Dietary ecology and niche separation among three closely related species (*Parapapio jonesi*, *Pp. whitei* and *Pp. broomi*) of South African Plio-Pleistocene Cercopithecoidea from Makapansgat Limeworks site.

NICOLAAS HOFMEYER FOURIE

Dissertation submitted in fulfillment of the requirement for the degree

Master of Science

in

Archaeology

In the Faculty of Science

University of Cape Town

February 2006

DECLARATION

I declare that his is work is my own, and has not been submitted before for any other degree at any other university.

Signed by candidate

N. H. Fourie

02 day of June 2006

ABSTRACT

Three sympatric, contemporaneous fossil cercopithecoid genera (*Cercopithecoides*, *Parapapio* and *Theropithecus*) are represented in assemblages from the Makapansgat Limeworks hominin locality in South Africa. The presence of such a variety of primate taxa in a single ecosystem at the same time suggests a certain degree of ecological and/or dietary differentiation between taxa. This research explores the possibility of dietary niche separation within this sample. Stable isotope ($^{13}C/^{12}C$, $^{18}O/^{16}O$) and trace-element (Sr, Ba, Ca) techniques for palaeodietary analysis are employed to investigate papionin dietary ecology, and especially to search for evidence of subtle niche separation between the more closely related, morphologically similar taxa of the genus *Parapapio*. Previous studies of fossil cercopithecoid dietary ecology report disjunctions between dietary and taxonomic groupings, possibly as a result of the use of fragmentary specimens or isolated teeth and ensuing taxonomic uncertainty, or perhaps because of problems in the taxonomy itself. Because such taxonomic uncertainties impede the interpretation of dietary data, craniometric analyses were also performed to ground the dietary interpretations in a morphological context. Only complete or partially complete cranial specimens from which morphological craniometric measurements could also be taken were sampled.. Dietary analyses indicated two widely differing dietary ecologies within the *Cercopithecoides williamsi* sample, consistent with published results for this taxon from Swartkrans and Sterkfontein. Results for *Theropithecus darti* indicated a predominantly C_4 diet. Two overlapping dietary ecologies, loosely correlated to taxonomic groupings, were found within the genus *Parapapio*; specimens attributed to *Pp. broomi* tended to have C_3-dominated diets with a larger rootstock component than *Pp. whitei* and *Pp. jonesi,* which included more C_4 grasses in their diet. The morphological analyses found no clear taxonomic signal in the craniometric data for *Parapapio,* suggesting that the current taxonomic assignments of *Parapapio* specimens are problematic. Additionally, for all of the analysed anatomical regions, the *Parapapio* sample was no more variable than the single geographically circumscribed extant chacma baboon sample. To sum, while biogeochemical dietary indicators indicate distinct dietary ecologies within and between genera, disjunctions exist between the dietary categories and the taxonomic assignment of specimens. Given these results, and in light of the taxonomic concerns highlighted by the craniometric investigation, reinvestigation of papionin taxonomy at Makapansgat may be warranted.

ACKNOWLEDGEMENTS

The last three years, especially the last year, have been an incredible learning and growing experience for me. The path over these years – two of which have been dedicated to this project – took a few interesting twists and turns, involved unrelated adventures and activities, and ended in two major projects, one of which is still ongoing at the time of the submission of this thesis. These multiple experiences were in a large part due to the efforts of my supervisors, Prof. Julia Lee-Thorp and Dr. Becky Ackermann. Whether it was securing a place on an international field school, sending me sample collecting, arranging the transport of samples from far places, helping me with applying for funding, helping me through my first conference presentations and posters, or being generally supportive and interested in my other university related activities, they have been an enormous source of inspiration and support. I would like to thank them for their mentorship, friendship, and their patient help, advice and comments throughout this project. I doubt I can ever adequately express the gratitude I feel.

I owe a special thanks to Prof. Julia Lee-Thorp and Dr. Matt Sponheimer for letting me use some of their unpublished isotope and trace-element data. I also owe Dr. Becky Ackermann special thanks for patiently guiding me through craniometric techniques and the world of multivariate statistics. I'm also very grateful to Dr. Daryl Codron for always being ready to assist me with whatever isotope, trace-element, or ecology issue I was battling with.

I would like to thank Mr. John Lanham for his help and friendship; his help with the mass spec and a range of other problems and difficulties for which one can rely on him to come up with a fix, was crucial to the completion of this project. Prof. Judith Sealy was always ready with advice and encouragement whenever I knocked on her door, and I truly appreciate that. I am also grateful to Dr. Andreas Spath and his staff in the ICP-MS lab in the Geology Department UCT for preparing and running the fossil samples for trace-element composition.

I thank Dr. Mike Raath of the Bernard Price Institute for Palaeontological Research (BPI) and the Department of Anatomical Sciences at the University of the Witwatersrand for access to the fossil primate material from Makapansgat, and Ms. Denise Hamerton from the Iziko Natural History Museum, Cape Town, for making the baboon collection at the museum available to me for craniometric sampling. I am

very grateful to PAST (Palaeo-Anthropology Scientific Trust) and the NRF (National Research Foundation) for providing the funding that made this research possible.

Finally, I would like to thank all my friends and colleagues who have been a tremendous source of encouragement to me. I am very grateful to my parents, Jan and Penny Fourie, and my sister, Hermien Fourie, as well as the rest of my family, who have been understanding and supportive in everything that I have endeavoured to do. With out their love and support I would not have gotten very far. I owe special thanks to my sister who at very short notice, during a very busy week, made the drawings of the baboon crania used in the illustrations in the craniometric section of this thesis. I am also very grateful to my uncle, Flip du Plessis, who passed away last year, and my aunt, Hermien du Plessis, for their investment in my university career and future.

CONTENTS

LIST OF FIGURES

LIST OF TABLES

APPENDICES

CHAPTER 1

INTRODUCTION

Extant papionins have been considered and investigated as models for various aspects of hominin evolution and ecology over the last thirty years (e.g. Jolly, 1970; Dunbar, 1976; Rose, 1976; Jolly, 2001; DHooghe *et al.*, 2004; Harvati *et al.*, 2004; Alberts *et al.*, 2005). South African Plio-Pleistocene fossil cercopithecoids may be useful in this context, as they were broadly contemporaneous and sympatric with the South African hominins and shared the same environments. Data from fossil primate taxa, in conjunction with data generated from extant primate taxa, can be useful in modelling and understanding dietary breadth, inter- and intra-taxon dietary variability. By refining paleaodietary reconstructions in fossil primates, specific dietary components may become more readily identifiable and dietary and behavioural responses to specific environmental factors may become evident. A more detailed understanding of Plio-Pleistocene primate community ecology will also broaden and refine our general understanding of the greater community ecology at fossil hominin localities. Working towards such a refined understanding of fossil primate dietary ecology and primate community ecology may provide a more appropriate framework from which to interpret and understand hominin dietary ecology.

A rich array of primate taxa are represented in the Plio-Pleistocene deposits of the South African karstic cave sites. Thus far, all recovered fossil primate specimens from South African Plio-Pleistocene sites are thought to belong to the family Cercopithicidae. Two sub-families, Cercopithicinae and Colobinae, are represented by four genera and up to twelve species, and one genus and one species, respectively (Freedman, 1957; Brain, 1981; Delson, 1992; Delson, 1993). All the South African Plio-Pleistocene Cercopithicinae genera belong to the tribe papionini (Freedman, 1957; Brain, 1981; Delson, 1992; Delson, 1993). Most extant members of this tribe in Africa are medium body-sized terrestrial primates inhabiting a wide range of habitats. There are currently far fewer extant papionin taxa in Africa than there were in the Plio-Pleistocene, and these are widely distributed across the continent; few are truly sympatric or even parapatric. Only *Papio h. hamadryas* and *Theropithecus gelada* occupy the same habitats, and this is facilitated by distinct niche separation and specific dietary specialisation on the part of *T. gelada* (Dunbar and Dunbar, 1974).

Some species/subspecies of *Papio* are parapatric (Zinner *et al.*, 2001). In such areas of parapatry, species borders are either maintained or hybrid zones develop (Nagel, 1970; Kummer, 1971; Nagel,1973; Kawai and Sugwara, 1976; Phillips-Conroy and Jolly, 1981; Alberts and Altmann, 2001).

During the Plio-Pleistocene in South Africa, up to five papionin taxa and one colobine taxon were sympatric or parapatric at some sites (Freedman, 1970). There is no modern analogue to this situation among extant papionin taxa. Furthermore, because all Plio-Pleistocene papionin taxa were terrestrial, and many were morphologically very similar, there is limited morphological evidence for dietary/niche specialisation. This unusual ecological situation is exemplified at the Plio-Pleistocene hominin locality of Makapansgat Limeworks in the Limpopo Province of South Africa. Here, five different fossil cercopithecoid taxa are thought to have been sympatric/parapatric during the Plio-Pleistocene. One is a colobine, while four of these taxa were papionins, of which three (genus: *Parapapio*) appear to have been very closely related. How did so many primate taxa manage to cohabit in the same environment, which they shared with a large variety and number of other herbivorous and omnivorous fauna?

The above scenario is not absent among other primates. For example, various species of guenons, which are skeletally relatively indistinct from one another cohabit in Africa (Gautier-Hion, 1980; Gautier-Hion and Gautier, 1986; Ham, 1995). However, these monkeys are arboreal and avoid competition by occupying different overlapping vertical eco-niches and/or by following differing dietary ecologies (Gautier-Hion, 1980; Gautier-Hion and Gautier, 1986; Mitani, 1991; Schoeninger *et al.*, 1997; Ramakrishnan and Coss, 2001). All the South African Plio-Pleistocene fossil cercopithecoid taxa are thought to have been terrestrial, or at least partially terrestrial, thus excluding the possibility of diversifying into different vertical eco-niches. Four of the five taxa at Makapansgat Limeworks are thought to have been largely terrestrial. Thus, even though the single colobine could have occupied a more arboreal eco-niche, there are still four competing terrestrial taxa. Nonetheless, in order for such a number of taxa to be supported within the same ecosystem at the same time, it is reasonable to expect a certain degree of ecological and/or dietary differentiation between taxa (Gautier-Hion, 1980; Gautier-Hion and Gautier, 1986; Mitani, 1991; Schoeninger *et al.*, 1997; Carter, 2001; Ramakrishnan and Coss, 2001). If this were the case, it would be expected that these ecological and/or dietary

differences should be detectable through chemical dietary indicators, distinctive dental wear and/or subtle morphological differences between these taxa. This project aims to investigate such dietary and ecological differences between the five fossil cercopithecoid taxa found at Makapansgat Limeworks.

The dietary ecology of the representatives of three sympatric, contemporaneous fossil cercopithecoid genera (*Cercopithecoides*, *Parapapio* and *Theropithecus*) from the Makapansgat Limeworks hominin locality in South Africa is here investigated through stable isotope and trace-element techniques. The representatives of these three genera are thought to have occupied distinct dietary niches, representing a terrestrial mixed C_4 ecology (*Theropithecus*) (Benefit and McCrossin, 1990), a semi-arboreal ecology (*Cercopithecoides*) (Benefit and McCrossin, 1990; Delson, 1992; El-Zaatari *et al.*, 2005) and a mixed C_3/C_4 terrestrial ecology (*Parapapio*) (Benefit and McCrossin, 1990; Luyt, 2001; Codron, 2003; Codron *et al.*, 2005; El-Zaatari *et al.*, 2005). Stable isotope and trace-element techniques for palaeodietary analysis are employed to investigate the dietary ecology of the members of these three genera, and to search for evidence of subtle niche separation between the more closely related, morphologically similar taxa of the genus *Parapapio*. A multi-layered approach to palaeodietary analysis is taken; a suite of five biogeochemical palaeodietary indicators is used to investigate subtle dietary differences between these taxa, as each indicator is sensitive to dietary or behavioural components to which others are insensitive. In this way it is hoped that subtle as well as broader dietary differences between taxa will be detected.

Particular emphasis will be made in this study on the genus *Parapapio,* as its abundance (i.e. number of specimens) and diversity (i.e. number of species) at Makapansgat allow for assessment of inter- and intra-taxa dietary variation, which might provide evidence for subtle dietary niche separation. This genus currently consists of three morphologically similar species (*Pp. jonesi*, *Pp. broomi* and *Pp. whitei*) in South Africa that differ primarily in size. The three species were originally distinguished on the bases of molar size, *Pp. whitei* having the largest and *Pp. jonesi* having the smallest molars (Broom, 1940). Subsequently, further refinements have been made in the identification of the three species, but differences in molar size between the three species remain the fundamental and most discriminating difference (Freedman, 1957). In other aspects of morphology, these species appear to be relatively homogenous. All three species have been described from the same deposits

at Makapansgat Limeworks (Freedman, 1957, 1976; Brain, 1981) while the same species have also been found to be synchronous and sympatric at a number of other fossil hominin localities (Freedman, 1957, 1970, 1976; Brain, 1981; Benefit and McCrossin, 1990; Elton, 2001). These three species show no obvious morphological adaptations that would suggest different dietary ecologies. Ecological and dietary differences between these closely related taxa, if they exist, may be identifiable through fine-grained analysis of chemical dietary indicators.

There are various well-established techniques for palaeodietary analysis, each with its own limitations, which have been employed to investigate the dietary ecology of Plio-Pleistocene faunas. Approaches that use dental morphology to gauge dietary adaptations are useful for identifying broad dietary categories, but are often not capable of distinguishing between more subtle dietary differences and dietary variability within a taxon (Benefit and McCrossin, 1990). Such approaches are unable to assess behavioural /dietary plasticity not represented in tooth morphology, although they are useful for identifying evolutionary adaptations and trends. Dental micro-wear studies are also useful for identifying broad dietary categories, and can be used to identify specific dietary components and/or the consistency of these components. However, micro-wear studies are limited by the effects of the "last meal," which disproportionately represents the damage on the tooth surface. Perhaps more importantly, a major limitation is the substantial overlap between effects and data of the dietary categories used (Grine, 1986, 1987; Teaford and Oyen, 1989; Grine *et al.*, 2002; El-Zataari *et al.*, 2005). Although both these techniques provide unique evolutionary and dietary information, they lack the degree of resolution needed to distinguish between closely related taxa which may differ in more subtle aspects of their diet and ecology than can be accurately detected and characterised by the analysis of dental morphology or wear.

Stable isotope and trace-element techniques for palaeodietary analysis have both been useful for the investigation of broad dietary differences among taxa. When used in combination, these biogeochemical tools are potentially more powerful, and may detect more subtle differences (Carter, 2001; Schoeninger *et al.*, 1997; Sillen, 1988; Sponheimer and Lee-Thorp, in press). These techniques directly measure diet by analysing the abundance of certain elements, usually trace-elements, and/or the isotopic composition of certain chemical constituents of animal tissues which are directly derived from the diet. Isotope and trace-element data reflect the actual

average diet consumed, averaged over a period of several years to a few weeks, depending on the tissue that is analysed. These techniques are sensitive to inter- and intra-species dietary variability, and no assumptions need to be made about taxonomic uniformitarianism or behavioural plasticity. It is also increasingly possible to begin investigating and identifying subtle dietary differences thanks to advances in the understanding of stable isotope and trace-element patterns in extant - and palaeo-ecosystems. This facilitates the interpretation of isotopic and trace-element data of selected taxa in the context of a faunal community ecology as derived from an understanding of extant and palaeo-ecosystems (e.g. Sillen, 1988; Sillen, 1992; Sponheimer, 1999; Sponheimer and Lee-Thorp, 2001; Sponheimer and Lee-Thorp, 2003a).

In this study, the stable isotope ratios of carbon ($^{13}C/^{12}C$) and oxygen ($^{18}O/^{16}O$), as well as strontium (Sr), barium (Ba) and calcium (Ca) abundances, are measured in order to detect the presence and contribution of certain dietary components. Using stable carbon isotope ratios, it is possible to distinguish between C_4 photosynthesising plants (e.g. grasses and sedges) and C_3 photosynthesising plants (e.g. trees and shrubs) and their products (e.g. seeds and fruits). Stable oxygen isotope ratios are useful in identifying likely sources of metabolic water in an animal's diet (e.g. from food water or meteoric surface water), from which aspects of behaviour can inferred (e.g. whether an animal is an obligate drinker or not). Sr/Ca and Ba/Ca ratios are useful in identifying the dietary contribution of certain plants and plant parts such as rootstocks and grasses. Our understanding of the latter two trace-element ratio patterns in African ecosystems is still in its naissance. For those dietary components for which little data is available (e.g. fruits), a heaver reliance on the theoretical understanding of trace-element abundances is necessary. Furthermore, Sr/Ca and Ba/Ca intraspecific variability is known to be high within any given taxon and area. Sufficient sample sizes are thus important in order to characterise a given taxon (Sillen, 1988; Sponheimer and Lee-Thorp, in press). This is not always feasible when working with fossil material and cautions that results for individual specimens should not be over-interpreted.

The tissues of animals which consume these plants/plant parts, themselves reflect the isotopic and trace-element composition of the plants that make up their diet. By understanding the isotope and trace-element patterns in natural systems, it is possible to tease apart whether different taxa in African ecosystems consume different

proportions of grass to other vegetation (based on $^{13}C/^{12}C$) (e.g. Ambrose and DeNiro, 1986; Lee-Thorp *et al.*, 1989b; Sponheimer, 1999; Panarello and Fernandez, 2002; Sponheimer *et al.*, 2003a, 2003b, 2005b), and/or have different sources for metabolic water (based on $^{18}O/^{16}O$) (e.g. Bocherens *et al.*, 1996; Kohn, 1996; Schoeninger and Valley, 1996; Cerling *et al.*, 1997; Sponheimer and Lee-Thorp, 1999c; Carter, 2001, Sponheimer and Lee-Thorp, 2001), and/or utilise different plant parts (based on Ba, Sr, Ca) (e.g. Runia, 1987; Sillen, 1992; Lee-Thorp and Sponheimer, 2003; Sponheimer *et al.*, 2005a, 2005b; Sponheimer and Lee-Thorp, in press). The patterns of the relevant isotope and trace-element abundances in natural systems and their use as dietary discriminators are described in more detail in Chapter III.

A number of studies have employed these techniques to investigate the ecology of extant and Plio-Pleistocene primate communities or individual taxa (Lee-Thorp *et al.*,1989b; Schoeninger *et al.*, 1997, 1998, 1999; Carter, 2001; Luyt, 2001; Sponheimer and Lee-Thorp, 2001; Codron, 2003; Thackeray and Myer, 2004; Codron *et al.*, 2005). Studies using fossil primate material have often been of limited use as dietary groupings do not always correlate accurately with the taxonomic assignment of specimens, and it is unclear how to interpret such disjunctions on the basis of isotope data alone. For instance, in such cases are the specimens identified incorrectly or are the taxonomic categories themselves problematic? Previous isotope based studies have pointed strongly to bimodal distributions of dietary habits for at least two of the taxa/genera included in this study (Luyt, 2001; Codron, 2003; Codron *et al.*, 2005). Extreme dietary variability is not unheard of amongst closely related primate species, but it is unusual. Such taxa (like baboons) with very variable diets are usually distributed over many, often extremely different habitats, and their diets reflect adaptations to these ecologically variable and extreme environments. This is not the case for the South African hominin bearing fossil sites that have been studied to date as they represent environments of reasonably similar habitat composition (Reed, 1997; Pickering *et al.*, 2004). The bimodality and variability of the dietary data reported for some taxa (Luyt, 2001, Codron, 2003; Codron *et al.*, 2005) from these sites are therefore somewhat unusual given the palaeoenvironmental setting. These apparently anomalous dietary patterns as well as concerns raised by morphologists (Maier, 1970; Jones, 1978; Brian, 1981; Delson, 1992; Thackeray and Myer, 2004) indicate that there may be flaws and inconsistencies in the taxonomy and identification of these taxa. Unreliable identification of specimens and possible flaws

in the taxonomy of South African Plio-Pleistocene cercopithecoids, impede the interpretation of patterns in the dietary data, since the patterns often don't match the taxonomic composition of the sample used.

Some of these difficulties regarding the secure identification of specimens and possible flaws in the taxonomy, encountered in studies of fossil primate dietary ecology relate to the nature of the samples used in these studies. Most studies investigating the dietary ecology of Plio-Pleistocene primates use isolated teeth or dentognathic fragments for analysis (Codron, 2003; Codron *et al.*, 2005; El-Zaatari *et al.*, 2005). The identification of isolated and fragmented specimens is very difficult because there are often no really discrete morphological features on these specimens that can be used to accurately distinguish between closely related taxa. Using such fragmentary isolated specimens therefore appears to be somewhat problematic because various taxa are morphologically very similar and not easily distinguishable from one another (Broom, 1940; Maier, 1970; Freedman, 1976; Delson, 1992). These difficulties regarding the correct identification of specimens and their implications for the interpretation of palaeodietary analyses are further compounded by uncertainties regarding the taxonomy of the South African Plio-Pleistocene Cercopithecoidea as a whole. It has been noted by previous researchers that some taxonomic units may in fact not reflect real biological units (Maier, 1970; Freedman, 1976; Delson, 1992). These problems and their implications for palaeodietary analysis are discussed further in Chapter II.

If specimens are incorrectly identified, dietary patterns in the data are lost and dietary differences between taxa are obscured by undue within-taxon variability. This study attempts to deal with this problem by only sampling complete or partially complete cranial specimens from which morphological craniometric measurements could also be taken. In this way higher confidence can be placed in the taxonomic assignment of specimens. Furthermore, the craniometric data can be analysed using multivariate statistical techniques, in order to further investigate remaining concerns around the identification and classification of specimens. It is hoped that these precautions will provide a more secure taxonomic context within which to investigate subtle dietary /ecological differences between these closely related taxa.

Additionally, this study focuses on material from a single site in order to further limit the introduction of excessive variability; even though this may imply smaller sample sizes, problems with comparing different periods and places can be avoided.

Different localities may have supported different macro-habitats and or micro habitats, which could have responded differently to climatic changes associated with different periods. Such factors would complicate isotopic and trace-element dietary analysis. Working with specimens from one site and a narrow sequence within that site means that all specimens would have experienced similar taphonomic and sedimentary influences. They are therefore likely to have been subject to similar diagenetic influences. Furthermore, a number of isotope and palaeoecology studies have been done on the fossil mammal communities from Makapansgat Limeworks site (Eizenhart, 1974, Partridge, 1975; Reed, 1996, 1997, 1998; Sponheimer, 1999; Sponheimer *et al.*, 1999; Sponheimer *et al.*, 2001; Sponheimer and Lee-Thorp, 2003b). The isotope and trace element data, and ecological, climatological and environmental information from these studies will provide a ready framework for interpreting the fossil cercopithecoid data.

This investigation therefore differs from previous investigations of Plio-Pleistocene cercopithecoid dietary ecology in a number of important ways. Firstly, a suite of dietary indicators are used to investigate broad as well as subtle dietary differences. Secondly, only complete or partially complete cranial specimens from a narrow sequence in a single site were sampled. Thirdly, specimens were subjected to morphometric analysis to investigate taxonomic concerns, and thus provide a more secure taxonomic context for the interpretation of dietary data. It should be noted that the craniometric analysis conducted in this study does not attempt to definitively settle taxonomic concerns regarding the genus *Parapapio*. It is done purely to facilitate dietary analysis by correlating dietary groupings to independently generated craniometric groupings. The results from this investigation may, however, provide insight into broader taxonomic issues.

A review of the relevant literature regarding the South African Plio-Pleistocene Cercopithecoidea and in particular the three genera used in this study is given in Chapter II. Stable isotope and trace-element techniques of palaeodietary analysis are described in Chapter III. Sampling protocol, sample preparation, stable isotope-, trace-element analysis, craniometric techniques and morphometric analyses are described in Chapter IV. The results for stable isotope, trace-element analysis and craniometric investigation are presented in Chapter V and VI. The results are consolidated and discussed in Chapter VII.

CHAPTER 2

SOUTH AFRICAN PLIO-PLEISTOCENE CERCOPITHECOIDEA

This chapter presents a brief review of the taxonomic history and dietary ecology of the relevant Plio-Pleistocene cercopithecoid taxa from karstic cave sites in South Africa. Problems concerning the current taxonomy of the relevant taxa are discussed in the final section.

2.1. South African Plio-Pleistocene Cercopithecoidea

The brecciated cave deposits from numerous karstic caves sites in South Africa were commercially mined at the end of the nineteenth century, and it was through such mining activity that interest was first drawn to the fossiliferous breccias. Although various geologists, palaeontologists and naturalists started collecting specimens from the caves during this time, no systematic research was conducted until after the discovery of the Taung child in 1924 (Dart, 1925a). This discovery prompted renewed scientific interest in the deposits, and various researchers started to re-examine existing collections and the cave sites themselves (see discussion in Freedman, 1957).

The first cercopithecoid fossils were discovered at Taung, a lime quarry approximately 100km north of Kimberley and 400km south-west of Sterkfontein (Fig. 2.1), and were announced in 1920 by SH Haughton at a Royal Society of South Africa meeting (Freedman, 1957). Subsequently, primate fossils were discovered at Makapansgat, Sterkfontein, Swartkrans and other hominid-bearing karstic cave sites. The fossil primate collection grew to consist of two sub-families, five genera and a large and varying number of species (Freedman, 1957; Brain, 1981; Delson, 1992; Delson, 1993). The majority of fossil primates from these South African Plio-Pleistocene deposits belong to the family Cercopithecidae and the sub-families Cercopithecinae and Colobinae. The Papionini make up the largest group within the Plio-Pleistocene Cercopithecinae, being represented by four to five genera; *Papio*, *Parapapio*, *Dinopithecus* (*Papio*), *Gorgopithecus* and *Theropithecus*. The sub-family Colobinae is only represented by one genus and one species; *Cercopithecoides*

williamsi. The current taxonomy of the South African fossil Cercopithecoidea has not changed substantially since Freedman's extensive review (Freedman, 1957). The classification scheme of South African fossil Cercopithecoidea used in this study is taken from Brain (1981) and Delson (1992, 1993) and is shown in Appendix A-1.

Figure 2.1. Map of South Africa, showing the most important Plio-Pleistocene hominin localities.

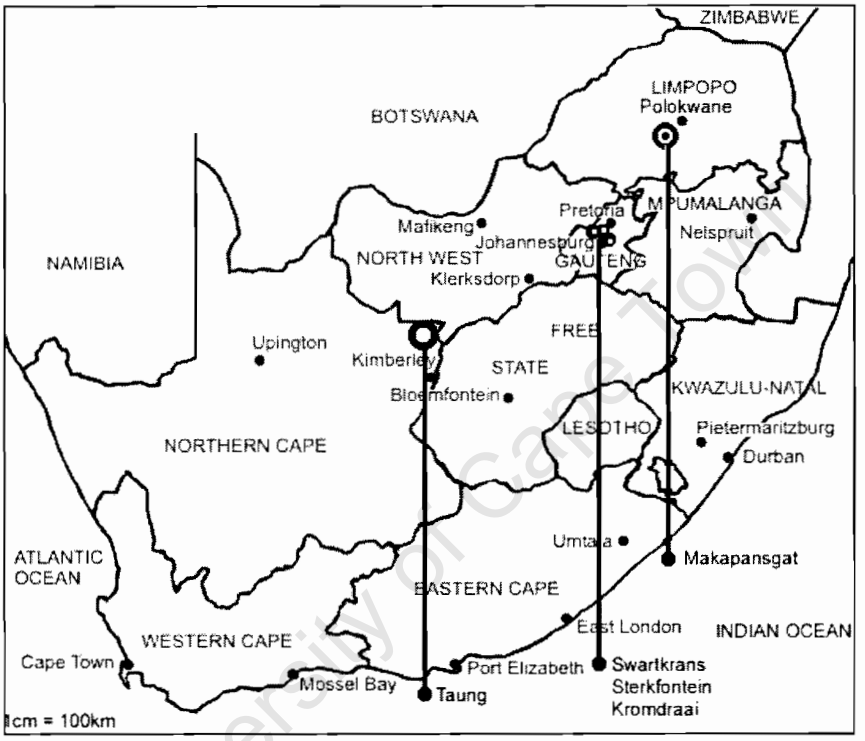

Within the genus *Parapapio*, three species have been described from Makapansgat, Sterkfontein and Swartkrans; *Parapapio whitei*, *Pp. broomi* and *Pp. jonesi* (Freedman, 1976; Brain, 1981). They almost certainly coexisted at these sites, since there is no evidence for a chronocline within the deposits in which they are found. In other words, the three taxa are randomly distributed throughout the *Parapapio* bearing deposits; one species does not succeed the other in sequence (Freedman, 1957). They also coexisted at these sites with *Theropithecus darti* and *Cercopithecoides williamsi* (Freedman, 1976). At other sites such as Kromdraai, Bolt's Farm, and Cooper's Cave, one or a combination of the above mentioned taxa shared their environment with other papionin taxa such as *Papio robinsoni*, *P. angusticeps, Dinopithecus* (*Papio*) *ingens*, *Gorgopithecus major* and the Theropithecine *T. oswaldi* (Freedman, 1976). Sterkfontein and Swartkrans are relatively close to Cooper's Cave and Kromdraai,

and there are no apparent barriers that would have prevented cohabitation of any combination of the above-mentioned taxa at any of these sites. It is unlikely that the composition of the primate communities at any of these sites were isolated or stagnant. Even though a full complement of contemporaneous taxa is not represented in the fossil assemblages of every site, this does not mean that they were not present in those areas; differences between taphonomic processes or collecting agents at different sites may have skewed the representation of other contemporary primate taxa in the deposits (Brain, 1981).

All of the fossil Cercopithecoidea from the South African Plio-Pleistocene, including those from Makapansgat, are thought to have been terrestrial. Today the greatest numbers of sympatric primates are found in the tropical forest environments of Africa (Gautier-Hion, 1980; Gautier-Hion and Gautier, 1986; Ham, 1995), Asia (Ramakrishnan and Coss, 2001) and South- and Central America (Mitani, 1991). They avoid competition through dietary specialization and/or by occupying different vertical layers in the forest, from the forest floor to the highest reaches of the canopy (Gautier-Hion, 1980; Gautier-Hion and Gautier, 1986; Mitani, 1991; Schoeninger *et al.*, 1997; Ramakrishnan and Coss, 2001). In other words, the diversity in these regions is enabled by niche separation. In order for a similar variety of species to coexist in a terrestrial environment it is reasonable to expect niche separation between species. Two of the fossil Theropithecine taxa do exhibit clear dental specialization. *Theropithecus oswaldi* and *T darti* exhibit a similar dental morphology to the modern *T. gelada*, suggesting a mainly gramnivorous diet (Brain, 1981; Benefit and McCrossin, 1990). *T. darti* has a shearing crest morphology (higher crests) which has been interpreted as suggesting greater folivory in this taxon than in either *T. oswaldi* or the extant *T. gelada* (Benefit and McCrossin, 1990). *C. williamsi* is also distinctive, with high-cusped molars and deep foveae consistent with the dental morphology of extant folivorous primates (Maier, 1970; Brain, 1981). However, there is little evidence of the kinds of major or distinct morphological or dental differences amongst the fossil papionins that would suggest niche separation. It is therefore surprising to find three or possibly four very closely related species in the genus *Parapapio* (*Parapapio antiquus*, *Pp. whitei*, *Pp. broomi* and *Pp. jonesi*) which are synchronous and sympatric – or at least parapatric – in such a saturated and competitive environment.

In the following section a brief review of the genus *Parapapio,* as currently understood, is given, along with a review of the two genera that were known to have coexisted with *Parapapio* at Makapansgat during Member 3 and 4 times.

2.1.1. *Parapapio*

The genus name *Parapapio* was given to a collection of small, short-snouted fossil baboons from Sterkfontein by TR Jones in 1937. Jones only recognized one species within this genus, which he called *Pp. broomi*. Broom (1940) later divided this single species into three species based purely on tooth size: the small *Pp. jonesi*, followed by the intermediate *Pp. broomi,* and the large *Pp. whitei*, this last taxon based on new specimens from Sterkfontein (Broom, 1940). Broom (1940) originally distinguished between the three taxa mainly on tooth size; this method of identification was later further developed by Freedman (1957) and other researchers (Maier, 1970; Freedman and Stenhouse, 1972). Freedman (1957, 1960, 1961, 1976) and others (Maier, 1970; Delson, 1992) emphasised, especially molar and pre-molar size, and non-metric differences in cranial morphology (e.g. muzzle morphology and shape of neurocranial components) between the three taxa. Molar dimensions appeared to play an important role in the identification of the three *Parapapio* taxa mainly due to a paucity of reasonably complete crania. In 1957, Freedman placed *Papio antiquus*, a small fossil baboon described from Taung (Haughton, 1920), into the genus *Parapapio*. The genus *Parapapio* currently consists of four species: *Pp. antiquus*, *Pp. jonesi*, *Pp. broomi* and *Pp. whitei*. *Pp. antiquus* is known only from Taung. (Haughton, 1920; Freedman 1957, 1970, 1976) *Pp. jonesi*, *Pp. broomi* and *Pp. whitei* have been identified at a number of sites including Taung, Sterkfontein, Swartkrans, Kromdraai and Makapansgat. *Pp. jonesi*, *Pp. broomi* and *Pp. whitei* form no discernable chronocline at any of the sites where they are sympatric (Freedman, 1957; Freedman, 1976; Brain, 1981), which would indicate that they coexisted. The genus is also represented in East Africa (Brain, 1981; Frost and Delson, 2002).

Based on a broad study of molar morphology using specimens from South African and East African sites, Benefit and McCrossin (1990) have suggested that South African *Parapapio* species were less frugivorous than East African *Parapapio* species, including more grasses and herbaceous foods in their diets. Dental wear studies of *Parapapio* specimens from South Africa have also inferred a significant grass component in their diet (El Zaatari *et al.*, 2005). Isotopic studies of teeth from Swartkrans and Sterkfontein have shown that the *Parapapio* species did rely – but

variably – on C_4 plants in their diets (Luyt, 2001; Codron, 2003; Codron *et al.*, 2005). They can best be described as terrestrial savannah primates, much like modern baboons but in many cases more substantially reliant on C_4 grasses. Both Luyt (2001) and Codron (2003) report a bimodal clustering of isotope data indicating two dietary groupings, which suggest two distinct sets of behaviours that might indicate taxonomic distinctiveness at the species level; these two sets of dietary behaviours do not correlate neatly with taxonomic assignments. This might suggest problems with the fossil taxonomy at these sites, because most of these isotope analyses were done on isolated teeth, which are readily subject to misidentification, and any such interpretations are somewhat problematic. These taxonomic concerns and complications are discussed in more detail in section 2.2 of this chapter.

2.1.2. *Theropithecus*

The fossil members of this genus are similar to modern gelada baboons (*Theropithecus gelada*), having high, flat faces, anterior teeth that are reduced relative to the molars, and molars with particularly high cusps. The genus was first described, based on material from Kenya, as *Simopithecus oswaldi* (Andrews, 1916). Broom and Jensen recovered the first South African specimen belonging to this genus in 1946 from Makapansgat Limeworks, but named it *Papio darti* (Broom and Jensen, 1946). Freedman (1957) recognized it as a *Simopithecus,* described all specimens from Makapansgat as *Simopithecus darti,* and designated the slightly larger and later form from Swartkrans *S. danieli*. Based on morphological, ecological and dietary similarities to modern gelada baboons, Jolly (1972) argued that *Simopithecus* be subsumed as a subgenus of Theropithecus. Later Delson (1993) deleted *Simopithecus* entirely from the taxonomy in favour of the genus name *Theropithecus*; he also placed *S. danieli* into *T. oswaldi*. Currently only two species of fossil Theropithecines are recognized from South African deposits: *Theropithecus darti* (only from Makapansgat) and *T. oswaldi*. Delson (1992) points out that the distinction between the two may be arbitrary, as it is based purely on differences in anterior tooth size.

The dietary characterization of the two species based on dental morphology and micro-wear supports the two species division as it currently stands (Benefit and McCrossin, 1990; El Zaatari *et al.*, 2005). Stable isotope analyses of tooth enamel of *T. oswaldi* indicate that this species relied heavily on C_4 grasses (Lee-Thorp *et al.*, 1989b; van der Merwe *et al.*, 2004) and had a diet similar to that of modern *T. gelada.*

Whether *T. darti* differed in its dietary ecology from *T. oswaldi*, as suggested by Benefit and McCrossin (1990), will be directly tested through stable isotope analysis in this investigation. If *T. darti* had a more folivorous diet than *T. oswaldi* it would be expected that *T. darti* specimens would yield more depleted (negative) stable carbon isotope ratios than *T. oswaldi* specimens.

2.1.3. *Cercopithecoides*

In the South African deposits, the genus *Cercopithecoides* is represented by only one species, *C. williamsi,* a medium to large-bodied colobine thought to be largely terrestrial (Benefit and McCrossin, 1990; Delson, 1992). The species was first described in South Africa by Mollet (1947), based on a single skull from Makapansgat. Subsequently, more specimens attributed to this species were described from Swartkrans, Taung, Sterkfontein, Kromdraai and Cooper's Cave (Brain, 1981; Freedman and Brain, 1972).

C. williamsi specimens exhibit a typical colobine dentition with molars having high cusps and deep foveae (Freedman, 1957; Brain, 1981; Maier, 1970), a characteristic of modern folivorous primates. The pattern of dental wear in this species appears to be related to grit in the diet, which suggests substantial terrestrial foraging (Delson, 1992; El Zaatari *et al.*, 2005). Postcrania also indicate a degree of terrestriality (Birchette, 1981; Leakey, 1982). This evidence is supported by limited isotopic data, which suggests that some *C. williamsi* individuals from Sterkfontein and Swartkrans included large quantities of C_4 type plants in their diets (Luyt, 2001; Codron, 2003; Codron *et al.*, 2005). Isotopic analysis also reveals a cluster of *C. williamsi* individuals with mostly C_3 diets (Luyt, 2001; Codron, 2003; Codron *et al.*, 2005), consistent with a largely arboreal folivorous diet. The cluster of specimens suggesting a significant C_4 component in the diet is surprising since all extant colobines are arboreal folivores restricted to the evergreen forests of tropical Africa. Furthermore, specimens belonging to both these dietary groupings, indicated by stable carbon isotope analysis, have been recovered from two different sites. At both sites there appears to be no obvious chronocline between specimens belonging to either dietary grouping. It has been suggested that this anomalous bimodal distribution in isotope values may be due to mis-identification of isolated teeth, or perhaps the presence of another as yet unrecognized species (Luyt, 2001; Codron, 2003, Codron *et al.*, 2005).

2.2. Taxonomic Concerns and Complications

While the broad framework of the current classification scheme of the Plio-Pleistocene South African Cercopithecoidea seems to be generally agreed upon (Maier, 1970; Jolly, 1972; Delson, 1973; Freedman, 1976; Brain, 1981; Benefit and McGrossin, 1990; Eisenhart, 1994; McKee and Keyser, 1994), it is also acknowledged that the classification of at least some genera may be problematic (Jones, 1978; Brian, 1981; Delson, 1992; Thackeray and Myer, 2004). The taxonomic validity of species belonging to the genus *Parapapio* has been increasingly questioned (Codron, 2003; Thackeray and Myer, 2004; Codron *et al.*, 2005), especially where the identifications are based on isolated teeth and where distinctions are made mainly on the bases of size (Maier, 1970; Delson, 1992; Thackeray and Myer, 2004). The taxonomic integrity of *Parapapio* sp. and the correct identification of specimens are essential to meaningfully interrogate isotopic and trace element data for evidence of niche separation (Codron, 2003; Codron *et al.*, 2005).

2.2.1. Taxonomic Assignment

Parapapio is distinguished from the *Papio* by their distinctive muzzle shape, generally shorter muzzle, lack of an ante-orbital drop, smaller teeth and smaller overall cranial size (Gear, 1926; Jones, 1937; Broom and Jensen, 1946; Freedman, 1957; Delson, 1992). However, Jones (1978) described extant *Papio h. ursinus* individuals from Zimbabwe with the same muzzle morphology as is typical of the *Parapapio*. He concluded that the muzzle morphology of *Parapapio* may not be sufficiently distinctive to distinguish between *Parapapio* and *Papio* specimens in fossil assemblages (Jones, 1978). If that is the case for muzzle morphology, the case for distinctions among isolated teeth is even more precarious. Freedman (1957) notes that there is no morphological difference between fossil *Papio* and *Parapapio* teeth; they differ only in size. Nonetheless, *Parapapio* specimens seem to have been routinely identified from dentognathic remains. This seems dangerous because large *Parapapio* teeth might easily be identified as belonging to one of the smaller *Papio* species or specimens or *vice versa*.

In spite of these difficulties, there has been a historical tendency to use dental measurements as the principal distinguishing characteristic between species in this genus (Freedman, 1976). Specimen M3065 – a partially complete cranium – is

described as being larger than a particularly large male *Pp. whitei* specimen, M3072, but is assigned to *P. broomi* based on dental dimensions (Maier, 1970). This has also been the case with a number of other specimens (e.g. M3051, M3060, M3061, M2961, M2962) (Maier, 1970; Freedman, 1976). When there is no consensus among researchers on the identification of near complete crania, or there are inconsistencies in the application of the classification criteria, it is reasonable to regard the taxonomic assignments within this genus with caution. The taxonomic assignment of isolated teeth and dentognathic specimens cannot safely be regarded as accurate. Delson (1992), Freedman (1976) and Maier (1970) recognized the arbitrary nature of taxonomic assignment based solely on the small differences in tooth size. Maier (1970) goes as far as cautioning that the taxonomic groupings of the genus *Parapapio*, as it stands, may not reflect real biological units. Thackeray and Myer (2004) argued that *Pp. broomi* and *P. jonesi* are males and females of the same species and that the overall range of variation in their combined dental measurements are consistent with that found in modern baboon populations. Whatever the case, it is evident that the historical taxonomic assignment of specimens is problematic, especially in the case of fragmentary dentognathic remains. The validity of the three species belonging to this genus needs to be reconsidered.

In particular, the taxonomy of the genus *Parapapio* is in need of rigorous revision using modern techniques. The complexity, application and analytical power of biometric techniques has significantly increased over the last two decades, as has our understanding of biological variation within taxa. Much of the theory behind the justification of the initial taxonomic assignments within the genus *Parapapio* may now be outdated. During the 1970s and the preceding decades, when the initial classification of this genus was put in place, relatively simple two-dimensional linear measurements were routinely used in biometric studies. However, such methods are somewhat insensitive to shape and make it difficult to account for the effects of size (Adams *et al.*, 2004). Since that time, multivariate approaches and current geometric morphometric methods have been extensively developed. Such methods are far more sensitive to shape, make it easier to remove non-shape induced variation, and allow for easy graphical representation (e.g. Adams *et al.*, 2004). Multivariate analyses have also been developed using three dimensionally digitised landmark data, which can be Procrustes rotated to remove size (e.g. Frost *et al.*, 2003), and multivariate statistics can now be easily and routinely performed on three dimensionally digitised landmark

data using large data sets. This was not possible or practical at the time that most of the fossil primate specimens were first described and analysed.

2.3. Plio-Pleistocene Cercopithecoid Palaeodiets and Palaeoecology

Six genera and roughly thirteen species of terrestrial Cercopithecoid primates are represented in the South African Plio-Pleistocene deposits. All of the South African Plio-Pleistocene Cercopithecoidea are thought to have been largely terrestrial, and would have therefore been in competition with each other, as well as with a large number and variety of Plio-Pleistocene herbivores and omnivores. It seems unlikely that South African Plio-Pleistocene environments were rich enough to support such a large number of ecologically similar taxa. There appears to be little overall niche specialization among these taxa, based on their morphology. The limited isotopic evidence thus far collected from Sterkfontien and Swartkrans indicate considerable dietary overlap between many taxa. There is overlap between taxa from different genera (e.g. *P. robinsoni*, *P. ingens* and *Parapapio* sp.) and an unusually large amount of variation within some taxa (e.g. *P. robinsoni*) (Codron, 2003).

If more than one *Parapapio* taxon is represented in the fossil sample, it would be expected that these taxa would exhibit differences in dietary ecology as a competition avoidance strategy. However, the apparent lack of evidence for ecological niche separation between different *Parapapio* taxa may be a result of incorrect identification of specimens and/or fundamental flaws in the taxonomy. In order to interpret the isotopic data and make meaningful observations about the diets of different taxa it is important that specimens are correctly identified. Isotopic analyses of fossil primate material are usually done using isolated teeth. Considering the difficulties in distinguishing between different species from isolated and fragmented specimens it is likely that many specimens are incorrectly identified. Misidentification of specimens, if it occurs, will mask real ecological distinctions. Anomalies in the dietary ecology of various taxa suggested by stable isotope analyses to date raise further questions about the integrity of the current taxonomic groupings and/or the identification of the fossil material analysed. Until the taxonomy of the Plio-Pleistocene Cercopithecinae of South Africa is more rigorously characterised, fragmented and isolated material cannot safely be used in biogeochemical and/or faunal analyses of closely related genera and taxa, such as the genus *Parapapio*.

These concerns can be at least partially addressed to facilitate dietary analysis. This can be achieved by using specimens which consist of near complete crania from synchronous deposits from a single site. Using a temporally and geographically restricted sample should limit temporally or geographically induced variability which may confuse taxonomic and ecological patterns in morphological and dietary analysis. Specimens can be morphometrically analysed using a large number of craniometric variables to investigate the existence of distinct morphotypes within the *Parapapio* sample and how these correlate to the taxonomic assignment of the specimens. This would provide a morphotypic framework, or at least a better understanding of the morphological affinities between specimens, through which to interpret patterns revealed by dietary analysis.

CHAPTER 3

STABLE ISOTOPE ECOLOGY AND TRACE-ELEMENT PATTERNS

This chapter describes basic principles in stable isotope ecology, and analysis. The basic principles of trace element analysis and its application to ecological studies are outlined. The use of fossil tooth enamel as isotopic archive and issues concerning diagenesis are also discussed.

STABLE ISOTOPES

3.1. Stable Carbon Isotope Dynamics and Fractionation in Biological Systems

Carbon has two stable light isotopes, ^{12}C and ^{13}C, the ratio of which are commonly used as tracers for biochemical pathways in foodwebs. The ^{13}C isotope of carbon has slightly different physicochemical properties to ^{12}C (O'Leary, 1993; Hoefs, 1997), resulting in differences in the way these two isotopes are treated during physical and chemical process. ^{13}C is strongly discriminated against during physical and biochemical processes in different parts of the carbon cycle. Stable carbon isotope composition is expressed as a difference relative to an international standard VPDB in parts per mille (‰) (Craig, 1957; Dawson and Brooks, 2001):

$$\delta = (R_{sample}/R_{standard}) - 1) \times 1000$$

R is the corresponding $^{13}C/^{12}C$.

3.1.1. Photosynthesis and Fractionation

In the 1970's stable isotope researchers observed that the stable carbon isotope composition in plants can be accurately predicted by the photosynthetic pathways followed, or vice versa (Smith and Epstein, 1971). Plants that are most depleted in ^{13}C use the Calvin Benson method of photosynthesis (C_3 – photosynthesis), while those following the Hatch-Slack method of photosynthesis (C_4 – photosynthesis) are less depleted in ^{13}C compared to atmospheric CO_2. These two categories of plants (hence referred to as C_3 and C_4 plants) discriminate against ^{13}C to different degrees during CO_2 fixation during photosynthesis.

In both C_3 and C_4 plants the first fractionation step occurs at the leaf surface where $^{13}CO_2$ is discriminated against more strongly than $^{12}CO_2$, due to stomatal effects and gas diffusion resistance at the leaf surface. ^{13}C is discriminated against by approximately 4.4‰ during diffusion at the leaf surface (O'Leary, 1993). $^{12}CO_2$ diffuses more easily through the stomata into the leaf than $^{13}CO_2$, because it is a lighter, smaller molecule (Farquhar *et al.*, 1982; van der Merwe and Medina, 1989). Further discrimination against $^{13}CO_2$ occurs to a minor degree during processes of dissolution, hydration and dissociation inside the leaf.

The greatest fractionation takes place during carboxylation (CO_2 – fixation) during which, in C_3 plants, carbon from the CO_2 is fixed as an organic three-carbon acid (phosphoglyceric acid – PGA), by the action of the enzyme ribulose biphosphate carboxylase (Rubisco) (Farquhar *et al.*, 1980; O'Leary, 1993; Hoefs, 1997). In C_4 plants, carbon from CO_2 is fixed in two stages. First carbon is fixed as a four-carbon acid (oxaloacetic acid – OAA) by the action of the enzyme phosphoenol pyruvate carboxylase (PEP). In a second step CO_2 is released elsewhere and completely converted by Rubisco as in C_3 plants. Since Rubisco discriminates more strongly against ^{13}C than does PEP, the result is that less ^{13}C is fixed as part of the three-carbon organic acid during carboxylation in C_3 plants than in C_4 plants (Farquhar *et al.*, 1982, O'Leary, 1988).

The result is that C_3 and C_4 plant have distinct $^{13}C/^{12}C$ ratios. Plants using C_3 photosynthesis are depleted in ^{13}C and exhibit $\delta^{13}C$ values ranging globally between -24‰ and -31‰ (Smith and Epstein, 1971; Vogel *et al.*, 1978; Vogel, 1980). C_4 photosynthesising plants are enriched in ^{13}C compared to C_3 plants and exhibit $\delta^{13}C$ values of between approximately -10‰ and -14‰ (Smith and Epstein, 1971).

C_4 plants are more efficient at limiting water loss and maintaining high rates of photosynthesis than C_3 in very hot and/or arid conditions. C_4 plants adopted an adaptive strategy to lower photorespiration by maintaining high CO_2 concentrations within the leaf. Due to maintaining high CO_2 to O_2 concentrations in the leaf C_4 plants can maintain higher and more efficient rates of photosynthesis. This also means that they can keep their stomata closed for longer periods of time and thus limit water loss due to respiration. C_4 plants thus fix CO_2 more efficiently than C_3 plants, using less time and water. C_4 plants are mainly grasses, certain sedges and shrubs of the lower latitudes. They are mainly found in tropical or arid environments and are virtually

absent in more temperate regions of the world (Smith and Epstein, 1971; Tieszen *et al.*, 1979; Ehleringer *et al.*, 1997).

3.1.2. Fractionation Between Diet and Consumer Tissue

Stable carbon isotope behaviour and patterns in biological systems are relatively well understood. $\delta^{13}C$ ratios are routinely used with a high degree of confidence in dietary studies of modern and fossil animal communities (Ambrose and DeNiro, 1986; Lee-Thorp *et al.*, 1989b; Panarello and Fernandez, 2002; Sponheimer *et al.*, 2003a, 2003b, 2003c). However the use of $^{13}C/^{12}C$ ratios is limited in that they can only be used to distinguish between broad categories of plants at the base of the foodweb, and their relative contributions to diet.

When these plants are consumed by animals, further isotope effects occur in the apportionment of carbon, and in the formation of those tissues. Due to mass balance effects in which waste products (eg. urea and feces) tend to be depleted in ^{13}C, most tissues are more enriched in the heavier isotope relative to the isotopic composition of the diet. The difference varies between tissue types depending on their composition. Although not always well-understood, the diet-to-tissue differences are relatively consistent. Hence the dietary "signal" is maintained in the tissue. This phenomenon has been demonstrated by controlled feeding studies on a variety of animals (Ambrose and Norr, 1993; Tieszen and Fagre, 1993; Ambrose, 2000; Sponheimer *et al.*, 2003c, 2003d) as well as in field ecological studies (Ambrose and DeNiro, 1986; Lee-Thorp *et al.*, 1989b; Panarello and Fernandez, 2002; Sponheimer *et al.*, 2003a, 2003b). Thus it is possible to broadly infer an organism's diet from the carbon isotope composition of its tissues. Animals will preferentially metabolize molecules containing lighter isotopic species as their molecular and chemical bonds require less energy to break than that of heavier isotopes (Kendall and Caldwell, 1998). Different tissues in an organism's body may therefore have different $\delta^{13}C$ values depending on their metabolic pathways. Further fractionation occurs because different tissues are synthesised from different constituents of the diet (Ambrose and Norr, 1993), tissues differ in composition and because different tissues have different turnover rates (Lee-Thorp *et al.*, 1989a; Bell *et al.*, 2001). Proteinaceous tissues derive mainly from the protein component of the diet (Tieszen and Fagre, 1993). Tooth enamel derives from a combination of all the elements of an animal's diet since apatite forms in equilibrium with blood bicarbonate levels (Krueger and Sullivan, 1984; Lee-Thorp *et al.*, 1989a).

Once formed tooth enamel does not remodel. There is an enrichment of approximately 12 - 14‰ $\delta^{13}C$ between diet and tooth enamel bioapatite carbonates (Krueger and Sullivan, 1984; Lee-Thorp *et al.*, 1989a; Balasse, 2002).

This biogenic signal in tooth enamel may be influenced in fossils (compared to modern animals) to a small degree by diagenesis. This possibility can be assessed and controlled for by interpreting $\delta^{13}C$ values of a taxon in relation to the $\delta^{13}C$ values of strict browsing and grazing fauna from the same deposits. Furthermore, as a result of the continuous and large-scale use of fossil fuels since the early twentieth century there has been a global decrease in the $\delta^{13}C$ of atmospheric carbon dioxide of approximately 1.5‰ (Friedli *et al.*, 1986; Marino and McElroy, 1991). This change is transmitted throughout the entire food web. In order to compare $\delta^{13}C$ values from older material against those from modern foodwebs, 1.5‰ should be added to values obtained from material postdating 1950.

Modern grazers in African savannah ecosystems like zebra (*Equus burchelli*) or graminivorous primates like gelada baboons (*Theropithecus gelada*) with a mostly C_4 diet would be expected to have enamel carbonate $\delta^{13}C$ values between 1‰ and -2‰ (Lee-Thorp *et al.*, 1989b; Sponheimer and Lee-Thorp, 2001). African browsers, such as kudu (*Tragelaphus strepsiceros*) or arboreal folivorous primates such as colobus monkeys (*Colobus* sp.) with exclusively C_3 diets would be expected to have enamel carbonate $\delta^{13}C$ values between -13‰ and -17‰ (Carter, 2001; Sponheimer and Lee-Thorp, 2001). Mixed feeders, herbivores that browse and graze to varying degrees can be distinguished by having intermediate $\delta^{13}C$ values falling between the $\delta^{13}C$ values of browsing and grazing end members species. The relative amounts of C_4 to C_3 plants in the diet can be roughly estimated using a mixing chart.

3.2. Stable Oxygen Isotopes

Oxygen has three stable isotopes, ^{16}O, ^{17}O and ^{18}O. ^{18}O is more abundant than ^{17}O and the $^{18}O/^{17}O$ ratio is considered to be constant (Hoefs, 1997). Therefore only the $^{18}O/^{16}O$ ratios are determined in ecological, metabolic and climatic studies. The$^{18}O/^{16}O$ ratio is routinely obtained during stable carbon isotope measurement from enamel carbonates. Because ^{18}O is a slightly larger and heaver isotope than ^{16}O it is sensitive to physical and chemical processes undergone by water (Dansgaard, 1964). Oxygen in animal tissues mainly derives from oxygen bound in water, with a further component from oxygen bound in food (e.g. in carbohydrates). The $\delta^{18}O$ values of

meteoric water have been found to vary with altitude, latitude, temperature and precipitant (Dansgaard, 1964). Stable oxygen isotope composition is expressed as a delta (δ) ^{18}O value in parts per mil (‰), relative to an international standard, Standard Mean Ocean Water (SMOW) or VPDB for carbonates (Craig, 1961):

$$\delta = (R_{sample}/R_{standard}) - 1) \times 1000$$

R is the corresponding $^{18}O/^{16}O$

3.2.1 Stable Oxygen Isotopes in Foodwebs

Animals obtain all their body water from surface water or water in the food they eat. Both enamel phosphate and carbonate stable oxygen isotope composition is a function of the stable oxygen isotope composition water entering the body as drinking water and water bound in food (Longinelli, 1966; Epstein *et al.*, 1977; Longinelli, 1984; Luz *et al.*, 1984; Kohn, 1996). Water from both sources are incorporated into the body water pool, body water thus represents an average of total water intake. Simply put, tissue $\delta^{18}O$ reflects body water $\delta^{18}O$ and therefore reflects the combined $\delta^{18}O$ of all water entering the body as drinking water and food water, set against the water which leaves the body (Luz *et al.*, 1984).

The stable oxygen isotope composition of meteoric water has a predictable relationship to latitude, altitude, temperature and precipitation (Dansgaard, 1964). Thus the analysis of $^{18}O/^{16}O$ ratios in animal tissues across sites/regions can yield information about local climatic and hydrological conditions (Longinelli, 1984).

There are also differences between the stable oxygen isotope composition of meteoric surface water and food water, which become useful in within-site faunal comparisons. Water containing the lighter isotope of water (^{16}O) evaporates preferentially from the leaf surface. Consequently the water retained in the leaf is enriched in ^{18}O (Epstein *et al.*, 1977). Animals that obtain most of their drinking water from the food they eat would tend to be more enriched in ^{18}O than animals that obtain most of their water from meteoric surface water (Gonfiantini, 1965; Kohn, 1996; Sponheimer and Lee-Thorp, 1999; Carter, 2001). The underground storage organs of plants are more depleted than their leaves as these parts of the plant derives its water from ground water, which resembles meteoric surface water in its oxygen isotope composition, and is not affected by evaporative discrimination against H_2O^{18}

(Gonfiantini, 1965; Epstein *et al.*, 1977; Sternberg, 1989). The stable oxygen isotope composition of animal tissues, within similar environments, can reveal behavioural and dietary differences between animals. Besides behavioural and dietary factors, thermophysiological adaptations can also have an effect on stable oxygen isotope composition of animal tissues. H_2O^{16} is preferentially lost during sweating or panting (Kohn, 1996; Kohn *et al.*, 1996), animals that rely heavily on such methods of thermoregulation may also have more enriched $\delta^{18}O$ values.

Various authors (Bocherens *et al.*, 1996; Schoeninger and Valley, 1996; Sponheimer and Lee-Thorp 1999; Lee-Thorp and Sponheimer, 2005) have demonstrated diet-related difference in $\delta^{18}O$ values between browsers and grazers that are ultimately linked to their drinking habits. Most grazers are obligate drinkers while browsers can be non-obligate drinkers. Browsers from South African Plio-Pleistocene fossil sites have more enriched $\delta^{18}O$ values than sympatric grazers, a pattern also found in modern animal communities in East (Kohn, 1996) and southern Africa (Sponheimer and Lee-Thorp, 1999; Lee-Thorp and Sponheimer 2005). Fossil browsers from Swartkrans had mean $\delta^{18}O$ values of 37.7‰ ± 1.7 and grazers had mean $\delta^{18}O$ values of 34‰ ± 1.6 (relative to VPDB) (Sponheimer and Lee-Thorp, 1999).

It is thought that grasses are more parched than the leaves of more deeply rooted plants during dryer parts of the year and that browsers would therefore ingest more water with their food compared to grazers. In addition browsers are able to concentrate their urine as a result of their higher protein diets, and hence are less reliant on drinking water. Hence, grazers obtain more of their metabolic water from ^{18}O depleted meteoric surface water (Sponheimer *et al.*, 1999), while browsers obtain more metabolic water from ^{18}O enriched leaf water (Kohn, 1996; Sponheimer and Lee-Thorp, 1999). Grazers would also be compelled to drink more or more regularly than browsers, grazers would therefore be more depleted in ^{18}O than browsers.

Oxygen isotope ratios have also been used to discriminate between eco-niches of sympatric forest primates (Carter, 2001). For example Carter (2001) found that the bone apatite of high canopy primates (*Procolobus badius* and *Colobus guereza*) in Ugandan forest ecotones had substantially higher $\delta^{18}O$ values (0.80 ± 0.71‰) compared to mid canopy primates (*Cercopithecus ascanius* and *Lophocebus albegina*) (-0.83 ± 0.43 ‰). Both high and mid canopy primates had higher $\delta^{18}O$ values than

more terrestrial low canopy taxa such as olive baboons (*Papio h. anubis*), which had relatively low $\delta^{18}O$ values (-1.82 ± 0.38‰) (Carter, 2001). Interestingly, sympatric terrestrial chimpanzees had intermediate $\delta^{18}O$ values perhaps indicating a substantial reliance on canopy fruits.

However these differences do not necessarily represent universal trends but are often locally defined. $\delta^{18}O$ values must be interpreted within the context of an environmentally circumscribed animal community where the behavioural and dietary characteristics of the various taxa have been moderately well characterised through stable carbon isotope - and faunal analysis. $\delta^{18}O$, if interpreted with in these parameters, can complement and refine the dietary, behavioural and physiological characterisation of the selected taxa (Bocherens *et al.*, 1996; Kohn, 1996; Schoeninger and Valley, 1996; Cerling *et al.*, 1997; Sponheimer and Lee-Thorp, 1999; Carter, 2001).

TRACE-ELEMENTS

3.3. Sr/Ca and Ba/Ca Ratios as Dietary Indicators

Strontium (Sr) and barium (Ba) are alkaline earth elements, which structurally resemble calcium (Ca) and do not have any known physiological function (Schroeder *et al.*, 1972). Sr, Ba an Ca are Group II elements on the periodic table and as such possess similar physico-chemical properties (Nielsen, 1986; Ezzo, 1994; Coursey *et al.*, 2005). Sr and Ba can also substitute for Ca in various metabolic processes in plants and animals (Klepinger, 1984; Ezzo, 1994). The levels of Sr and Ba in plants are generally the same as the substrates they grow in, which is dependant on local geology (Ezzo, 1994; Toots and Voorhies, 1965). The baseline levels of Sr and Ba vary with geology and are decreased in wet well-drained soils as apposed to dry, poorly drained soils (Mitchell, 1955; Sillen and Kavanagh, 1982). The alkaline earth elements can therefore only be used as dietary indicators within a circumscribed geological area. Different types of plants within the same area may have different abundances of Sr and Ba (Sponheimer and Lee-Thorp, 2006) and different plant parts may exhibit different abundances (Menzel and Heald, 1955; Iserman, 1981; Runia 1987). Animals discriminate very strongly against the heavier and larger atoms of Sr and Ba during nutrient absorption and physiological processes. The process by which Ca is preferentially absorbed and the heavier alkaline earth elements are actively

discriminated against is known as biological purification or "biopurification" (Comar *et al.*, 1957).

More than 90% of the body's Sr and Ba are found in the skeleton (Elias et al., 1982; Klepinger, 1984; Ezzo, 1994). Skeletal components are thus ideal for trace-element analysis. However when bone fossilises it undergoes substantial structural and chemical changes. Exogenous carbonates and minerals are incorporated into the bone during the fossilisation process and the biogenic trace-element component of the bone may be significantly altered. Although it may be possible to recover some of the biogenic trace-element composition from fossil bone, using their solubility characteristics, the chemical procedures are tedious (Sillen 1981, 1986; Sealy and Sillen, 1988; Sealy *et al.*, 1991). More recently tooth enamel have been shown to be far more resistant to post-depositional diagenetic alteration than bone (Lee-Thorp *et al.*, 1989b; Lee-Thorp and van der Merwe, 1991; Wang and Cerling, 1994; Sponheimer and Lee-Thorp, 1999; Lee-Thorp and Sponheimer, 2003). Consequently fossil tooth enamel requires far less rigorous pre-treatment. Modern and fossil tooth enamel has been shown to provide reliable biogenic signals of dietary Sr and Ba (Sillen, 1992; Lee-Thorp and Sponheimer, 2003; Sponheimer *et al.*, 2005). Ca is proportionally much more abundant than Sr and Ba, and because Sr and Ba follow the same biochemical pathways as Ca during metabolic processes, the abundance of Sr and Ba in tissues are usually expresses as a ratio to Ca.

3.3.1. Strontium

The most abundant isotope of Sr (82.58%) has an atomic number of 88 ($p^+ = 38$, $n^0 = 50$), atomic mass of 87.62amu and an atomic radius of 2.45Å whereas the most abundant isotope of Ca (96.94%) has an atomic number of 40 ($p^+ = 20$, $n^0 = 20$), atomic mass of 40.078amu and diameter of 2.23Å (Coursey *et al.*, 2005). As Sr is a substantially larger and heavier atom than Ca it is discriminated against during nutrient absorption and the biopurification of Ca at each level of the food chain (Burton *et al.*, 1999). The ratio of Sr to Ca thus decreases from plant to herbivore to faunivore (Elias *et al.*, 1982; Sillen, 1992; Ezzo, 1994; Sillen *et al.*, 1995; Burton *et al.*, 1999). The Sr/Ca ratio in bone has been used with certain limitations as a trophic level indicator within an environment (Sealy and Sillen, 1988; Sillen, 1992; Ezzo, 1994; Sillen *et al.*, 1995; Burton *et al.*, 1999). Furthermore, the incorporation of Sr into bone is negatively correlated to the Ca content of the diet (Lambert and Weydert-

Hofmeyer, 1993). In other words the less Ca is available in the diet the more readily Sr is incorporated during biological apatite synthesis. A decreased availability of Ca is often associated with high dietary fibre as fibre binds with the Ca and decreases its availability (Lambert and Weydert-Hofmeyer, 1993). There is thus a positive correlation between bone Sr content and the fibre content of the diet.

It has also been shown that different plant parts contain different amounts of Sr (Menzel and Heald, 1955; Iserman, 1981; Runia 1987). In plants the larger, heavier Sr atoms are discriminated against during capillary transport of minerals in solution to different parts of the plant (Burton *et al.*, 1999; Sillen *et al.*, 1995). Roots and stems tend to have relatively higher concentrations of Sr; with nutrient transport in the xylem sap to the leaves and fruits the concentration of Sr decreases. Leaves thus have lower Sr/Ca ratios than roots and stems (Burton *et al.*, 1999) and fruits may have lower Sr/Ca ratios than leaves. Furthermore, grasses in African ecosystems have been found to have higher concentrations of Sr than leaves of dicotyledonous plants (Sponheimer and Lee-Thorp, 2006). Thus Sr/Ca ratios can be used to discriminate between grass, leaf/fruit and underground plant organs (Runia, 1987; Sillen *et al.*, 1995; Burton *et al.*, 1999; Sponheimer *et al.*, 2005). Since the Sr/Ca ratio of an animal's tissue is directly derived from its diet it should be possible to discriminate between the importance of different plant parts and/or different plants in an animal's diet (Sillen, 1988, 1992; Sponheimer and Lee-Thorp, 2006).

3.3.2. Barium

The most abundant isotope of Ba (79.7%) has an even larger and heavier atom than Sr, with an atomic number of 138 ($p^+ = 56$, $n^0 = 82$), atomic mass of 137.327amu and atomic diameter of 2.78Å (Coursey *et al.*, 2005). Ba atoms are larger and more than three times as heavy as Ca atoms. Subsequently it is even more strongly discriminated against during the biopurification of Ca (Burton *et al.*, 1999). Thus similarly to Sr/Ca, the Ba/Ca ratio shows a strong trophic level reduction (Klepinger, 1984; Burton *et al.*, 1999). Sponheimer *et al.* (2005) have shown, by proxy, that grasses have substantially higher Ba/Ca ratios than roots and tubers, both of which show high Sr/Ca ratios. A combination of Sr/Ca and Ba/Ca ratios can thus be useful in discriminating between plants and plant parts that are not distinct in their Sr/Ca or carbon isotope ratios. For example a high Ba/Ca ratio would be consistent with a mainly C_4 diet which can be corroborated by stable carbon isotope analysis. An enriched $\delta^{13}C$ values and high

Sr/Ca ratios together with a low Ba/Ca would suggest a C_4 diet with a substantial component of roots/corms or rhizomes. Ba/Ca and Sr/Ba ratios has the potential to bring greater resolution to dietary analysis as it can be used to discriminate between dietary constituents to which Sr/Ca and $\delta^{13}C$ analysis are insensitive. As for Sr/Ca ratios, the use of Ba/Ca and Sr/Ba ratios as dietary indicators must be employed cautiously and where possible in conjunction with other dietary indicators. Sr/Ca and Ba/Ca have also been found to have a high natural variability within a taxon or area (Sillen, 1988; Sponheimer and Lee-Thorp, in press). Sufficient sample sizes are therefore important to accurately characterise a taxon in term of Sr/Ca and Ba/Ca. The nature of fossil samples and the available fossils meeting the sample criteria limits the sample sizes in this investigation. Variability in such small samples as well as individual specimens should thus not be over interpreted.

Sr/Ba ratios have also been used as an expression of the relative amounts of Sr and Ba in an animal tissue (Burton and Price, 1990, 1991; Gilbert *et al.*, 1994; Sponheimer and Lee-Thorp, in press). By expressing the relative abundances of Sr and Ba as a Sr/Ba ratio, it has been found that clearer distinctions can be made between certain dietary categories than by using Sr/Ca and Ba/Ca ratios (Burton and Price 1990, 1991; Gilbert *et al.*, 1994, Sponheimer and Lee-Thorp, in press). For instance, browsers and grazers from Kruger National Park have very different Sr/Ca and Ba/Ca ratios and have similar Sr/Ba ratios, while carnivores are clearly distinguished from these taxa in their much higher Sr/Ba ratios (Sponheimer and Lee-Thorp, in press).

3.4. Fossil Tooth Enamel as an Archive of Biogeochemical Information

Tooth enamel is nearly entirely anorganic and consists of bio-apatite similar to hydroxyl apatite ($Ca_{10}[PO_4]_6[OH]_2$). Carbonate will usually substitute at phosphate sites as a structural carbonate and/or less often substitutes at hydroxyl sites (Rey *et al.*, 1991). Sr or Ba may substitute at Ca sites in the lattice during synthesis. Tooth enamel bio-apatite thus contains biogenic carbon, oxygen, Sr and Ba. Stable oxygen and carbon isotope ratios can thus be measured from the enamel carbonate. The isotopic composition and trace element abundances of the tooth enamel apatite have been shown to reflect the isotopic composition (Ambrose and Norr, 1993; Tieszen and Fagre, 1993) and trace element abundances of the entire, integrated diet. This relationship has been verified and refined for stable isotopes through controlled

feeding studies and the routine isotopic analysis of modern and fossil tooth enamel in ecological and dietary studies (Ambrose and Norr, 1993; Tieszen and Fagre, 1993; Bocherens *et al.*, 1996; Cerling *et al.*, 1997; Sponheimer and Lee-Thorp, 1999; Sponheimer and Lee-Thorp, 2001; Balasse, 2002; Lee-Thorp and Sponheimer, 2003b).

However the various constituent elements and chemical groups in fossil apatite may be replaced or contaminated by diagenetic carbonates, Sr and Ba during burial and fossilisation (Sillen, 1986; Lee-Thorp and van der Merwe, 1987; Wang and Cerling, 1994; Kohn *et al.*, 1999, Lee-Thorp and Sponheimer, 2003). This may offset or obscure the biogenic signal in the enamel. The degradation and diagenetic alteration of calcified tissues are exacerbated by combination of heat, moisture and bacterial interference (Lee-Thorp and Sponheimer, 2003). During the burial and fossilisation exposure to heat, moisture and bacterial activity provide opportunities for indigenous ions in the calcified tissues to be replaced by exogenous ions from the surrounding matrix during processes of dissolution, recrystallisation and crystal growth (Lee-Thorp, 2002; Lee-Thorp and Sponheimer, 2003). Foreign apatitic and non-apatitic minerals, such as pyrites and silicates, may also be deposited in spaces left in the calcified tissue by decomposed and leached organic material (Hassan *et al.*, 1977).

The extent of diagenesis depends on the depositional environment and the nature of the calcified tissues. Calcified tissues such as bone and tooth dentine apatite are more porous, less crystalline and contain a relatively high proportion of organic material. Such tissues are more likely to undergo more substantial diagenesis (Koch *et al.*, 1997). Dense, non-porous and highly crystalline tissues such as tooth enamel apatite are more resistant to diagenesis and likely to yield a more reliable biogenic signal (Luz and Kolodny, 1985; Lee-Thorp and van der Merwe, 1987; Lee-Thorp *et al.*, 1989b; Sponheimer and Lee-Thorp, 1999; Lee-Thorp *et al.*, 2003). Processes of dissolution, recrystallisation and crystal growth would occur less readily in enamel apatite, reducing opportunities for diagenetic contamination during burial processes (Lee-Thorp, 2002). Tooth enamel does undergo some post-mortem diagenesis, but the biogenic signal remains largely intact. The effects of diagenetic carbonates can be mediated through careful acid pre-treatment of samples, however not all diagenetic carbonates can be removed in this way. Carbon and oxygen isotope ratios may still be offset against values obtained for modern animals with similar diets (Lee-Thorp *et al.*, 1989b). Nonetheless, at South African karstic cave sites large differences remain

between the stable carbon isotope ratios of grazers and browsers. Other taxa can be safely compared with each other within this framework of end values for entirely C_3 and C_4 diets (Lee-Thorp *et al.*, 1989b). Similarly, stable oxygen isotope ratios obtained from the enamel carbonate of various Plio-Pleistocene taxa from South African karstic cave sites produce similar patterns to their ecological equivalents in modern systems. The $\delta^{18}O$ values obtained from fossil enamel carbonate, from at least some sites, are therefore believed to be largely intact biogenic signals.

$\delta^{13}C$ and $\delta^{18}O$ values are obtained from fossil enamel carbonates in palaeodietary studies of fossil animal communities (Lee-Thorp *et al.*, 1989b; Sponheimer *et al.*, 1999; Lee-Thorp *et al.*, 2000; Sponheimer *et al.*, 2001; Lee-Thorp and Sponheimer, 2003; Lee-Thorp *et al.*, 2003; Luyt and Lee-Thorp, 2003; Sponheimer and Lee-Thorp, 2003; Sponheimer *et al.*, 2005). Furthermore, enamel bio-apatite from Makapansgat, where all samples for this study originate, has not been significantly affected by diagenetic processes and all analyses to date have produced reliable biogenic $\delta^{13}C$ and $\delta^{18}O$ signals (Sponheimer *et al.*, 1999; Sponheimer *et al.*, 2001; Lee-Thorp and Sponheimer, 2003). It is thus likely that biogenic isotope and trace-element signals in fossil tooth enamel bio-apatite can be successfully used to investigate subtle dietary differences between related taxa.

3.5. Dietary Reconstruction

By combining Sr/Ca, Ba/Ca and $\delta^{13}C$ and $\delta^{18}O$ data these dietary indicators can be a powerful tool for investigating subtle dietary differences. Similar approaches have shown some positive results in studies of the dietary ecology of extant primate and faunal communities. Using stable isotopes of carbon, oxygen and nitrogen Carter (2001) was able to distinguish between vertical econiches among African forest primates. The diets and habitat use of various new world monkeys have similarly been investigated by using carbon and nitrogen isotopes (Schoeninger *et al.*, 1997). The combination trace-elements and stable isotope have not previously been applied to extant fossil primate dietary ecology, although promising results have been reported in studies of other mammalian taxa. Sillen (1988), using stable carbon and oxygen isotope data as well as Sr/Ca ratios, was able to identify specific dietary components and behaviours in various taxa, as well as lactation and pregnancy. More recently the combination of carbon isotope data and Sr/Ca, Ba/Ca and Sr/Ba ratios have been used to investigate South African *Australopithecus africanus* diets (Sponheimer and Lee-

Thorp, in press). This included a survey of these indicators in extant as well as fossil faunal communities and has complemented and expanded the existing understanding of patterns of trace-element abundances in extant and extinct foodwebs.

Through such studies certain combinations of dietary indicators have been identified with specific dietary and behavioural components. For example; high Sr/Ca and Ba/Ca ratios combined with enriched $\delta^{13}C$ values would indicate a C_4 grass diet. But high Sr/Ca and low Ba/Ca ratios together with depleted $\delta^{13}C$ values would suggest a C_3 diet with a heavy reliance on high Sr/Ca, low Ba/Ca C_3 plants and plant parts such as roots and tubers. High Sr/Ca and low Ba/Ca ratios with enriched $\delta^{13}C$ values would be consistent with a diet rich in C_4 rootstocks. $\delta^{18}O$ values will add further ecological and behavioural information. It should be possible to characterise the relative reliance of the selected fossil cercopithecoid taxa on specific foods and hopefully be able to distinguish ecologically between different taxa in this way.

CHAPTER 4

MATERIALS AND METHODS

This chapter describes briefly the stratigraphy and palaeoecology of Makapansgat Limeworks Site from which the samples in this study were obtained. I proceed to describe in detail the sampling strategy and procedures, and analytical methods. They include experiments to refine the laboratory preparation protocol for the stable isotope ratio analysis of fossil tooth enamel, in order to minimise damage.

4.1. Makapansgat Limeworks

The Makapansgat Limeworks (24.54° S; 29.25° E) is situated in the Makapan Valley, approximately 225 km north of Johannesburg and close to the town of Mokopane (formally known as Potgietersrust) in the Limpopo Province of South Africa. The area's geology is dominated by the Transvaal Supergroup. Solution cavities occur in dolomites of the Malmani Subgroup which overlays the Black Reef Quartzite formation (McFadden *et al.*, 1979). Makapansgat Limeworks Cave site is one of a number of fossiliferous infillings in the valley and consists of a number of chambers made up of solution cavities. In the early 20th century the deposits were extensively mined for the lime-rich travertine. These mining activities brought to light the fossiliferous deposits and stimulated academic interest in the sites. In 1925b Raymond Dart first described Makapansgat Limeworks as a site showing evidence of early human (hominid) occupation. Later in 1947, James Kitching recovered a portion of an *Australopithecus africanus* brain case from an old mine dump (Maguire, 1998). This led to the hand sorting of the mining rubble and systematic excavations at the site, which continues up to the present.

4.1.1. Stratigraphy

The site represents one of the oldest hominid bearing deposits in South Africa. Five members have been identified; the oldest (Member 1) is thought to be between 4.2 to 3.6 Ma (Partridge *et al.*, 2000) and the youngest (Member 5) about 1.6 - 1.8Ma (Vrba, 1995). Member 3 and 4 consist of a fossil-rich grey breccia and a less fossiliferous pink breccia respectively; the pink breccia (member 4) being especially rich in primate material (Maier, 1972; Maguire, 1998; Partridge, 2000). Biostratigraphy

tentatively places Member 3 to between 2.9 Ma and 2.7 Ma and Member 4 to between 2.5 Ma and 2.7 Ma (Delson, 1984; Vrba, 1995). Magnetostratigraphic methods of dating have provided slightly older dates for Members 3 and 4 of approximately 3.33Ma to 3.11Ma and 3.11Ma to 2.58Ma respectively (Partridge *et al.*, 2000). Palaeomagnetic dates for the Makapansgat members have been considered to be somewhat contentious as the cave stratigraphy of Makapansgat Limeworks is extremely complex and not yet fully understood. Magnetostratigraphic methods used so far assume that different members or parts of members were accumulated and deposited in succession but Maguire (1985) argues that parts of what are considered different members may have accumulated contemporaneously. Based on such an understanding of the depositional history of the cave deposits as well as palaeoenvironmental and faunal evidence she argued that Members 3 and 4 may represent a single member or are at least not significantly distinct as depositional and environmental events (Maguire 1985, 1998). For the purposed of this investigation, Members 3 and 4 will be treated as broadly contemporaneous representing more or less similar environmental conditions.

4.1.2. Palaeoecology

Studies of the palaeoenvironments of the Makapan Valley suggest that a mosaic of habitats existed during Member 3 and 4 times. Various approaches and combinations of approaches to palaeonenvironmental reconstruction (e.g. ecomorpholical, faunal composition and stable isotope) have characterised Makapansgat Member 3 vegetation structure as consisting of bushland and riparian woodland with nearby wetlands (Reed, 1998; Sponheimer *et al.*, 1999; Sponheimer *et al.*, 2001a; De Gusta and Vrba, 2003; Sponheimer and Lee-Thorp, 2003b). This in combination with evidence from microfaunal (Pocock, 1987) analyses and palynological (Zavada and Cadman, 1993) studies suggests that substantial wooded environments existed at Makapansgat during Member 3 times and that patches of grassland existed in the vicinity of the site (Sponheimer *et al.*, 1999; Sponheimer *et al.*, 2001a; Sponheimer and Lee-Thorp, 2003).

Member 4 is thought to have supported similar habitats although it may have been more wooded as suggested by the high frequency of primates in the Member 4 deposits (Reed, 1997; Reed, 1998). However Reed also points out that differences in faunal composition might equally be the result of different taphonomic histories rather

than differing environments (Reed, 1997; Reed, 1998). Member 3 faunal material was accumulated primarily by hyenas (Maguire, 1980) and Member 4 by leopards and birds of prey (Maguire, 1980; Reed, 1996) thus skewing the representation of certain taxa. Both Member 3 and 4 palaeoenvironments appear to have been mainly closed environments dominated by bushland, with riparian woodlands and nearby limited wetlands and substantial patches of grassland (Reed, 1997; Reed, 1998; Sponheimer *et al.*, 1999; Sponheimer *et al.*, 2001a; Sponheimer and Lee-Thorp, 2003). Members 3 and 4 are thus treated as representing a single environmental regime for the purposes of this investigation.

4.2. Sampling Strategy

All fossil primate specimens used in this study were recovered from Makapansgat Limeworks Members 3 and 4. These deposits yielded a substantial number of *Parapapio* specimens assigned to three species (*Pp. whitei*, *Pp. broomi* and *Pp. jonesi*), as well as *Theropithecus darti* and *Cercopithecoides williamsi* specimens. These specimens were recovered from mining rubble, sorted based on the colour and sedimentary composition of the breccia matrix, and therefore attributed with reasonable confidence to specific members of the *in situ* depositional sequence (Maguire, 1998; Partridge, 2000).

There are several advantages to working with material from a single site even though this may imply smaller sample sizes, as problems with comparing different periods and places can be avoided. Different localities may have supported different macro-habitats and/or micro-habitats, which could have responded differently to climatic changes associated with different periods. Such factors may complicate isotopic and trace-element dietary analysis.

As discussed in Chapter 2, section 2.2., the identification and classification of the fossil *Parapapio* based on isolated teeth is problematic. In order to avoid this problem as far as possible, tooth enamel was sampled only from complete or partially complete cranial specimens from which craniometric data could *also* be obtained. This approach allowed for independent assessment of morphometric variation and co-variation with taxonomic groupings (as assigned), and the genus as a whole against an extant chacma baboon (*Papio hamadryas ursinus*) model. It would also assist in placing those *Parapapio* specimens which have not been assigned to one of the three *Parapapio* species. Different dietary ecologies, as inferred from dietary indicators,

can then be correlated or taxonomic or morphotypic groupings confirmed or revealed by craniometric analysis. Only adult individuals with erupted third molars were sampled. The tooth enamel of the third molar is laid down in the post-juvenile phase of development (Reid *et al.*, 1998) and therefore would reflect biogeochemical signals laid down under normal or near normal adult physiological and dietary conditions.

T. darti and *C. williamsi* were also sampled in order to test dietary predictions based on dental morphology and dental wear. *T. darti* is considered distinct from *T. oswaldi* in being slightly smaller, although there is some doubt as to the biological validity of these two species (Delson, 1992) *T. darti* is thought, based on differences in dental morphology and dental wear, to have included more fruit in its diet (Benefit and McCrossin, 1990) than did *T. oswaldi* and modern *T. gelada*, both of which rely/relied heavily on grasses (Lee-Thorp *et al.*, 1989; Lee-Thorp and van der Merwe, 1993; Codron *et al.*, 2005). It will be tested through stable isotope analysis of the enamel carbonate of *T. darti* whether it included more C_3 foods in its diet compared to *T. oswaldi*.

C. williamsi belongs to the subfamily Colobinae, of which all extant members are strict arboreal folivores. Analysis of *C. williamsi* post-cranial elements (Birchette, 1981; Leakey, 1982) and dental wear (Delson, 1992) suggests that this fossil colobine was at least partially, if not largely, terrestrial. Stable isotope analyses of *C. williamsi* specimens from Sterkfontein and Swartkrans have revealed the presence of two distinct dietary ecologies within this taxon; one is consistent with a mostly C_4 diet and the other a more heavily C_3 diet (Luyt, 2001; Codron, 2003; Codron *et al.*, 2005). It will be tested whether *C. williamsi* from Makapansgat also exhibits such disparate dietary behaviours. *T. darti* and *C. williamsi* will also conveniently serve as morphological outgroups for craniometric analysis. Nineteen specimens were sampled for this study, sixteen of which belong to the genus *Parapapio*, two *C. williamsi* and one *T. darti*. Specimens are listed in Table 4.1 below; more extensive specimen information is supplied in Appendix A-2.

Table 4.1. List of specimens sampled for stable isotope and trace-element analysis.

MP Accession no.	M Accession no.	Taxon	Sex
MP36	M236	*Cercopithecoides williamsi*	
MP3A	M203	*C. williamsi*	M
MP239		*Parapapio* sp.	F
	M3133	*Parapapio* sp.	
	M3147	*Parapapio* sp.	
	M3079	*Parapapio* sp.	F
	M3084	*Parapapio* sp.	
MP208		*Parapapio* sp.	
MP151	M3037	*Pp. broomi*	
MP2	M202	*Pp. broomi*	M
MP170	M3056	*Pp. broomi*	F
MP75	M2961	*Pp. jonesi*	M
MP173	M3051	*Pp. jonesi*	M
	M3070	*Pp. whitei*	F
MP76	M2062	*Pp. whitei*	M
MP119	M3005	*Pp. whitei*	F
MP164	M3050	*Pp. whitei*	
MP223		*Pp. whitei*	M
MP222		*Theropithecus darti*	F

4.3. Fossil Tooth Enamel Sampling

Tooth enamel for stable isotope and trace element analyses are sampled at the same time and undergo the same pre-treatment. About 2mg of tooth enamel powder is needed for isotope analysis and 2mg for trace element analysis, allowance should also be made for material lost during pre-treatment. In total 5 to 7 mg of tooth enamel was required from each specimen sampled. This raised concerns that the destructive sampling may result in the loss of the original dimensions of the sampled teeth. Therefore the effects of different sampling techniques were tested on modern baboon teeth using a diamond-tipped microdrill. Various dimensions of the teeth were measured before and after sampling using digital callipers. It was found that abrasion of the buccal/lingual surfaces of the tooth did not produce measurable changes in the dimensions of the tooth. Permission was subsequently granted to sample 19

specimens. Only third molars were sampled. All of the sampled specimens had broken or damaged third molars. Where possible teeth were sampled preferentially along these broken enamel surfaces of the tooth, in order to minimise sampling damage to the outer surfaces. Only buccal/lingual and mesial/distal surfaces were sampled thus avoiding damage to occlusal surfaces.

4.4. Pre-Treatment

4.4.1. Pre-Treatment Protocol

Although enamel is relatively impervious to diagenesis, nevertheless some contamination by exogenous carbonates may have occurred in fossil enamel, which could alter the biogenic isotopic and trace-element composition. Organic contaminants, such as humic acids, were removed by sodium hypochlorite treatment. Simple diagenetic carbonate and soluble apatite carbonates and organic contaminants can be partially removed by an acid pre-treatment procedure (Lee-Thorp *et al.*, 1989b; Koch *et al.*, 1997; Sponheimer 1999). This has become a standard procedure for isotopic analysis of fossil enamel carbonate. Material from Makapansgat has been subjected to intensive studies about their preservation status, the efficacy of pre-treatment and the effects of these on biogenic isotopic signals retained in the fossils (Sponheimer and Lee-Thorp, 1999; Lee-Thorp and Sponheimer, 2003). These studies have shown that fossil enamel from Makapansgat is relatively well preserved and has retained its biogenic isotope signals with a high degree of integrity (Sponheimer and Lee-Thorp, 1999; Lee-Thorp and Sponheimer, 2003). The enamel samples used in this study are believed to have retained reliable biogenic isotope signals. With appropriate pre-treatment of the enamel, stable isotope analysis will produce reliable results reflecting real biogenic signals minimally offset by diagenetic effects.

Due to the fragile nature the teeth and the small enamel surfaces exposed for sampling, relatively small samples of powder tooth enamel were collected. A proportion of a sample is inevitably lost during the pre-treatment procedure to chemical and mechanical processes. At least 3mg of sample is needed after pre-treatment in order to perform both stable isotope analysis and trace-element analysis. In order to check what proportion of a sample was likely to be lost during pre-treatment and how such losses could be minimised; a number of variants of the standard pre-treatment protocol were performed on tooth enamel from a large

Chalicothere (*Ancylotherium hennigi* - M156) tooth from Makapansgat Limeworks member 3. This specimen would have experienced similar depositional fossilisation processes as the fossil cercopithecoid specimens from Makapansgat.

The following protocol is used in the pre-treatment of fossil enamel in our laboratory. The enamel powder is agitated with 1ml of 1.75% solution of bleach (NaOCl – sodium hypochlorite) in a micro-centrifuge tube, and left for 45 min. The NaOCl removes all organic contaminants from the sample. The sample is then centrifuged for 30 seconds and rinsed 3 times with distilled water, mixing and centrifuging the sample between every rinse. The sample is then mixed with 1ml of a 0.1M solution of acetic acid (CH_3OOH) and left to react for 15 minutes. This step dissolves the diagenetic carbonates which dissolve more readily than bound structural carbonates in the enamel powder. The sample is then rinsed and centrifuged 3 times as before. The centrifuge tube is covered with parafilm and left to dry overnight in a freeze dryer. An extra step was added to the protocol by treating the sample with acetone (C_3H_6O) for 30min to eliminate organic adhesives or varnishes often used to treat fossils. In order to minimise losses during pre-treatment procedures, different reaction times for the different steps in the protocol were used. Since the samples were somewhat smaller than those that would usually be treated with this protocol, it was reasoned that reactions with contaminating components in the enamel would be completed in less time than for larger samples and that if the smaller sample was left to react for the normal length of time some of the biogenic carbonate would also be lost. Decreasing reaction times would limit such a loss of biogenic material, but if the reaction times were not long enough diagenetic contaminants would not be effectively removed and the resulting isotopic signal would be offset. A series of protocols using different combinations of reaction times were thus used and samples were analysed to check whether exogenous carbonate components had been effectively removed.

4.4.2. Experimental Variants of Pre-Treatment Protocol

Five different pre-treatment procedures were used which differed only in the length of time that the enamel powder was exposed to 0.1M acetic acid and NaOCl solutions. Each pre-treatment procedure was replicated three times using 5mg samples of enamel powder in 1.5ml centrifuge tubes with sharply tapering ends. Thin tapered 2ml pipette tips were used to pipette reagents in and out of the tubes. These measures help to minimise mechanical losses of material. Three blanks were also prepared for each

pre-treatment procedure. The centrifuge tubes were weighed and 5mg of enamel powder deposited in each. Tubes were weighed before and after pre-treatment, to enable calculation of the amount of powder lost during pre-treatment.

Five sets consisting of three samples and three blanks were thus treated using the following 5 pre-treatment procedures. The stable carbon and oxygen isotope ratios of all three samples from each pre-treatment procedure was determined to check whether differing reaction times and additional treatments affected the isotopic signal of the enamel thus monitoring the efficacy of the pre-treatment procedure in removing exogenous carbonates from the fossil enamel. The five variations of the pre-treatment procedure for enamel carbonate are listed in Table 4.2 below.

Table 4.2. Reactions times for different steps of pre-treatment procedure for enamel carbonate.

	Acetone (C_3H_6O)	1.75% NaOCl	0.1M CH_3OOH
Pre-treatement	Reaction Time (min)	Reaction Time (min)	Reaction Time (min)
I		45	15
II		15	10
III		15	5
IV		15	rinse
V	30	15	rinse
Untreated		15 (distilled water)	rinsed (distilled water)

4.4.3. Results

Pre-treatments I - III resulted in the lowest percentage loss of enamel powder per sample (n = 9, 38.5 ± 1.6%). Pre-treatments IV and V, where the enamel powder was only rinsed in the 0.1M acetic acid solution, resulted in slightly higher percentage loss of enamel powder per sample (n = 6, 42.3 ± 2.6%). The addition of the acetone treatment seems to have no effect on the amount of material lost during pre-treatment to either mechanical or chemical processes. Differences in the amount of material lost during the different pre-treatment variants were not statistically significant (Kruskal-Wallis ANOVA, $p > 0.05$). Table 4.3 lists the percentage loss for each pre-treatment. The blank shows that 13.8 ± 2.4% (n = 3) of a sample is lost to mechanical processes.

Table 4.3. $\delta^{13}C$ and $\delta^{18}O$ values and percentage loss of enamel sample for samples of *Chalicothere* tooth enamel using different variations of the pre-treatment protocol.

Pre-Treatment	n	$\delta^{13}C$ (‰)	STD (‰)	$\delta^{18}O$ (‰)	STD (‰)	Mean % Sample Lost	STD
I	3	-10.6	0.2	1	0.2	38.3	1.8
II	3	-10.7	0.1	0.9	0.3	39.1	4.4
III	3	-10.7	0.1	1	0.02	38.1	1.5
IV	3	-10.6	0.1	0.9	0.3	42.3	2.1
V	2	-10.2	0.6	1.3	0.1	42.3	2.8
Untreated	3	-4.7	0.07	0.9	0.2	13.8	2.4

28.5 ± 0% (n = 6) of a sample was lost to chemical processes when pre-treatment IV-V was used. 24.3 ± 0.5% (n = 9) of the sample was lost to chemical processes when pre-treatments I - III were used. Although this difference is not statistically significant (Mann-Whitney U, $p > 0.05$), this may suggest that during procedures (I – III) with longer acid reaction times (5 – 15min) some of the dissolved carbonate is recrystallising when using small powdered samples. The exogenous carbonates react and dissolve almost instantly when the acid is added as is evidenced when samples were only rinsed with acid as in pre-treatment IV and V. During these two pre-treatment protocols the acid and the dissolved carbonates were removed before recrystallisation of these carbonates could take place. However, different pre-treatment procedures appear to have no significant effect on the $\delta^{13}C$ (-10.6‰ ± 0.2‰, n = 15) and $\delta^{18}O$ (+1‰ ± 0.1‰, n = 15) values obtained for the enamel. They seem to be equally effective for removal of exogenous carbonates. The stable isotope results are presented in Table 4.3. The individual results for each sample, standards and calibration curves are presented in Appendix B-1.

The results for the untreated sample very clearly show the presence of diagenetic carbonate in the enamel. Untreated samples yielded much more positive $\delta^{13}C$ values, about 6‰ more enriched than treated samples. These positive $\delta^{13}C$ values for the untreated sample also approach the $\delta^{13}C$ values for the matrix in which the fossils are encased. In most cases enough sample was left after pre-treatment to conduct both stable isotope and trace-element analysis. Although the effects of the recrystallised exogenous carbonates seem to have a negligible effect on the biogenic isotope signals of the samples it was felt that a conservative approach should be taken to pre-

treatment. Pre-treatment V yielded a somewhat higher $\delta^{13}C$ standard deviation, this is probably due to some of the reactants used in pre-treatment, specifically acetone, not having being thoroughly removed during the final rinsing step of one of the three samples. The five pre-treatment variants seem to work equally well in removing diagenic contanimants. It was decided to use pre-treatment V for the fossil cercopithecoid enamel samples since even though a greater weight percentage of the sample is lost, it is less likely that recrystallisation of carbonates would occur during this pre-treatment variant, while anthropogenic contaminants, such as glues and resins are also removed.

4.5. Stable Isotope Mass Spectrometry

Pre-treated fossil enamel powder was weighed out (2 mg) and reacted with phosphoric acid (H_3PO_4) at 70°C, and the resultant CO_2 was cryogenically distilled, in a Kiel II autocarbonate device. The dry CO_2 was introduced into a Finnigan Matt 252 mass spectrometer (Finnigan, Bremen) for measurement of the isotopic ratios of carbon and oxygen. As per convention, $^{13}C/^{12}C$ and $^{18}O/^{16}O$ ratios are expressed as delta values (δ) in parts per thousand (‰), relative to the VPDB standard as follows:

$$\delta X = (R_{sample}/R_{standard}) - 1) \times 1000$$

where X is ^{13}C or ^{18}O and R is the corresponding $^{13}C/^{12}C$ or $^{18}O/^{16}O$ ratio. Sample results were calibrated using an international carbonatite standard (NBS18), one inter-laboratory standard (Cararra Z) and one internal marble standard (Cavendish Marble) of known isotopic composition. Replicates of these standards were used to determine analytical precision and to derive calibration equations. Analytical precision was 0.1‰ for $^{13}C/^{12}C$ and 0.2‰ for $^{18}O/^{16}O$. All $^{13}C/^{12}C$ or $^{18}O/^{16}O$ ratios were calibrated using a linear ($y = mx + c$) regression equation derived from comparison of observed values versus known values for the standards. Appendix C-1 provides details of standards and the derived calibration equations.

4.6. Trace-Element Analysis by ICP-MS (Inductively Coupled Plasma Mass Spectrometry)

The remaining sample, usually between 1 and 2 mg of pre-treated material, was prepared for trace-element analysis on a Perkin-Elmer ELAN 6000 inductively coupled plasma mass spectrometer (ICP-MS). Samples were weighed into teflon beakers and dissolved in 1ml of $HF:HNO_3$ (3:1). The beakers were closed and left on a hotplate for 48 hours. The beakers were then opened, the contents evaporated until incipient dryness. The sample residues were then twice dissolved in 2ml of HNO_3 and evaporated to dryness. The dried sample was then dissolved in a 5% HNO_3 solution containing 10ppb Re, Rh, In and Bi as internal standards. The samples were then analysed on the ICP-MS for Mn, Zn, Sr, Ba and Ca content. Trace-element amounts are expressed in parts per million (ppm). Results were standardized against artificial multi-element standards. Replicate analysis of the international rock standard BHVO-1 gave a procedural error of better than 3%.

4.7. Craniometrics

4.7.1. Materials

All specimens sampled for isotope and trace-element analyses, as well as other suitable specimens from Makapansgat curated at the Department of Anatomy at the University of the Witwatersrand, were used in the craniometric analyses. Dental measurements for each specimen were also taken (*Parapapio*, n = 19; *Cercopithecoides*, n = 1; *Theropithecus*, n = 2). Only adult specimens were used for craniometric analysis. Suitable specimens included cranial specimens which were relatively complete and exhibited limited plastic distortion. A sample of 30 chacma baboon crania from the Iziko Natural History museum in Cape Town was digitized and measured for comparative purposes. Table 4.4 lists all fossil specimens which were digitised for craniometric analysis; the list of modern baboon crania used for comparative purposes appears in Appendix A-2.

Table 4.4. List of fossil cercopithecoid specimens digitised for craniometric analysis.

MP Accession no.	M Accession no.	Taxon	Sex
MP3A	M203	*Cercopithecoides williamsi*	M

MP239		*Parapapio* sp.	F
	M3133	*Parapapio* sp.	
	M3147	*Parapapio* sp.	
	M3079	*Parapapio* sp.	F
	M3084	*Parapapio* sp.	
	M3078	*Parapapio* sp.	
MP167	M3053	*Parapapio* sp.	
MP47/MP92/MP5	M624	*Parapapio* sp.	
MP208		*Parapapio* sp.	
MP2	M202	*Pp. broomi*	M
MP170	M3056	*Pp. broomi*	F
	M3065	*Pp. broomi*	M
MP75	M2961	*Pp. jonesi*	M
	M3070	*Pp. whitei*	F
MP76	M2062	*Pp. whitei*	M
MP119	M3005	*Pp. whitei*	F
MP164	M3050	*Pp. whitei*	
MP223		*Pp. whitei*	M
MP221		*Pp. whitei*	M
MP222		*Theropithecus darti*	F
	M3073	*T. darti*	

4.7.2. Coordinate Landmark Data and Inter-Landmark Distances

Thirty-six craniometric landmarks (after Singleton, 2002), along with three standard dental measurements, were collected from both samples. Table 4.5 below lists the landmarks and dental measurements used in this study, and their abbreviations.

Table 4.5. Landmark data collected, and their abbreviations.

Landmarks	Abbreviation
Facio-Cranium	
Midsagittal	
Prosthion	**PR**
Nasospinale	**NS**
Rhinion	**RH**
Nasion	**NA**
Glabella	**GL**
Bilateral Right	
Premax/max (R)	**PM** (R)
Superior premaxilary suture (R)	**SPS** (R)

Zygomaxillary inferior (R)	**ZI** (R)
Zygomaxillary superior (R)	**ZS** (R)
Fronto malare orbitale (R)	**FMO** (R)
Orbital notch (R)	**ON** (R)
Fronto malare temporale (R)	**FMT** (R)
Bilateral Left	
Premax/max (L)	**PM** (L)
Superior premaxillary suture (L)	**SPS** (L)
Zygomaxillary inferior (L)	**ZI** (L)
Zygomaxillary superior (L)	**ZS** (L)
Fronto malare orbitale (L)	**FMO** (L)
Orbital notch (L)	**ON** (L)
Fronto malare temporale (L)	**FMT** (L)
Neuro-Cranium	
Midsagittal	
Bregma	**BR**
Bilateral Right	
Temporal/frontal/parietal suture (R)	**TP** (R)
Porion (R)	**P** (R)
Bilateral Left	
Temporal/frontal/parietal suture (L)	**TP** (L)
Porion (L)	**P** (L)
Basi-Cranium	
Midsagittal	
Basion	**BA**
Ophistion	**OPI**
Inion	**I**
Bilateral Right	
M1 lingual (R)	**M1L** (R)
Distal M3 (R)	**DM3** (R)
Jugular (R)	**JP** (R)
Occipital/temporal (R)	**OT** (R)
Bilateral Left	
M1 lingual (L)	**M1L** (L)
Distal M3 (L)	**DM3** (L)
Jugular (L)	**JP** (L)
Occipital/temporal (L)	**OT** (L)
Dental Measurements	
Bucco-lingual (Anterior)	**BL** (A)
Bucco-lingual (Posterior)	**BL** (B)
Mesio-distal	**MD**

Three-dimensional craniometric landmark coordinate data were collected using a Microscribe 3-DX digitiser and Inscibe-32 software (Immersion Corp., San Jose, CA). The skull was mounted to record the landmarks on the dorsal aspect. Landmarks on each were recorded three times in succession. Great care was taken not to move the specimen during digitising. Replications of landmarks were taken successively in order to minimise handling and remounting of the fragile fossil specimens. Inter-landmark distances were calculated for each replication and the average inter-landmark distances of the three replications were used in further analyses. Coordinate data could not be averaged in the same way. The first replication of coordinates was used in all analyses for both the fossil and extant samples.

Fossil crania were often incomplete and were missing a number of landmarks on at least one side. The morphometric (PAST) and statistical (STATISTICA) programs used cannot accommodate missing data and therefore only complete subsets of coordinate landmark data common to as many of the fossil specimens as possible can be used for further analysis. However this often excluded too many variables or fossil specimens. Because of these issues, five subsets consisting of a varying number and combination of landmarks and specimens were selected and used in further analysis. The composition of each of the five subsets used for this study is given in Table 4.6. Subsets were selected either to maximise the number of variables (i.e. landmarks and inter-landmark distances) whilst still maintaining a meaningful compliment of fossil specimens (e.g. subsets I to IV), or to maximise the numbers of fossil specimens in a subset (e.g. Subset IV and V). In this way no fossil specimens were excluded from analysis. All possible inter-landmark distances were calculated for the five subsets of landmarks.

Dental measurements consisted of maximum mesio-distal (anterior and posterior) and buccal-lingual measurements of the third molars of all specimens, extant and fossil, that retained these teeth. These measurements were taken using a pair of digital callipers. Each measurement was repeated three times and the average used for further analysis.

Table 4.6. Specimen and inter-landmark distance composition of Subsets I to V

Subset I
Specimens
MP170,MP164,M3065,M3133,MP75,MP2
Inter-Landmark Distances
NA-GL, NA-TP(R), NA-BR, NA-ON(L), GL-TP(R), GL-BR, GL-ON(L), TP(R)-BR, TP(R)-ON(L), BR-ON(L)}
Subset II
Specimens
MP221,MP2,MP170,MP223,M3065,M3070
Inter-Landmark Distances
ZI(R)-NA, ZI(R)-ZS(R), ZI(R)-FMO(R), ZI(R)-ON(R), ZI(R)-GL, ZI(R)-ON(L), NA(R)-ZS(R), NA-FMO(R), NA-ON(R), NA-GL, NA-ON(L), ZS(R)-FMO(R), ZS(R)-ON(R), ZS(R)-GL, ZS(R)-ON(L), FMO(R)-ON(R), FMO(R)-GL, FMO(R)-ON(L), ON(R)-GL, ON(R)-ON(L), GL-ON(L)}
Subset III
Specimens
M3084,MP239,M3073,MP221,MP2,MP170,MP223,M3065,M3070
Inter-Landmark Distances
NA-ZS(R), NA-FMO(R), NA-ON(R), NA-GL, NA-ON(L), ZS(R)-FMO(R), ZS(R)-ON(R), ZS(R)-GL, ZS(R)-ON(L), FMO(R)-ON(R), FMO(R)-GL, FMO(R)-ON(L), ON(R)-GL, ON(R)-ON(L), GL-ON(L
Subset IV
Specimens
MP47,MP3078,MP221,MP223,M3084,MP239,M3070,MP208,M3073,MP3
Inter-Landmark Distances
PR-NS, PR-PM(R), PR-RH, PR-NA, PR-PM(L), PR-ZS(L), NS-PM(R), NS-RH, NS-NA, NS-PM(L), NS-S(L), PM(R)-RH, PM(R)-NA, PM(R)-PM(L), PM(R)-ZS(L), RH-NA, RH-PM(L), RH-ZS(L), NA-PM(L), NA-ZS(L), PM(L)-ZS(L)
Subset V
Specimens
MP167,MP47,MP3078,MP221,MP119,MP223,M3084,MP239,M3070,M3079,MP208,M3073,MP3,MP222
Inter-Landmark Distances
PR-PM(R), PR-NA, PR-PM(L), PM(R)-NA, PM(R)-PM(L), NA-PM(L)

4.7.3. Statistical Analyses

4.7.3.1. Procrustes Analysis

Landmark configurations were Procrustes transformed using the PAST ver.1.34 morphometrics software package (Hammer, Harper and Ryan, 2005). Procrustes transformation scales specimen configurations to unit centroid size and superimposes them to minimise summed squared distances for all landmarks. Specimen configurations are thus oriented to a common origin and the effects of gross size are removed; the point scatter produced around any given landmark thus represents shape variation. Even though Procrustes removes the effects of gross size it cannot correct for allometric effects. Procrustes transformed coordinate data therefore still retains size-correlated as well as size-independent components of shape.

4.7.3.2. Principal Components and Principal Coordinates Analysis

Principal Components Analysis (PCA) and Principal Coordinate analysis (PCoord), translated the data (inter-landmark or Procrustes transformed landmark coordinates) into a matrix of full rank. Each vector generated by this matrix is uncorrelated and ordinated according to the amount of variance it explains. Two vectors are represented as components of a two dimensional graph and specimens were ordinated relative to the major axis of variation. Principal coordinate analysis is similar to PCA but Procrustes transformed 3D landmark coordinates (x, y and z coordinates) are used rather than representing each landmark as a single variable.

Inter-landmark distances were subjected to PCA analysis. Variable loadings on principal component axes pinpoint variables with large negative or positive coefficients, which identifies them as significantly influential variables on that principal component. Through plots of various principal component axes based on PCA of the inter-landmark distances for each subset, the relationship (in terms of size, size-correlated shape and other aspects of shape) between the different specimens within that subset could be investigated. By investigating the variable loadings along the different axis, as well as referring back to the inter-landmark distances for individual specimens, differences between specimens and patterns in the data could be tied back to differences in the size and shape of influential anatomical regions of the cranium, specific to that subset of data.

Specimen loadings on the coordinate axes generated by PCoord analysis of Procrustes transformed coordinate data for the different subsets were plotted against the geometric means of specimens based on the inter-landmark distances of that subset in order to identify allometric effects. A significant linear correlation between the specimen loadings and the geometric means indicated whether shape differences, as expressed along the relevant coordinate axis, were related to size. In this manner it was possible to distinguish when size-correlated versus size-independent shape was being summarised along an axes, further facilitating the interpretation of differences between specimens and taxa.

For each of the five analyses, three sets of PCA and PCoord analyses were performed. Firstly, the subset of variables for the extant chacma baboon sample was analysed. This indicated whether PCA and PCoord analyses could distinguish between male and female specimens based on the particular subset of data and whether shape differences between the sexes were allometric. It also helped to identify the most significant anatomical differences between male and female, and large and small specimens. Secondly, the same variable subset of the fossil subsample was subjected to PCA and PCoord analysis. Differences in the size and shape between fossil specimens were investigated this way. Once again it could also be ascertained whether shape differences were correlated to size and whether size was related to sex and/or taxon. It could thus be inferred whether patterning in the fossil subsample was due to sexually dimorphic components in the data or reflected taxonomic differences. Thirdly, PCA and PCoord analyses were performed on the entire subset of variables, combining the extant chacma baboon sample and the fossil subsample in the same analysis. This allowed for the fossil subsample and the extant sample to be compared on aspects of size, shape and variability in those components. Again by inspection of variable loadings and raw inter-landmark distances, differences, similarities and overlap between sexes and taxa in the size and shape of significant anatomical regions of the cranium as specified by the subset, could be characterised. PCoord analysis would further indicate whether similarities in size necessarily translates into similarities in shape and provides a more powerful tool to asses shape differences and variability. Most importantly, this third step allows for comparison of variability in the size and shape of *Parapapio* with that of the extant chacma baboon sample.

CHAPTER 5

RESULTS:
STABLE ISOTOPE AND TRACE-ELEMENT ANALYSES

In this chapter the results of stable isotope and trace-element analyses for fossil cercopithecoid specimens from Makapansgat Limeworks Members 3 and 4 are presented. The results are discussed using the most recent taxonomic assignment of the specimens based on the most recent re-evaluation of taxonomic assignments of specimens (Freedman, 1960; Maier, 1970; Eisenhart, 1974; Freedman, 1976) or taxonomic assignments currently used in publications (Al-Zaatari *et al.*, 2005; Williams *et al.*, in press). Dietary habits of these fossil cercopithecoid specimens are deduced and compared to each other and to the broader contemporaneous fossil community based on existing isotope and trace element data for a suite of fauna from Makapansgat Member 3 and 4. Statistical analyses were not performed on the data because the sample sizes are small and statistical results would not be particularly meaningful.

5.4. Stable Isotope Data

All $\delta^{13}C$ and $\delta^{18}O$ data for fossil tooth enamel carbonate are shown in Appendix C-2 and C-3. Stable isotope data for enamel carbonate of contemporaneous fossil grazers, browsers and mixed feeders from Makapansgat Members 3 an 4 have been included in the graphs presenting $\delta^{13}C$ and $\delta^{18}O$ data, as references for pure C_3 and C_4 diets and for comparative purposes. Fossil fauna enamel carbonate stable isotope data are from Sponheimer (1999), Sponheimer and Lee-Thorp (1999c), Sponheimr and Lee-Thorp (unpublished data), Sponheimer *et al.* (1999). Stable isotope data for a sample of extant chacma baboons from Codron (2003) are shown for comparative purposes. The $\delta^{13}C$ data for the extant chacma baboon enamel carbonate have been adjusted for the 20th century fossil fuel effect on atmospheric CO_2 $^{13}C/^{12}C$ ratios.

In the plot of $\delta^{13}C$ vs. $\delta^{18}O$ (Fig. 5.1), the stable isotope results of *C. williamsi*, *T. darti* and *Parapapio* sp. are presented in the context of the broader community isotope ecology at Makapansgat. Enamel carbonate stable carbon and oxygen isotope ratios for browsing bovids, browsing giraffes, grazing bovids, grazing equids and grazing suids are taken from work by Sponheimer (1999), Sponheimer and Lee-Thorp (1999c), Sponheimer *et al.* (1999, 2001). *Parapapio* and the one *Cercopithecoides*

williamsi specimen's values fall in between those for browsing and grazing fauna at Makapansgat Limeworks, and are statistically significantly different to both groups (t-test, $p < 0.00001$ for *Parapapio* vs. browsers and *Parapapio* vs. grazers), indicating intermediate diets with both C_3 and C_4 sources.

In general these values are more enriched in ^{13}C than the enamel carbonate of the extant chacma baboons (*P. h. ursinus*) (Fig. 5.2) from woodland savannah habitats in the Waterberg, South Africa, about 100km to the west of Makapansgat. Chacma baboons from this region typically yielded a narrower and lower range of $\delta^{13}C$ enamel carbonate values between -13.5 and -10‰ (n = 10) (Codron, 2003) suggesting relatively minor contributions of C_4 plants (or possibly succulents) to their diets. The Waterberg $\delta^{13}C$ results seem typical, since broad sampling of extant chacma baboons from several savanna localities in South Africa, including the region around Mokopane (near Makapansgat), suggests that extant baboons in the savannah habitats of South Africa have predominantly C_3 diets with only small contributions from sources more enriched in ^{13}C (Codron *et al.*, 2005). Hence the Makapansgat *Parapapio* included a larger C_4 component in their diets than do savanna baboons in this region today. The small-bodied *Parapapio* included an eclectic mix of C_3 and C_4 plants and occupied a dietary niche, which shows little overlap with larger herbivorous taxa. The two *C. williamsi* specimens are markedly different to one another; one specimen groups with the mixed C_3/C_4 diet *Parapapio* and the other nearer the C_4 grazing fauna. *T. darti* clearly groups with the C_4 grazing fauna and is clearly distinguished from the *Parapapio* sample in having a largely C_4 dominated diet.

At Makapansgat Limeworks fossil browsers are more enriched in ^{18}O than fossil grazers and carnivores (Sponheimer, 1999) as seen in Fig. 5.1 and 5.3. This pattern has been observed in several modern faunal assemblages in southern Africa (Sponheimer and Lee-Thorp 2001, Lee-Thorp and Sponheimer, 2005). Higher $\delta^{18}O$ values in browsers may be linked to higher relative contributions of leaf water, which is ^{18}O-enriched due to evapotranspiration, compared to grazers and carnivores. All the fossil cercopithecoid specimens analysed in his study yielded enamel carbonate $\delta^{18}O$ values (1.1 to -5.8‰, -1.8 ± 1.5‰, n = 19) similar to the lower range of $\delta^{18}O$ values found for sympatric and contemporaneous fossil grazing taxa (2.3 to -5.7‰, -0.7 ± 1.7‰, n = 35) from Makapansgat Limeworks (Sponheimer and Lee-Thorp, 1999c).

Browsing taxa have significantly higher $\delta^{18}O$ (3.8 to -2.9‰, 1.5 ± 1.5‰, n = 28, t-test, $p < 0.0001$) compared to both grazing and cercopithecoid taxa. Notably the fossil cercopithecoid specimens were most similar in $\delta^{18}O$ to sympatric and contemporaneous fossil grazing suids (-3.1 ± 2‰, n = 5) and equids (-1.9 ± 0.8‰, n = 5) from Makapansgat Limeworks (Sponheimer and Lee-Thorp, 1999c). It is thought that suids include a substantial proportion of rootstocks in their diet (Sillen, 1988; Sponheimer and Lee-Thorp, 2005a; Sponheimer and Lee-Thorp, in press). The subterranean parts of plants (roots, tubers, corms, rhizomes) are ^{18}O-depleted relative to the above ground parts and resemble ground water in their $\delta^{18}O$ values (Gonfiantini, 1965; Epstein *et al.*, 1977; Sternberg, 1989). A large input of rootstocks from both C_3 and C_4 plants could explain the combination of intermediate carbon isotope values and deleted oxygen isotope values for *Parapapio*. Although faunivores (hyenas in this case) are not shown in Fig. 5.1, the range of $\delta^{18}O$ values (-3.9 to -2.2‰, -3 ± 0.9‰, n = 3) (Sponheimer and Lee-Thorp, unpublished data) overlaps with the cercopithecoid taxa. The relatively low $\delta^{18}O$ values of faunivores also suggest that animal foods may be depleted in ^{18}O (Tredget *et al.*, 1993; Sponheimer and Lee-Thorp, 1999). The combination of low $\delta^{18}O$ and intermediate $\delta^{13}C$ values for *Parapapio* might suggest that various rootstocks and/or animal foods may have been important dietary sources. A further non-competing explanation is that these primates were obligate drinkers.

Figure 5.1. Plot of $\delta^{13}C$ vs. $\delta^{18}O$ showing the relative position of fossil cercopithecoid taxa in the community ecology of Makapansgat Limeworks Members 3 and 4.

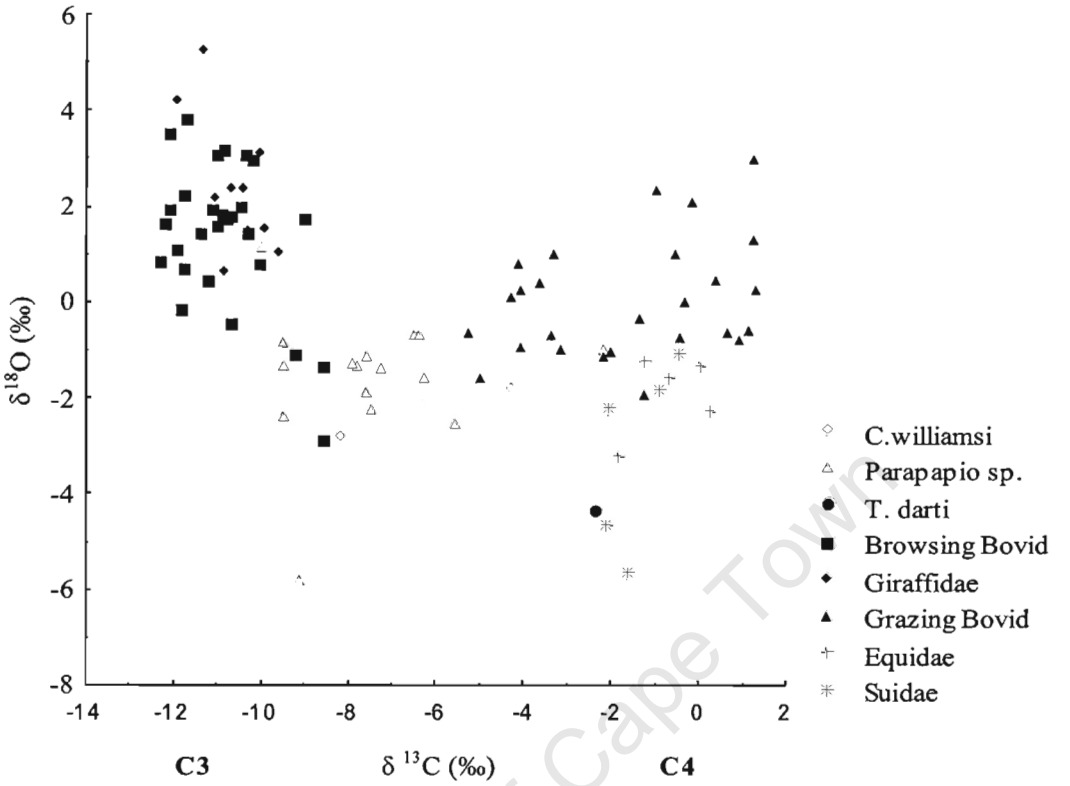

Pp. whitei and *Pp. jonesi* tooth enamel carbonate yielded similar mean $\delta^{13}C$ values of -6.6 ± 3.4‰ and a range of -5.6 to -9.5‰ (n = 5), and a mean -7 ± 0.7‰ and a range of -6.5 to -7.5‰ (n = 2) respectively (Fig. 5.2). Both *Pp. whitei* and *Pp. jonesi* enamel carbonate was generally more enriched in ^{13}C than *Pp. broomi* which yielded an average $\delta^{13}C$ value of -9 ± 1.3‰ and a range of -7.6 to -10‰ (n = 3). One *Pp. whitei* specimen, MP76 (Fig. 5.2), yielded a relatively low $\delta^{13}C$ value of -9.5‰ inconsistent with the range of values (-5.6 to -7.6‰ $\delta^{13}C$) obtained for the other four individuals attributed of this taxon. The $\delta^{13}C$ value of this individual accounts for the large standard deviation reported for the *Pp. whitei* group and the range overlap with the *Pp. broomi* group. The group consisting of unassigned *Parapapio* specimens yielded a wide range of $\delta^{13}C$ values (-2.2 to -9.5‰, -7.2 ± 2.4‰, n = 6), which overlaps with *Pp. whitei*, *Pp. jonesi* and *Pp. broomi* values. This would be expected if the unassigned specimens included representatives from all species (or dietary groupings). The high $\delta^{13}C$ value (-2.2‰) obtained for M3147 alone accounts for large range of $\delta^{13}C$ values reported for the unassigned *Parapapio* sample.

Pp. whitei (-0.7 to -2.5‰, -1.3 ± 07‰, n=5) and *Pp. jonesi* (-0.7 to -2.2‰, -1.4 ± 1.1‰, n = 2) both yielded similar $\delta^{18}O$ values to *Pp. broomi* (1.1 to -1.9‰, -0.7 ±

.6‰, n = 3) (Fig. 5.3). Only MP2 yielded a higher $\delta^{18}O$ value (1.1‰), but this value does not fall outside the range of variation observed for other fauna, fossil or extant (Codron 2003, Sponheimer and Lee-Thorp 1999). The unassigned *Parapapio* specimens yielded similar $\delta^{18}O$ values (-1 to -5.8‰, -2.2 ± 1.8‰, n = 6) to all three *Parapapio* taxa, as would be expected.

All *Parapapio* specimens, including the unassigned *Parapapio* and those assigned to *Pp. whitei*, *Pp. broomi* and *Pp. jonesi*, separate out into two $\delta^{13}C$ groupings, which overlap slightly (Fig. 5.2). This suggests the presence of two dietary groupings within the genus at Makapansgat. The largest and the smallest species of the genus have almost identical $\delta^{13}C$ values, which indicate that that they included substantial portion of C_4 foods in their diet. The $\delta^{13}C$ values for *Pp. broomi*, a species of intermediate size between *Pp. whitei* and *Pp. jonesi*, however, suggest a more C_3 dominated diet. There appear to be no differences in the $\delta^{18}O$ values between the three *Parapapio* taxa.

The two specimens of *C. williamsi* have very different $\delta^{13}C$ values indicating widely disparate inputs of C_4 foods. MP3A has a $\delta^{13}C$ value of -8.2‰ suggesting a diet largely composed of C_3. MP36 has a $\delta^{13}C$ value of -4.3‰ suggesting a mixed diet dominated by C_4 plants. *C. williamsi* dentition is typical of folivorous primates (Maier, 1970; Brain, 1981). Furthermore, this species belongs the subfamily Colobinae, of which all extant members are arboreal and are for the most part folivores. High contributions of C_4 are therefore surprising, as it implies a largely terrestrial grass-based diet. Dental wear and post-cranial anatomy studies of fossil *C. williamsi* , however, have suggested that they were an at least partially terrestrial taxon in the past (Benefit and McCrossin, 1990; Elton, 2001). Although only two individuals were analysed in this study, a bimodal distribution of $\delta^{13}C$ values was previously reported for *C. williamsi* specimens from Swartkrans and Sterkfontein (Luyt, 2001; Codron, 2003; Codron *et al.*, 2005). These studies sampled isolated teeth, therefore the possibility existed that some teeth in those studies were incorrectly identified. Alternatively, more than one taxon may be represented (Luyt, 2001; Codron, 2003). In this study, however, well-preserved crania that were confidently identified as *C. williamsi* were analysed, and these data support the presence of two distinct dietary eco-niches within this taxon(or alternatively and less plausibly, that diets were highly variable but only the extremes were captured in the sampling programme). Fig. 5.3 shows that both the *C. williamsi* specimens yielded similar $\delta^{18}O$

values (-1.8 and -2.8‰ respectively, -2.3 ± 0.7‰, n = 2) to *Parapapio* specimens (1.1‰ to -5.8‰, -1.6‰±1.4‰, n=16), with no significant difference.

The single *T. darti* specimen analysed here yielded a $\delta^{13}C$ value (-2.4‰) consistent with a largely C_4 diet similar to that of modern gelada baboons (*Theropithecus gelada*) and other fossil grazers in Makapansgat valley. Benefit and McCrossin (1990) suggested that *T. darti* was more folivorous than *T. oswaldi* based on molar crown morphology. The single specimen analysed here is indistinguishable in $\delta^{13}C$ from a larger dataset for *T. oswaldi* from Swartkrans and Sterkfontein, which indicates that this *T. darti* specimen consumed as much grass as *T. oswaldi*. Larger sample sizes are needed to confirm this characterisation. The $\delta^{18}O$ value for this specimen (MP222) was relatively low, overlapping with values of fossil grazing suids (Sponheimer and Lee-Thorp, 1999) and consistent with similarly lower $\delta^{18}O$ values for *T. oswaldi* specimens from Swartkrans (Codron, 2003). This implies that Theropithecine taxa relied more heavily on rootstocks (primarily grass roots) and/or meteoric surface water than did other contemporaneous primate taxa.

Figure 5.2. $\delta^{13}C$ values (‰) for fossil cercopithecoid sample, browsers and grazers from Makapansgat Limeworks Members 3 and 4 and extant baboons

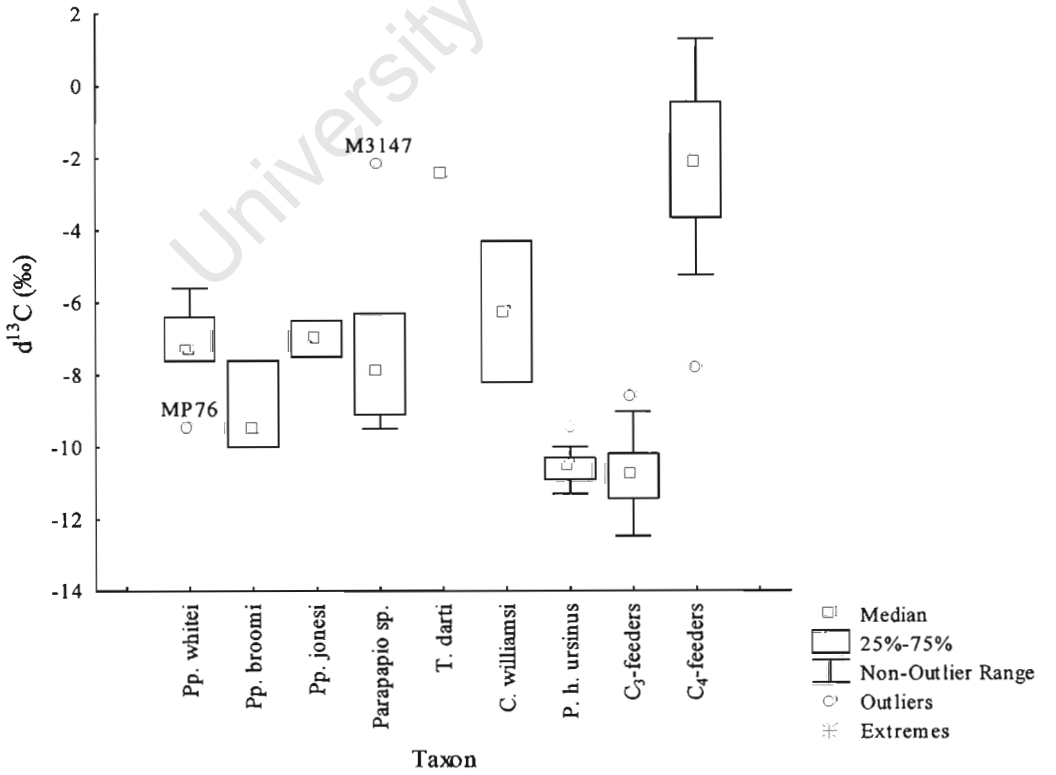

Figure 5.3. $\delta^{18}O$ values (‰) for fossil cercopithecoid sample, browsers and grazers from Makapansgat Limeworks Members 3 and 4 and extant baboons.

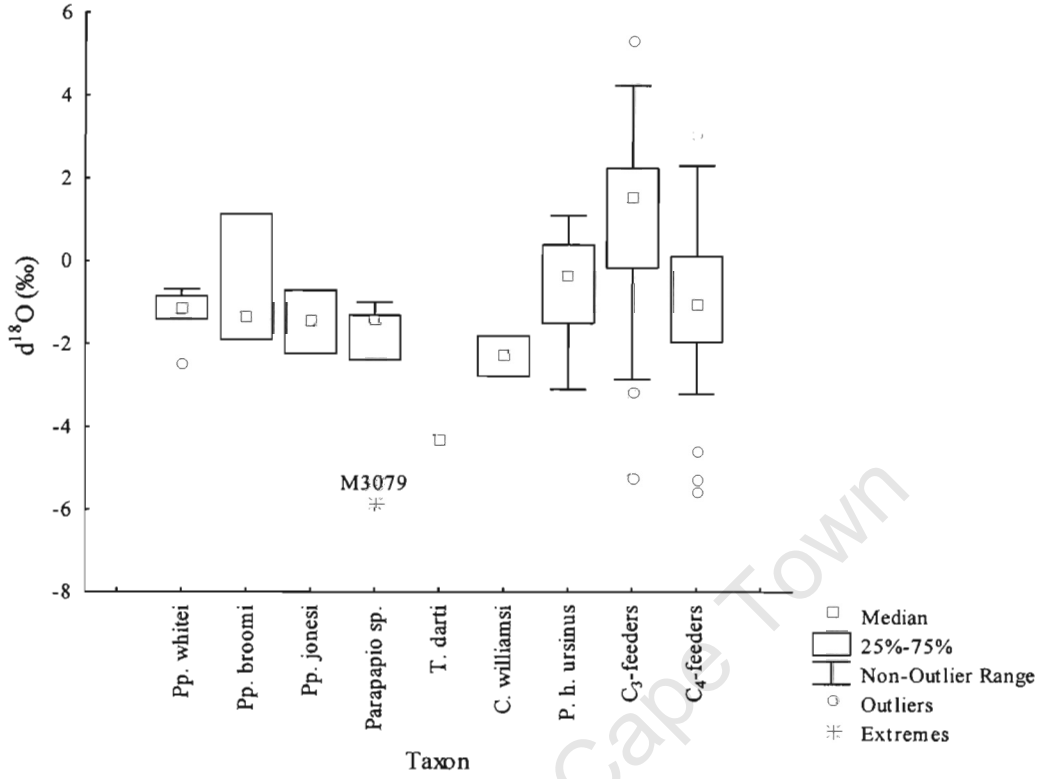

An unassigned *Parapapio* specimen, M3147, yielded a $\delta^{13}C$ value of -2.2‰, more consistent with values expected for Theropithecines. Such a high $\delta^{13}C$ value, implying a C_4-grass-dominated diet, has not been previously reported for any modern or fossil *Papio,* or *Parapapio,* species from South Africa (Luyt, 2001; Codron, 2003; Codron *et al.*, 2005). The $\delta^{18}O$ value is undiagnostic. Either this individual consumed grassy foods far in excess of the other members of this genus, or possibly, it may be that this specimen has been incorrectly identified. *T. darti* and larger *Parapapio* specimens overlap in size. In the past fossil *Theropithecus* specimens have been variously identified as *Papio* sp., *Parapapio* sp. or *Dinopithecus* sp. and vice-versa, and *Parapapio* sp. have been confused with *C. williamsi* (Freedman, 1975). Diagenesis does not offer a plausible explanation because all indicators including the amount of carbonate produced during analysis were normal. Furthermore all faunal enamel isotope analyses from Makapansgat have been shown to be reliable (Sponheimer and Lee-Thorp, 1999a; Sponheimer and Lee-Thorp, 2003b; Sponheimer, and Lee-Thorp, in press). The $\delta^{18}O$ value for M3079 (*Parapapio* sp.) of -5.8‰ fell outside the range of 1.1‰ to -2.8‰ for other *Parapapio* specimens in this study. The $\delta^{13}C$ value for M3079 was -9.1‰, consistent with a mainly C_3 diet which falls within the range of

values found for *Pp. broomi*. There is also nothing in the analysis of this specimen to suggest a significant diagenetic carbonate component or contamination as it did not produce an unduly large yield of carbonate, although diagenesis cannot be completely ruled out. Hence, overall the suite of analyses produced just one apparent outlier on the basis of $\delta^{13}C$ value (M3147) and another on the basis of the $\delta^{18}O$ (M3079); these two specimens have not been included further in investigation of the data.

5.5. Trace-Element Analysis of Fossil Cercopithecoid Specimens: Sr/Ca, Ba/Ca and Sr/Ba

All Ca, Sr and Ba data for fossil tooth enamel are shown in Appendix C-2 and C-3. Trace-element data of contemporaneous fossil grazers, browsers and mixed feeders from Makapansgat members 3 an 4 have been included in the graphs presenting trace-element data, as references for different dietary classes and for general comparative purposes. The Sr/Ca and Ba/Ca data for the Makapansgat fauna are taken from Sponheimer and Lee-Thorp (in press) and unpublished data by the same authors.

Fig. 5.4 to 5.6 below presents Sr/Ca vs. Ba/Ca ratios, Sr/Ca vs. $\delta^{13}C$ and Ba/Ca vs. $\delta^{13}C$ for a variety of faunal classes from Makapansgat Limeworks, Members 3 an 4, and provides a community ecology context for the interpretation of the Sr/Ca and Ba/Ca ratios observed for the fossil cercopithecoid sample. Although there is much overlap between faunal classes grazing taxa have significantly higher Sr/Ca and Ba/Ca ratios than browsing taxa (Sponheimer *et al.*, 2005; Sponheimer and Lee-Thorp; in press). Certain taxa also have Sr/Ca and Ba/Ca ratios consistent with inferred and observed diets; these include grazing fossil suids from Makapansgat (Sponheimer *et al.*, 2005; Sponheimer and Lee-Thorp, unpublished data) and extant mole rats (Sponhemer and Lee-Thorp, in press) which are consistent with diets rich in rootstocks. These patterns in Southern African fossil and extant faunal communities provide useful comparisons against which to interpret the fossil cercopithecoid data.

The plot of Sr/Ca vs. Ba/Ca (Fig.5.4) shows that *Parapapio* specimens as a group fall broadly between browsing and grazing taxa while overlapping with both. The *Parapapio* sample resembles both browsing and grazing taxa in Sr/Ca ratios (Fig. 5.5) although they tend to slightly higher end of Sr/Ca ratios, yielding none of the low Sr/Ca ratios more typical in browsers. The plot of Ba/Ca vs. $\delta^{13}C$ (Fig. 5.6) shows that the *Parapapio* sample resembles browsing taxa in their Ba/Ca ratios rather than grazing bovids, because they have relatively low Ba/Ca ratios. Another taxon which

shows a similar patterning are the fossil grazing suid specimens (*Potamochoeroides shawi*). Suids are thought to include a significant portion of roots, tubers, corms and rhizomes in their diet, which limited data suggest may be low in both Sr and Ba (Sponheimer *et al.*, 2005). The combination of relatively high but not distinct Sr/Ca ratios, and distinctively low Ba/Ca ratios, are consistent with a reliance on rootstocks in the diet.

The *T. darti* specimen, MP222, has a Sr/Ca ratio similar to the higher end observed for grazing taxa from Makapansgat (Fig. 5.5 and Fig. 5.7). At the same time it has a high Ba/Ca ratio (Fig. 5.6 and Fig. 5.8) which together with a high Sr/Ca ratio which would be consistent with gramnivory.

Figure 5.4. Plot of Sr/Ca vs. Ba/Ca showing the relative position of fossil cercopithecoid taxa in the community ecology of Makapansgat Limeworks Members 3 and 4.

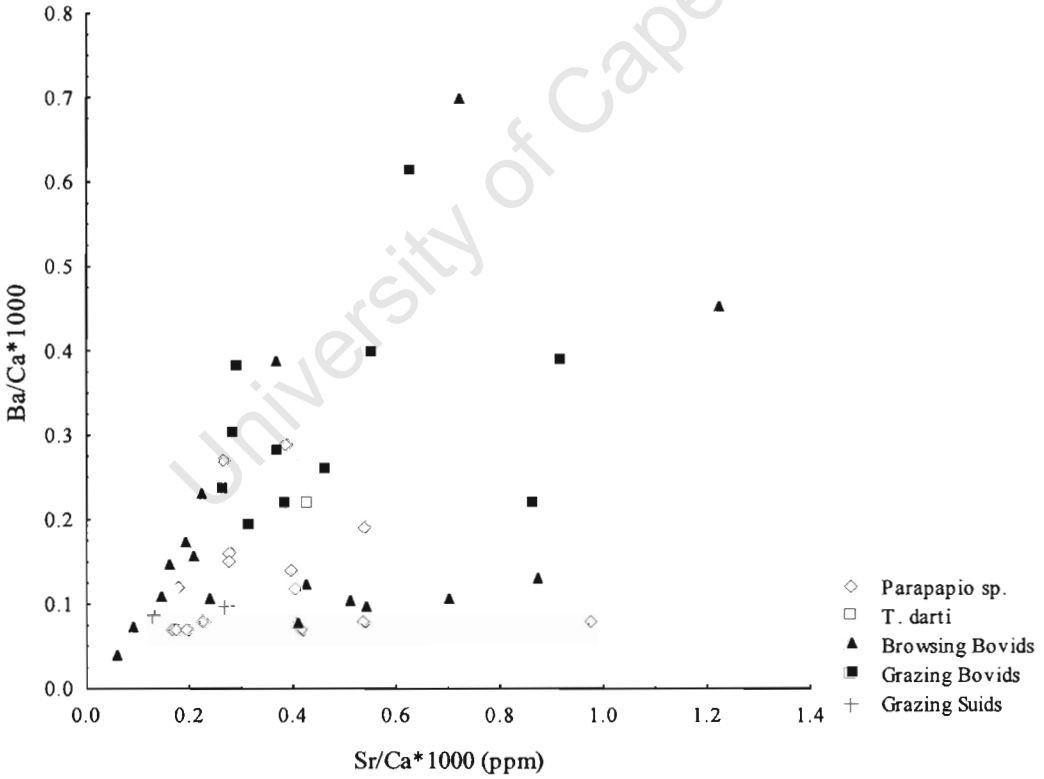

Figure 5.5. Plot of Sr/Ca vs. $\delta^{13}C$ showing the relative position of fossil cercopithecoid taxa in the community ecology of Makapansgat Limeworks Members 3 and 4.

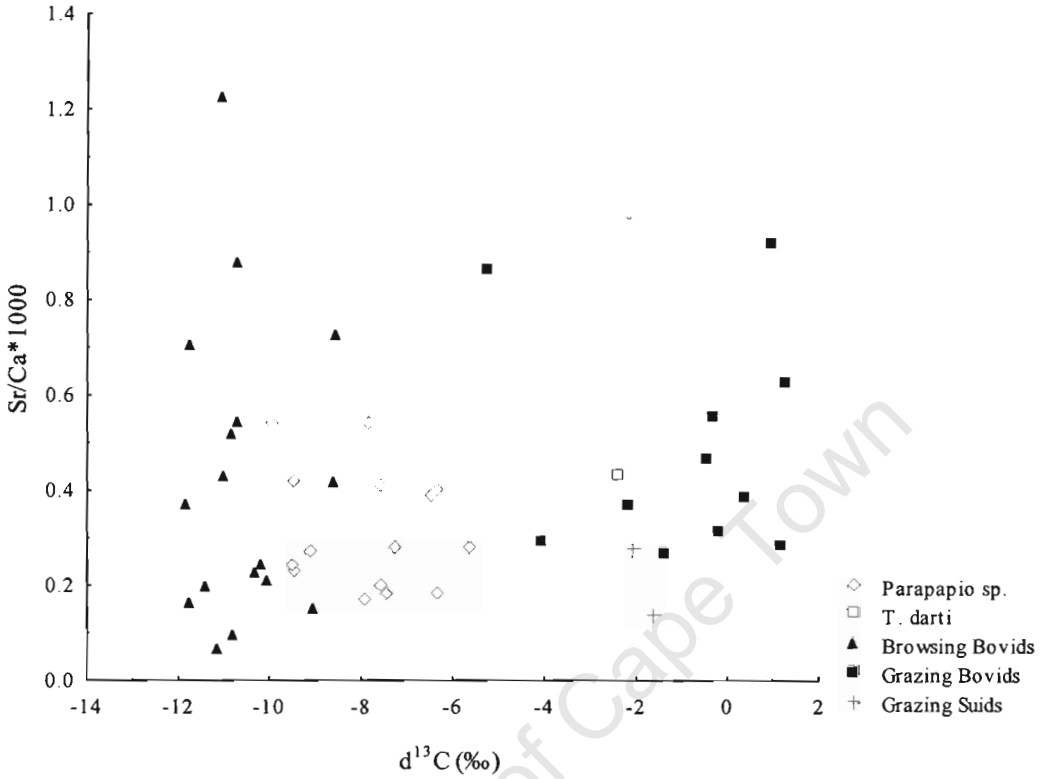

Figure 5.6. Plot of Ba/Ca vs. $\delta^{13}C$ showing the relative position of fossil cercopithecoid taxa in the community ecology of Makapansgat Limeworks Members 3 and 4.

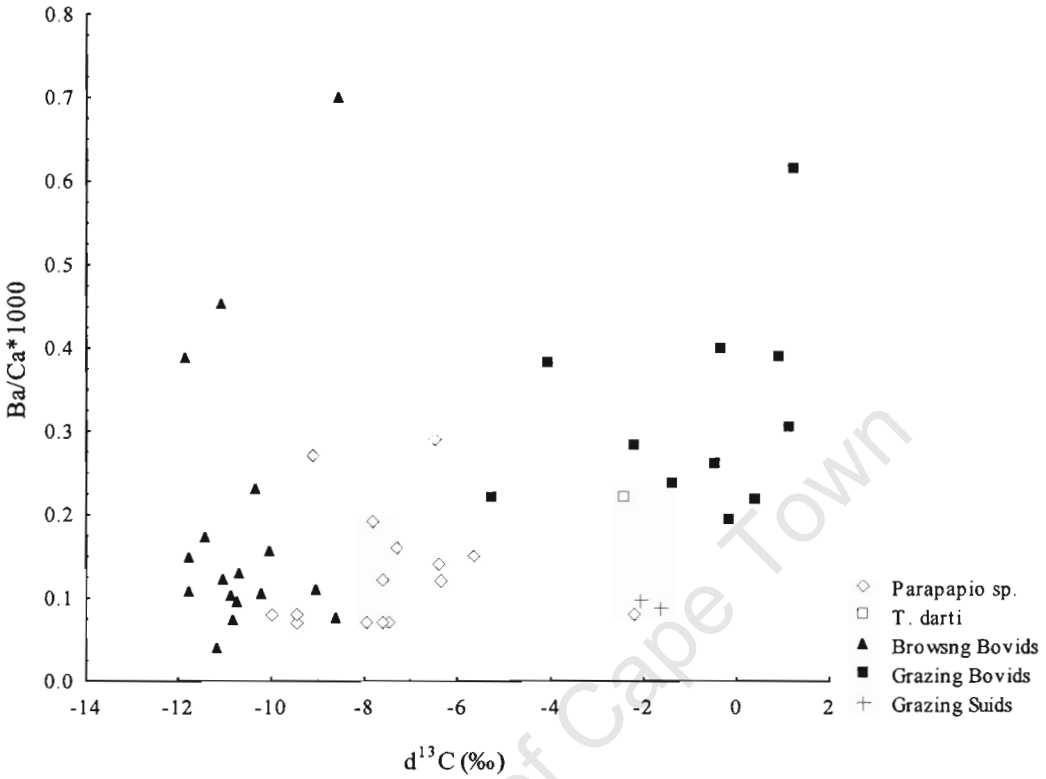

Pp. broomi yielded generally higher Sr/Ca ratios (0.41 to 0.23, 0.39 ± 0.16, n = 3) than *Pp. whitei* (0.40 to 0.20, 0.28 ± 0.07, n = 5) and *Pp. jonesi* (0.39 to 0.18, 0.28 ± 0.15 n = 2). The unassigned *Parapapio* specimens yielded a range of values (0.54 to 0.17, 0.32 ± 0.16, n = 5) representative of those observed for all *Parapapio* taxa.

There is substantial overlap in the Sr/Ca ranges (Fig. 5.7) between the three *Parapapio* taxa. All three taxa are broadly similar in their Sr/Ca ratios although *Pp. broomi* tends to a higher mean Sr/Ca ratio.

Pp. whitei specimens yielded generally higher Ba/Ca ratios (0.16 to 0.07, 0.13 ± 0.04, n = 4) than *Pp. broomi* specimens (0.12 to 0.08, 0.09 ± 0.02, n = 4), as might be expected due their more C_4 grass diet. The two *Pp. jonesi* specimens had widely different Ba/Ca ratios from one another. MP75 yielded the higher Ba/Ca ratio compared to all other fossil cercopithecpoid specimens in this study, a relatively high Sr/Ca ratio and a more depleted $\delta^{13}C$ value than the other *Pp. jonesi* specimen, MP173. The high Sr/Ca and Ba/Ca ratios for this specimen are consistent with grass and rootstocks in the diet; however the magnitude of the Ba/Ca ratio as compared to other specimens remains unusual. M3147 also yielded an anomalously high Sr

abundance. It yielded an unusually high Sr and Sr/Ca ratio inconsistent with the range of Sr and Sr/Ca values obtained for other fossil cercopithecoid specimens. M3147 yielded a Sr abundance (325ppm) more than three times that of the average for the genus *Parapapio* (93ppm). These higher values are more consistent with granitic-dominated geological zones (Sponheimer and Lee-Thorp, in press), and hence possibly this individual came from an area with a different geology. Unassigned *Parapapio* specimens (0.27 to 0.07, 0.14 ± 0.09, n = 5) yielded a range of Ba/Ca ratios overlapping with all three *Parapapio* taxa as would be expected if it consisted of representatives of all three taxa.

The generally lower Ba/Ca and relatively higher Sr/Ca, and low $\delta^{13}C$ values, for *Pp. broomi* compared to *Pp. whitei* and *Pp. jonesi* is consistent with a greater reliance on C_3 rootstocks than the other two *Parapapio* taxa. Sr/Ca and Ba/Ca ratios for specimens attributed to *Pp. whitei* and *Pp. jonesi* are also consistent with the inclusion of rootstocks in the diet but suggest perhaps a smaller rootstock input than *Pp. broomi.*

Samples for trace-element analysis were often very small as they represented the material left over after, sometimes, multiple isotopic analyses. MP76 represents one such very small sample. For this reason there was not enough material to measure its Ba abundance, but only yielded Sr and Ca abundances. Ba/Ca and Sr/Ba ratios could therefore not be calculated for this specimen.

Figure 5.7. Box and whiskers plot of Sr/Ca x 1000 ratios for fossil cercopithecoid taxa and faunal classes from Makapansgat Limeworks Members 3 and 4.

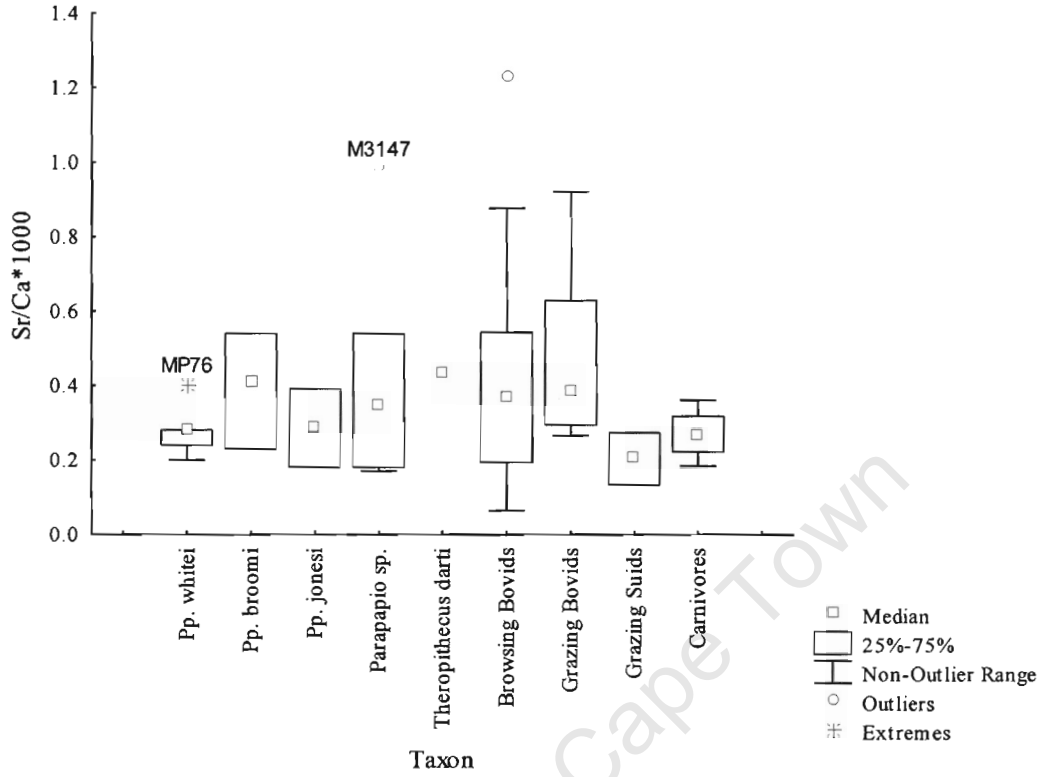

Figure 5.8. Box and whiskers plot of Sr/Ca x 1000 ratios for fossil cercopithecoid taxa and faunal classes from Makapansgat Limeworks Members 3 and 4.

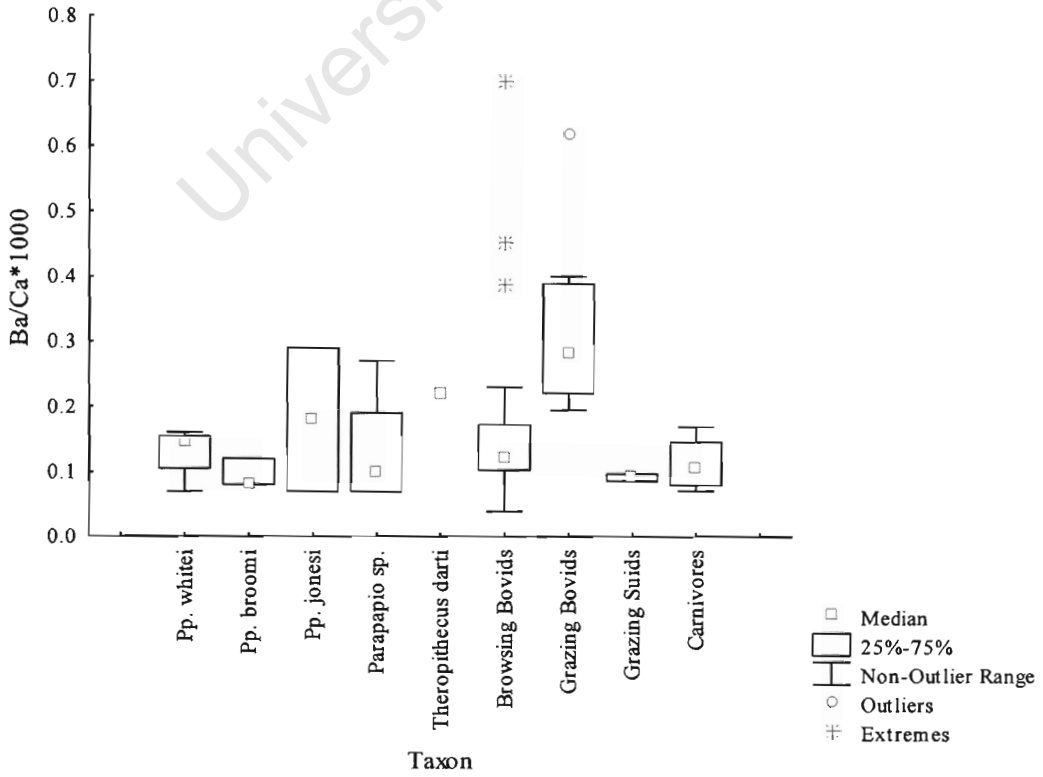

Sr/Ba ratios also clearly distinguished *Pp. broomi* from *Pp. whitei* and *Pp. jonesi*. *Pp. broomi* yielded higher mean Sr/Ba ratios (4.35 ± 2.1, n = 3) than *Pp. whitei* and *Pp. jonesi* specimens together (2.21 ± 0.64, n = 6.). *Pp. broomi* also yielded Sr/Ba ratios, which were relatively high compared to all other comparative taxa, including the grazing suids, and only overlapped with the higher end of the range of Sr/Ba ratios for browsing bovids. Sponheimer and Lee-Thorp (in press) report that mole rats, a taxon that largely feeds off rootstocks (Kingdon, 1997), yielded much higher Sr/Ba ratios than all other taxa. Hence, a plausible explanation for the high Sr/Ba observed for *Pp. broomi* would again reflect a greater dependence on rootstocks in this taxon than in *Pp. whitei* and *Pp. jonesi*.

Figure 5.9. Box and whiskers plot of Sr/Ba ratios for fossil cercopithecoid taxa and faunal classes from Makapansgat Limeworks Members 3 and 4.

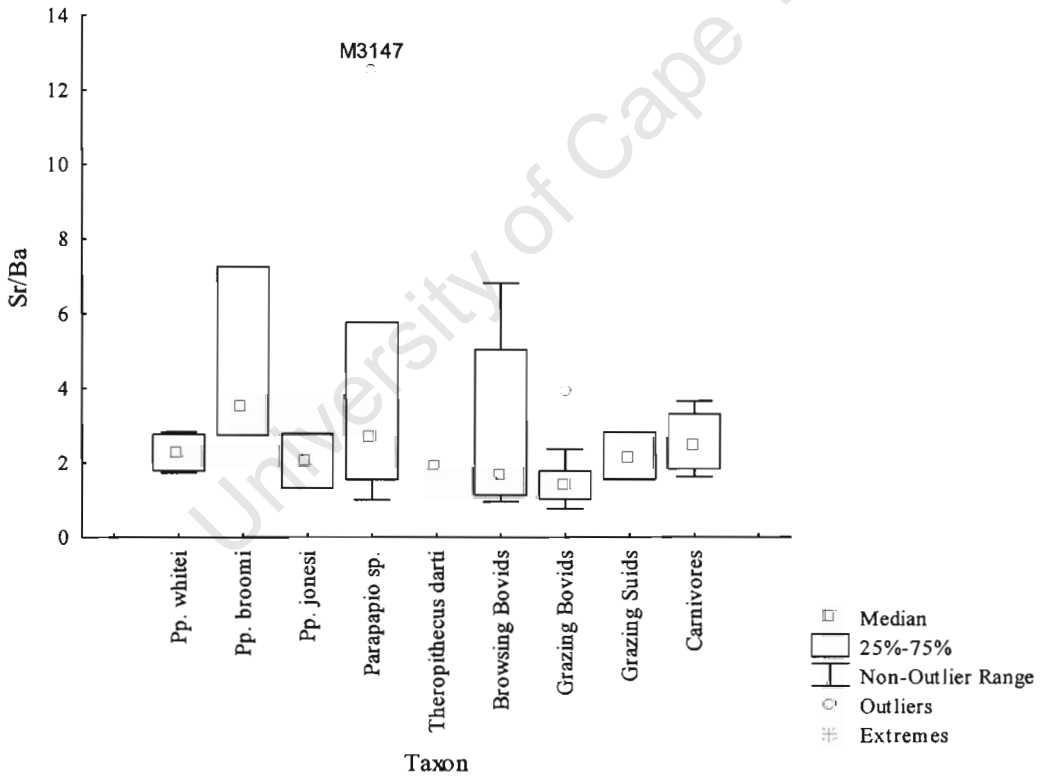

CHAPTER 6

RESULTS:
CRANIOMETRIC INVESTGATION

The results for the craniometric investigation of the selected Plio-Pleistocene cercopithecoid taxa from Makapansgat Limeworks are presented in this chapter. The results for Principal Components- and Principal Coordinates Analyses are presented for each subset of specimens. A full list of coordinate landmark data for all specimens is presented in Appendix D-1 and D-2. The most recent taxonomic assignment of specimens is used when referring to specimens.

6.1. Subset I

The six specimens that comprise Subset I along with the landmarks and inter-landmark distances they share in common are listed in Table 6.1.

Table 6.1. Details for specimens constituting Subset I.

Accession no.	Taxon	Sex
MP164	*Pp. whitei*	I
M3065	*Pp. broomi*	M
MP2	*Pp. broomi*	M
MP170	*Pp. broomi*	F
MP75	*Pp. jonesi*	M
M3133	*Parapapio* sp.	I
Anatomical Landmarks		
NA, GL, TP(R), BR, ON(L)		
Inter-Landmark Distances		
NA-GL, NA-TP(R), NA-BR, NA-ON(L), GL-TP (R) GL-BR, GL-ON(L), TP(R)-BR, TP(R)-ON(L), BR-ON(L)		

I = Indeterminate sex

M = Male

F = Female

6.1.1. Cluster Analysis of Inter-landmark Distances

6.1.1.1. Extant Baboon Sample

A single linkage cluster analysis (Fig. 6.1) performed on the sample of extant chacma baboons, based on the same subset of inter-landmark distances as Subset I, generally separates male and female specimens from each other, although there are some female specimens in the mainly male cluster. This separation probably reflects basic size and size-related shape differences between males and females.

Figure 6.1. A Tree diagram based on a single linkage cluster analysis performed on Subset I inter-landmark distances of the extant baboon sample. (n = 31, F = 14, M = 17)

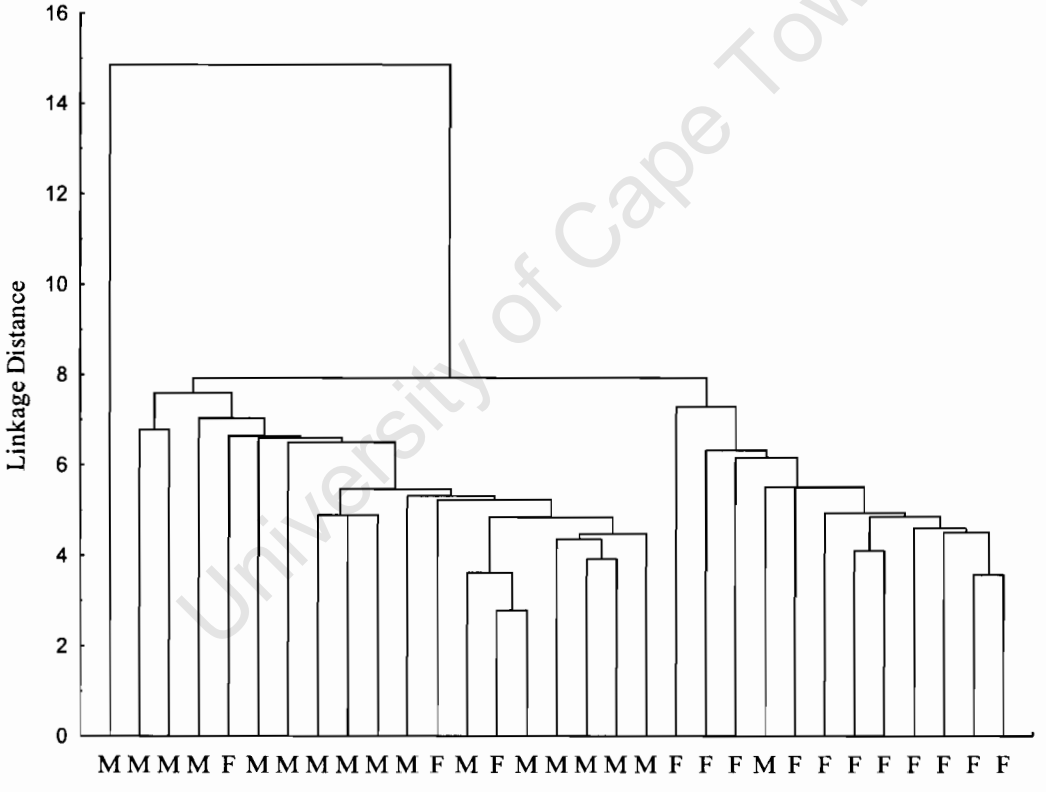

6.1.1.2. Fossil Cercopithecoid Sample

A single linkage cluster analysis (Fig. 6.2), performed on the Subset I fossil *Parapapio* specimen inter-landmark distances, did not separate specimens into distinct groups. Specimens belonging to the same taxon were not ordinated together or

separated from other taxa. There is also no separation between male and female specimens.

Figure 6.2. A Tree diagram based on a single linkage cluster analysis performed on Subset I inter-landmark distances of the Subset I fossil cercopithecoid subsample. (n = 6, *Pp. whitei* = 1, *Pp. broomi* = 3, *Pp. jonesi* = 1, *Parapapio* sp. = 1)

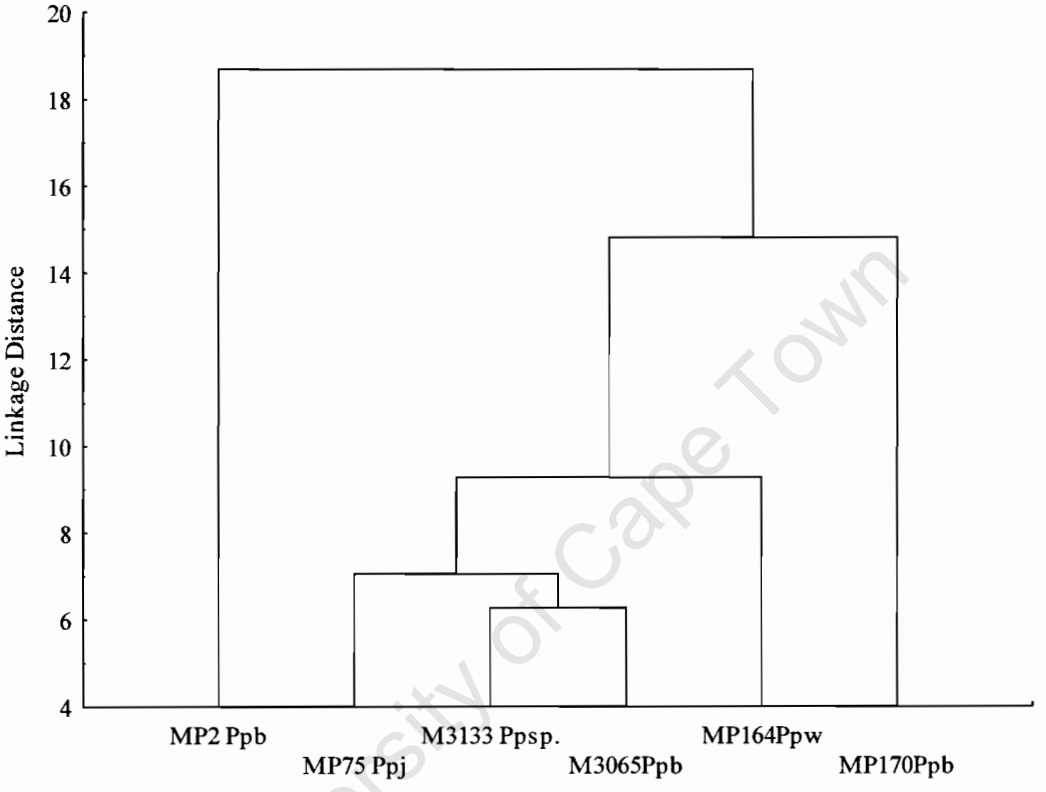

6.1.2. Principal Components Analysis and Principal Coordinates Analysis

6.1.2.1. Extant Baboon Sample

Plot of PC1 vs. PC2 based on PCA with 95% ellipses of Subset I inter-landmark distances for the extant baboon sample (Fig. 6.3) is shown below. PC1 explains 60% of the variance and ordinates male specimens more positively and female specimens more negatively along both the PC1 axis. All variables yielded positive loadings on the PC1, implying that PC1 represents size and size-related shape. Specimens that were more negatively placed along this axis exhibited shorter anterior neurocrania (NA-BR) than specimens with more positive ordinations. Weak polarisation of male and female specimens also occurs along the PC2 axis. The PC2 axis summarises 21% of the variance. PC2 contained a mixture of positive and negative loadings suggesting

that this component explains other aspects of shape. Variable loadings indicated that specimens that were more positively placed along this axis differed in the shape of the lateral anterior neurocranium around the region of the anterior frontal bone.

Figure 6.3. Plot of PC1 vs. PC2 based on PCA with 95% ellipses of Subset I inter-landmark distances for the extant baboon sample. (n = 31, F = 14, M = 17)

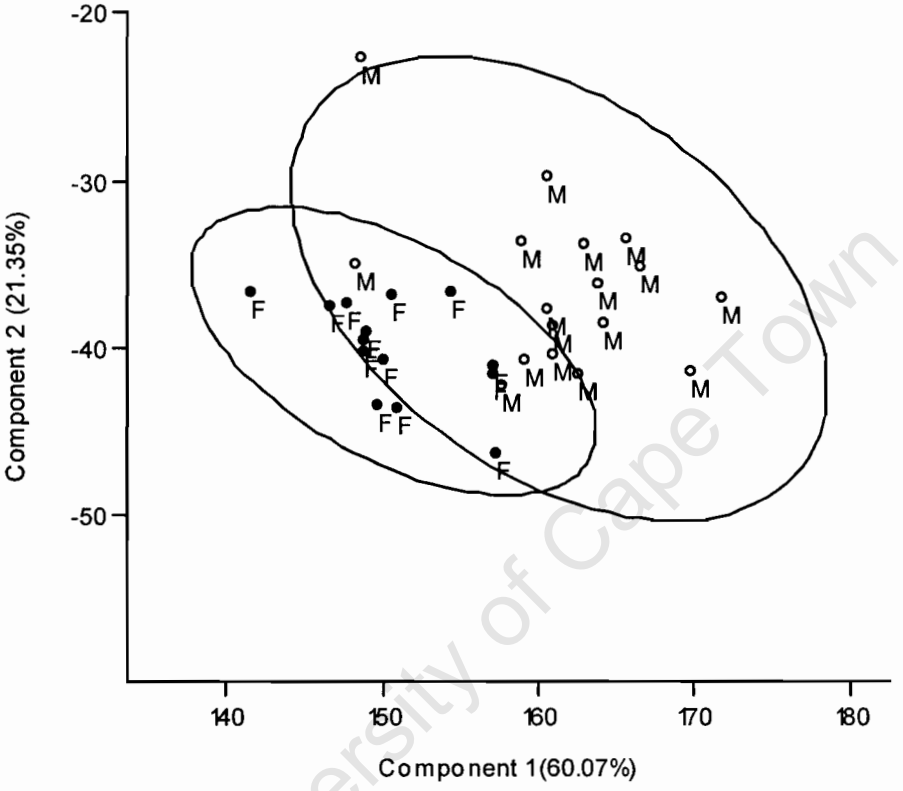

A stepwise Discriminant Function Analysis (DFA) was run on the Subset I inter-landmark distances to identify which inter-landmark distances were the most significant discriminators between larger and smaller specimens. NA-TP(R), TP(R)-BR, and NA-BR were the most significant discriminators between male and female specimens in the extant sample. These variables describe facets of the length between the anterior neurocranium and the upperface and the breadth of the anterior part of the parietal bone, as illustrated in Fig. 6.4 below.

Figure 6.4. Most significant discriminators between male and female baboon crania for Subset I inter-landmark distances.

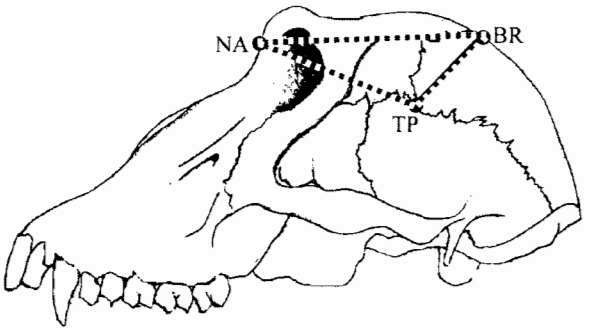

The plot of Coordinate 1 vs. Coordinate 2 (Fig. 6.5), based on a PCoord analysis of Procrustes-aligned coordinate data of Subset I coordinates of the extant chacma baboon sample, separates male and female specimens along the Coordinate 1 axis, as with PCA (Fig. 6.3) there was some overlap between male and female clusters. Coordinate 1 specimen loadings were significantly and moderately correlated to the geometric means of specimens across the extant chacma baboon sample ($r^2 = 0.38$, $p < 0.001$) implying that this axis summarises aspects of both size-correlated - and size-independent shape. The Coordinate 1 axis thus summarises a component of shape differences between larger and smaller specimens which in this case is appears to be related to sexual dimorphic differences in size and shape. Male specimens appear to differ from female specimens in aspects of size-correlated shape of the anterior neurocranium. Males tend to have somewhat longer anterior neurocrania than females, although as the analysis indicates there is some overlap between the sexes. The Coordinate 2 axis showed no such correlation, implying that only size-independent shape is summarised along this axis.

Figure 6.5. Plot of Coordinate 1 vs. Coordinate 2 based on PCoord with 95% ellipses of Subset I Procrustes-aligned coordinate data for the extant baboon sample. (n = 31, F = 14, M = 17)

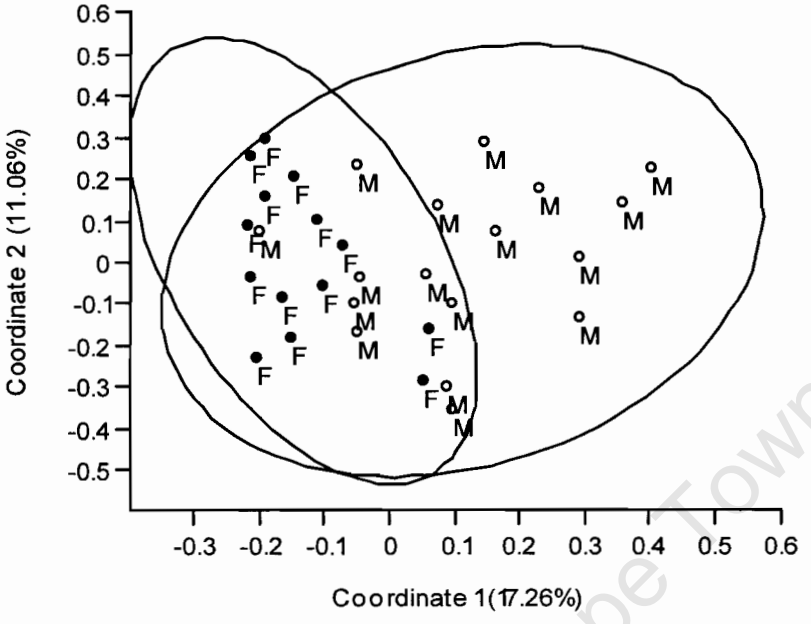

To summarise PCA and PCoord analysis of the extant chacma baboon sample for Subset I craniometric data indicates that the component 1 axes are able to distinguish between larger and smaller specimens in both size and size related shape for the given subset of variables. Male specimens have longer anterior neurocrania and higher nuerocrania than female specimens and fall more positively along the component 1 axes of both PCA and PCoord. It is therefore expected that the PCA and PCoord analyses of the fossil specimens, based on the same subset of data, should be able to discriminate between larger ad smaller specimens on the bases of size and size-related shape differences. Such polarisation in the fossil sample would be expected to occur along taxonomic and/or sexually dimorphic lines.

6.1.2.2. Fossil Cercopithecoid Sample

PC1 and PC2 (Fig. 6.6) summarise 55% and 35% of the variance, respectively. PC1 loadings are mostly positive with two very small negative loadings, which suggests that PC1 reflects mainly size and size-correlated shape differences. MP2 and MP170, a *Pp. broomi* male and female respectively, as in the cluster analysis, appear to be quite different from the other specimens and each other. They are widely separated from one another along the PC1 axis and widely separated from the other *Parapapio*

specimens along the PC2 axis. MP170 appears to have a longer dorsal anterior nuerocranium (NA-BR) than its male conspecific, MP2. Interestingly MP2 has very tall anterior neurocranium (BR-TP) relative to its length compared to other specimens. PC2 reflects the same combination of traits for MP2 and orients specimens with tall neurocrania more positively than specimens with shorter anterior neurocrania. Both MP2 and MP170 have similar relatively taller anterior neurocrania and upperface regions than all other specimens in this subsample. MP170 is furthermore absolutely larger than MP2 and the other *Parapapio* specimens in this subsample on inspection and comparison of geometric means. MP2 shows greater similarity to other specimens in this subsample with respect to its geometric mean than it does to MP170. It appears that the small negative loadings on both PC1 and PC2 are mostly related to MP2, as this specimen has an unusually tall anterior cranial vault for its length.

Figure 6.6. Plot of PC1 vs. PC2 based on PCA of Subset I inter-landmark distances for the Subset I fossil cercopithecoid subsample. (n = 6, *Pp. whitei* = 1, *Pp. broomi* = 3, *Pp. jonesi* = 1, *Parapapio* sp. = 1)

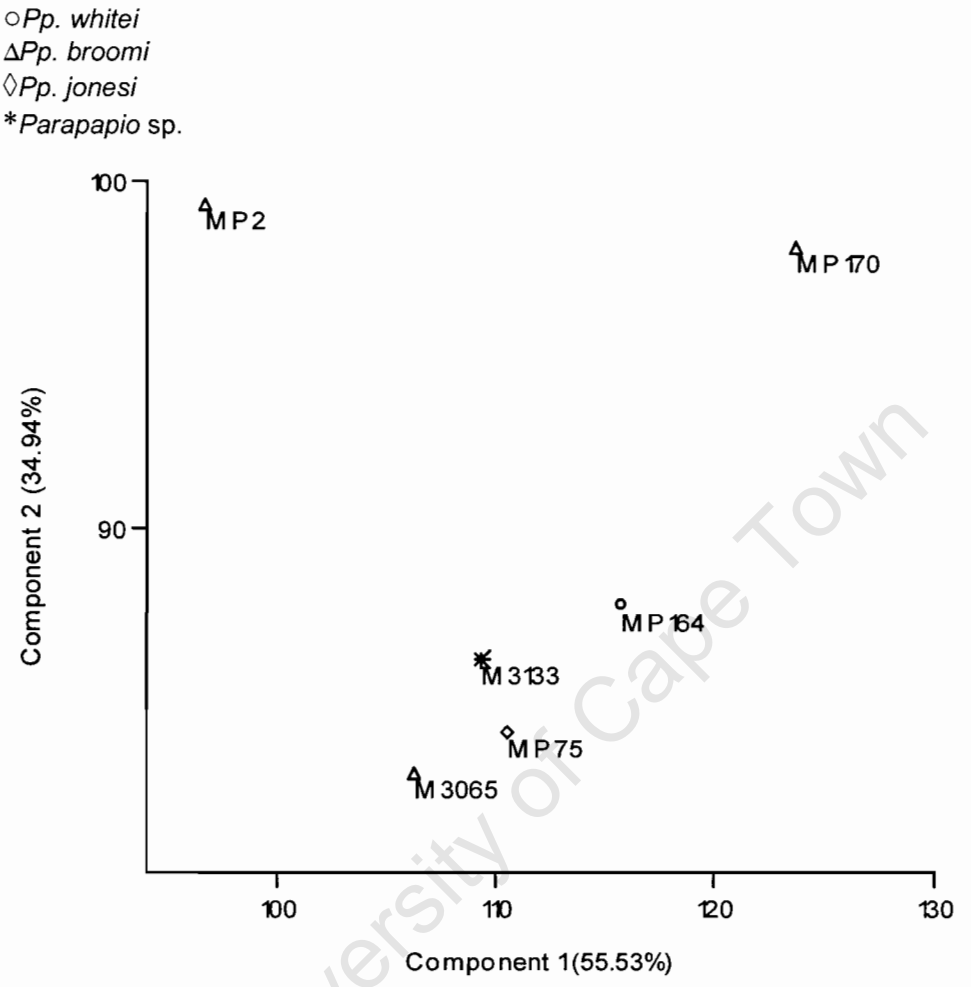

The plot of Coordinate 1 vs. Coordinate 2 (Fig. 6.7), based on PCoord analysis of Subset I Procrustes transformed coordinate data of the fossil cercopithecoid subsample, polarises specimens along the Coordinate 2 axis and separates MP2 from the rest of the subsample along the Coordinate 1 axis. Neither axis was significantly correlated to the geometric means across the *Parapapio* subsample suggesting that both axes explain size-independent shape in the anterior cranial vault. MP2 is consistently ordinated away from all other specimens in both cluster analyses, PCA and PCoord, suggesting a relatively tall and short anterior cranial vault for this specimen compared to other specimens in this sample.

Along the Coordinate 2 axis MP75 (*Pp. jonesi*, male) and MP164 (*Pp. whitei*) cluster together, as do MP3133 (*Parapapio* sp.) and MP3065 (*Pp. broomi*, male).

MP170 (*Pp. broomi*, female) does not group with other *Parapapio* specimens along the Coordinate 2 axis and does not differ from any of the other *Parapapio* specimens (except MP2) along the Coordinate 1 axis. MP170 resemble other specimens in a having relatively long anterior neurocranium but differed in having a relatively tall anterior cranial vault.

Figure 6.7. Plot of Coordinate 1 vs. Coordinate 2 based on PCoord of Subset I Procrustes transformed coordinate data for the Subset I fossil cercopithecoid subsample (n = 6, *Pp. whitei* = 1, *Pp. broomi* = 3, *Pp. jonesi* = 1, *Parapapio* sp. = 1)

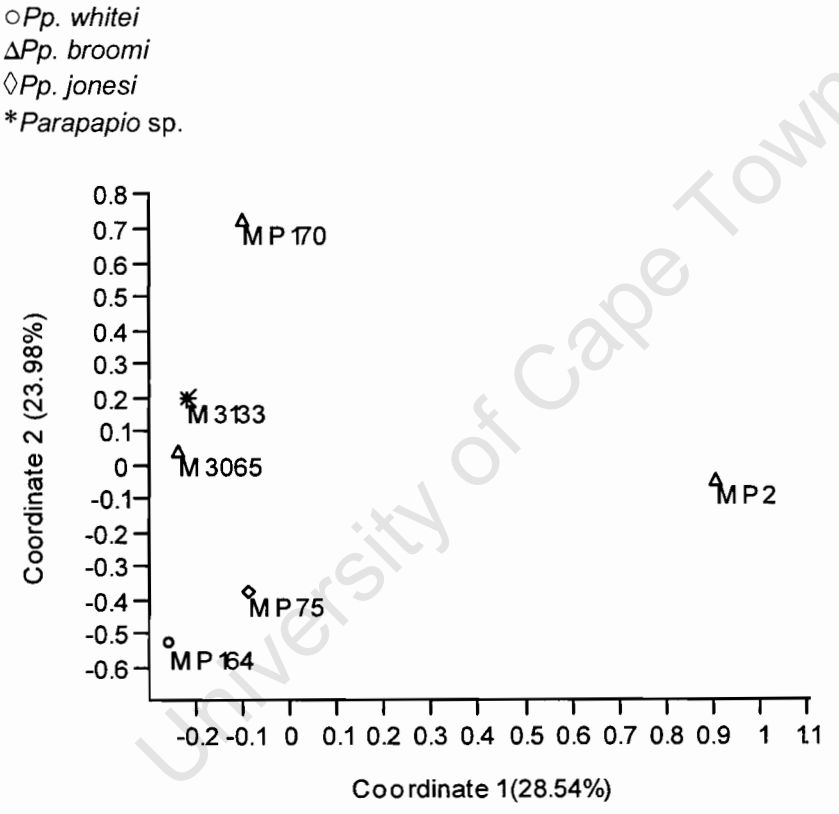

6.1.2.3. Fossil *Parapapio* vs. Extant Baboon Sample

Plots of PC1 vs. PC2 (Fig. 6.8), and Coordinate 1 vs. Coordinate 2 (Fig. 6.9), based on PCA and PCoord of Subset I data of the extant chacma baboons sample and the fossil cercopithecoid subsample, grouped *Parapapio* specimens on the margins of the female scatter on the plots along the component 1 axes. This patterning relative to the extant baboon sample probably reflects the relatively smaller size and related shape differences of the *Parapapio* specimens relative to the extant chacma baboon sample. However certain individuals, at least one *Parapapio*, specimen the large *Pp. broomi* female (MP170) fall within the scatter of extant female baboons suggesting that *Parapapio* individuals can have similar size and shape dimensions in the anterior neurocranium and upperface, within the range of variation of extant female chacma baboons. MP170 shows similarities in size (Fig. 6.8) and shape (Fig. 6.9) to the extant female chacma baboon sample. MP170 does however differ in shape as summarised along the Coordinate 2 axis (Fig. 6.9) from the extant female chacma baboon sample.

The overall extent of the variation within the main *Parapapio* cluster appears to be comparable to the extent of the variation within a single sex of the extant chacma baboon sample along the both the component 1 and 2 axes of the PCA and PCoord analyses. There appears to be no excessive variation within the main cluster of the *Parapapio* sample, contrary to what would be expected based on its apparent taxonomic composition. The data for this subset suggests that M3065, M3133, MP75 and M164 represent a single morphotype with respect to the anterior neurocranium.

Figure 6.8. Plot of PC1 vs. PC2 based on PCA of Subset I inter-landmark distances for the extant baboon sample and the Subset I fossil cercopithecoid subsample. (n = 37, *P. h. ursinus* = 31, *Pp. whitei* = 1, *Pp. broomi* = 3, *Pp. jonesi* = 1, *Parapapio* sp. = 1)

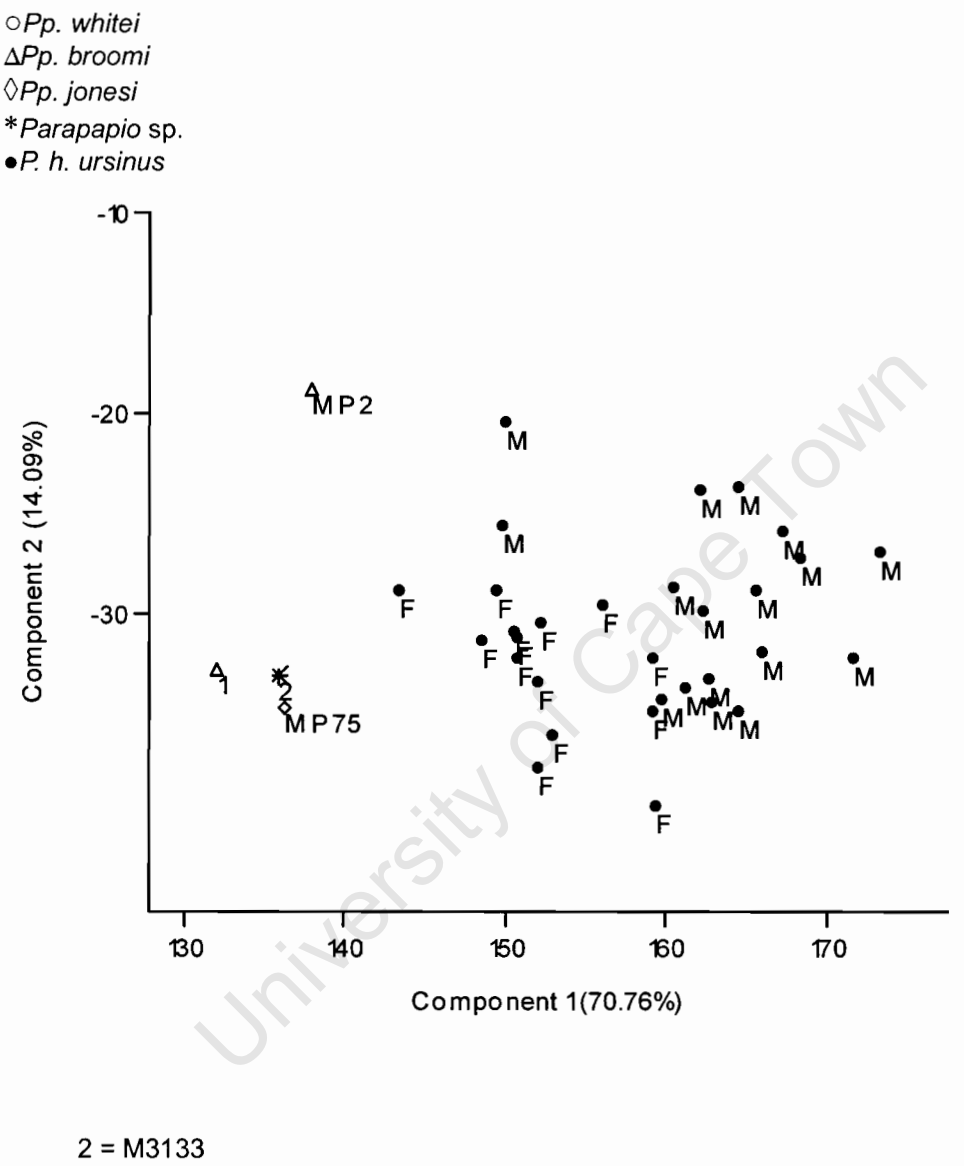

Figure 6.9. Plot of Coordinate 1 vs. Coordinate 2 based on PCoord of Subset I Procrustes transformed coordinate data for the extant baboon sample and the Subset I fossil cercopithecoid subsample. (n = 37, *P. h. ursinus* = 31, *Pp. whitei* = 1, *Pp. broomi* = 3, *Pp. jonesi* = 1, *Parapapio* sp. = 1)

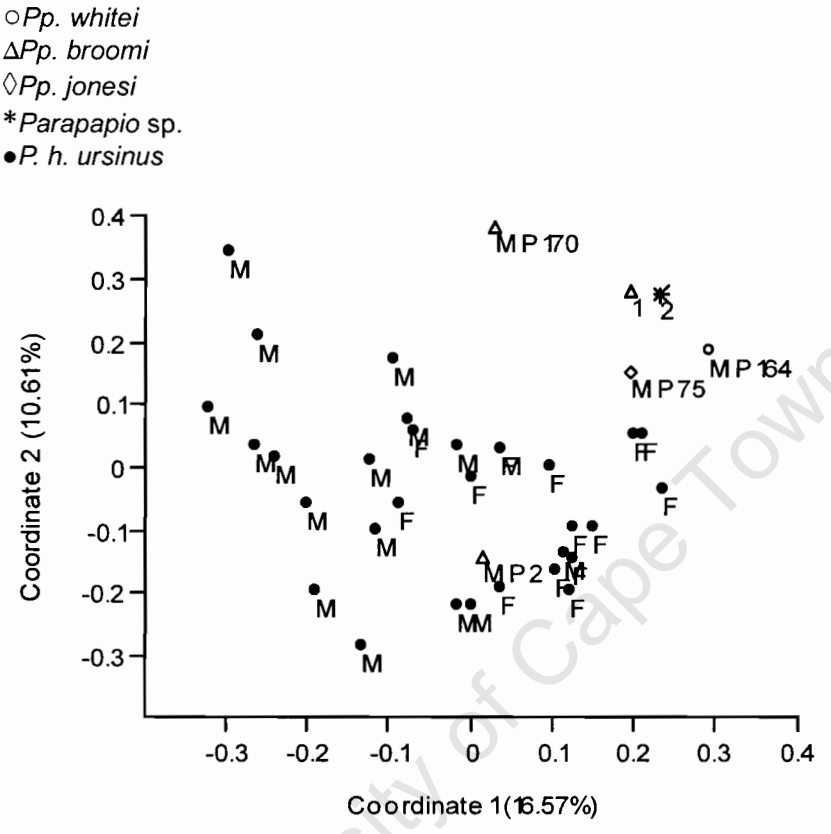

1 = M3065
2 = M3133

6.2. Subset II

The six specimens which comprise Subset II along with the landmarks and inter-landmark distances they share in common are listed in Table 6.2.

Table 6.2. Details for specimens that constitute Subset II.

Accession no.	Taxon	Sex
MP221	*Pp. whitei*	M
MP223	*Pp. whitei*	M
M3070	*Pp. whitei*	F
MP2	*Pp. broomi*	M
M3065	*Pp. broomi*	M
MP170	*Pp. broomi*	F
Anatomical Landmarks		
ZI(R), NA, ZS(R), FMO(R), GL, ON(R), ON(L)		
Inter-Landmark Distances		
ZI(R)-NA, ZI(R)-ZS(R), ZI(R)-FMO(R), ZI(R)-ON(R), ZI(R)-GL, ZI(R)-ON(L), NA(R)-ZS(R), NA-FMO(R), NA-ON(R), NA-GL, NA-ON(L), ZS(R)-FMO(R), ZS(R)-ON(R), ZS(R)-GL, ZS(R)-ON(L), FMO(R)-ON(R), FMO(R)-GL, FMO(R)-ON(L), ON(R)-GL, ON(R)-ON(L), GL-ON(L)		

6.2.1. Cluster Analysis of Inter-landmark Distances

6.2.1.1. Extant Baboon Sample

A single linkage cluster analysis (Fig. 6.10) performed on the sample of extant chacma baboons, based on the same subset of inter-landmark distances as Subset II, clearly separates male and female specimens from each other. This clustering probably reflects basic size and size-related shape differences between males and females. The accuracy of the clustering suggests that this set of inter-landmark distances accurately reflect differences between male and female specimens.

Figure 6.10. A Tree diagram based on a single linkage cluster analysis performed on Subset II inter-landmark distances of the extant baboons sample. (n = 31, F = 14, M = 17)

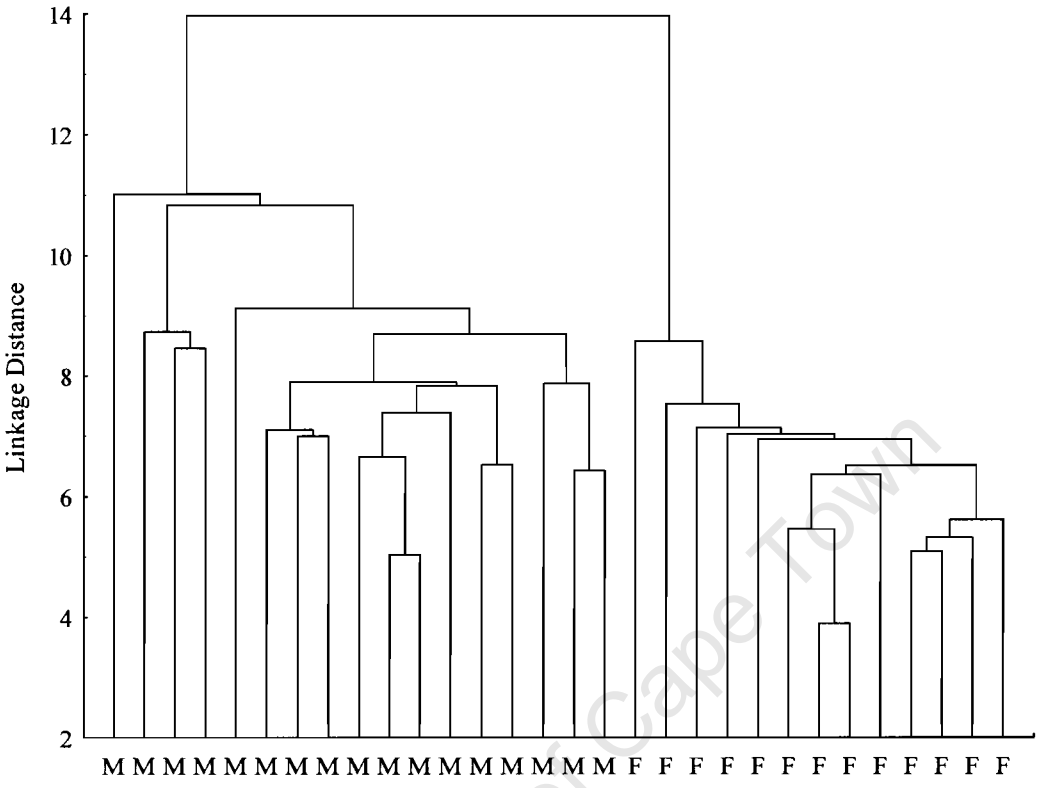

6.2.1.2. Fossil Cercopithecoid Sample

Figure 6.11. A Tree diagram based on a single linkage cluster analysis performed on Subset II inter-landmark distances of the Subset II fossil cercopithecoid subsample. (n = 6, *Pp. whitei* = 3, *Pp. broomi* = 3)

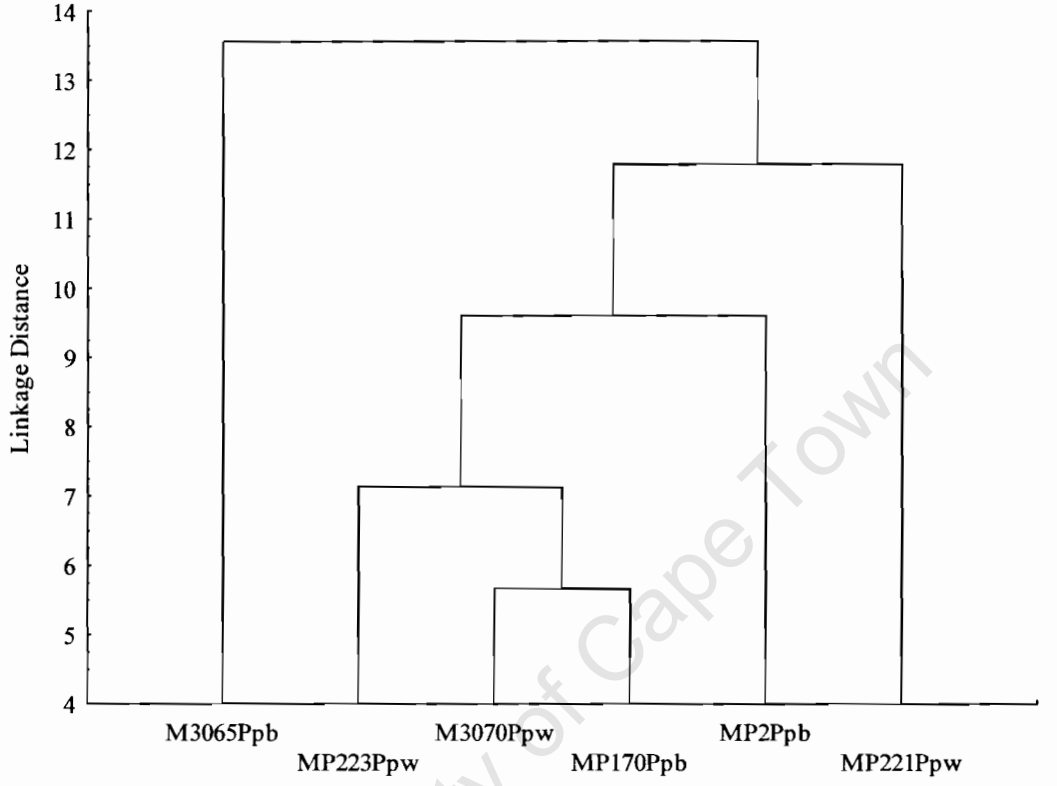

This subset consists of two male *Pp. whitei* and two male *Pp. broomi* specimens and it would be expected that specimens of the same sex and species should show the greatest affinity with one another. Contrary to this expectation the *Pp. whitei* male (MP223) shows greatest affinity to the male *Pp. broomi* (MP2). The two female specimens; M3070 (*Pp. whitei*, female) and MP170 (*Pp. broomi*, female) also show greater affinity with one another than with other specimens. This may suggest that these measurements reflect basic sex differences but are not sensitive to taxonomic differences. As with Subset I, specimens do not cluster together as would be predicted from their current taxonomic assignments.

6.2.2. Principal Components Analysis and Principal Coordinates Analysis

6.2.2.1. Extant Baboon Sample

The plot of PC1 vs. PC2 (Fig. 6.12), based on PCA of Subset II inter-landmark distances of the extant baboon sample, shows clear separation of male from female specimens along the PC1 axis. There appears to be no polarisation along the PC2 axis. Individual loadings for the PC1 axis are all positive whereas most loading on the PC2 axis are negative. This indicates that the PC1 axis mainly summarises size and size-related shape whereas the PC2 axis summarises other aspects of shape. It appears that specimens that are more positively ordinated along the PC1 axis differ considerably from specimens that fall more negatively along the same axis in the height and breadth of the infra-orbital and orbital regions of the midface. Male specimens appear to have taller infra-orbital regions (ZI-ZS, ZI-FMO) and larger orbits (e.g. ZS-ON, NA-FMO) than female specimens. The larger male specimens also appear to vary more in shape (PC2) than the smaller female specimens.

Figure 6.12. Plot of PC1 vs. PC2 based on PCA with 95% ellipses of Subset II inter-landmark distances of the extant baboon sample. (n = 31, F = 14, M = 17)

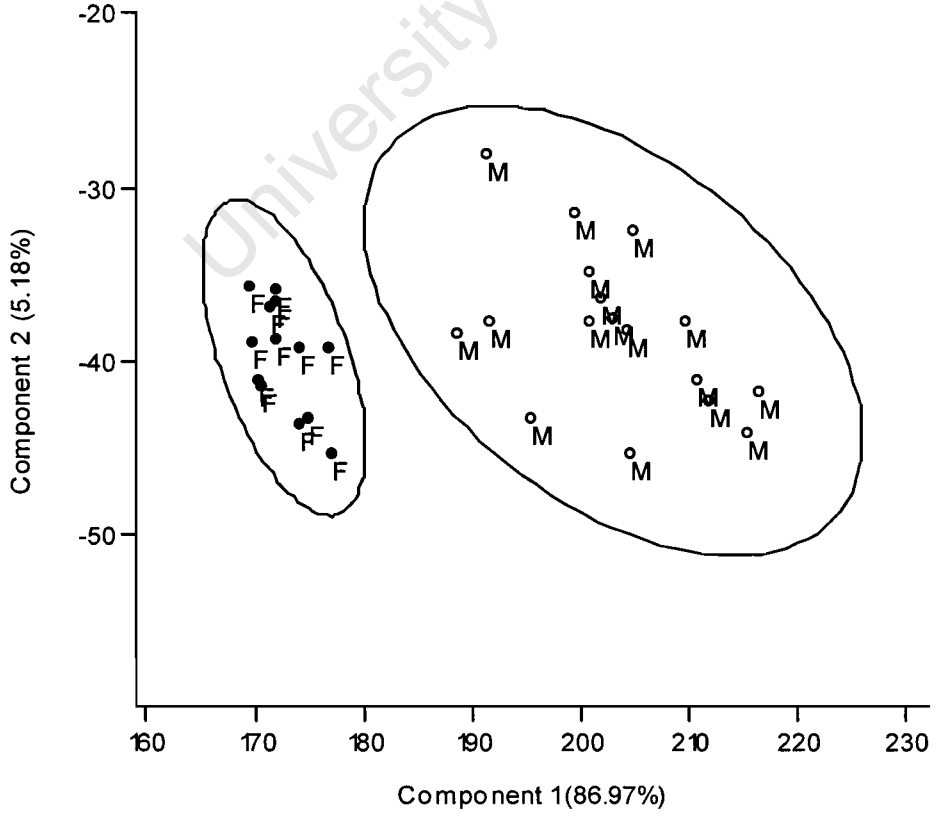

Stepwise DFA of Subset II inter-landmark distances identified only one variable as a significant discriminator; ZS(R)-FMO(R). However this may be because most of the inter-landmark distances for this subset measure the height and width of the upper-/midface around the infraorbital and orbital region. These measurements for the upper-/midface probably discriminate between male and female specimens equally well and in the same way, and thus duplicate one another in their discriminatory power. Fig. 6.13 and Fig. 6.14 below shows the most significant discriminator is shown as a white dotted line along with some of the non-significant inter-landmark distances, which are shown in black.

Figure 6.13. and **Figure 6.14.** Most significant discriminators between male and female baboon crania for Subset II inter-landmark distances.

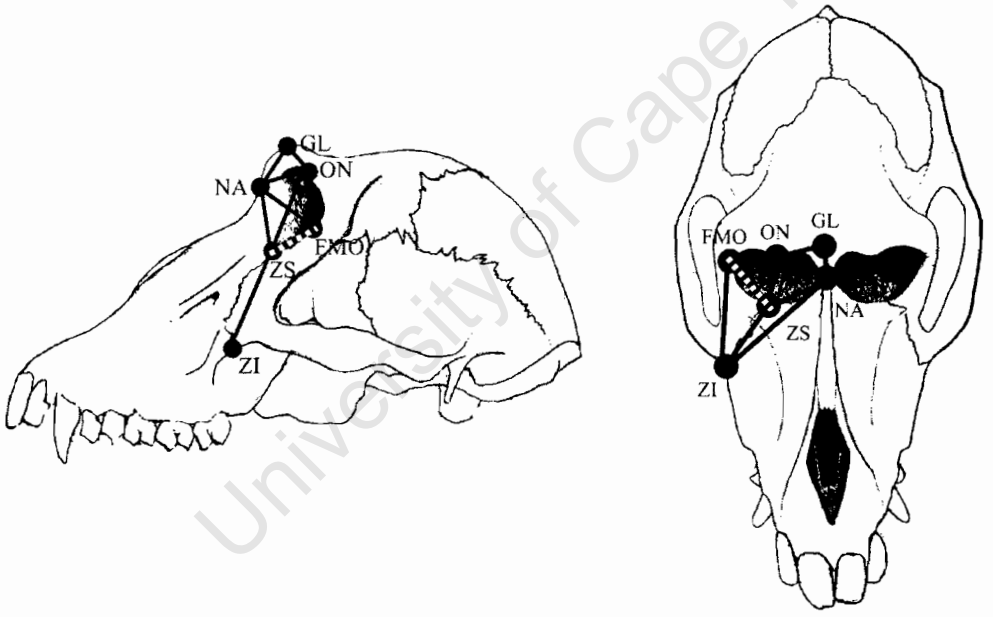

The plot of Coordinate 1 vs. Coordinate 2 (Fig. 6.15), based on a PCoord analysis of Subset II Procrustes transformed coordinate data of the extant chacma baboon sample, also weakly separates male and female specimens along the Coordinate 1 axis. Specimen loadings along the Coordinate 1 axis were significantly and moderately correlated to the geometric means of specimens across the extant chacma baboon sample ($r^2 = 0.47$, $p < 0.0001$) implying that this axis summarises aspects of both size-related – and size-independent shape. There appears to be no polarisation of sexes along the Coordinate 2 axis, which probably mostly summarises size-independent shape. Specimens that are more negatively positioned along the Coordinate 1 axis

have longer and broader infraorbital and orbital regions than specimens that fall more positively along the same axis; differences separating specimens along this axis relate to differences in the shape of these regions of the midface.

Figure 6.15. Plot of Coordinate 1 vs. Coordinate 2 based on PCoord with 95% ellipses of Subset II Procrustes transformed 3D coordinate landmark data for the extant baboon sample. (n = 31, F = 14, M = 17)

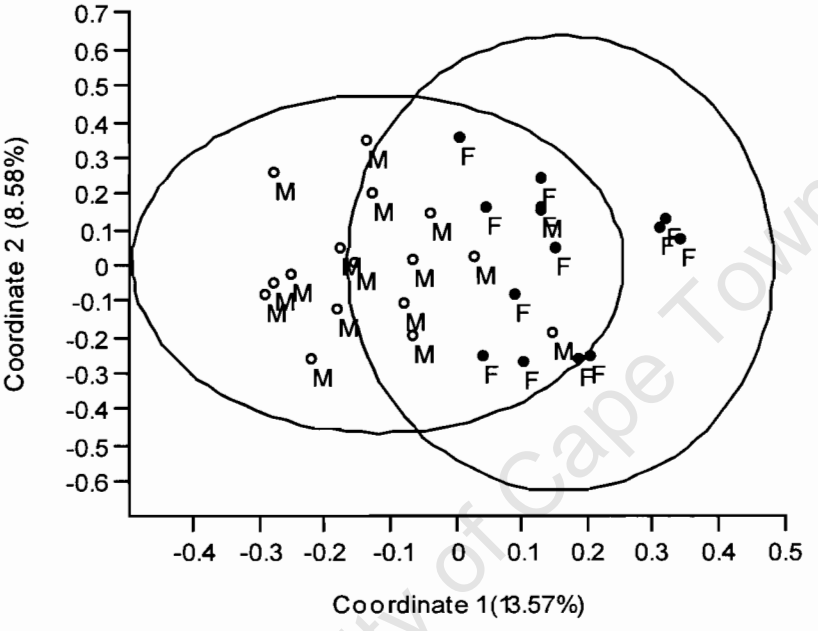

6.2.2.2. Fossil Cercopithecoid Sample

PC1 vs. PC2 based on a PCA of Subset II inter-landmark distances of the *Parapapio* subsample are summarised in Fig. 6.16 below. PC1 explains 62% of the variance and PC2 explains 22% of the variance. Loadings on PC1 are all positive and the majority of loadings on PC2 are positive. This indicates that PC1 reflects mainly size and size-related shape and PC2 reflects other aspects of shape. Specimens that fall more positively along the PC1 axis exhibit a relatively tall upper-/midface and long supraorbital margin relative to specimens that fall more negatively along the same axis. Specimens that are more positively ordinated along the PC2 axis exhibit a relatively short interorbital region (GL-NA) and relatively large orbits compared to specimens that fall more negatively along this axis.

Specimens are not clearly clustered along either axis. Although MP3070 (*Pp. whitei*, female), MP170 (*Pp. broomi*, female) and MP223 (*Pp. whitei*, male) seem to be more

closely associated with each other and have somewhat smaller orbital regions than MP221(*Pp. whitei*, male) and MP2 (*Pp. broomi*, male), these latter two specimens exhibit somewhat shorter interorbital regions than the former pair. M3065 (*Pp. broomi*, male) appears to differ from the main body of specimens along the PC1 axis, having a relatively short upper-/midface and a short supraorbital margin. Within this subset there appears to be no clear polarisation between different taxa or differently sexed specimens with regards to size and shape as reflected in inter-landmark distances.

The plot of Coordinate 1 vs. Coordinate 2 (Fig. 6.17), based on a PCoord analysis of Procrustes transformed coordinate data of the fossil cercopithecoid subsample, show similar patterns observed to those in cluster analysis and PCA. Specimen loadings on either axis were not found to be significantly correlated to the geometric means of specimens across the fossil cercopithecoid subsample, implying that size-correlated shape is not summarised in either axis. There appears to be no clustering along either axis. Specimens are relatively evenly distributed along the Coordinate 2 axis, while only M3065 (*Pp. broomi*, male) appears to be separated along the Coordinate 1 axis, implying a difference in the shape of the orbital region. PCoord reveals no affinities between specimens that can be correlated to their current taxonomic assignment or sex identification.

Figure 6.16. Plot of PC1 vs. PC2 based on PCA of Subset II inter-landmark distances for the Subset II fossil cercopithecoid subsample. (n = 6, *Pp. whitei* = 3, *Pp. broomi* = 3)

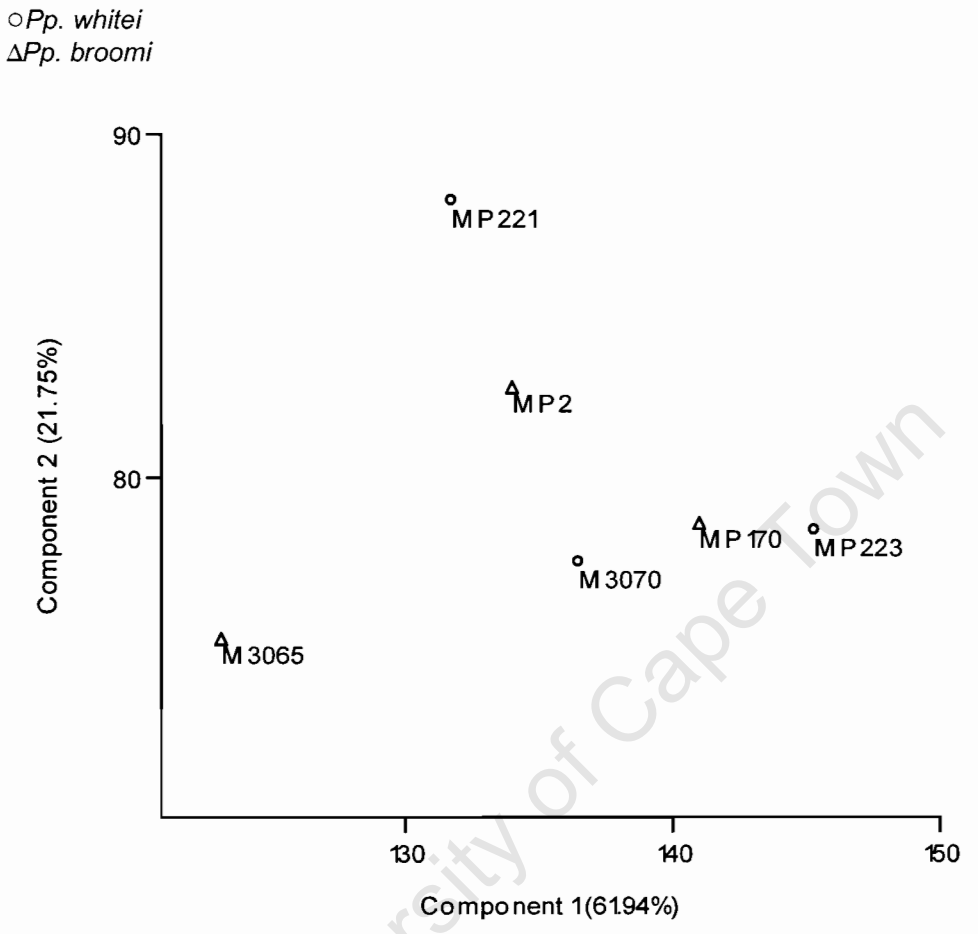

Figure 6.17. Plot of Coordinate 1 vs. Coordinate 2 based on PCoord of Subset II Procrustes transformed coordinate data for the Subset II fossil cercopithecoid subsample. (n = 6, *Pp. whitei* = 3, *Pp. broomi* = 3)

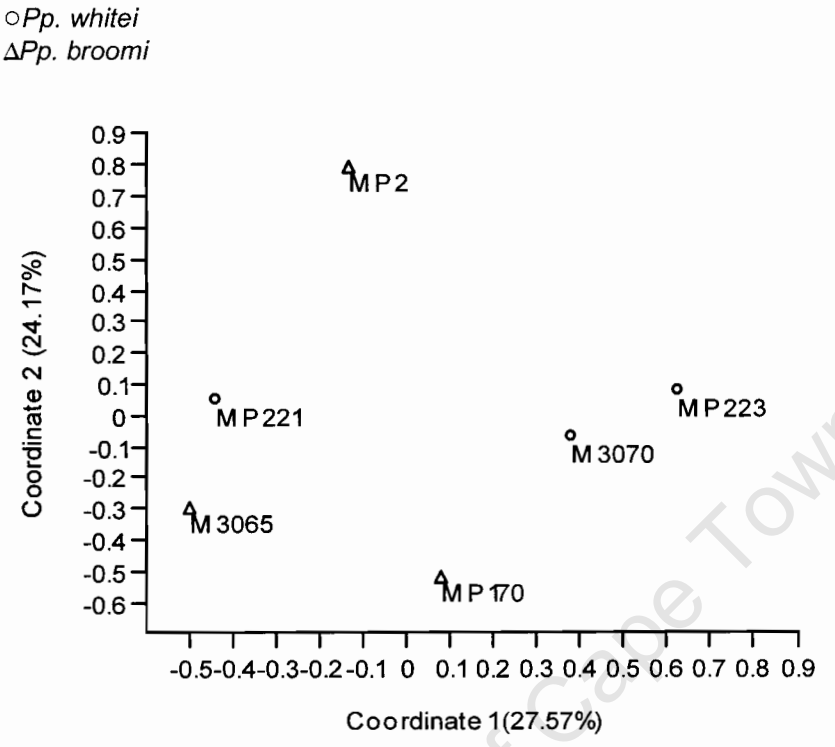

6.2.2.3. Fossil *Parapapio* vs. Extant Baboon Sample

In the plot of PC1 vs. PC2 (Fig. 6.18), based on a PCA of Subset II inter-landmark distances for both the extant chacma baboon and fossil cercopithecoid sample, PC1 explains 87% of the variance and all loadings on this axis are positive, indicating that size and size-related shape is summarised along this axis. PC2 explains 5% of the variance and has a mixture of positive and negative loadings, indicating that it primarily summarises other aspects of shape. *Parapapio* specimens cluster with female chacma baboons in this analysis. Most specimens resemble the extant female chacma sample in having a relatively shorter upper-/midface (PC1) compared to male chacma baboon specimens and resemble the chacma baboon sample in general in aspects of the shape of the upper-/midface and orbital region (PC2), suggesting that *Parapapio* has a relatively tall upper-/midface and large orbits comparable to the extant chacma baboon sample. M3065 is distinguished from the extant female chacma baboons sample as having a relatively short upper-/midface and orbital region, where

as MP223 is distinguished from the main cluster as it has a somewhat larger longer orbital region. Most of the *Parapapio* specimens tend to the outer edge of the female baboon scatter as result of their slightly smaller size of their orbital region and shorter upper-/midface.

Figure 6.18. Plot of PC1 vs. PC2 based on PCA of Subset II inter-landmark distances for the extant baboon sample and the Subset II fossil cercopithecoid subsample (n = 37, *P. h. ursinus* = 31, *Pp. whitei* = 3, *Pp. broomi* = 3).

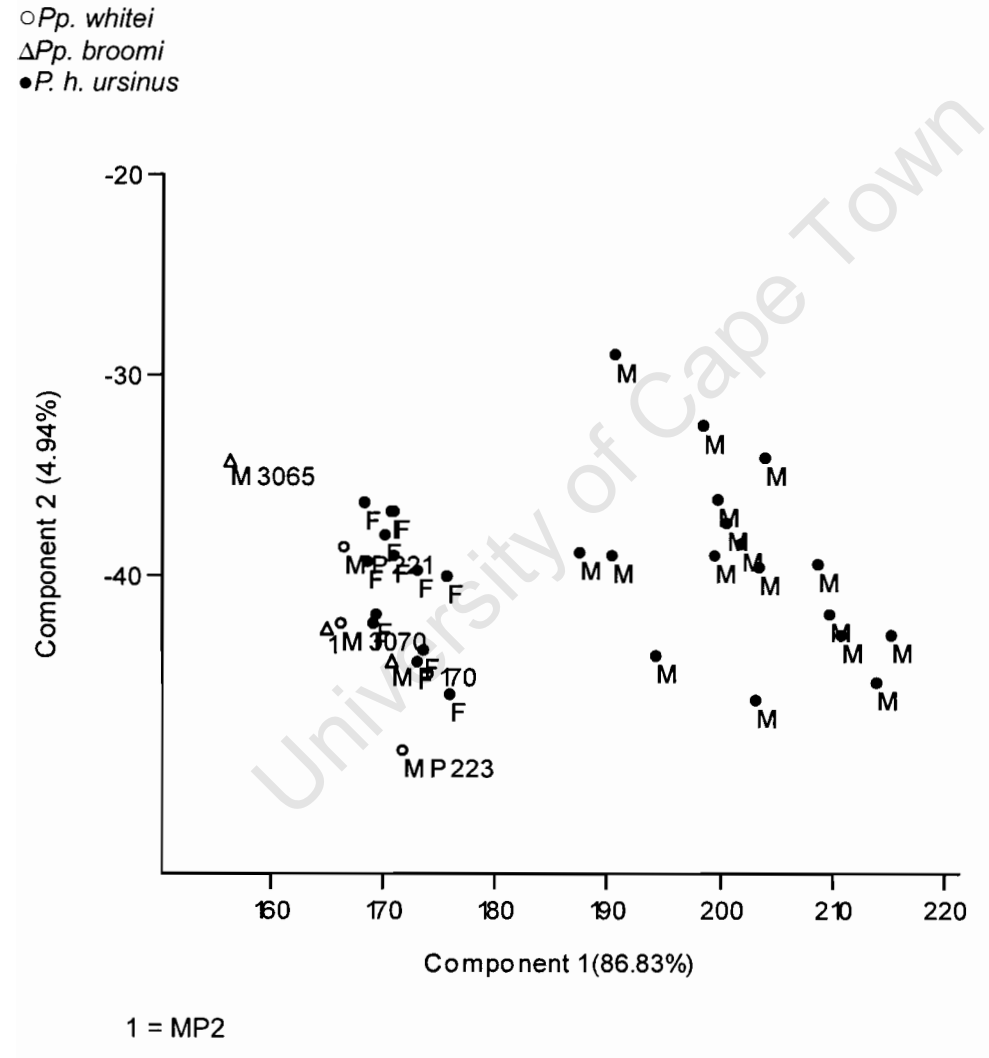

The plot of Coordinate 1 vs. Coordinate 2 (Fig. 6.19), based on PCoord analysis of Subset II Procrustes transformed coordinate data, clearly separated male specimens from female specimens for the extant chacma baboon sample and *Parapapio* from the baboon sample. Polarisation occurs along both the Coordinate 1 and Coordinate 2

axis. Differences among the three groups along the Coordinate 1 axis reflect both differences in size-correlated shape and size-independent shape of the upper-/midface and orbital region perhaps related to the size differences between the different groups. Female chacma baboon specimens are smaller than males, and *Parapapio* specimens tend to resemble smaller female specimens in aspects of size. Differences along the Coordinate 2 axis reflect differences in size-independent shape of these same regions. The *Parapapio* sample clearly differs in the shape of the upper-/midface and orbital region from the extant chacma baboon sample. Furthermore, compared to the extant chacma baboon sample the *Parapapio* sample forms a relatively tight cluster which does not vary more than the extant sample.

Figure 6.19. Plot of Coordinate 1 vs. Coordinate 2 based on PCoord of Subset II Procrustes transformed coordinate data for the extant baboon sample and the Subset II fossil cercopithecoid subsample (n = 37, *P. h. ursinus* = 31, *Pp. whitei* = 3, *Pp. broomi* = 3)

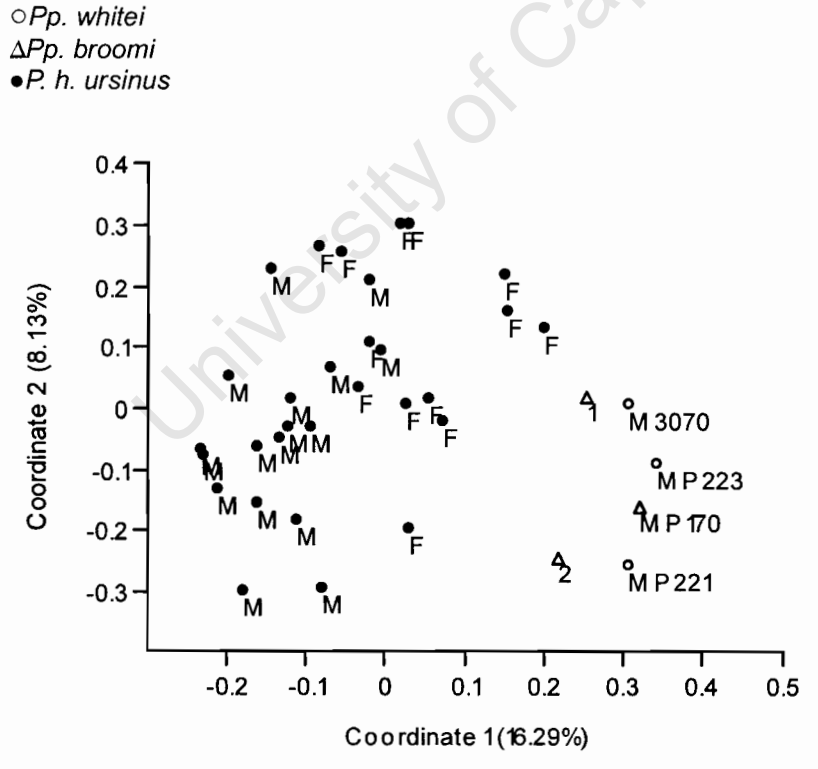

1 = MP2
2 = M3065

6.3. Subset III

The nine specimens which comprise Subset III along with the landmarks and inter-landmark distances they share in common are listed in Table 6.3.

Table 6.3. Details for specimens that constitute Subset III.

Accession no.	Taxon	Sex
MP221	*Pp. whitei*	M
MP223	*Pp. whitei*	M
MP3070	*Pp. whitei*	F
MP2	*Pp. broomi*	M
M3065	*Pp. broomi*	M
MP170	*Pp. broomi*	F
MP239	*Parapapio* sp.	F
M3084	*Parapapio* sp.	I
M3073	*T. darti*	I
Anatomical Landmarks		
NA, ZS(R), FMO(R),ON(R),ON(L),GL		
Inter-Landmark Distances		
NA-ZS(R), NA-FMO(R), NA-ON(R), NA-GL, NA-ON(L), ZS(R)-FMO(R), ZS(R)-ON(R), ZS(R)-GL, ZS(R)-ON(L), FMO(R)-ON(R), FMO(R)-GL, FMO(R)-ON(L), ON(R)-GL, ON(R)-ON(L), GL-ON(L)		

6.3.1. Cluster Analysis of Inter-landmark Distances

6.3.1.1. Extant Baboon Sample

A single linkage cluster analysis (Fig. 6.20) performed on the sample of extant chacma baboons based on the same subset of inter-landmark distances as Subset III, did not separate male and female specimens from each other. Chacma baboons are highly sexually dimorphic and a clear separation between the sexes would be expected. This particular subset of measurements does not appear to capture differences related to sexual dimorphism.

Figure 6.20. A Tree diagram based on a single linkage cluster analysis performed on Subset III inter-landmark distances of the extant baboons sample. (n = 31, F = 14, M = 17)

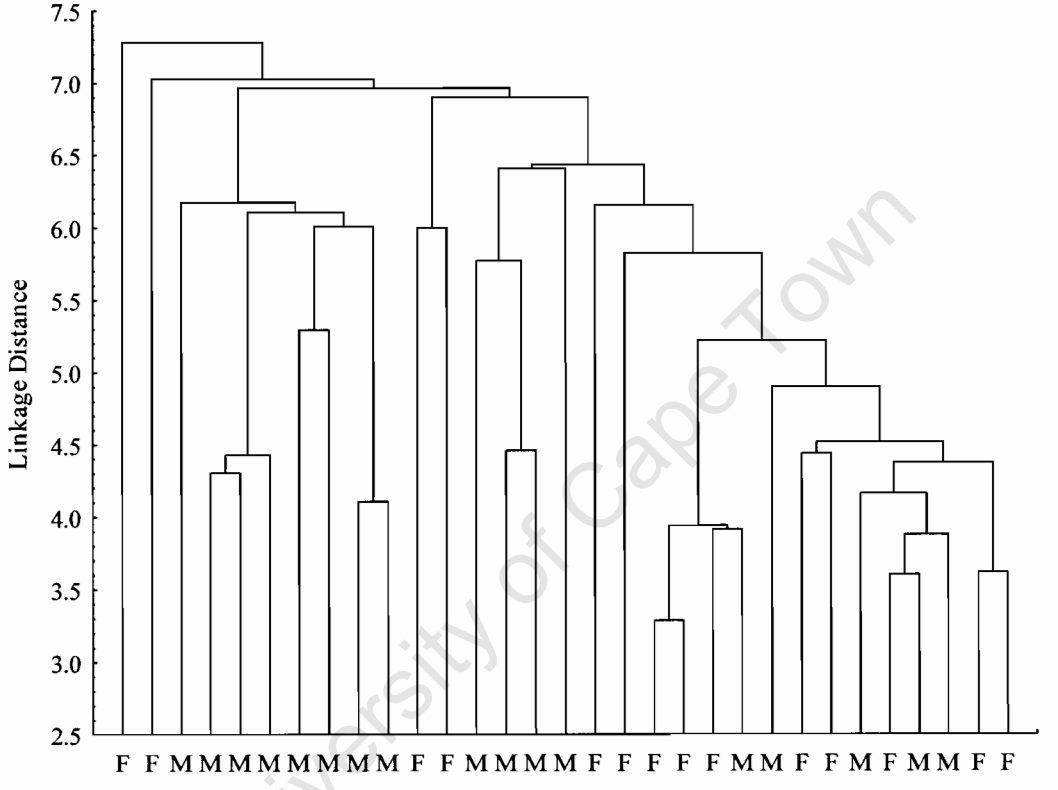

6.3.1.2. Fossil Cercopithecoid Sample

A single linkage cluster analysis (Fig. 6.21) performed on the Subset III fossil cercopithecoid subsample yielded two apparent clusters. M3065 (*Pp. broomi*, male), M3070 (*Pp. whitei*, female), MP239 (*Parapapio* sp. female) and M3073 (*T. darti*) clustered together and was separated from (*Parapapio broomi*, male), MP223 (*Pp. whitei*, male), MP170 (*Pp. broomi*, female) and M3084 (*Parapapio* sp.) which formed the second cluster. It would be expected that specimens of the same taxonomic affinity would cluster together, but this does not appear to be the case. It also does not appear that specimens are separated into different sexes, but this is not surprising

since the cluster analysis of the extant chacma baboon sample was unable to differentiate between male and female specimens given this particular set of variables.

Figure 6.21. A Tree diagram based on a single linkage cluster analysis performed on Subset I inter-landmark distances of the Subset III fossil cercopithecoid subsample. (n = 9, *Pp. whitei* = 3, *Pp. broomi* = 3, *Parapapio* sp. = 2, *T. darti* = 1).

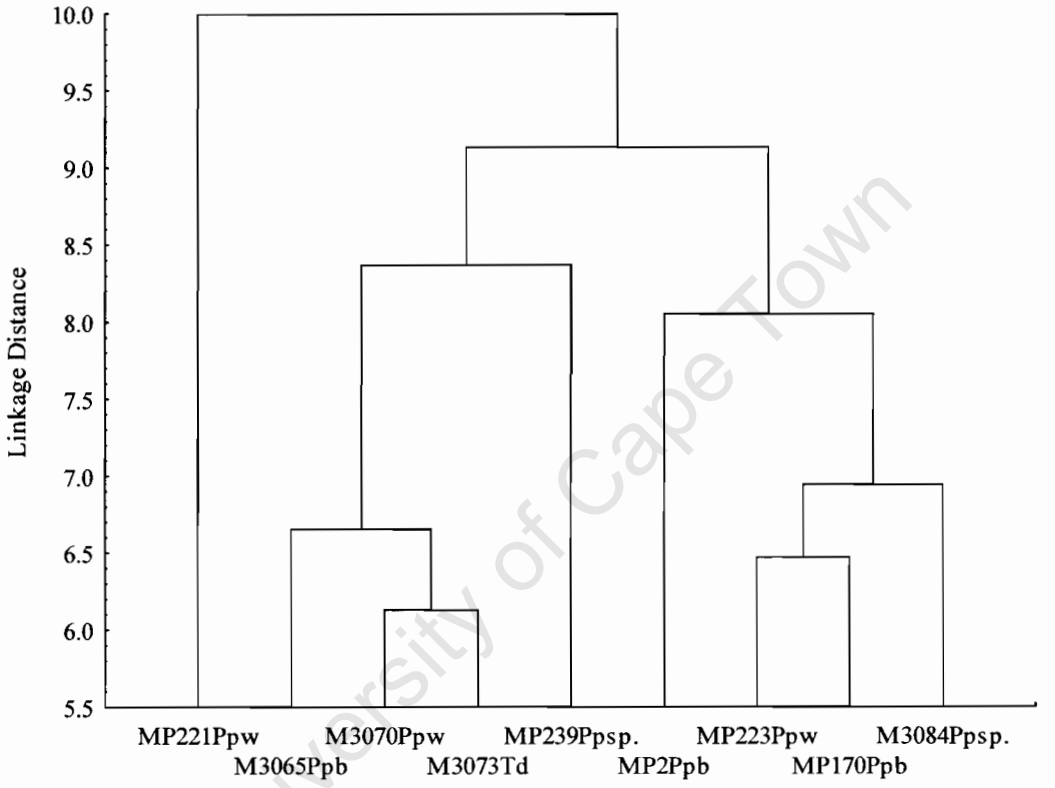

6.3.2. Principal Components Analysis and Principal Coordinates Analysis

6.3.2.1. Extant Baboon Sample

Surprisingly the plot of PC1 vs. PC2 (Fig. 6.22), based on Subset III inter-landmark distances of the extant chacma baboons sample, was able to discriminate between male and female specimens in the extant chacma baboon sample. PC1 summarises 75% of the variation and appears to reflect size and size-related shape, since all the loadings on this axis are positive. Male and female specimens are separated along this axis. Specimens with relatively tall (ZS-ON), large orbits and long supraorbital margins (FMO-ON, ON-GL) fall more positively along the PC1 axis than specimens

with smaller, shorter orbits and upperfaces. It also appears that the generally larger male specimens vary more along the PC1 axis than do females. PC2 yielded a mixture of positive and negative loadings, implying that this axis summarises other aspects of shape. There is no apparent polarisation along the PC2 axis which summarises for 8% of the variance. Male and female specimens appear to differ in the size, but not in the shape of the orbital region. PCA indicates that the Subset III variables mainly reflect simple size differences between male and female specimens. It is not clear why cluster analysis was unable to discriminate between male and female specimens.

Figure 6.22. Plot of PC1 vs. PC2 based on PCA with 95% ellipses of Subset III inter-landmark distances for the extant baboon sample. (n = 31, F = 14, M= 17)

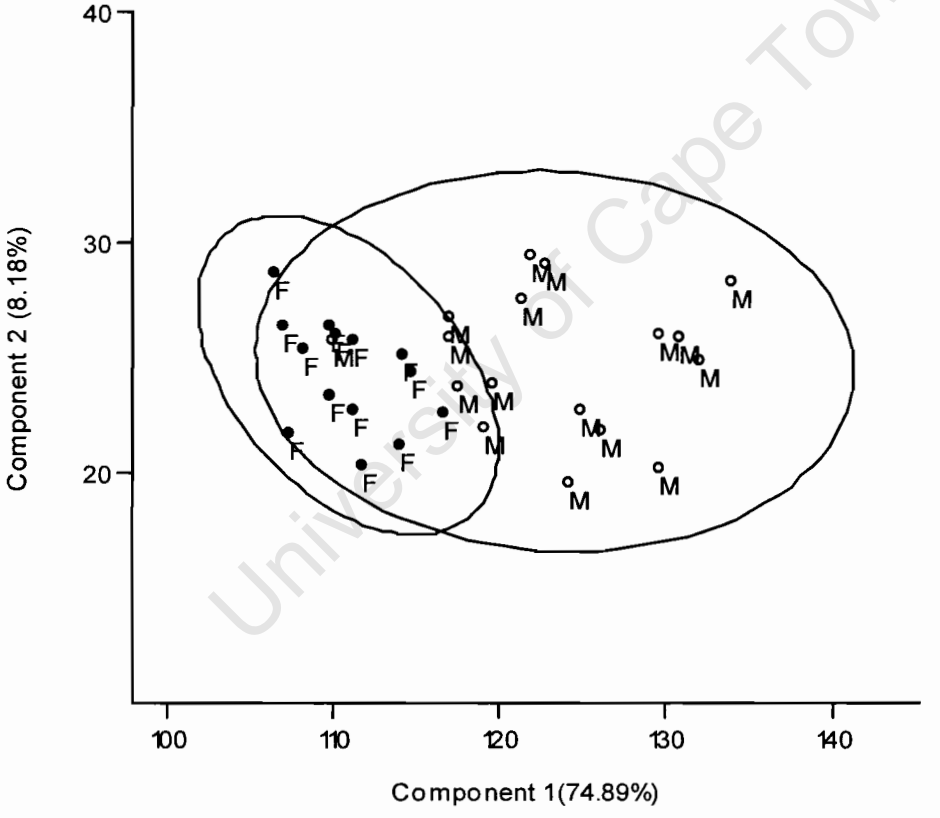

Stepwise Discriminant Function Analysis only yielded one significant discriminating inter-landmark distance; NA-FMO(R). As with the previous subsets this may be because most of the inter-landmark distances for Subset III measure the same differences between individuals (height and width of the orbital region) and are more or less equal in their discriminatory power. Some inter-landmark distances are shown in Fig. 6.23 and Fig. 6.24 below to demonstrate the dimensions recorded by

Subset III variables. The most significant discriminator (NA-FMO(R)) is indicated by the white dotted line.

Figure 6.23. and **Figure 6.24.** Most significant discriminators between male and female baboon crania for Subset III inter-landmark distances.

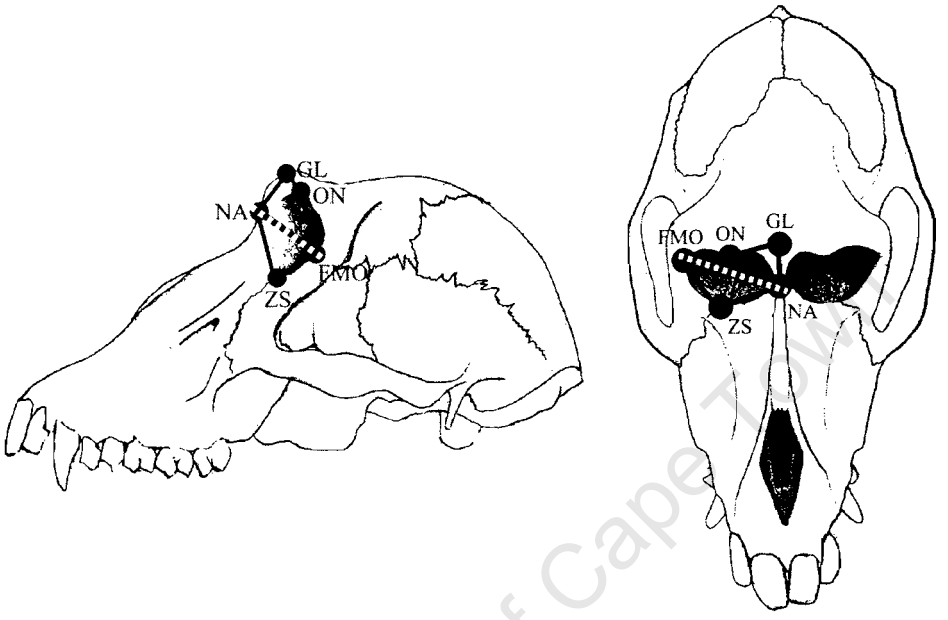

The plot of Coordinate 1 vs. Coordinate 2 (Fig. 6.25), based on a PCoord analysis of Subset III Procrustes transformed coordinate data of the extant chacma baboon sample, analysis was unable to distinguish between male and female specimens in the extant chacma baboon sample confirming the indications observed in the PCA (Fig. 6.22) that male and female specimens do not differ in the shape of the orbital region regardless of differences in size between the sexes. However, it does appear that specimen loadings on the Coordinate 1 axis are significant and moderately correlated to the geometric means of specimens across the extant baboon sample ($r^2 = 0.40$, $p < 0.001$) indicating that this axis is influenced by size-correlated shape, implying that the shape differences along the Coordinate 1 axis are correlated to size differences but not size as a function of sex.

Figure 6.25. Plot of Coordinate 1 vs. Coordinate 2 based on PCoord with 95% ellipses of Subset III Procrustes transformed coordinate data for the extant baboon sample. (n = 31, F = 14, M = 17)

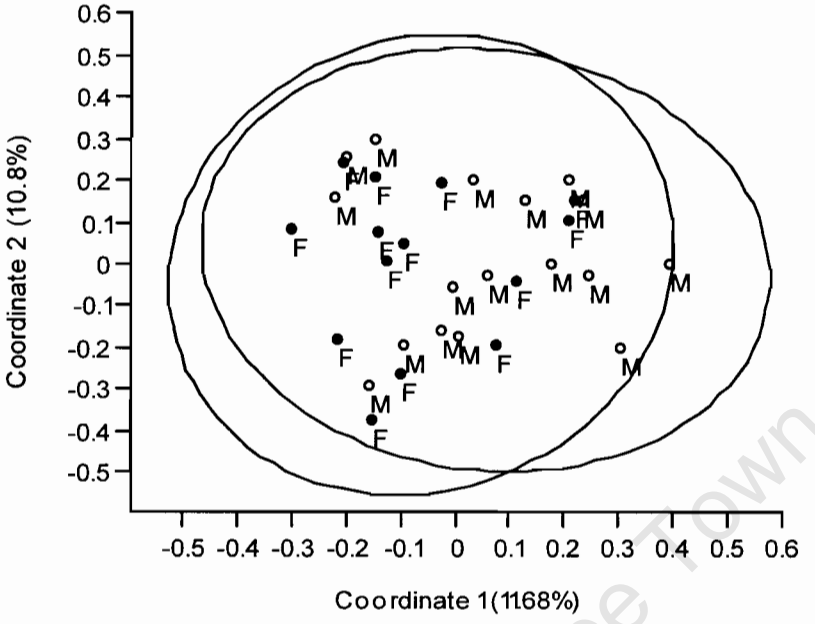

6.3.2.2. Fossil Cercopithecoid Sample

Plot of PC1 vs. PC2 (Fig. 6.26), based on a PCA of Subset III inter-landmark distances of the fossil cercopithecoid subsample, shows some separation of specimens along the PC1 axis which accounts for 51% of the variance. All loadings on PC1 are positive indicating that it mainly reflects size and size-correlated shape. PC2 explains 26% of the variance and about half the loadings on PC2 are negative indicating that it summarises other aspects of shape. Specimens with large, tall orbits and long supraorbital margins fall more positively along the PC1 axis. Specimens which fall more positively along the PC2 axis have relatively broad orbits but a relatively short interorbital region compared to specimens which fall more negatively along this axis. The separation along the PC1 axis suggests two size groupings and mirrors the result of the cluster analysis for this subsample. MP221 appears to occupy a more positive position along the PC2 axis which may be heavily influenced by its noticeably shorter interorbital region (NA-GL). PCA does not clearly distinguish between *Parapapio* and *Theropithecus* and does not group *Parapapio* specimens according to their current taxonomic affinities.

Figure 6.26. Plot of PC1 vs. PC2 based on PCA of Subset III inter-landmark distances for the Subset III fossil cercopithecoid subsample. (n = 9, *Pp. whitei* = 3, *Pp. broomi* = 3, *Parapapio* sp. = 2, *T. darti* = 1)

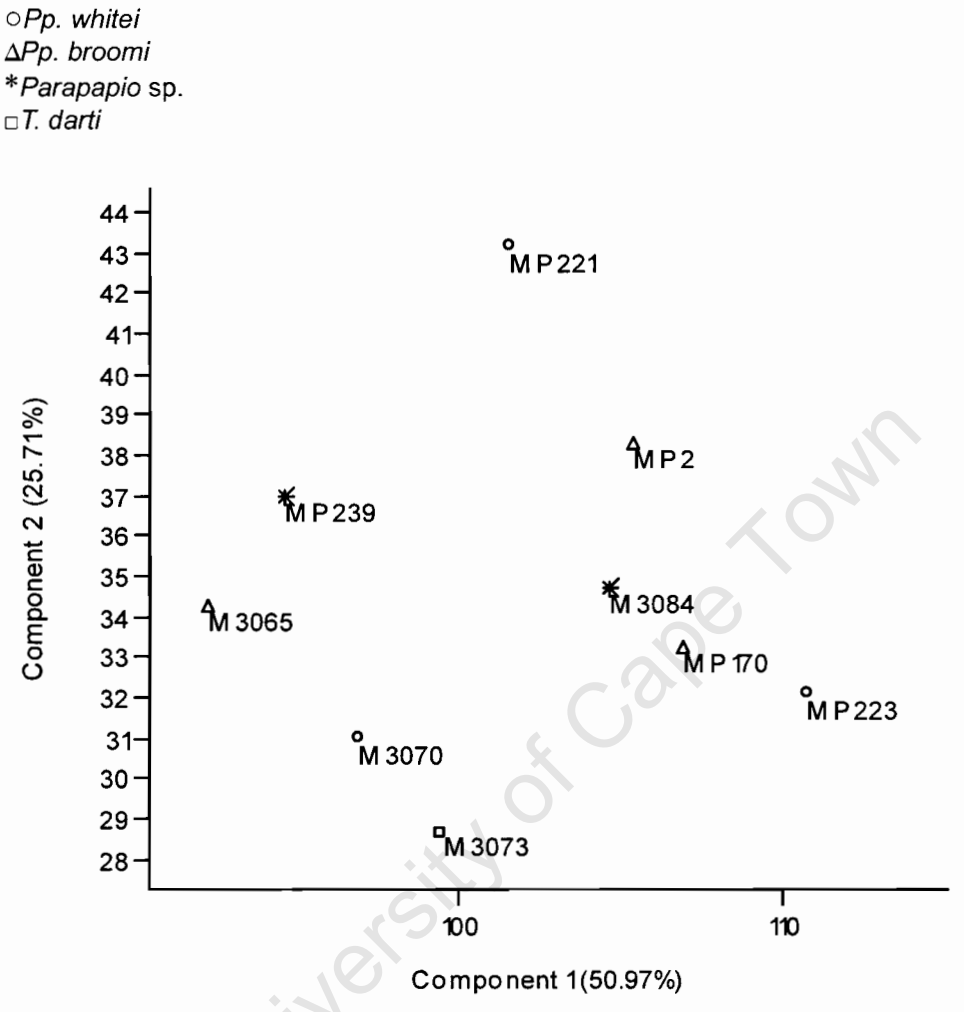

The plot of Coordinate 1 vs. Coordinate 2 (Fig. 6.27), based on PCoord analysis of Subset III coordinate data for the fossil cercopithecoid subsample, shows some polarisation along the Coordinate 2 axis. Neither axis is significantly correlated to the geometric means across the fossil subsample, indicating that both axes mainly summarise aspects of size-independent shape. There appears to be some separation between specimens along the Coordinate 2 axis indicating a size-independent shape difference around the orbital regions between specimens. This separation between specimens does not correlate the pattern observed in the plot of PC1 vs. PC2. Furthermore there appears to be no taxonomic signal in the data distinguishing different *Parapapio* taxa from one another. The data was also unable to clearly distinguish between the *T. darti* specimen (M3073) and the *Parapapio* subsample. A

close affinity in the shape of the orbital region is also indicated between the *T. darti* specimen and the relatively large female *Pp. broomi* specimen (MP170).

Figure 6.27. Plot of Coordinate 1 vs. Coordinate 2 based on PCoord of Subset III Procrustes transformed coordinate data for the Subset III fossil cercopithecoid subsample. (n = 9, *Pp. whitei* = 3, *Pp. broomi* = 3, *Parapapio* sp. = 2, *T. darti* = 1)

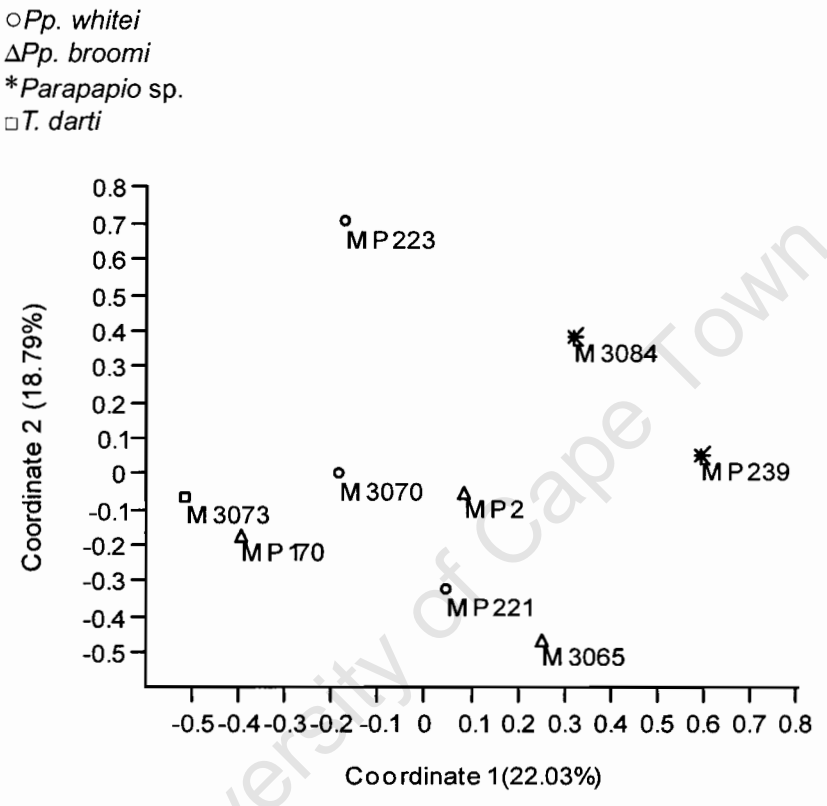

6.3.2.3. Fossil *Parapapio* vs. Extant Baboon Sample

Plot of PC1 vs. PC2 (Fig. 6.28) and Coordinte1 vs. Coorinate2 (Fig. 28) based on a PCA and a PCoord analysis of Subset III inter-landmark distances and Procrustes transformed coordinate data of the fossil cercopithecoid subsample and the extant chacma baboon sample are presented below. PC1 accounts for 75% variation and reflects mainly size. Larger, mostly male *Parapapio* specimens fall well within the extant female chacma baboon range along the PC1 axis indicating a similarity in size. MP170, a female *Pp. broomi* appears to be quite large as it is associated with this group. The *Parapapio* subsample appears to have a similar range of variation to the extant chacma baboon sample along the PC2 axis. Only one individual MP221 (*Pp.*

whitei, male) falls out side of this range along the PC2 axis, but falls within the range along the PC1 axis, reflecting a similarity in size and a difference in shape, probably related to its unusually short interorbital region. PCA only weakly distinguishes the *T. darti* specimen (M3073) from the *Parapapio* subsample and the extant chacma baboon sample as it lies immediately outside the bottom edge of the range for these two samples.

The fossil cercopithecoid subsample is clearly separated from the extant chacma baboon sample along the Coordinate 1 axis of the plot of Coordinate 1 vs. Coordinte2 (Fig. 6.29). This suggests that although they may share similarities in aspects of size of the orbital region and upperface they clearly differ in the shape of the orbital region from one another. The extent of the variation in shape along the Coordinate 2 axis also does not exceed the extent of the variation observed for the extant chacma baboon sample. MP221, although it differed from the main *Parapapio* sample in some aspects of the interorbital region (Fig. 6.28), does not differ in shape of the orbital region from the main body of the *Parapapio* subsample and neither does the *T. darti* specimen (M3073).

Figure 6.28. Plot of PC1 vs. PC2 based on PCA of Subset III inter-landmark distances for the extant baboon sample and Subset III fossil cercopithecoid subsample. (n = 40, *P. h. ursinus* = 31, *Pp. whitei* = 3, *Pp. broomi* = 3, *Parapapio* sp. = 2, *T. darti* = 1)

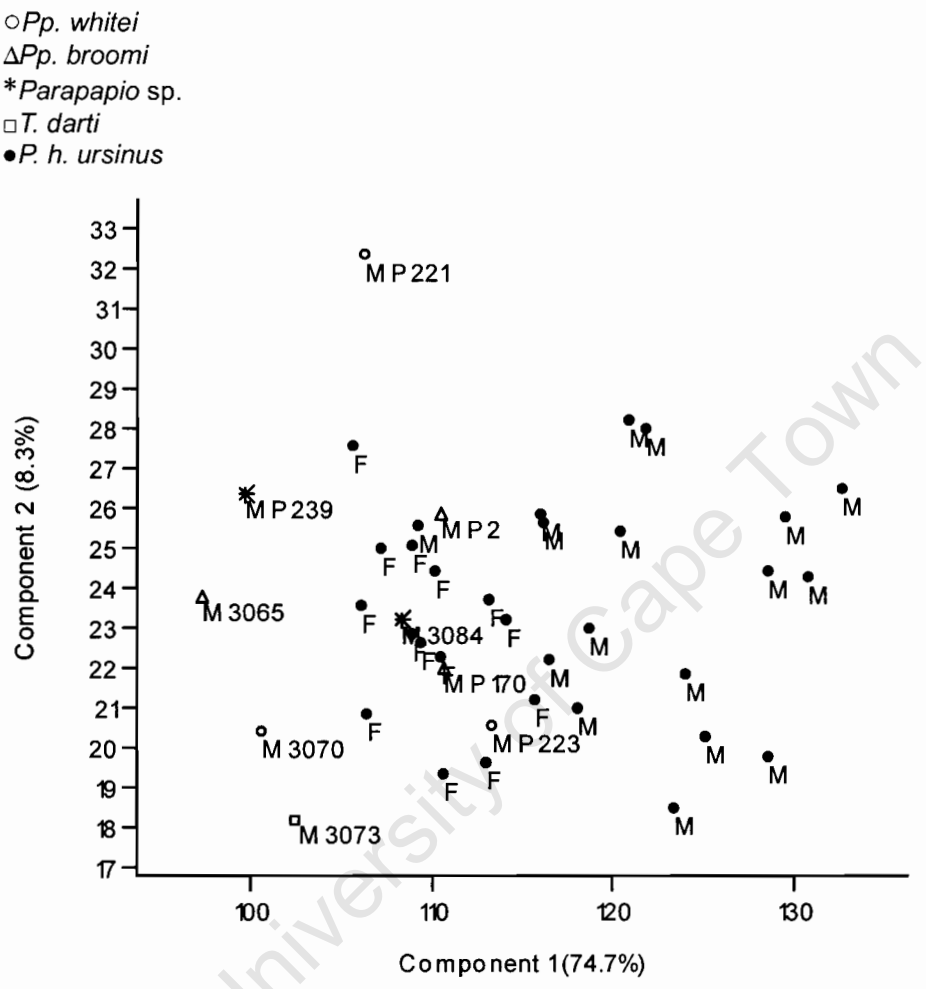

Figure 6.29. Plot of Coordinate 1 vs. Coordinate 2 based on PCoord of Subset III Procrustes transformed coordinate data for the extant baboon sample and the Subset III fossil cercopithecoid subsample. (n = 40, *P. h. ursinus* = 31, *Pp. whitei* = 3, *Pp. broomi* = 3, *Parapapio* sp. = 2, *T. darti* = 1)

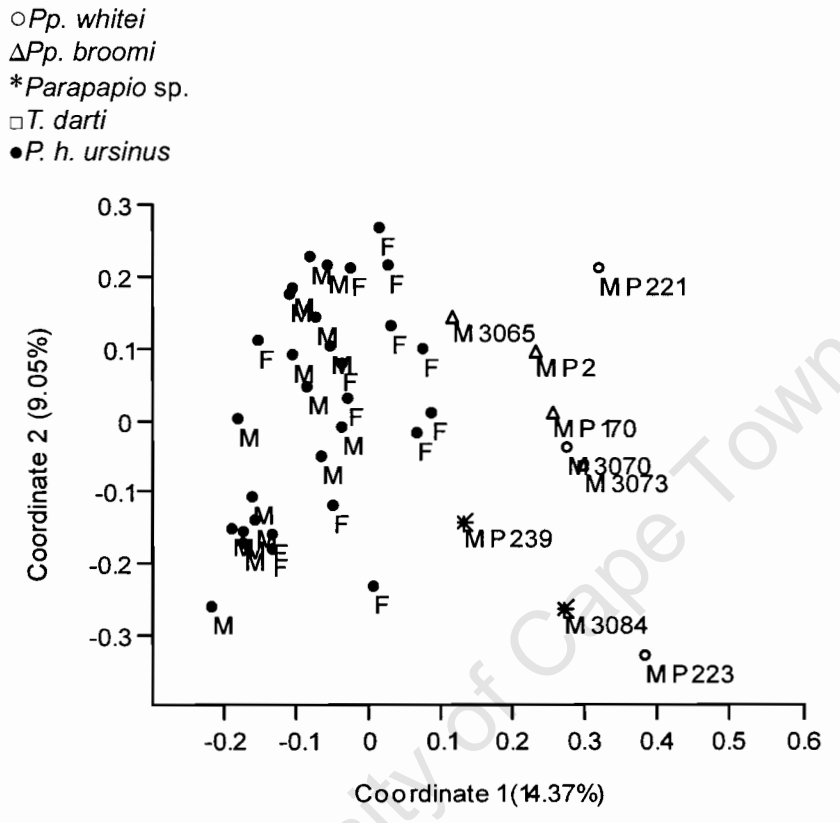

6.4. Subset IV

The ten specimens which comprise Subset IV along with the landmarks and inter-landmark distances they share in common are listed in Table 6.4.

Table 6.4. Details of specimens that constitute Subset IV.

Accession no.	Taxon	Sex
MP221	*Pp. whitei*	M
MP223	*Pp. whitei*	M
M3070	*Pp. whitei*	F
MP239	*Parapapio* sp.	F
M3084	*Parapapio sp.*	I
MP208	*Parapapio sp.*	I
MP47	*Parapapio sp.*	I
M3078	*Parapapio sp.*	I
M3073	*T. darti*	I
MP3	*C. williamsi*	M
Anatomical Landmarks		
PR, NS, PM(R), RH, NA, PM(L), ZS(L)		
Inter-Landmark Distances		
PR-NS, PR-PM(R), PR-RH, PR-NA, PR-PM(L), PR-ZS(L), NS-PM(R), NS-RH, NS-NA, NS-PM(L), NS-S(L), PM(R)-RH, PM(R)-NA, PM(R)-PM(L), PM(R)-ZS(L), RH-NA, RH-PM(L), RH-ZS(L), NA-PM(L), NA-ZS(L), PM(L)-ZS(L)		

6.4.1. Cluster Analysis of Inter-landmark Distances

6.4.1.1. Extant Baboon Sample

A single linkage cluster analysis (Fig. 6.30) performed on the sample of extant chacma baboons, based on the same subset of inter-landmark distances as Subset IV, clearly separates male and female specimens from each other. This separation probably reflects basic size and size-related shape differences between males and females. The accuracy of the clustering suggests that this set of inter-landmark distances is reflects sexual dimorphism.

Figure 6.30. A Tree diagram based on a single linkage cluster analysis performed on Subset IV inter-landmark distances of the extant baboon sample. (n = 31, F = 14, M = 17)

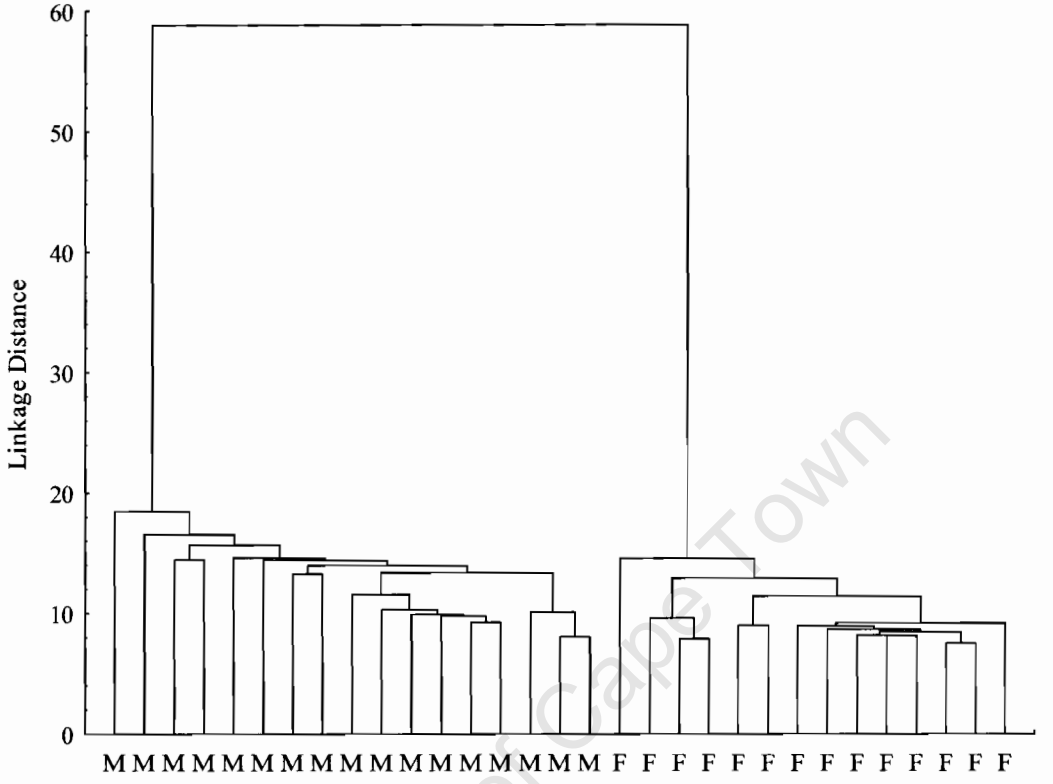

6.4.1.2. Fossil Cercopithecoid Sample

A single linkage cluster analysis (Fig. 6.31) performed on the Subset IV fossil cercopithecoid subsample yielded two main clusters. An unassigned *Parapapio* specimen (MP47) and the *T. darti* specimen (M3073) group together with the relatively larger male *Pp. whitei* (MP221 and MP223) specimens. The second cluster consists of unassigned *Parapapio* specimens, a *Pp. whitei* female (M3070) and a *C. williamsi* specimen (MP3). Cluster analysis is unable to discriminate *T darti* (M3073) and *C. williamsi* (MP3) from *Parapapio* specimens.

Figure 6.31. A Tree diagram based on a single linkage cluster analysis performed on Subset IV inter-landmark distances of the Subset IV fossil cercopithecoids (n = 9, *Pp. whitei* = 3, *Parapapio* = 4, *T. darti* = 1, *C. williamsi* = 1)

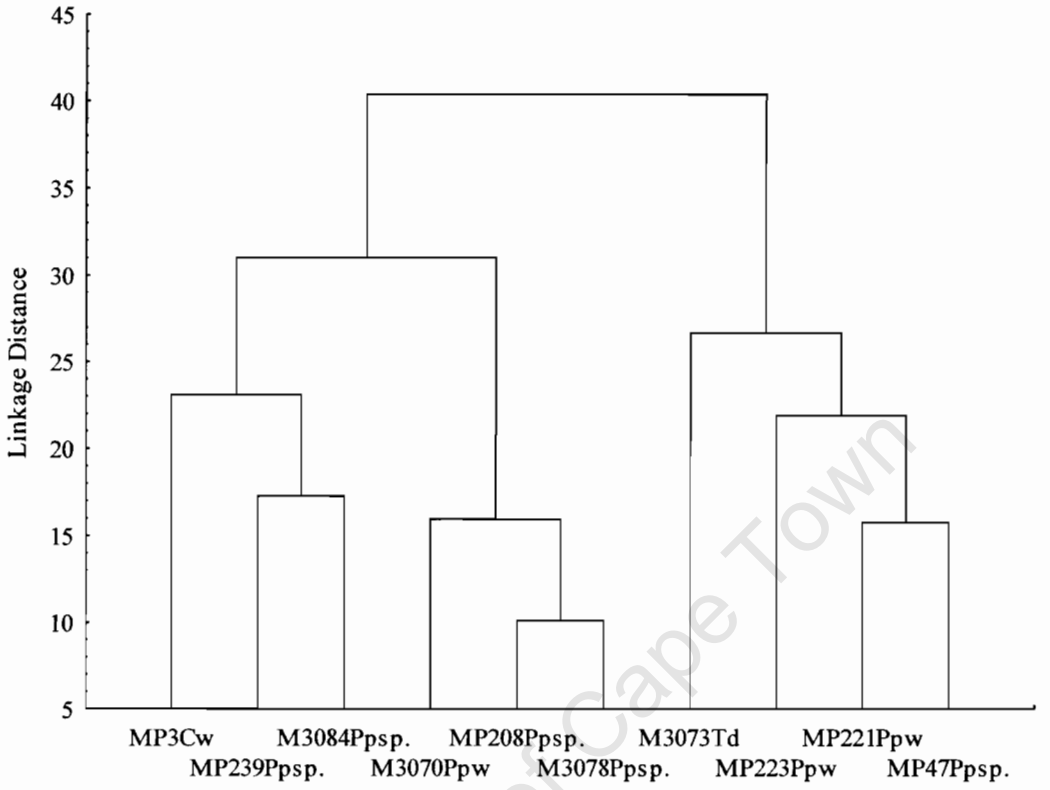

6.4.2. Principal Components Analysis and Principal Coordinates Analysis

6.4.2.1. Extant Baboon Sample

Male and female specimens are clearly separated along the PC1 axis in the plot of PC1 vs. PC2 (Fig. 6.32), based on a PCA of Subset IV inter-landmark distances of the extant chacma baboon sample. PC1 explains 97% of the variance and all loadings on the PC1 axis are positive indicating that it mainly reflects size and size-correlated shape. Males and females are primarily distinguished from one another based on differences in the length of the muzzle (e.g. NS–NA, PR-NA, PR-ZS) Specimens with relatively long muzzles were more positively oriented along the PC1 axis than specimens with short muzzles. The PC2 axis yielded a large number of negative loadings implying that it summarises other aspects of the shape of the muzzle. No separation between sexes occurred along this axis.

Figure 6.32. Plot of PC1 vs. PC2 based on PCA with 95% ellipses of Subset IV inter-landmark distances for the extant baboon sample. (n = 31, F = 14, M= 17)

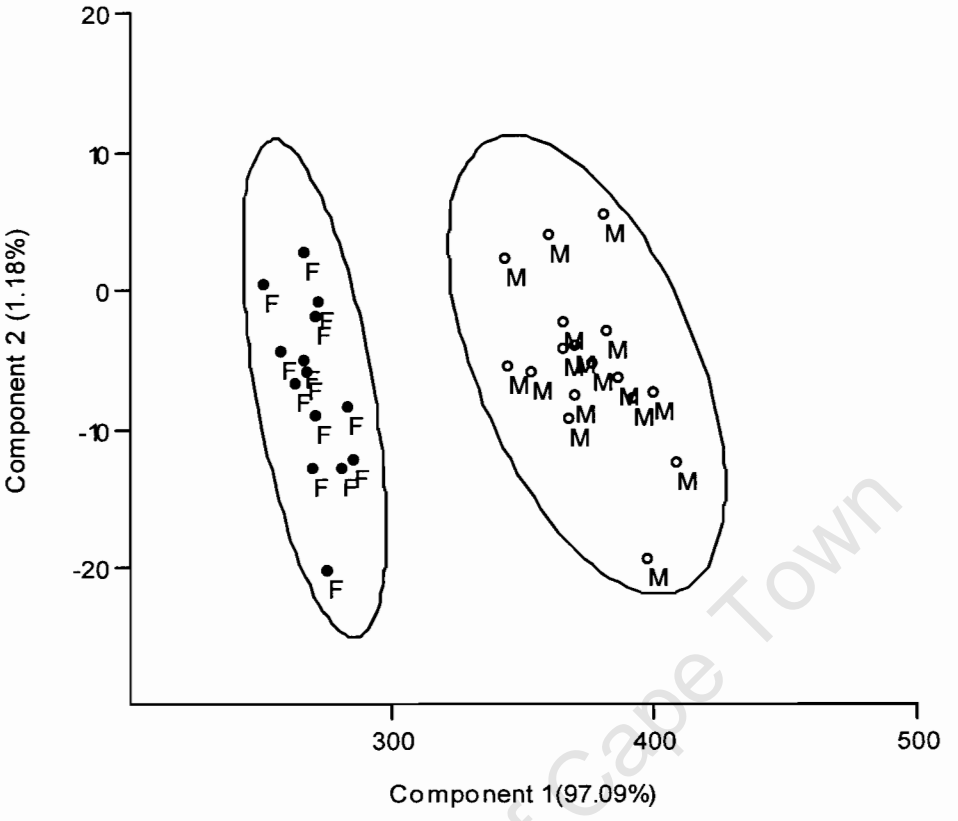

Stepwise Discriminant Function Analysis of Subset IV inter-landmark distances indicated NS-NA to be the most significant discriminator between male and female specimens. Males and females have markedly different mean NS-NA distances; 123 ± 5mm (n = 17) and 88 ± 3mm (n = 14) respectively. NS-NA is indicated as a dotted line on the Fig. 6.33. As can be seen in Fig. 6.33 below most of the Subset IV inter-landmark distances measure the length of the muzzle region. The NS-NA measurement was found to be the most powerful discriminator, but most other measures of the length of the muzzle were also good discriminators as they in part duplicate measurements of the same aspects of the muzzle.

Figure 6.33. Most significant discriminators between male and female baboon crania for Subset IV inter-landmark distances.

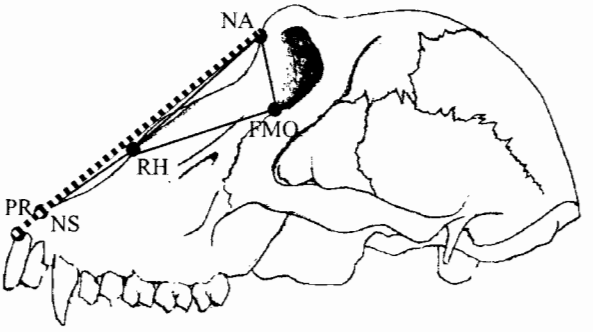

Plot of Coordinate 1 vs. Coordinate 2 (Fig. 6.34), based on a PCoord analysis of Subset IV Procrustes transformed coordinate data of the extant chacma baboon sample, also clearly separates male and female specimens along the Coordinate 1 axis. Males with longer muzzles fall more negatively along the Coordinate1 axis, while females with shorter, less dorsally oriented muzzles fall more positively along the same axis. There appears to be no separation of the sexes along the Coordinate 2 axis. Specimen loadings along both the Coordinate 1 axis ($r^2 = 0.54$, $p < 0.0001$) and the Coodinate2 axis ($r^2 = 0.7$, $p < 0.0001$) are significantly correlated to the geometric means of specimens across the sample. This indicates that both axes summarise aspects of size-correlated shape. Differences in the shape of the muzzle are linked to sexually dimorphic patterns of size difference in the length of the muzzle region. The sexual dimorphic aspect of this size related shape is apparent on the Coordinate 1 axis which correlates well with the patterning of the same specimens along the PC1 axis (Fig. 6.33).

Figure 6.34. Plot of Coordinate1 vs. Coordinate 2 based on PCoord with 95% ellipses of Subset IV Procrustes transformed coordinate data for the extant baboon sample. (n = 31, F = 14, M= 17)

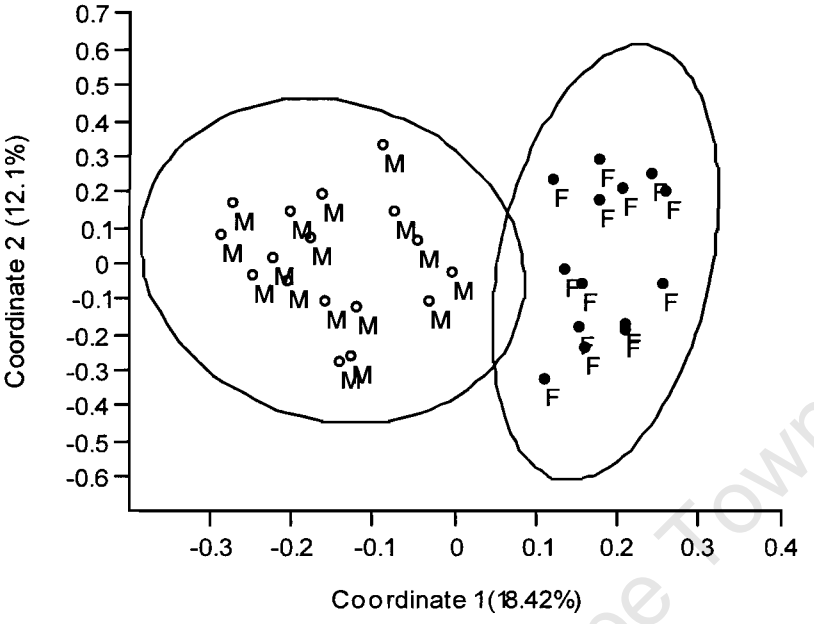

6.4.2.2. Fossil Cercopithecoid Sample

PC1 vs. PC2 (Fig. 6.35), based on a PCA of Subset IV inter-landmark distances of the fossil cercopithecoid subsample, separates specimens along the PC1 axis and the PC2 axis. PC1 accounts for 90% of the variance and PC2 for 6% of the variance. PC1 reflects size and size-correlated shape while the majority of the loadings on PC2 are negative implying that this axis summarises other aspects of shape. Specimens that fall more positively along the PC1 axis have relatively long muzzles compared to specimens that fall less positive positions along this axis. Specimens to the right on PC1 have particularly long muzzles (77 ± 7 mm, n = 4) and specimens to the left have relatively short muzzles (55 ± 4 mm, n = 6). Specimens that fall more positively along the PC2 have a relatively short anterior muzzle, specifically related to the length of the nasal aperture (NS-RH).

MP3 (*C. williamsi*) does seem to be separated from the *Parapapio* specimens along the PC2 axis reflecting its relatively short muzzle and substantially longer nasal aperture. MP3 falls within the range of muzzle lengths for the specimens along the left on the PC1 axis which are characterised by somewhat shorter muzzle lengths, most notably in their NS-NA measurements. Other specimens with shorter muzzles, mainly

consist of female *Parapapio* and unassigned and unsexed *Parapapio* specimens, whereas the specimens which fall to the right on this axis consist of two male *Pp. whitei* specimens and one unassigned and unsexed *Parapapio* specimen. The polarisation along the PC1 axis may suggest a sexual dimorphic signal within the sample. Furthermore M3084 and MP239 resemble one another in having relatively long nasal apertures compared to M3070, M3078 and MP208, although M3084 and M239 and M3070, M3078 and MP208 have similar overall muzzle lengths.

Figure 6.35. Plot of PC1 vs. PC2 based on PCA of Subset IV inter-landmark distances for the Subset IV fossil cercopithecoid subsample. (n = 9, *Pp. whitei* = 3, *Parapapio* sp. = 4, *T. darti* = 1, *C. williamsi* = 1)

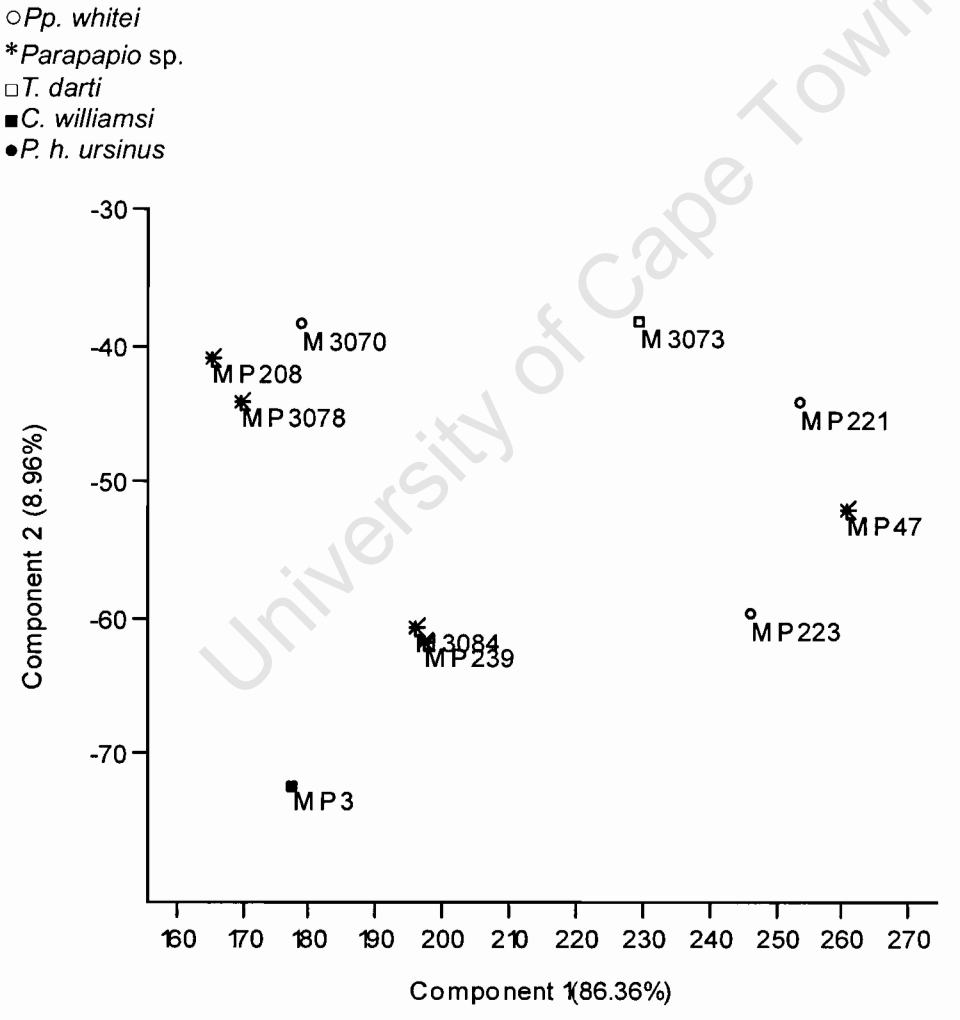

The plot of Coordinate 1 vs. Coordinate 2 (Fig. 6.36), based on a PCoord analysis of Subset IV Procrustes transformed coordinate data, generally ordinates specimens

relative to one another in a similar pattern as the plot of PC1 vs. PC2 (Fig. 6.35). The specimen loadings on the Coordinate 1 axis were significantly and moderately correlated ($r^2 = 0.5$, $p < 0.05$) to the geometric means for specimens across the fossil subsample, indicating that this axis summarises aspects of size-correlated shape. No such correlation was found for the Coordinate 2 axis. Specimens with shorter muzzles are ordinated more negatively on the Coordinate 1 axis and specimens with longer muzzles more positively. The *C. williamsi* specimen (MP3) is clearly separated from the papionin subsample along the Coordinate 2 axis. This indicates that *C. williamsi* shares aspects of size-correlated shape in the muzzle to the smaller *Parapapio* specimens, but differs significantly in size-independent shape of the muzzle. PCoord could not distinguish between the *T. darti* (M3073) specimen and larger *Parapapio* specimens, perhaps indicating a close affinity between early *Theropithecus* and *Parapapio* in muzzle shape and size. Interestingly, the relatively large, long muzzled male *Pp. whitei* specimen (MP223) shows greater affinity in size-dependant shape to smaller relatively short-muzzled specimens than to other relatively larger specimens.

Figure 6.36. Plot of Coordinate 1 vs. Coordinate 2 based on PCoord of Subset IV Procrustes transformed 3D coordinate landmark data for the Subset IV fossil cercopithecoid subsample. (n = 9, *Pp. whitei* = 3, *Parapapio* sp. = 4, *T. darti* = 1, *C. williamsi* = 1)

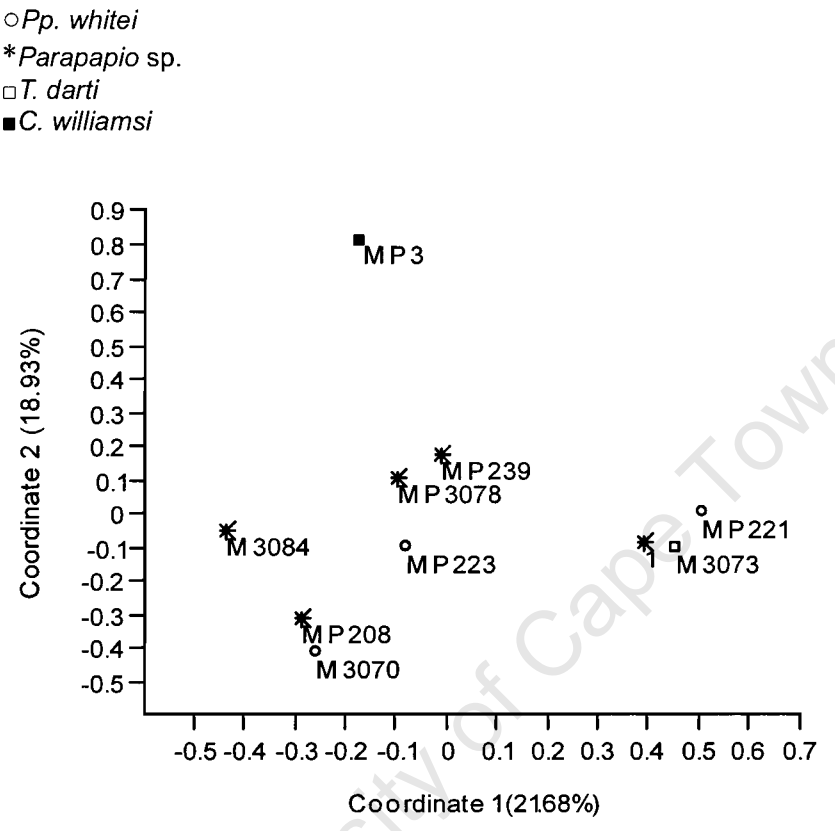

1 = MP47

6.4.2.3. Fossil *Parapapio* vs. Extant Baboon Sample

In the plot of PC1 vs. PC2 (Fig. 6.37), based on a PCA of Subset IV inter-landmark distances of both the extant chacma baboon sample and the fossil cercopithecoid subsample, the fossil sample is separated from the extant female sample along the PC1 axis, which reflects basic size and size-related shape differences in the length of the muzzle. This is expected as *Parapapio* is differentiated from *Papio* by a generally shorter muzzle (Jones, 1937; Freedman, 1957). Some fossil specimens overlap with the range of the extant female chacma baboon sample. The fossil subsample also displays a similar range of variation along both axes to what is observed in the extant

chacma baboon sample. The *C. williamsi* specimen (MP3) is ordinated away from the general papionin sample along both axes. Three *Parapapio* specimens (MP208, M3084 and MP223) fall somewhat more negatively along the PC2 than most extant chacma and other *Parapapio* specimens due to the relatively longer nasal apertures and/or anterior muzzle regions within these specimens compared to other papionin specimens in the analysis.

Figure 6.37. Plot of PC1 vs. PC2 based on PCA of Subset IV inter-landmark distances for the extant baboon sample. (n = 40, *P. h. ursinus* = 31, *Pp. whitei* = 3, *Parapapio* sp. = 4, *T. darti* = 1, *C. williamsi* = 1)

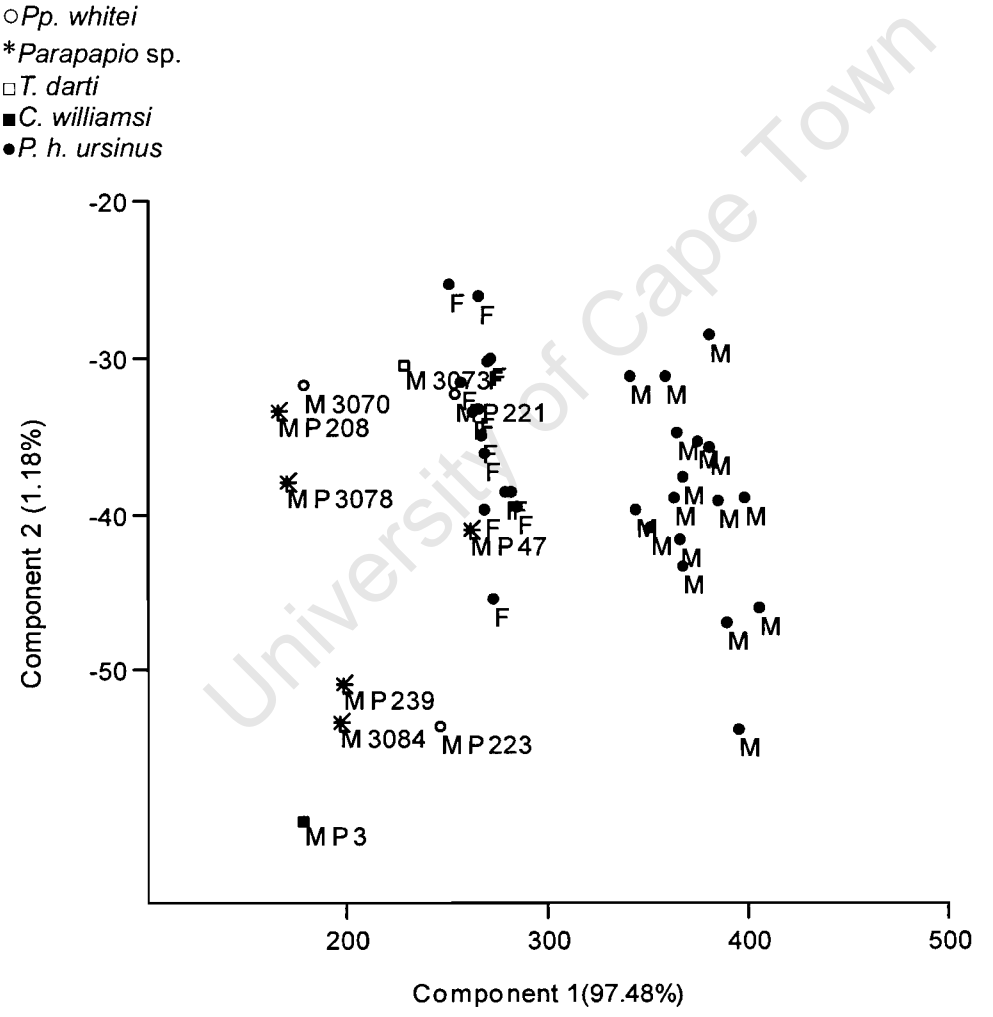

The plot of Coordinate 1 vs. Coordinate 2 (Fig. 6.38), based on a PCoord analysis of Subset IV Procrustes-aligned coordinate data for both the extant chacma baboon sample and the fossil cercopithecoid subsample, clearly distinguishes between male

and female baboon specimens along both the Coordinate 1 and Coordinate 2 axis. The fossil sample is also distinguished from the baboon sample along the Coordinate 1 axis, but has a similar position as the extant male chacma baboon sample along the Coordinate 2 axis. This would indicate that the fossil *Parapapio* sample clearly differs in both size-correlated - and size-independent shape of the muzzle from the extant chacma baboon sample. Although the larger *Parapapio* specimens and the *T. darti* specimen clearly form a subgroup showing greater affinity with the extant chacma baboon sample than do the smaller *Parapapio* specimens with respect to size-dependant shape of the muzzle region, they nonetheless stay distinct from the extant chacma sample, perhaps reflecting a sexually dimorphic pattern in the shape of the muzzle. The *Parapapio* sample does not appear to vary more than the extant chacma sample along either axis.

Figure 6.38. Plot of Coordinate 1 vs. Coordinate 2 based on PCA of Subset IV Procrustes transformed coordinate data for the extant baboon sample and the Subset IV fossil cercopithecoid subset. (n = 40, *P. h. ursinus* = 31, *Pp. whitei* = 3, *Parapapio* sp. = 4, *T. darti* = 1, *C. williamsi* = 1)

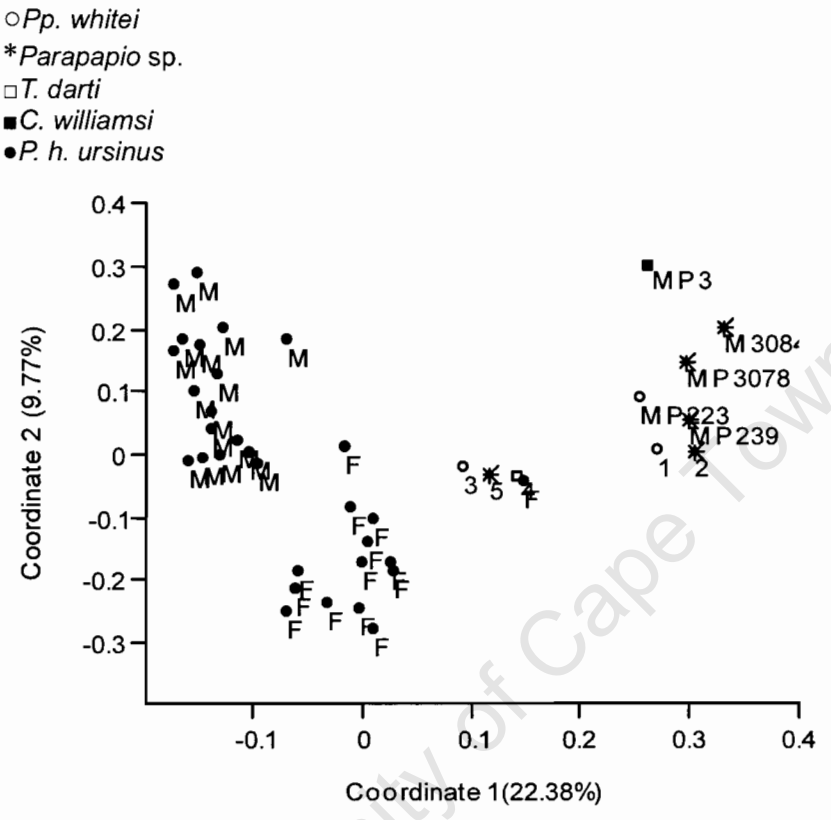

1 = M3070
2 = MP208
3 = MP221
4 = M3073
5 = MP47

6.5. Subset V

The fourteen specimens which comprise Subset V along with the landmarks and inter-landmark distances they share in common are listed in Table 6.5.

Table 6.5. Details of specimens that constitute Subset V.

Accession no.	Taxon	Sex
MP221	*Pp. whitei*	M
MP223	*Pp. whitei*	M
M3070	*Pp. whitei*	F
MP119	*Pp. whitei*	F
MP239	*Parapapio* sp.	F
M3079	*Parapapio sp.*	F
M3084	*Parapapio sp.*	I
MP208	*Parapapio sp.*	I
MP167	*Parapapio sp.*	I
MP47	*Parapapio sp.*	I
M3078	*Parapapio sp.*	I
MP222	*T. darti*	F
M3073	*T. darti*	I
MP3	*C. williamsi*	M
Anatomical Landmarks		
PR, PM(R), NA, PM (L)		
Inter-Landmark Distances		
PR-PM(R), PR-NA, PR-PM(L), PM(R)-NA, PM(R)-PM(L), NA-PM(L)		

6.5.1. Cluster Analysis of Inter-landmark Distances

6.5.1.1. Extant Baboon Sample

A single linkage cluster analysis (Fig. 6.39) performed on the sample of extant chacma baboons based on the same subset of inter-landmark distances as Subset V, clearly separates male and female specimens from each other. This separation probably reflect simple size and size-related shape differences between male and female specimens for this set of inter-landmark distances, similar to Subset IV since both Subset IV and V inter-landmark distances relate mainly to the length of the midface and muzzle.

Figure 6.39. A Tree diagram based on a single linkage cluster analysis performed on Subset V inter-landmark distances of the extant baboons sample. (n = 31, F = 14, M = 17)

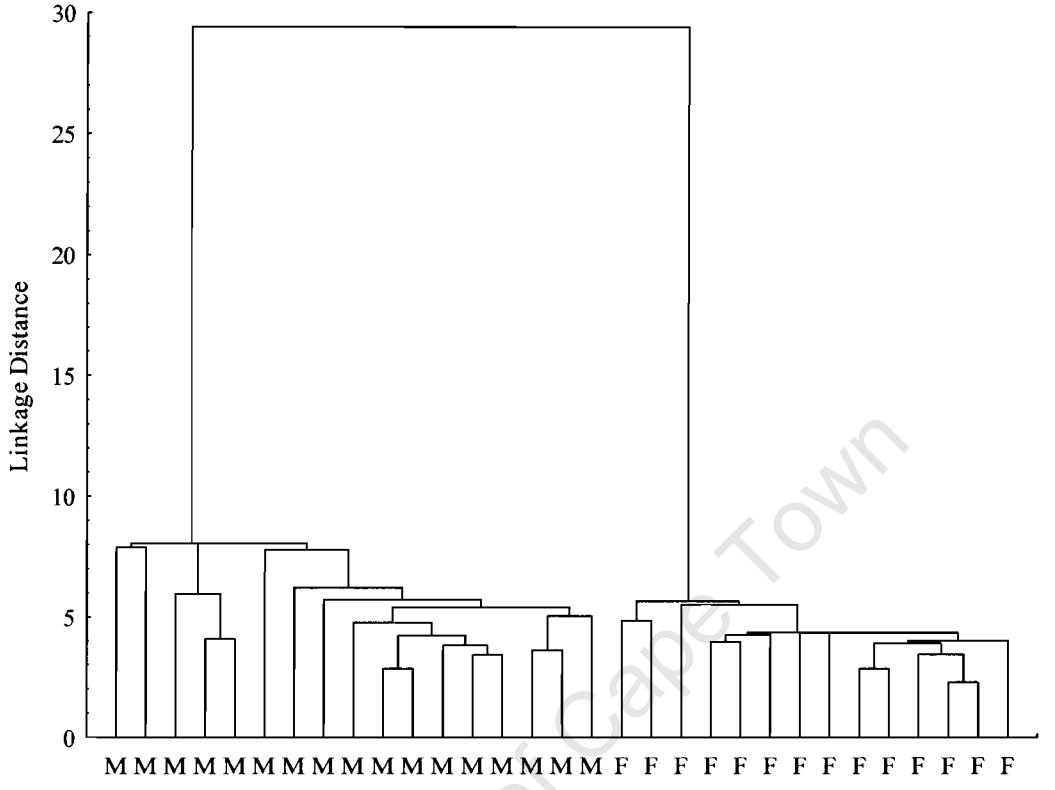

6.5.1.2. Fossil Cercopithecoid Sample

A single linkage cluster analysis (Fig. 6.40) performed on the Subset V fossil cercopithecoid subsample separated specimens into two groups. The relatively larger male *Pp. whitei* specimens (MP221 and MP223) and *T. darti* specimens (MP222 and M3073) and MP47 group together as in Subset IV analysis, while the second group consists of four female specimens (2 *Pp. whitei* and 2 *Parapapio* sp.), four unassigned *Parapapio* specimens and the *C. williamsi* specimen (MP3). This suggests that this subset of measurement is sensitive to differences in size and size-correlated shape of the muzzle between the sexes but not between different taxa.

Figure 6.40. A Tree diagram based on a single linkage cluster analysis performed on Subset IV inter-landmark distances of the Subset V fossil cercopithecoid subsample. (*Pp. whitei* = 4, *Parapapio* sp. = 7, *T. darti* = 2, *C. williamsi* = 1)

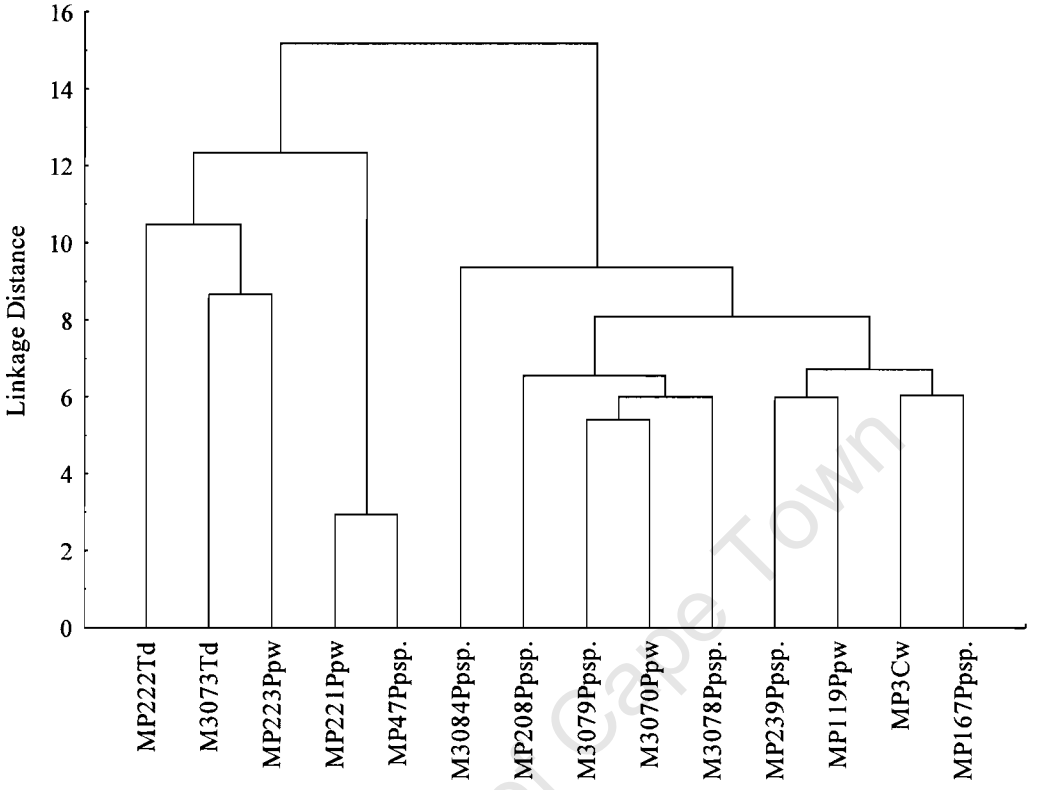

6.5.2. Principal Components Analysis and Principal Coordinates Analysis

6.5.2.1. Extant Baboon Sample

The plot of PC1 vs. PC2 (Fig. 6.41), based on a PCA of Subset V inter-landmark distances of the extant chacma baboon sample clearly clusters male and female specimens along the PC1 axis. PC1 summarises 99% of the variation and all loadings on PC1 are positive indicating that PC1 mainly reflects size and size-related shape. Specimens are clearly and accurately differentiated along the PC1 axis with no overlap between the sexes suggesting very sexually dimorphic muzzle lengths (NA-PR) for male and female chacma baboon specimens. Subset V variables mainly characterise the length of the muzzle region which appears to be very sexually dimorphic in the extant chacma baboon sample. PC2 contains a mixture of both positive and negative loadings implying that this axis summarises other aspects of shape. There is no apparent polarisation along the PC2 axis which summarises less than 1% of the variation, although the larger male specimens appear to vary more

along the PC2 axis than the smaller female specimens due to differences in the lengths of the components that make up the total muzzle length, similar to the relationships described for the anterior and posterior portions of the muzzle in Subset IV analyses. Loadings along this axis suggest that males are more variable in posterior muzzle length (NA-PM) relative to anterior muzzle length (PM-PR). Male specimens may therefore have shorter posterior muzzle regions than would be expected relative to their anterior muzzle regions.

Figure 6.41. Plot of PC1 vs. PC2 based on PCA with 95% ellipses of Subset V inter-landmark distances for the extant baboon sample. (n = 31, F = 14, M= 17)

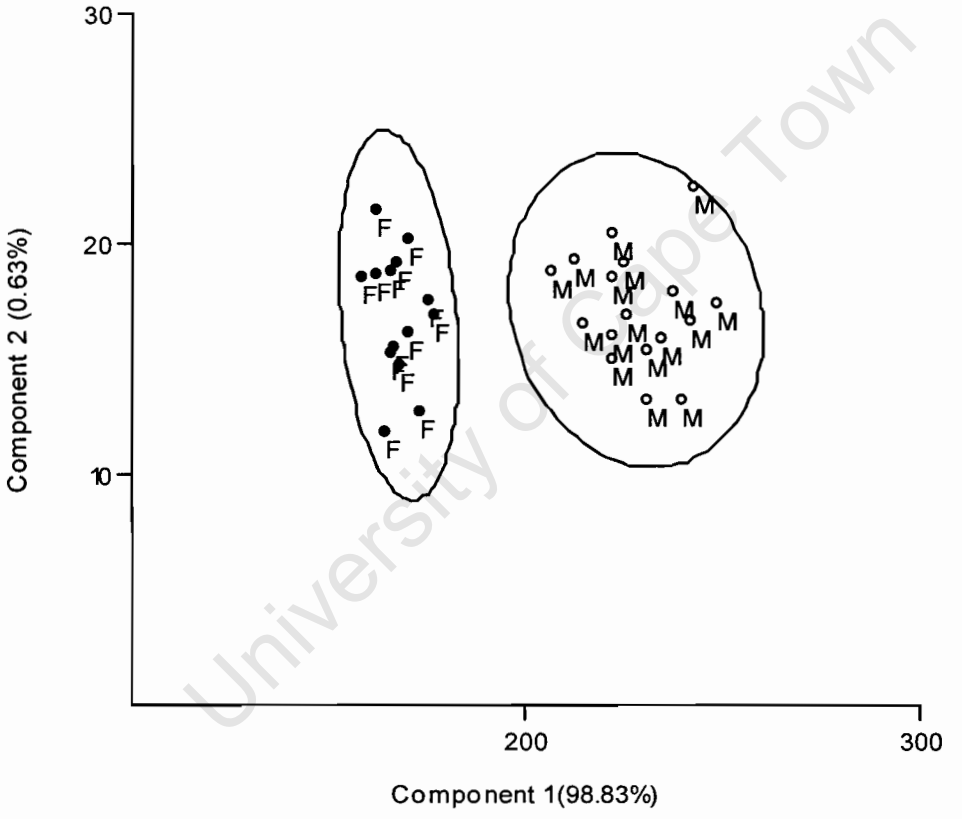

As with Subset IV analysis the Stepwise Discriminant Function Analysis identified a measure of muzzle length (NA-PR) as the most significant discriminator. Again most the variables in this subset measure length of the midface and muzzle and appear to be duplicating one another in their discriminatory power. The inter-landmark distances are illustrated in Fig. 6.42 below; NA-PR is indicated by the dotted line.

Figure 6.42. Most significant discriminators for Subset V inter-landmark distances for distinguishing between male and female baboon crania.

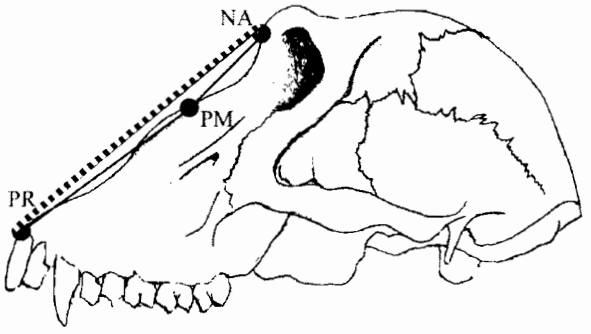

The plot of Coordinate 1 vs. Coordinate 2 (Fig. 6.43), based on a PCoord of Procrustes transformed Subset V coordinate data of the extant chacma baboon sample distinguished between male and female specimens along the Coordinate 1 axis. The Specimen loadings on the Coordinate 1 axis was found to be significantly and moderately correlated to the geometric means of specimens across the extant chacma baboon sample ($r^2 = 0.41$, $p < 0.001$) indicating that this axis summarises size-correlated shape variation in the midface and muzzle. There also appears to be weak polarisation along the Coordinate 2 axis with female specimens tending to the lower end of the axis. This axis was also found to be significantly and moderately correlated to the geometric means across the extant chacma baboon sample ($r^2 = 0.4492$, $p < 0.0001$), implying that some aspects of size-correlated shape is also summarised along the Coordinate 2 axis. Subset V coordinate data appear to be sensitive to size-correlated shape differences in the muzzle and midface of male and female chacma baboons probably reflecting the shorter, less dorsally oriented muzzle of females relative to the longer, more prognathic, dorsally oriented male muzzle.

Figure 6.43. Plot of Coordinate 1 vs. Coordinate 2 based on PCoord with 95% ellipses of Subset V Procrustes transformed coordinate data for the extant baboon sample. (n = 31, F = 14, M= 17)

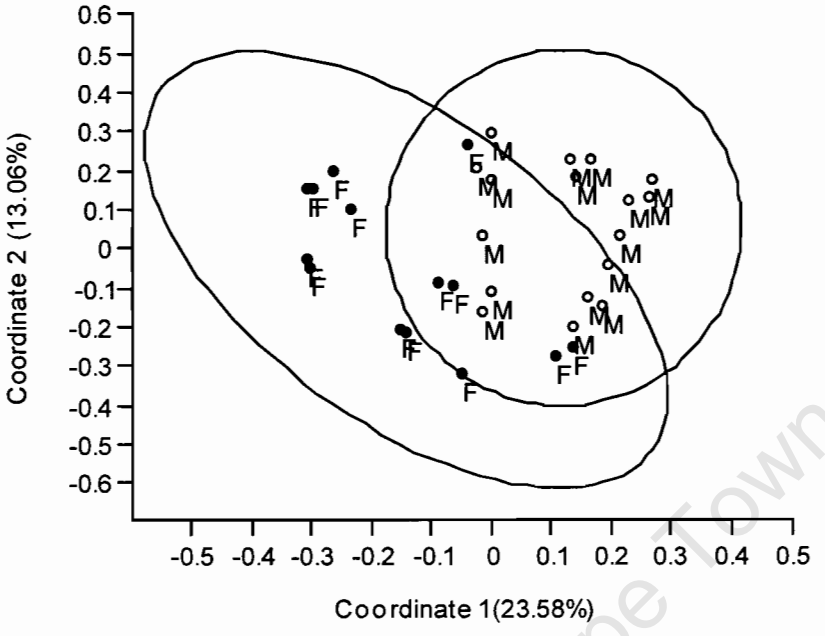

6.5.2.2. Fossil Cercopithecoid Sample

The plot of PC1 vs. PC2 (Fig. 6.44), based on a PCA of Subset V inter-landmark distances of the fossil cercopithecoid subsample, resembles the results of the cluster analysis and of the Subset IV PCA analysis. Specimens with long muzzles are associated with one another to the right on the PC1 axis and specimens it short muzzles to the left on the PC1 axis. PC1 accounts for 95% of the variance and summarises size and size-correlated shape. PC2 contains some negative loadings indicating that it summarises other aspects of shape. Specimens with relatively narrow muzzles and shorter posterior muzzle regions fall more positively along this axis. However, no clear polarisation occurs along this axis, except for MP222 (*T. darti*), which is clearly differentiated from the rest of the sample along this axis. MP222 and M3073, both *T. darti* specimens, resemble each other in the length of the muzzle but appear to differ in some aspect of the shape of the muzzle. MP222 appears to have a narrower muzzle and a shorter posterior region of the muzzle than the *Parapapio* specimens and M3073. *T. darti* specimen (M3073) is not differentiated from the *Parapapio* subsample along either PC1 or PC2. The *C. williamsi* specimen (MP3)

clusters with the smaller shorter muzzled *Parapapio* specimens to the left of the PC1 and is also not differentiated from the *Parapapio* sample along the PC 2 axis.

Figure 6.44. Plot of PC1 vs. PC2 based on PCA of Subset V inter-landmark distances for the Subset V fossil cercopithecoid subsample. (*Pp. whitei* = 4, *Parapapio* sp. = 7, *T. darti* = 2, *C. williamsi* = 1)

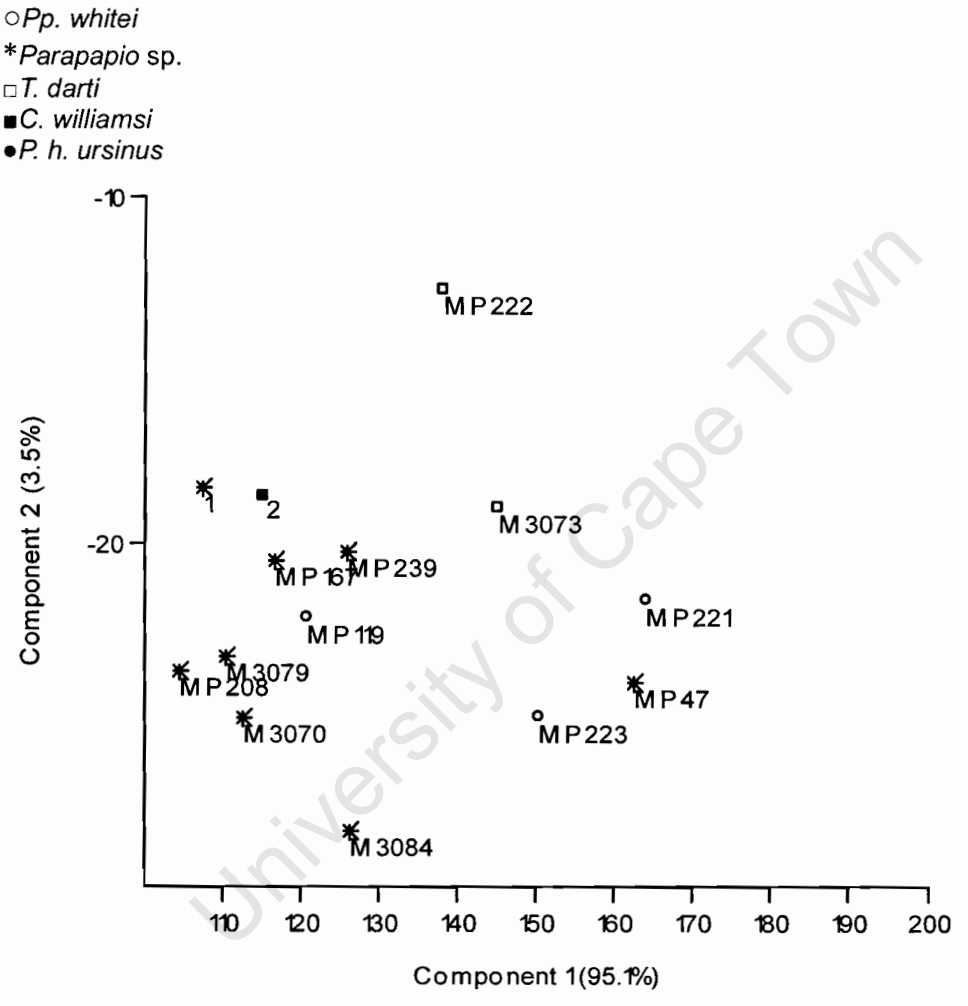

1 = M3078
2 = MP3

There does appear to be some weak polarisation along the Coordinate 1 axis of the plot of Coordinate 1 vs. Coordinate 2 (Fig. 6.45), based on a PCoord analysis of Subset V Procrustes rotated coordinate data of the fossil cercopithecoid subsample. The polarisation along the Coordinate 1 axis does not resemble groupings observed in the PCA analysis. However it does appear that the larger *Parapapio* specimens (MP221, MP223 and MP47) do cluster toward the left on the Coordinate 1 axis but at

the same time they also associate with other *Parapapio* specimens which in the PCA analysis appeared dissimilar in size to these specimens. The specimen loadings on the Coordinate 1 axis was also found to be significantly and moderately correlated to the geometric means of specimens across the fossil cercopithecoid subsample ($r^2 = 0.43$, $p < 0.05$), implying that the Coordinate 1 axis summarises aspects of size-correlated shape as well as size-independent shape. This would suggest that the unassigned *Parapapio* specimens, which cluster with the larger male *Pp. whitei* specimens, although somewhat smaller, differ from the other *Parapapio* specimens in size-independent shape of the muzzle. The Coordinate 2 axis shows no correlation with the geometric means across the subsample which suggest that it reflects a size-independent component. Interestingly Subset V data are unable to distinguish the *T. darti* specimen (M3073) and the *C. williamsi* specimen (MP3) from the *Parapapio* subsample. Only MP222 is clearly dissociated from the *Parapapio* subsample in shape along the Coordinate 2 axis.

Figure 6.45. Plot of Coordinate 1 vs. Coordinate 2 based on PCoord of Subset V Procrustes transformed coordinate data for the Subset V fossil cercopithecoid subsample. (*Pp. whitei* = 4, *Parapapio* sp. = 7, *T. darti* = 2, *C. williamsi* = 1)

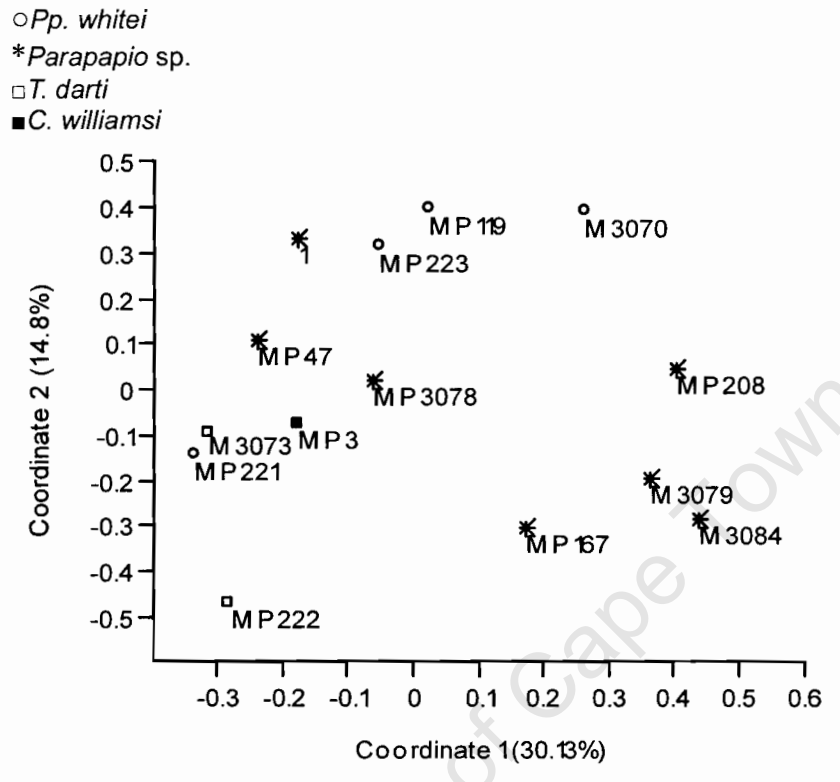

1 = MP239

6.5.2.3. Fossil *Parapapio* vs. Extant Baboon Sample

The plot of PC1 vs. PC2 (Fig. 6.46), based on a PCA of Subset V inter-landmark distances of the extant chacma baboon sample and the fossil cercopithecoid subsample is presented in below. Male, female and fossil cercopithecoid specimens are distinguished along the PC1 axis. PC1 explains 99% of the variance and only has positive loading suggesting that size and size-correlated shape is summarised along this axis. Fossil cercopithecoid specimens appear to be consistently smaller in muzzle length than the extant chacma baboon sample, although some of the larger fossil specimens (MP21, MP223 and MP47) overlap with the female chacma baboon sample. The *Parapapio* subsample does not appear to vary significantly more than the extant chacma sample and appears to replicate some aspects of the sexual dimorphic signal in the extant chacma baboon sample. The *T. darti* specimen MP222 is clearly

distinguished from the papionin sample and appears to differ mainly in aspects of the width of the muzzle and the length of the posterior part of the muzzle.

Figure 6.46. Plot of PC1 vs. PC2 based on PCA of Subset V inter-landmark distances for the extant baboon sample and Subset V fossil cercopithecoid subsample (n = 45, *P. h. ursinus* = 31, *Pp. whitei* = 4, *Parapapio* sp. = 7, *T. darti* = 2, *C. williamsi* = 1)

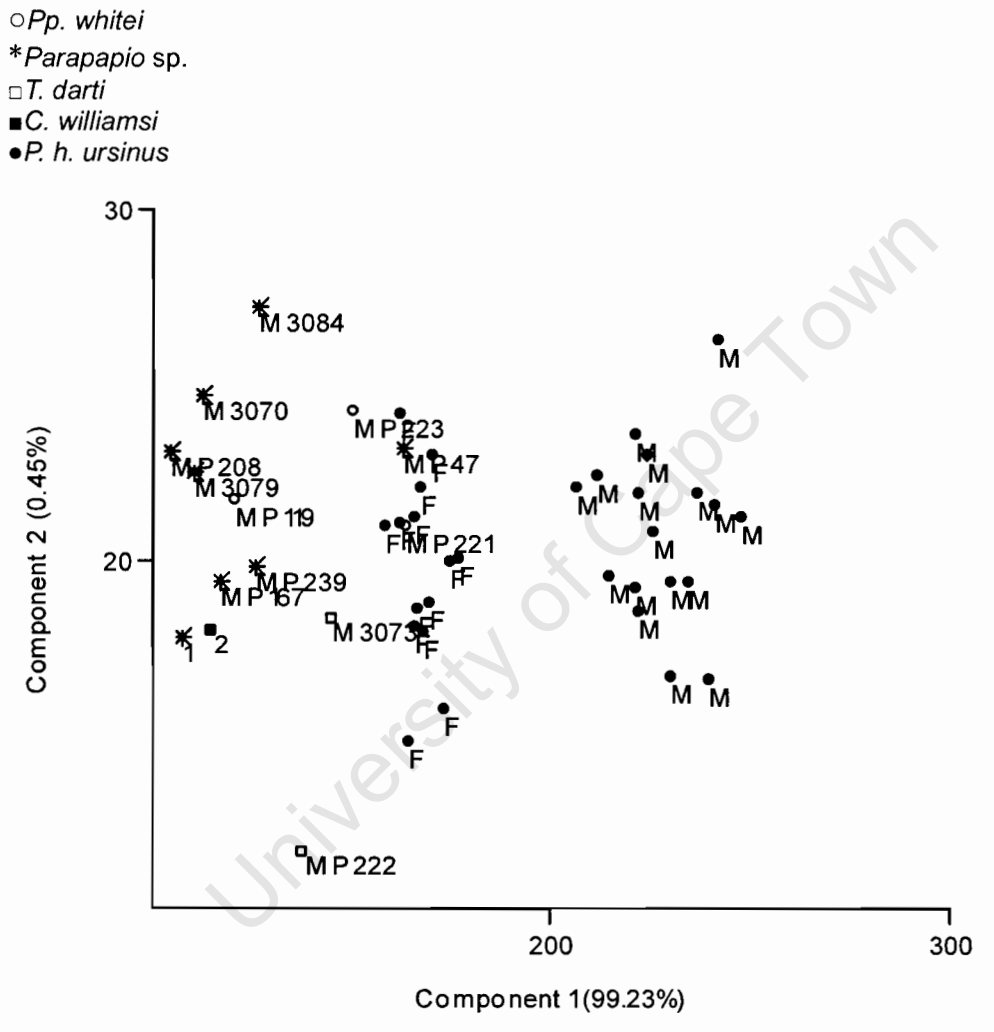

1 = M3078
2 = MP3

The plot of Coordinate 1 vs. Coordinae2 (Fig. 6.47), based on a PCoord analysis of Subset V Procrustes rotated coordinate data, reflects a similar patter to PCA (Fig. 6.46). Male, female chacma baboon and fossil cercopithecoid specimens are weakly separated from one another in shape along the Coordinate 1 axis, as there appears to be considerable overlap between the three groups. The larger fossil specimens (MP222, M3073 and MP221) seem to show some shape affinities with both the male

and the female extant chacma baboon sample in the shape of the muzzle and midface. The *Parapapio* subsample does not appear to vary more than the extant chacma sample along the Coordinate 2 axis, which summarises size-independent shape. However the *Parapapio* subsample does appear to vary more along the Coordinate 1 axis than the extant chacma baboon sample. The *T. darti* specimens (MP222 and M3073) lei within the extant chacma baboon scatter indicating similarity in size-correlated and size-independent shape of the muzzle.

Figure 6.47. Plot of Coordinate 1 vs. Coordinate 2 based on PCoord of Subset V Procrustes transformed coordinate data for the extant baboon sample and the Subset V fossil cercopithecoid subsample. (n = 45, *P. h. ursinus* = 31, *Pp. whitei* = 4, *Parapapio* sp. = 7, *T. darti* = 2, *C. williamsi* = 1)

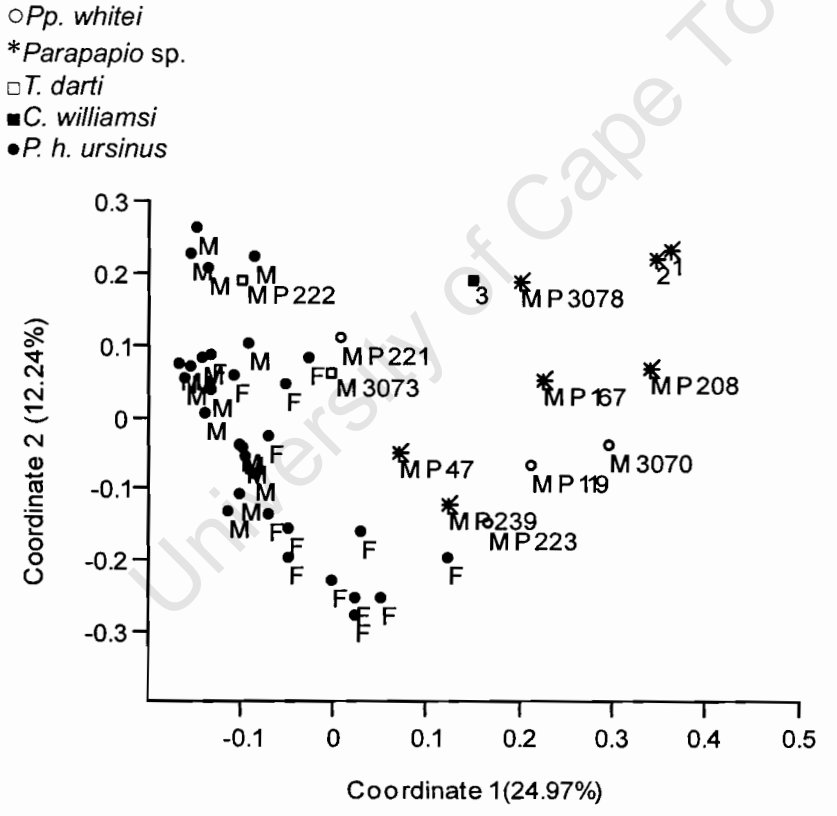

1 = M3084
2 = M3079
3 = MP3

6.6. Analysis of Dental Measurements

A summery of the measurements for three dimensions of the right third molars of eleven Parapapio specimens and twenty-seven exant chacma baboons specimens are given in Table 6.6 below.

Table 6.6. Summery of measurements of right third molar of fossil *Parapapio* specimens and the extant chacma baboon sample.

		Buccal-Lingual Posterior (mm)			Buccal-Lingual Anterior (mm)			Mesio-Distal (mm)		
Taxon	n	range	mean	std	range	mean	std	range	mean	std
Pp. whitei	4	9.0-11	10.2	0.8	12.1-12.9	12.5	0.4	11.5-12.5	12.5	0.5
Pp. broomi	3	8.5-9.3	9	0.4	10.5-11.8	11	0.5	10.5-11.8	11	0.7
Pp. jonesi	1								12.6	
Parapapio sp.	3	8.3-10.2	9.4	1	11.2-12.5	11.6	0.7	10.8-13.5	11.6	1.6
P. h. ursinus, male	15	9.5-11.5	10.4	0.7	11.5-12.5	12	0.5	13-15	14	0.6
P. h. ursinus, female	12	9.5-11	9.8	0.5	10.6-12.5	11.6	0.5	12-13.7	12.7	0.5

The plot of the first two PC axes (Fig. 6.48) based on a PCA analysis of the measurements of the three dimensions recorded for the right third molars of *Parapapio* specimens which preserved these dental dimensions separate specimens along the PC1 axis. All the loadings on this axis were positive, indicating that it mainly summarises size. PC1 summarises 84% of the size variance in the data. Specimens were separated along the PC1 axis along taxonomic lines as would be expected. Molar size should be a good predictor of taxon since molar size was a key aspect in the historical identification of the taxa and the subsequent assignment of *Parapapio* specimens to each of the three taxa (Broom, 1940; Freedman, 1957). *Pp. whitei* specimens (MP119, MP223 and MP76) group together as would be expected. Examination of the raw data confirms that they have larger measurements on all three dimensions than all other specimens. An unassigned *Parapapio* specimen (M3147) is also associated with this group and yielded comparable measurements to *Pp. whitei* specimens in this group. Surprisingly M3070, a *Pp. whitei* female, shows greater affinities to the *Pp. broomi* group than the *Pp. whitei* group. This may be due to female *Pp. whitei* having smaller molars than males but MP119, also a female *Pp. whitei* specimen has distinctly larger molars, more similar to male *Pp. whitei*

specimens. M3070 has relatively short buccul-lingual posterior and mesio-distal lengths similar to *Pp. broomi*, but a relatively long buccul-lingual anterior length more typical of the other *Pp. whitei* specimens. The female *Pp broomi* specimens and the other unassigned *Parapapio* specimens generally have smaller third molars than both male and female specimens attributed to *Pp. white.*

Inspection of the individual measurements (Appendix D-3) for each of the three dimensions of the third molars confirm that *Pp. whitei* specimens are larger than *Pp. broomi* specimens for buccul-lingual posterior and buccul-lingual anterior lengths. There is some overlap in mesio-distal distances between *Pp. whitei* specimens and *Pp. broomi*. MP173 was the only *Pp. jonesi* specimen to preserve any dental dimensions. Surprisingly it had a mesio-distal length greater than any of the *Pp. whitei* and *Pp. broomi* specimens contrary to what would be expected from the smallest *Parapapio* taxon. This dimension may have been exaggerated by a crack running through the tooth between the two cusps which may have contribute as much as 1mm to the measurement. Nonetheless, a mesio-distal measurement of 11.6mm still places it in the range of measurements found for *Pp. whitei* and *Pp. broomi*.

Figure 6.48. Plot of PC1 vs. PC2 based on PCA of three dimensions of the right third molar of selected *Parapapio* specimens. (n = 10, *Pp. whitei* = 4, *Pp. broomi* = 3, *Parapapio* sp. = 3)

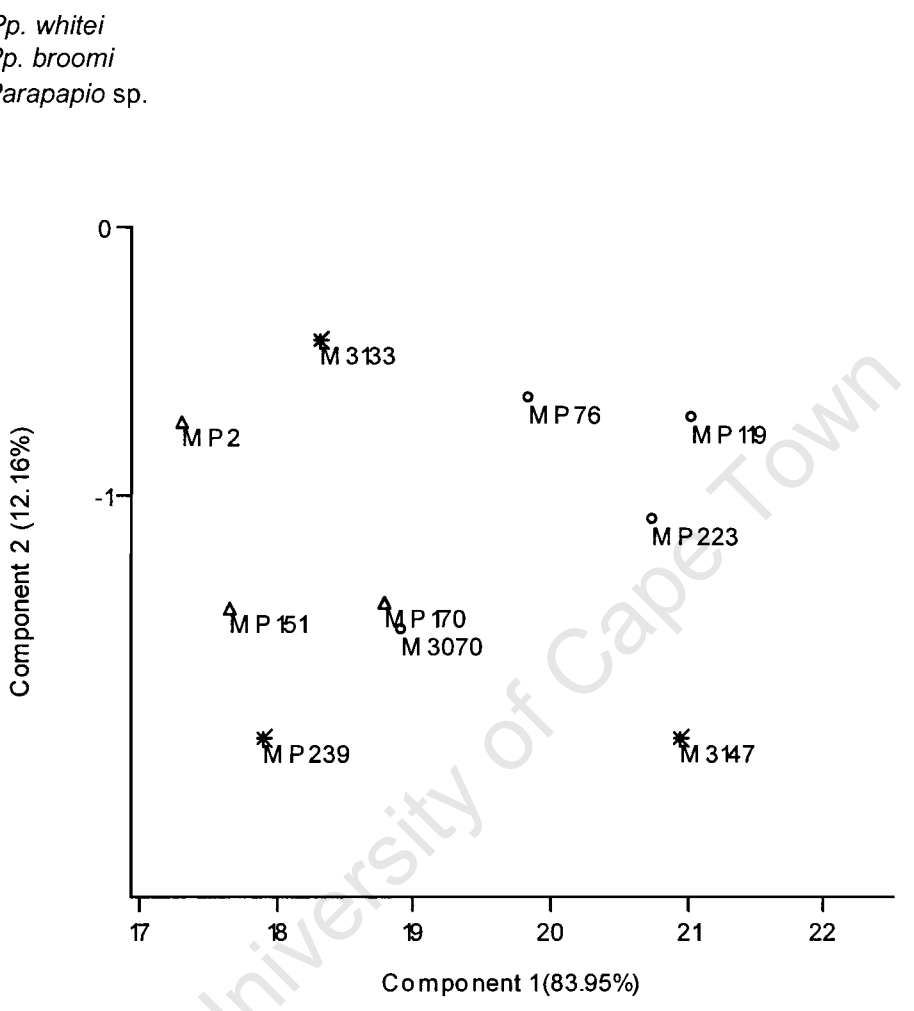

When the dimensions of the third molars of fossil *Parapapio* sample was compared to the extant chacma baboon sample (Fig. 6.49), the fossil *Parapapio* sample were somewhat smaller but showed considerable overlap with the female portion of the extant chacma sample. All loadings on PC1, which summarises 78% of the variance, were positive indicating that this axis summarises aspects of size. The mesio-distal variable yielded a negative loading on the PC2 axis suggesting that some aspect other than size was also being reflected on the PC2 axis. This axis mainly distinguished between *Parapapio* and the extant chacma sample suggesting some difference in the mesio-distal aspect between *Parapapio* and extant chacma baboons. Furthermore,

there also did not appear to by any undue variability in the *Parapapio* sample compared to the extant chacma sample.

Figure 6.49. Plot of PC1 vs. PC2 based on PCA of three dimensions of the right third molar of selected *Parapapio* specimens and the extant

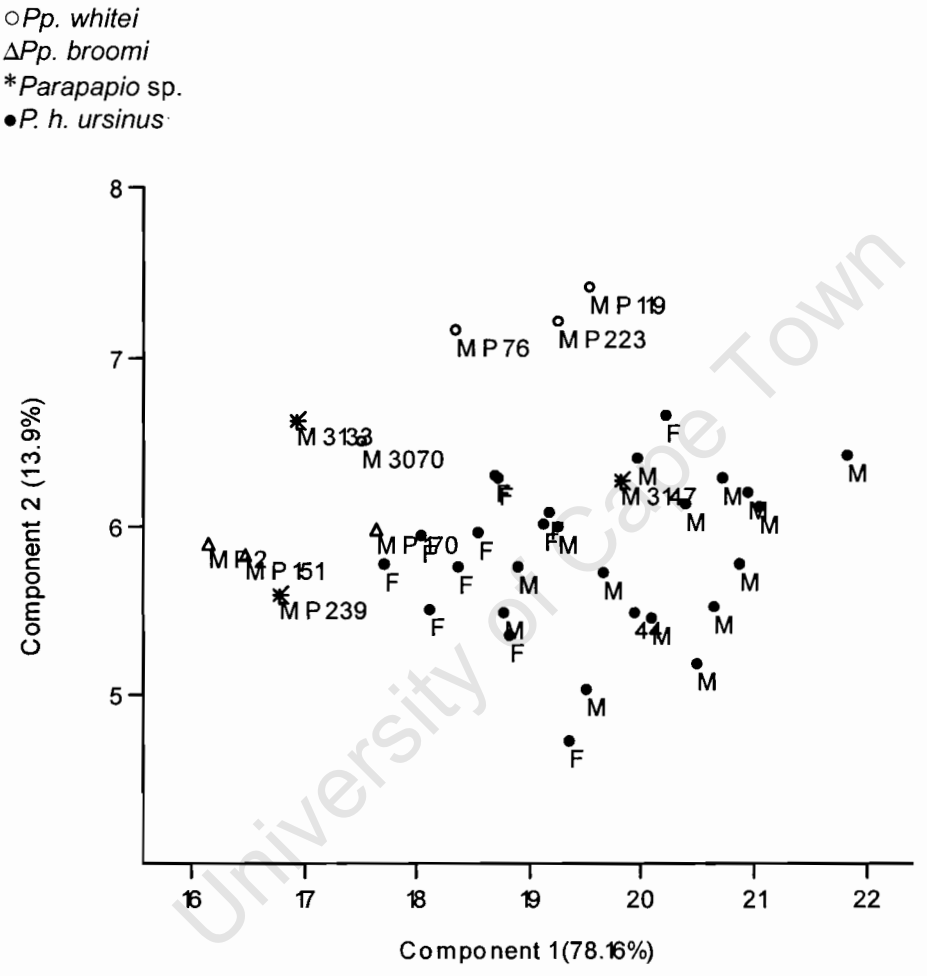

CHAPTER 7

DISCUSSION

In this chapter the results reported in chapters 5 and 6 are summarised, interpreted and discussed. The results of stable isotope and trace-element analyses, reported in chapter 5, are discussed first, followed by discussion of the results of the craniometric investigation. Stable isotope and trace-element analyses are then considered in light of the implications of the craniometric analyses. Improvements and limitations of the approach taken in this study and directions for future research in the palaeoecology of Plio-Pleistocene cercopithecoids are considered. Finally, the above discussion is summarised and some general conclusions are drawn.

7.2. Stable Isotope and Trace-element Analysis of Fossil Cercopithecoid Specimens

The ecological position of *Parapapio* as a group within the community ecology of Makapansgat during Member 2 and 3 times is striking, as *Parapapio* appears to neatly fill the gap between browsing and grazing taxa (Fig. 5.1, Chap. 5). The *Parapapio* diet appears to be a truly mixed diet, which included relatively high proportions of both C_3 and C_4 foods. *Parapapio* yielded relatively low $\delta^{18}O$ ratios similar to water-dependant taxa such as suids and equids. However, *Parapapio*'s $\delta^{13}C$ values were dissimilar to these taxa, and indicated a stronger C_3 component in the diet. Given this combination, we can deduce that their C_3 foods were unlikely to be leaves but rather ^{18}O-depleted rootstocks. The inclusion of a significant fruit component to the diet can however not be discounted. The combination of Sr/Ca, Ba/Ca and Sr/Ba ratios in the *Parapapio* sample resemble the results for fossil suids (from Sponheimer and Lee-Thorp, unpublished data), extant warthogs (Sponheimer and Lee-Thorp, 2005) and extant mole rats (Sponheimer and Lee-Thorp, in press). These animals include significant but varying proportions of rootstocks in their diet. In summary, the relatively low $\delta^{18}O$ and $\delta^{13}C$ values observed for *Parapapio*, suggests that they were frequent drinkers and/or partook of C_3 or C_4 rootstocks, while the trace-element composition is consistent with a reliance on the underground parts of plants.

Within the genus *Parapapio*, stable isotope and trace-element analyses identify two overlapping dietary groupings. Stable carbon isotope analysis identifies a ^{13}C-enriched and a ^{13}C-depleted group. The former consists mostly of specimens attributed to *Pp. whitei* and *Pp. jonesi,* while the latter is comprised mostly of specimens attributed to *Pp. broomi*. There were no noticeable differences between *Parapapio* taxa in $\delta^{18}O$, suggesting that all were obligate drinkers. Although these dietary groupings are grossly correlated to taxonomic groupings, individual specimens within *Pp. whitei* (MP76) and *Pp. broomi* (MP170) yielded $\delta^{13}C$ values unlike those of the majority of specimens within their respective taxa; MP76 (*Pp. whitei*) yielded a $\delta^{13}C$ signal more typical of *Pp. broomi* and MP170 (*Pp. whitei*) yielded a $\delta^{13}C$ signal more typical of *Pp. whitei*. This might indicate that the two specimens have been incorrectly identified, since their ecological affinities do not match their taxonomic affinities. Alternatively, this could hint at dietary variability within each taxon, with the ranges of this variability currently skewed by the small sample sizes; larger sample sizes may reflect greater variability and in effect close the ecological gap between different taxa. However, as the $\delta^{13}C$ data stand, they suggest that *Pp. whitei* and *Pp. jonesi* included similar amounts of C_4 foods in their diets, and that *Pp. broomi* included more C_3 foods in its diet at Makapansgat. A similar bimodal distribution of $\delta^{13}C$ values is reported for *Parapapio* specimens from Sterkfontein, where specimens attributed to *Pp. broomi* and *Pp. jonesi* were more ^{13}C-enriched than specimens attributed to *Pp. whitei* (Codron *et al.*, 2005). Furthermore, both groups of ^{13}C-enriched *Parapapio* specimens from Sterkfontein (n = 7, mean = -7.5 ± 1.1‰ $\delta^{13}C$) and Makapansgat (n = 6, mean = -6.8 ± 0.8‰ $\delta^{13}C$) indicates a similar reliance on C_4 resources. Interestingly the Sterkfontein Member 4 (~2.4 – 2.6 Ma) environments may have been more wooded than the Makapansgat Member 3 (~3 Ma) environs, with a smaller open grassland component (Reed, 1997; Bamford, 1999). Even within a more densely wooded environment *Parapapio* taxa still chose to substantially exploit the limited grassland components. It is worth noting that the taxonomic affinities of the two dietary groups at Sterkfontein and Makapansgat differ. At Sterkfontein it is *Pp. whitei* that is characterised by a more C_3–oriented diet, whereas at Makapansgat it is *Pp. broomi* that fits that dietary profile. Samples from Sterkfontein were mainly derived from isolated teeth and it was also noted that dietary groupings corresponded relatively poorly to the taxonomic assignment of specimens. Therefore, it is possible that the lack of similarity between the two sites results from the problematic

taxonomic identification of *Parapapio* specimens from isolated teeth at Sterkfotein. Alternatively, as indicated by the craniometric analysis of the Makapansgat material, the three-species breakdown of *Parapapio* may not reflect real biological units, and therefore much of the noise and lack of correlation in the data may be due to this problem. More rigorous taxonomic investigations may resolve some of these disparities.

Sr/Ca, Ba/Ca and Sr/Ba ratios revealed further dietary differences between taxa and specimens, and also identified two overlapping dietary groupings within the fossil *Parapapio* sample, corresponding to the dietary groupings observed for $\delta^{13}C$. Sr/Ca and Ba/Ca have been found to be relatively variable (Sillen, 1988), especially in primary consumers (Burton *et al.*, 1999), and may produce a relatively large range of values for a specific taxon (Sillen, 1988). Here, the identification of patterning within such relatively variable indicators may be considered to be an indication of real dietary differences. *Pp. whitei* specimens tended to have generally lower Sr/Ca ratios, higher Ba/Ca ratios and lower Sr/Ba ratios than *Pp. broomi* specimens. This difference was particularly apparent in the distribution of Ba/Ca and Sr/Ba ratios. Although *Pp. whitei* Sr/Ca ratios appeared to be generally low, *Pp. broomi* Sr/Ca ratios appeared to be quite variable and did not cluster tightly. The combination of $\delta^{13}C$, Sr/Ca, Ba/Ca and Sr/Ba ratios observed for the various *Parapapio* taxa in the sample is consistent with the interpretation that *Pp. broomi* specimens included substantially more C_3 rootstocks in their diet than *Pp. whitei* specimens. The two *Pp. jonesi* specimens yielded widely different Sr/Ca and Ba/Ca ratios to one another. MP75 yielded a high $\delta^{13}C$ signal consistent with a significant C_4 component in the diet and high Sr/Ca and Ba/Ca ratios, while MP173 yielded a lower $\delta^{13}C$ value and low Sr/Ca and Ba/Ca ratios. This latter combination has not been identified elsewhere. Given the high natural intra-specific variability of these trace-elements, and the small sample sizes in this study, results from individual specimens, however, should not be over interpreted. As emphasised by Sillen (1988), sufficient sample sizes are necessary in order to confirm dietary characterisations that are made based on this set of trace-element ratios. Notwithstanding the need for larger sample sizes and the nature of Sr/Ca and Ba/Ca variability, some of the variability in the combinations of dietary signals may be due to specific dietary inputs not yet modelled in modern African savannah ecosystems.

Taken together, the current stable isotope and trace-element data from *Parapapio* samples from Swartkrans, Sterkfontein, and Makapansgat indicate the presence of two identifiable but overlapping dietary regimes that are not particularly well correlated to the current specimen identifications (Codron, 2003; El-Zaatari *et al.*, 2005). Importantly, the apparent dietary groupings revealed by the analyses presented here do not necessarily argue for the presence of two distinct taxa at Makapansgat, but only points out two different dietary ecologies. These differences may reflect dietary shifts that result from environmental changes over time. Several thousand if not tens of thousands of years may be represented within the Member 3 and 4 deposits at Makapansgat, during which time environmental oscillations could have occurred.

The isotopic variability, and by extension the dietary variability, of the *Parapapio* sample from Makapansgat does not exceed the variability observed within several extant populations of baboons from the Awash Valley, Ethiopia, measured over several decades (Fourie, unpublished data). However, this comparison should not be taken too far since the Awash Valley in Ethiopia represents a much more extreme and arid environment to that which would have been present during Makapansgat Members 3 and 4 times. Nonetheless, given the time depth of the *Parapapio* bearing deposits and taxonomic composition of the *Parapapio* sample at Makapansgat, dietary variability within the sample may be expected to be somewhat exaggerated compared to a extant analogue viewed over a comparatively short period of time. This does not discount the possibility that subtle but distinct dietary ecologies and/or species may be represented within the sample. Further research on well provenanced and securely identified samples is clearly needed to confirm dietary characterisations and the nature dietary variability within these fossil taxa, in order to be certain about the dietary ecology and niche separation within *Parapapio*.

The results for the two *C. williamsi* specimens compared well with results for this same taxon reported by Codron (2003) and Codron *et al.*, (2005). One specimen (MP3A) yielded a $\delta^{13}C$ value consistent with a mixed/C_3-oriented diet, while the other specimen (MP36) yielded a $\delta^{13}C$ value consistent with a mostly C_4 diet. Such a disparity in diets within a single taxon is unusual, and implies that these individuals were exploiting two completely distinct ecological niches. It has been noted that this taxon appears to be post-cranially adapted to a terrestrial lifestyle while retaining a dental morphology typical of folivorous colobines (Benefits and McCrossin, 1991). Dental wear studies have also suggested a terrestrial diet including a substantial

amount of grasses (Al-Zaatari *et al.*, 2005). Some C_4 dietary contribution is to be expected, but a C_4-dominated diet is not, given the taxonomic affinities and dental morphology of this taxon. Codron (2003) has argued that such a disparate signal is unlikely to be due to temporal shifts in ecology, as such a radical dietary shift over a relatively short period of time (in evolutionary terms) seems unlikely. It has been tentatively suggested that the existence of a second species of *Cercopithecoides* at Sterkfontein and Swartkrans may be the most parsimonious explanation for the existence of two such distinctive dietary ecologies within the *C. williamsi* sample (Codron, 2003; Codron *et al.*, 2005). The results of this study are consistent with this hypothesis, and extend the range of this observation to Makapansgat Members 3 and 4. Previously two species of *Cercopithecoides* were recognised based on slight morphological differences, but *C. molletti* was later collapsed into *C. williamsi* by Freedman (1976). The ecological data suggests that the taxonomy of *Cercopithecoides* should be reinvestigated, and the merits of *C. molletti* reconsidered. The presence of two distinct dietary ecologies within this (relatively) morphologically homogenous taxon has implications for paleoecological reconstructions. *C. williamsi* is an extinct colobine monkey, and all extant colobine monkeys are strict arboreal folivores living in wooded environments. The presence of *Cercopithecoides* sp. in fossil assemblages has therefore often been interpreted as indicating the presence of more closed wooded habitats in palaeoenvironmental reconstructions (e.g. WoldeGabriel *et al.*, 1994). Yet the data presented here for *C. williamsi*, in conjunction with the dietary data from Swartkrans and Sterkfontien (Codron *et al.*, 2005), stress again that assumptions about ecological uniformitarianism based on taxonomic affinities may not always be valid and require testing.

Finally, the results of this study also offer some insights into the dietary ecology of *Theropithecus*. The *T. darti* (MP222) specimen yielded a $\delta^{13}C$ value consistent with a predominantly C_4 diet with a small C_3 component. This specimen also yielded relatively high Sr/Ca and Ba/Ca ratios consistent with a high proportion of above ground plant parts. The $\delta^{13}C$ value for this specimen is nearly identical to the mean $\delta^{13}C$ values reported for *T. oswaldi* from Swartkrans (Lee-Thorp *et al.*, 1989b; Codron *et al.*, 2005). Taken together, these data question interpretations – based on small molar morphology and dental wear differences (Benefit and McCrossin, 1990) – that *T. darti* had a more frugivorous and folivorous diet than *T. oswaldi.* Rather, $\delta^{13}C$ and

trace-element data suggest that *T. darti* and *T. oswaldi* both relied heavily on C_4 grasses.

7.1. Craniometric Assessment of Fossil Cercopithecoid Taxa from Makapansgat Limeworks Site

The main reason for choosing relatively complete specimens for isotopic analysis, rather than fragmentary remains or isolated teeth, was that it provided morphological context for interpreting the results. One of the expectations was that any dietary distinctions found would most likely occur along taxonomic lines. This was not the case. Certainly the results showed distinct size and shape differences among fossil cercopithecoids. Some of these differences may reflect sexual dimorphism in the sample. PCA of Subsets III, IV and V inter-landmark data appeared to discriminate between larger and smaller fossil cercopithecoid specimens with respect to the orbital region and the length of the muzzle and midface. Larger specimens for these subsamples were usually male, and smaller specimens were usually female, although a large proportion of these subsamples often consisted of unassigned and unsexed *Parapapio* specimens. It is therefore not entirely clear whether the polarisation of specimens is specifically related to a sexually dimorphic pattern in the data or distinct taxonomic morphotypes, although separation along the PC1 axis for Subsets IV and V suggest the former. Similarly, PCoord analysis was not able show any consistent association between specimens of the same species or sex. For example, in Subset I PCoord the *Pp. jonesi* specimen MP75 and the *Pp. whitei* specimen MP164 clearly paired together more closely than to any other specimens with respect to the shape of the anterior neurocranium.

Certain individual specimens stand out in their extreme size. MP221 and MP223 (*Pp. whitei*, males) were consistently identified as relatively large specimens by PCA. This grouping of *Pp. whitei* specimens away from other *Parapapio* specimens based on size fits well with the definition of *Pp. whitei* as the largest of the three *Parapapio* taxa at Makapansgat. MP47 is a relatively large unassigned *Parapapio* specimen associated closely with MP221 and MP223 on PC1 and PC2 in the analyses of Subset IV and V inter-landmark distances. Surprisingly, MP170, a female *Pp. broomi* specimen, was also larger than all conspecifics. This specimen was most closely associated with the two large male *Pp. whitei* specimens (MP221 and MP223) in

aspects of the orbital region and midface. However none of these specimens differed consistently in shape from other smaller *Parapapio* specimens. PCoord did not separate these "large" *Parapapio* specimens from smaller *Parapapio* specimens. PCoord of subsets II, IV and V did not indicate that MP221 and MP223 shared any great affinities in size-independent shape of the orbital region (Subset II) and size-correlated shape of the muzzle (Subset IV and V). MP221 and MP223 often shared greater shape affinities (both size-correlated and size-independent) with other specimens than with each other. Only MP170 appeared to differ in both size and size-independent shape of the anterior neurocranium (Subset I) from other specimens, but appeared quite similar to the specimens in shape and size of the orbital region and midface (Subset II).

Despite the presence of consistent size and/or shape differences among certain specimens throughout these analyses, there was no consistent taxonomic patterning to these differences. The *Pp. broomi* male (MP2) and the *Pp. broomi* female (MP170) differed substantially in size and shape of the anterior neurocranium from other *Pp. whitei*, *Pp. broomi* and *Pp. jonesi* specimens, and also differed from one another in the PCA of Subset I inter-landmark distances. In the PCA of Subset II and III inter-landmark distances, they appear to associate with MP221 and MP223, indicating greater similarity in size and shape with these two male *Pp. whitei* specimens than with other *Pp. broomi* specimens. The *Pp. jonesi* specimen (MP75) did not appear to be smaller or different to other *Parapapio* specimens regardless of their taxonomic assignment. No patterned differences between *Pp. whitei* and *Pp. broomi* specimens were consistently apparent in PCA or PCoord analysis across any of the subsets. Therefore, although there appear to be distinct differences in shape and size among the fossil *Parapapio* specimens, these differences appear to be, in part, related to sexual dimorphism and not to taxonomic differences.

The relatively large *T. darti* specimens, M3073 and MP222, tended to associate with the larger *Parapapio* specimens along the PC1 axes. MP222 (*T. darti*, female) differed substantially from *Parapapio* specimens along the PC2 axis and the Coordinate 2 axis (Subset V), implying a shape difference in the muzzle region, whereas M3073 (*T. darti*) fell within the range for *Parapapio* specimens along the PC2 axis and Coordinate 2 axis for Subsets IV and V. Yet while *T. darti* specimens showed substantial similarity in size and shape with the larger *Parapapio* specimens, it is important to note that the *Theropithecus* sample is extremely small, and M3073 in

particular may represent an outlier. *Theropithecus* might appear as a distinct cluster from *Parapapio* if a larger sample were used, although some overlap between the genera is to be expected (Singleton, 2002). Furthermore some shape and size overlap between *Theropithecus* and *Parapapio* may not necessarily be unusual since at ~3Ma *Theropithecus* and *Papio* are still relatively close to the basal split between the two genera, somewhat earlier in the Pliocene (~4 – 3.75Ma) (Leakey, 1993; Newman *et al.*, 2004).

When the extant and fossil samples are analysed together two patterns emerge. First, there appears to be some overlap between the two groups, with larger *Parapapio* specimens falling within the female extant chacma baboon range. Larger specimens such as MP170 (Subset II and III), MP47 (Subset III, IV and V), MP221 (Subset IV and V), and MP223 (Subset IV and V) regularly fall within the range of the extant female chacma sample for size and shape of the orbital regions, upper midface and muzzle. However, *Parapapio* did appear distinctive from the extant chacma baboon sample in the size and shape of the anterior neurocranium, PCoord analyses of the subsets showed more distinct shape differentiation between the *Parapapio* sample and the extant chacma baboon sample. This implies that *Parapapio*, although similar to the chacma sample in certain anatomical regions of the cranium, differed substantially and consistently from the extant chacma baboon sample in both size and shape.

The second interesting result to emerge from the pooled analyses is that the entire *Parapapio* sample did not usually appear to be more variable than the extant chacma baboon sample, in aspects of size or shape, even though greater intra-specific variability in the fossil sample was expected to some extent due to the inclusion of multiple taxa and the possibility of temporal depth (Williams *et al.*, in press). Additionally, the extant baboon sample is derived from a geographically restricted population of a single subspecies of baboon, which is unlikely to be an adequate model for size and shape variation across the fossil sample. Despite this, the fossil *Parapapio* sample did not vary more than the extant baboon sample for any of the anatomical regions of the skull that were analysed by PCA or PCoord. Arguments for multiple taxa based on excessive variation in the fossil *Parapapio* sample, at least within this sample from Makapansgat and for the variables analysed here, are inconsistent with the craniometric data presented here.

Finally, it is necessary to consider the dental dimensions of the fossil samples, especially as *Parapapio* species have been mainly defined and distinguished from one

another based on the relative size of the post-canine dentition (e.g. Broom, 1940; Freedman, 1957; Maier, 1970; Freedman, 1976). In general, dental measurements were correlated to taxonomic assignments, although *Pp. whitei* and *Pp. broomi* show overlap in dental dimensions. However, this correlation has little meaning, as comparing these dimensions can only yield results consistent with the previous taxonomic order, because the taxa themselves have been defined by the dimensions of the post-canine teeth. Interestingly, if the M3 data is viewed in the absence of specimen identifications, then the points appear as a continuum rather than representing discreet metric clusters. This does not disprove the presence of more than one species in the fossil *Parapapio* sample, but it does suggest a more complex relationship between taxa if more than one is represented in the sample.

Surprisingly, the *Pp. jonesi* specimen MP173 had an unexpectedly large mesio-distal measurement for its M3, comparable to sizes found for *Pp. whitei* in this study. This measurement may be slightly exaggerated because the M3 has a substantial crack through the tooth between the two cusps which may contribute up to 1mm to the mesio-distal measurement. But even correcting for this, it would still be a surprisingly large measurement that is inconsistent with the taxonomic position of *Pp. jonesi*. MP173 was originally described as relatively large specimen, with size and shape affinities to *Pp. whitei* and *Pp. broomi* specimens (Maier, 1970). The dimensions of the premolars weighed heavily in its assignment to *Pp. jonesi* even though it was acknowledged that the molars were larger than would be expected for a *Pp. jonesi* specimen (Maier, 1970). This example further illustrates the problematic nature of the original criteria for taxonomic assignment for *Parapapio* specimens, especially specimens consisting of isolated teeth or dentognathic specimens.

Parapapio specimens also show substantial overlap with the female cluster of the extant chacma baboon sample in the measured dimensions of the M3. It is therefore likely that the dimensions of the post-canine teeth of *Parapapio* may in some cases not be distinguishable from other fossil papionin taxa such as *Papio robinsoni* or *P. h. ursinus*. Dental dimensions alone should therefore not be used to distinguish between *Parapapio* and other papionin taxa. Furthermore, it is implicit in the *Parapapio* literature that small post canine teeth/tooth equals a small specimen. The three species are commonly described as representing three different size categories, when in fact those size categories appear only to apply to the post canine tooth size and not to the whole specimen. MP173, although not included in the craniometric analysis, is a

relatively large specimen but it has small pre-molars and therefore was assigned to the 'smaller' of the three *Parapapio* species. Similarly, MP2, identified as a *Pp. broomi* male (Freedman 1960), yielded some of the smallest M3 measurements, while craniometric analysis indicated it was of intermediate to large size relative to other specimens in Subsets I, II and III. In Subset I, MP75, identified as a *Pp. jonesi* male (Maier 1970), exhibits size affinity with a *Pp. broomi* male, M3065, and shape affinity with an unsexed *Pp. whitei* specimen, MP164. Yet Maier (1970) identifies it as the smallest of the three *Parapapio* species, since the mesio-distal length of the M3 falls below the (then) observed range for *Pp. broomi,* and despite the fact that its bucco-lingual measurements fall within the range of *Pp. broomi*. Smaller post-canine teeth do not necessarily imply a small specimen. The assumption that *Pp. jonesi* specimens are absolutely smaller than *Pp. broomi* specimens, and that *Pp. broomi* specimens are absolutely smaller than *Pp. whitei* specimens, does not appear to hold.

Taken together, the craniometric and dental analyses indicate that the taxonomic assignment of specimens within this sample, and by extension within and among samples from other sites, may be substantially flawed. The data did not yield any taxonomic signal which would indicate the presence of multiple taxa within this sample, although the possibility that multiple taxa are present is not entirely discounted. Historical classification criteria for *Parapapio* taxa and the taxonomic assignment of *Parapapio* specimens are clearly problematic. Future research should review the taxonomy and the individual taxonomic assignments of specimens using large samples from various sites. This will help us to understand the nature of the variation reported for the fossil samples, and might reveal temporally correlated trends between sites. Such a comprehensive review using multiple sites and appropriately constructed extant models will yield a more reliable and thoroughly understood taxonomy. This is crucial if further research into the biology and ecology of Plio-Pleistocene cercopithecoid taxa is to yield meaningful results.

CONCLUSION

This study has provided the first fine-grained dietary data on well preserved and more securely identified partially complete cranial *Parapapio* specimens, in an attempt to circumvent taxonomic uncertainties inherent in using isolated teeth and dentognathic specimens. Dietary indicators suggest that two overlapping dietary

ecologies are represented in the *Parapapio* sample. These dietary groups are loosely correlated to specimens attributed to *Pp. broomi*, which appear to have had a mixed C_3 diet with substantial input from rootstocks, and to specimens attributed to *Pp. whitei/Pp. jonesi*, which appear to have had a mixed C_4 diet with a lesser rootstock component.

Craniometric analyses found no taxonomic signal, and no consistent craniometric affinities could be demonstrated between specimens assumed to belong to the same species. These analyses also highlighted inconsistencies in the current taxonomic identification of specimens. Although not discounting the possibility that more than one taxon may be present in the *Parapapio* sample, the data does not support such a conclusion. In the context of the craniometric analyses, it would appear that two overlapping dietary ecologies are present within a single taxon. This is not necessarily surprising, as many papionin taxa are very adaptable generalists, capable of exploiting a wide range of habitats and resources (Hall, 1961; DeVore and Hall, 1965; Hamilton III *et al.*, 1978). The bimodality in the dietary signal of the *Parapapio* sample from Makapansgat members 3 and 4 may reflect a predictable dietary response to climatic and environmental oscillations over time. Alternatively, the two observed dietary ecologies may be due to the presence of two ecologically distinct taxa in the *Parapapio* sample. It may be that the variables (and variable combinations) used for the craniometric analyses were not appropriate for distinguishing between these closely related taxa.

Although not conclusive, craniometric and dietary data suggest that *Parapapio* at Makapansgat could represent a single taxon with an eclectic and adaptable dietary ecology. This characterisation must be further tested by the morphometric analysis of larger samples of *Parapapio* from various sites, as well as more extensive dietary analyses of well provenanced and securely identified specimens. Furthermore, the dietary data suggests that *T. darti* – or at least the individual sampled here – did not have a diet that differed from *T. oswaldi*, and that *C. williamsi* at Makapansgat exhibits two very different dietary ecologies, as has been found at other sites (Luyt, 2001; Codron, 2003; Codron *et al.*, 2005). These results also demonstrate that that the biogenic signal in fossil tooth enamel can be retained with enough integrity to reveal subtle dietary differences.

The data presented in this investigation of *Parapapio* dietary ecology and morphology have implications for paleodietary analysis, palaeoenvironmental

reconstruction and biostratigraphic studies of hominin localities. Firstly, craniometic data for this sample highlights incongruities in the identification of specimens, and raises questions about the validity of the three species breakdown of *Parapapio*. These concerns are reinforced by the dietary data, which only distinguished between two dietary ecologies in the *Parapapio* sample supposedly consisting of three species. This study was done using relatively well provenaced and securely identified cranial specimens, yet uncertainties regarding the taxonomic assignment of specimens and the taxonomy of the genus investigated still presented difficulties for the interpretation of dietary data. This emphasises the danger of working with highly fragmentary, poorly identified material. Secondly, such taxonomic concerns must first be addressed for fossil cercopithecoid taxa if they are to be safely and effectively used in biostratigraphic studies (Delson, 1984; McKee *et al.*, 1995). Thirdly, neither the presence of *C. williamsi* nor the general abundance of primate taxa and specimens at Makapansgat can be assumed to indicate a wooded component. It appears that *C. williamsi* at Makapansgat had a much more terrestrial ecology than would be predicted from its taxonomic affiliations or dental morphology; this inference is consistent with data from Swartkrans and Sterkfontein (Codron, 2005; Codron *et al.*, 2005). All the cercopithecoid taxa from Makapansgat Members 3 and 4 exhibited diets reflecting an open-habitat component and cannot safely be used to as indicators of more closed environments.

Finally, this investigation has shown that it possible to detect subtle dietary differences between related taxa using stable isotope and trace-element tools. However the dietary, ecological and behavioural information yielded by these techniques only give part of the dietary, ecological and behavioural picture of the animal. Only through a synthesis of functional morphology, dental wear and biogeochemical techniques can a more holistic picture of the ecology of the animals investigated be arrived at, as each provides unique biological, evolutionary and behavioural information. Future palaeo-dietary studies should attempt to apply the full suite of techniques in order to attain greater resolution and tease apart ecological relationships and dietary components in fossil foodwebs.

REFERENCES

Ackermann RR. 2003. Using extant morphological variation to understand fossil relationships: a cautionary tale. South African Journal of Science 99: 255-258

Adams DC, Rohlf FJ, Slice DE. 2004. Geometric morphometrics: ten years of progress following the 'revolution'. Italian Journal of Zoology 71: 5-16

Alberts SC, Altmann J. 2001. Immigration and hybridization patterns of yellow and anubis baboons in and around Amboseli, Kenya. American Journal of Primatology 53: 139-154

Alberts SC, Hollister-Smith JA, Mututua RS, Sayialel SH, Muruthi PM, Warutere JK, Altmann J. 2005. Seasonality and long term change in a savanna environment. In: Brockman DK, van Schaik CP, editors. Seasonality in primates: studies of living and extinct non-human primates. Cambridge: Cambridge University Press: p157-197

Ambrose SH. 1991. Effects of diet, climate and physiology on nitrogen isotope abundances in terrestrial foodwebs. Journal of Archaeological Science 18: 293-317

Ambrose SH. 2000. Controlled diet and climate experiments on nitrogen isotope ratios of rats. In: Ambrose SH, Katzenberg MA, editors. Biogeochemical approaches to paleodietary analysis. New York: Plenum Publishers. p243-258

Ambrose SH, DeNiro M. 1986. The isotopic ecology of East African mammals. Oecologia 69: 395-406

Ambrose SH, Norr L. 1993. Experimental evidence for the relationship of the carbon isotope ratios of whole diet and dietary protein to those of bone collagen and carbonate. In: Lambert JB, Grupe G, editors. Prehistoric human bone: archaeology at molecular level. New York: Springer

Ambrose SH, Butler BM, Hanson DB, Hunter-Anderson RL, Krueger HW. 1997. Stable isotope analysis of human diet in the Marianas Archipelago, Western Pacific. American Journal of Physical Anthropology 104: 343-361

Andrews CW. 1916. Note on a new baboon (*Simopithecus oswaldi*, gen. et sp.n.) from the (?) Pliocene of British East Africa. Annals of the Magazine of Natural History 18: 410-419

Balasse M. 2002. Reconstructing dietary and environmental history from enamel isotopic analysis: time resolution of intra-tooth sequential sampling. International Journal of Osteoarchaeology 12: 155-165

Bamford M. 1999. Pliocene fossil woods from an early hominid cave deposit, Sterkfontein, South Africa. South African Journal of Science 95: 231-236

Bell LS, Cox G, Sealy J. 2001 Determining life history trajectories using bone density fractionation and stable isotope measurements: a new approach. American Journal of Physical Anthropology 116: 66-79

Benefit BR, McCrossin ML. 1990. Diet, species diversity and distribution of African fossil baboons. Kroeber Anthropological Society Papers 70-71:

Birchette MG. 1981. Postcranial remains of cercopithecoides. American Journal of Physical Anthropology 54: 201

Bocherens H, Koch P, Mariotti A, Geraads D, Jaeger J. 1996. Isotopic biogeochemistry (^{13}C, ^{18}O) of mammalian enamel from African Pleistocene hominin sites. Palaios 11: 306-318

Boutton TW. 1991. Stable carbon isotope ratios of natural materials: II. Atmospheric, terrestrial, marine and freshwater environments. In: Coleman DC, Fry B, editors. Carbon Isotope Techniques. San Diego: Academic Press. p173-183

Brain CK. 1958. The Transvaal ape-man bearing cave deposits. Transvaal Museum Memoirs 11: 1-18

Brain CK. 1981. The fossil animals. In: CK Brain, editor. The hunters or the hunted?: an introduction to African cave taphonomy. Chicago: University of Chicago Press. p147-190

Brock A, McFadden PL, Patridge TC. 1977. Preliminary palaeomagnetic results from Makapansgat and Swartkrans. Nature 266: 249-250

Broom R. 1940. The South African Pleistocene cercopithecoid apes. Annals of the Transvaal Museum 20: 89-100

Broom R, Jensen JS. 1946. A new fossil baboon from the caves at Potgietersrust. Annals of the Transvaal Museum 20: 337-340

Burton JH, Price TD. 1990. Paleodietary applications of barium values in bone. Proceedings of the 27th international symposium on archaeometry, Heidelberg.

Burton JH, Price D, Middleton WD. 1999. Correlation of bone Ba/Ca and Sr/Ca due to biological purification of calcium. Journal of Archaeological Science 26: 609-616

Carter ML. 2001. Sensitivity of stable isotopes (^{13}C, ^{15}N and ^{18}O) in bone to dietary specialization and niche separation among sympatric primates in Kibale National Park, Uganda. Unpublished Ph. D. thesis. University of Chicago.

Cerling TE, Harris JM, Ambrose SH, Leaky MG, Solounias N. 1997. Dietary and environmental reconstruction with stable isotope analysis of herbivore tooth enamel from the Miocene locality of Fort Ternan, Kenya. Journal of Human Evolution 33: 635-650

Codron DM. 2003. Dietary ecology of chacma baboons (*Papio ursinus* (Kerr, 1792)) and Pleistocene Cercopithecoidea in savanna environments of South Africa. University of Cape Town. Masters Thesis

Codron D, Luyt J, Lee-Thorp JA, Sponheimer M, DeRuiter D, Codron J. 2005. Utilization of savanna-based resources by baboons during the Plio-Pleistocene. South African Journal of Science 101: 254-248

Comar C, Russel RS, Wasserman RH. 1957. Strontium calcium movement from soil to man. Science 126: 485-496

Coursey JS, Schwab DJ, Dragoset RA. 2005. Atomic weights and isotopic compositions (version 2.4.1). [Online] Available: http://physics.nist.gov/Comp [2005, Sept 16] National Institute of Standards and Technology, Gaithersburg, MD

Craig H. 1957. Isotopic standards for carbon and oxygen and correction factors for mass-spectrometric analysis of carbon dioxide. Geochimica et Cosmochimica Acta 12: 133-149

Craig H. 1961. Standard for reporting concentrations of deuterium and oxygen-18 in natural waters. Science 133: 1833-1834

Dansgaard W. 1964. Stable isotopes in precipitation. Tellus 16: 436-468

Dart R. 1925a. *Australopithecus africanus*, man-ape from South Africa. Nature 115: 195-199

Dart R. 1925b. A note on Makapansgat: a site of early human occupation. South African Journal of Science 22: 454

Dawson TE, Brooks PD. 2001. Fundamentals of stable isotope chemistry measurement. In: Unkovitch M, Pate J, McNiell A, Gibbs JD, editors. Stable

isotope techniques in the study of biological processes and functioning of ecosystems. Dortrecht: Kluwer Academic Press. p1-18

DeGusta D, Vrba E. 2003. A method for inferring paleohabitats from the functional morphology of bovid astragali. Journal of Archaeological Science 30: 1009-1022 .

DHoogh TM, Mwenda JM, Hill JA. 2004. The baboon as a nonhuman primate model for the study of human reproduction. Gynecologic and Obstetric Investigation 57: 1-60

Delson E. 1973. Fossil colobine makeup of the circum-Mediterranean region and the evolutionary history of the Cercopithecoidea (Primates, Mamalia). Ph. D. dissertation. Columbia University

Delson E. 1984. Cercopithoid biochronology of the African Pliocene: correlation between eastern and southern hominid bearing localities. Courier Forschunstinstitute Senckenberg 69: 119-218

Delson E. 1992. Evolution of Old World Monkeys. In: Jones JS, Martin RD, Pilbeam D, Bunney S, editors. Cambridge Encyclopedia of Human Evolution. Cambridge: Cambridge University Press. p 217-222

Delson E. 1993. *Theropithecus* fossils from Africa and India and the taxonomy of the genus. In: Jablonski NG, editor. The rise and fall of a primate genus. Cambridge: Cambridge University Press. p157-189

Donnely SM, Kramer A. 1999. Testing for multiple species in fossil samples: an evaluation and comparison of tests for equal relative variation. American Journal of Physical Anthropology 108: 507-529

Dunbar RIM. 1976. Australopithecine diet based on a baboon analogy. Journal of Human Evolution 5: 161-167

Dunbar RIM, Dunbar EP. 1974. Ecological relations an niche separation between sympatric and terrestrial primates in Ethiopia. Folia Primatologia 21: 36-60

Eisenhart WL. 1974. The Fossil Cercopithecoids of Makapansgat and Sterkfontien. B. A. thesis, Department of Anthropology, Harvard Colledge.

Ehleringer JR, Cerling TE, Helliker B. 1997. C_4 photosynthesis, atmospheric CO_2 and climate. Oecologia 112: 285-299

Elias RW, Hirao Y, Patterson CC. 1982. The circumvention of the natural biopurification of calcium along nutrient pathways by atmospheric inputs of industrial lead. Geochimica et Cosmochimica Acta 46: 2561-2580

Elton S. 2001. Locomotor and habitat classifications of cercopithedoid post cranial material from Sterkfontein member 4, Bolt's Farm and Swartkrans members 1 and 2, South Africa. Palaeontologia Africana 37: 115-126

El-Zaatari S, Grine FE, Teaford MF, Smith HF. 2005. Molar microwear and dietary reconstructions of fossil cercopithecoidea from the Plio-Pleistocene deposits of South Africa. Journal of Human Evolution: 1-26

Epstein S, Thompson P, Yapp CJ. 1977. Oxygen and hydrogen isotopic ratios in plant cellulose. Science 198: 1209-1215

Ezzo JA. 1994a. Putting the "chemistry" back into archaeological bone chemistry analysis: modeling potential paleodietary indicators. Journal of Anthropological Archaeology 13: 1-34

Ezzo JA. 1994b. Zinc as a paleodietary indicator: an issue of theoretical validity in bone-chemistry analysis. American Antiquity 59: 606-621

Farquhar GH, von Caemmerer S, Berry JA. 1980. A biochemical model of photosynthetic CO_2 assimilation in leaves of C_3 species. Planta 149: 78–90.

Farquhar GD, O'Leary MH, Berry JA. 1982. On the relationship between carbon isotope discrimination and intercellular carbon dioxide concentration in leaves. Australian Journal of Plant Physiology 9: 121-137

Farquhar GD, Ehleringer JR, Hubick KT. 1989. Carbon isotope discrimination and photosynthesis. Annual Review of Plant Physiology and Plant Molecular Biology 40: 503-537.

Freedman L. 1957. The fossil Cercopithecoidea of South Africa. Annals of the Transvaal Museum 23:122-213

Freedman L. 1960. Some new fossil cercopithecoid specimens from Makapansgat, South Africa. Palaeontologia Africana 7: 7-45

Freedman L. 1961. New cercopithecoid fossil, including a new species, from Taung, Cape Province, South Africa. Annals of the South African Museum 46: 1-10

Freedman L. 1970. A new checklist of fossil cercopithecoidea of South Africa. Palaeontologia Africana 13: 109-110

Freedman L. 1976. South African fossil Cercopithecoidea: a re-assessment including a description of new material from Makapansgat, Sterkfontien and Taung. Journal of Human Evolution 5: 297-315

Freedman L, Brain CK. 1972. Fossil cercopithecoid remains from the Kromdraai Australopihecine site (Mammalia: Primates). Annals of the Transvaal Museum 28: 1-16

Freedman L, Brain CK. 1977. A reexamination of the cercopithecoid fossil from Swartkrans (Mammalia: Cercopithecoidea). Annals of the Transvaal Museum 30: 211-218

Freedman L, Stenhouse NS. 1972. The *Parapapio* specimens of Sterkfontein, Transvaal, South Africa. Palaeontologia 14: 93-111

Friedly H, Lotscher H, Oesschger H, Siegenthaler U. 1986. Ice core records of the $^{13}C/^{12}C$ ratio of atmospheric CO_2 in the past two centuries. Nature 324: 237-238

Frost SR, Delson E. 2002. Fossil Cercopithecidea from the Hadar Foramation and surrounding areas of the Afar Depression, Ehtiopia. Journal of Human Evolution 43: 687-748

Frost SR, Marcus LF, Bookstein FL, Reddy DP, Delson E. 2003. Cranial allometry, phylogeography and systematics of large bodied Papionins (Primates: Cercopithecinae) inferred from geometric morphometric analysis of landmark data. The Anatomical Record Part A 275A: 1048-1072

Gautier-Hion A. 1980. Seasonal variation of diet related to species an sex in a community of *Cercopithecus* monkeys. Journal of Animal Ecology 49: 237-269

Gautier-Hion A., Gautier J. 1986. Sexual dimorphism, social units and ecology among sympatric forest guenons. Symposia of the Society for the Study of Human Biology 24: 61-77

Gear JHS. 1926. A preliminary account of the baboon remains froim Taungs. South Afrian Journal of Science 23: 731-747

Gilbert C, Sealy J and Sillen A. 1994. An investigation of barium, calcium and strontium as palaeodietary indicators in the Southwestern Cape, South Africa. Journal of Archaeological Science 21: 173-184

Grine FE. 1986. Dental evidence for dietary differences in Australopithecine and Paranthropus: a quantitative analysis of permanent molar microwear. Journal of Human Evolution 15: 783-822

Grine FE. 1987. Quantitative analysis of oclussal micowear in Australopithecus and Paranthropus. Scanning Microcopy 1: 647-656

Grine FE, Ungar PS, Teaford MF. 2002. Error estimates in dental microwear quantification using SEM. Scanning Microscopy 24: 144-153

Ham R. 1995. Polyspecific association between grey-cheeked mangabeys (*Cercocebus albigena*) and four sympatric primate species in the Lopé Reserve, Gabon. [Abstract from 1995 Spring meeting Primate Society of Great Britain, University of Edinburgh; April, 95]. Folia Primatologia 64: 100.

Harvati K, Frost SR, McNulty KP. 2004. Neanderthal taxonomy reconsidered: implications o 3D primate models of intra- and interspecific differences. Proceedings of the National Academy of Sciences 101: 1147-1152

Hassan A. 1977. Mineralogical studies of bone apatite and their imlplication for radiocarbon dating. Radio Carbon 19: 364-374

Hughton SH. 1925. A note on a the occurrence of a pecies of baboon in lime depsits near Taungs. Transvaal Royal Society of South Africa 12: lxviii

Hoefs J. 1997. Stable isotope geochemistry (fourth edition). Berlin: Springer-Verlag.

Iserman K. 1981. Uptake of stable strontium by plants and effects on plant growth. In: Skoryna SC, editor. Handbook of sable strontium. New York: Plenum Press. p 65-86

Jolly CJ. 1970. The seed-eaters: A new model of hominid differentiation based on a baboon analogy. Man 5: 1-26

Jolly CJ. 1972. The classification and natural history of *Theropithecus* (*Simopithecus*) (Andrews, 1916) baboons of the African Pleistocene. Bulletin of the British Museum of Natural History (Geology) 22: 1-123

Jolly CJ. 2001. Papionin analogies for human evolution. Yearbook of Physical Anthropology 44: 178-204

Jones TR. 1937. A new fossil primate from Sterkfontein, Krugersdorp, Transvaal. South African Journal of Science 33: 709-728

Jones TR. 1978. The skull and mandible of the South African baboon: a morphological study. Johannesburg: Witwatersrand University Press.

Kelley J, Plavcan MJ. 1998. A simulation test of hominid species number at Lufeng, China: implications for the use of the coefficient of variation in paleotaxonomy. Journal of Human Evolution 35: 577-596

Kendall C, Caldwell EA. 1998. Fundamentals of isotope geochemistry. In: Kendall C, McDonnell JJ, editors. Isotope Tracers in Catchment Hydrology. Amsterdam: Elsevier Science B. V. p51-86

Kingdon J. 1997. The Kingdon field guide to African mammals. New York: Academic Press

Kitching JW. 1953. A new species of fossil baboon from Potgietersrust. South African Journal of Science 50: 66-69

Klepinger LL. 1984. Nutritional assessment from bone. Annual Review of Anthropology 13: 75-96

Koch PL, Turos N, Fogel ML. 1997. The effects of sample treatment on the isotopic integrity of carbonate in biogenic hydroxylapatite. Journal of Archaeological Science 24: 417-429

Kohn MJ. 1996. Predicting animal $\delta^{18}O$: accounting for diet and physiological adaptation. Geochimica and Cosmochimica Acta 60: 4811-4829

Kohn MJ, Schoeninger MJ, Barker W. 1999. Altered sates: effects of diagenesis on fossil tooth chemistry. Geochimica et Cosmochimica Acta 63: 2737-2747

Kohn MJ, Schoeninger MJ, Valley JW. 1996. Herbivore tooth oxygen isotope composition: the effects of diet and physiology. Geochimica et Cosmochimica Acta 60: 3889-3896

Krueger HW, Sullivan CH. 1984. Models for carbon isotopr fractionation between diet and bone. In: Turnland JF, Johnston PE, editors. Stable isotopes in nutrition. ACS Symposium Series, 258, American Chemical Society. p. 205-222

Kummer H. 1971. Primate societies: group techniques of ecological adaptation. Chicago: Aldine

Lambert JB, Weydert-Hofmeyer JM. 1993. Dietary inferences from bone. In: Lambert JB, Grupe G, editors. Prehistoric human bone – archaeology at the molecular level. Springer-Verlag. p217-229

Leaky MG. 1982. Extinct large colobines from the Plio-Pleistocene of Africa. American Journal of Physical Anthropology 58: 153-172

Leaky MG. 1993. Evolution of *Theropithecus* in the Turkana basin. In: Jablonski N, editor. *Theropithecus*: the rise and fall of a primate genus. Cambridge: Cambridge University Press. p85-125

LeGros RZ, LeGros JP, Trautz OR, Klein E. 1969. Two types of carbonate substitution in apaptite structure. Experientia 24: 5-7

Lee-Thorp JA. 1989. Stable isotopes in deep time: the diets of fossil fauna and hominids. Ph.D thesis, University of Cape Town.

Lee-Thorp JA. 2002. Two decades of progress towards understanding fossilization processes and isotopic signals in calcified tissue minerals. Archaeometry 44: 435-446

Lee-Thorp JA, Sponheimer M. 2003. Three case studies used to reassess the reliability of fossil bone and tooth enamel isotope signals for paleodietary studies. Journal of Anthropological Archaeology 22: 208-216

Lee-Thorp JA, van der Mewre NJ. 1987. Carbon isotope analysis of fossil bone apatite. South African journal of Science 83: 712-715

Lee-Thorp JA, van der Merwe NJ. 1993. Stable carbon isotope studies of Swartkrans fossils. Transvaal Museum Monographs 8: 251-256

Lee-Thorp JA, Sealy JC, van der Merwe NJ. 1989a. Stable carbon isotope ratio differences between bone collagen and bone apatite, and their relationship to diet. Journal of Archaeological Science. 16: 585-599

Lee-Thorp JA, Sponheimer M, van der Merwe NJ. 2003. What do stable isotopes tell us about hominid dietary and ecological niches in the Pliocene? International Journal of Osteoarcaeology 13: 104-113

Lee-Thorp JA, van der Merwe NJ, Brain CK. 1989b. Isotopic evidence for dietary differences between two extinct baboon species from Swartkrans. Journal of Human Evolution. 18: 183-190

Lee-Thorp JA, van der Merwe NJ, Brain CK. 1994. Diet of *Australopithecus robustus* at Swartkrans from stable carbon isotopic analysis. Journal Human Evolution. 27: 361-372

Longinelli A. 1966. Ratios of ^{18}O: ^{16}O in phosphate and carbonate from living and fossil marine organisms. Nature 211: 923-927

Longinelli A. 1984. Oxygen isotopes in mammal bone phosphate: a new tool for paleaohydrological and palaeoclimatological research? Geochimica et Cosmochimica Acta 48: 385-390

Luyt CJ. 2001. Revising palaeoenvironment from the hominid-bearing Plio-Pleistocene sites: new isotopic evidence from Sterkfontein . Unpublished Masters Thesis. University of Cape Town

Luz B, Kolodny Y. 1985. Oxygen isotope variations in phosphate of biogenic apatites iv. Mammal teeth and bones. Earth and Planetary Science Letters 75: 29-36

Luz B, Kolodny Y, Horowitz M. 1984. Fractionation of oxygen isotopes between mammalian bone-phosphate and environmental drinking water. Geochimica et Cosmochimica Acta 48: 1689-1693

Maier W. 1970. New fossil Cercopithecoidea from the lower Pleistocene cave deposits of the Makapansgat Limeworks, South Africa. Palaeontologia Africana 13: 69-109

Maier W. 1972. The first complete skull of *Simipithecus darti* from Makapansgat, South Africa and its systematic position. Journal of Human Evolution 1: 395-405

Maguire JM. 1998. Makapansgat: a guide to the palaeontological and archaeological sites of the Makapansgat Valley. Pretoria: Desktop Creations.

Marino BD, McElroy MB. 1991. Isotopic composition of atmospheric CO_2 inferred from carbon in C_4 plant cellulose. Nature 349: 127-131

McFadden PL, Brock A, Patridge TC. 1979. Palaeomagnetism and the age of the Makapansgat hominid site. Earth and Planetary Science Letters 44: 373-382

McKee JK, Keyser AW. Craniodental remains of *Papio angusticeps* from Haasgat cave site, South Africa. International Journal of Primatology 15: 823-841

Menzel RG, Heald WR. 1955. Distibution of potassium rubidium, caesium, calcium and strontium within plants grown in nutrient solutions. Soil Sience 80: 287-293

Mitchell RL. 1955. Trace elements in soils. In: Bear FE, editor. Trace elements in soils. New York: Reinhold. p253-258

Mitani M. 1991. Niche overlap and polyspecific association among sympatric Cercopithecoids in the Campo Animal Reserve, Southwestern Cameroon. Primates: 32, 137-151.

Mollett O. 1947. Fossil mammals from the Makapan Valley, Potgietresrust. I. Primates. South African Journal of Science 43: 295-303

Nagel U. 1970. Social organisation in a baboon hybrid zone. Procedures of the 3rd International Congress on Primatology: 223-233

Nagel U. 1973.A comparison o anubis baboons, hamadryas baboons and their hybrids at a species order in Ethiopia. Folia Primatologia 19: 104-165

Newman TK, Jolly CJ, Rogers J. 2004. Mitochondrial phylogeny and systematics of baboons (*Papio*). American Journal of Physical Anthropology 124: 17-27

Nielsen FH. 1986. Other elements: Sb, Ba, B, Br, Cs, Ge, Rb, Ag, Sr, Sn, Ti, Zr, Be, Bi, Ga, Au, In, Nb, Sc, Te, Tl, W. In: Mertz W, editor. Trace-elements in human and animal nutrition. Orlando: Acadmic Press. p. 415-463

O'Leary M. 1993. Biochemical basis for carbon isotope fractionation. In: Ehleringer JR, Hall AE, Farquhar GD, editors. Stable isotopes and stable cabon-water relations. New York: Acaemic Press. p 19-28

Panarello HO, Fernandez J. 2002. Stable carbon isotope measurements on hair from wild animals from altiplanic environments of Jujuy, Argentina. Radiocarbon 44: 709-716

Patridge TC. 1973. Geomorphological dating of cave openings at Makapansgat, Sterkfontein, Swartkrans and Taung. Nature 246: 75-79

Partridge TC. 2000. Hominid bearing cave and tufa deposits. In: Partridge TC, Maud RR, editors. The Cenozoic of Southern Africa. New York: Oxford University Press. p 100-131

Partridge TC, Latham AG, Heslop D. 2000. Appendix on magnetotratigraphy Makapansgat, Sterkfontein, Taung and Swartkrans. In: Partridge TC, Maud RR, editors. The Cenozoic of Southern Africa. New York: Oxford University Press. p126-129

Pickering TR, Clarke RJ, Heaton JL. 2004. The context of Stw573 an early hominid skull and skeleton from Sterkfontein Member 2 taphonomy and paleoenvironment. Journal of Human Evolution 46: 279-297

Phillips-Conroy JE, Jolly CJ. 1981. Sexual dimorphism in two subspecies of Ethiopian baboons (*Papio hamadryas*) and their hybrids. American Journal of Physical Anthropology 56 (2): 115-129

Pocock, TN. 1987. Plio-Pleistocene fossil mammalian microfauna of Southern Africa - a preliminary report including description of two new fossil muroid genera (Mammalia: Rodentia). Palaeontologia Africana 26. p 69-91

Ramakrishnan U, Coss RG. 2001. A comparison of sleeping behaviour of three sympatric primates. Folia Primatologia 72: 51 – 63

Rose MD. 1976. Bipedal behavior of olive baboons (*Papio anubis*) and its relevance to an understanding of the evolution of human bipedalism. American Journal of Physical Anthropology 44: 247-261

Reed KE. 1996. The paleoecology of Makapansgat and other Afican Plio-Pleistocene hominid localities. P.hD. Dissertation, State University of New York at Stony Brook.

Reed KE. 1997. Early hominid evolution and ecological change through the African Plio-Pleistocene. Journal of Human Evoltion 32: 289-322

Reed KE. 1998. Using large mammal communities to examine ecological and taxonomic organisation and predict vegetation in extant and extinct assemblages. Paleobiology 32: 384-408

Reid DJ, Schwartz GT, Dean C, Chandrasekera. 1998. A histological reconstruction of dental development in the common chimpanzee, *Pan troglodytes.* Journal of Human Evolution 35: 427-448

Rey C, Renugupalakrishnan V, Shimizu M, Collins B, Glisher MJ. 1991. A resolution enhanced Fourier transform infrared spectroscopic study of the environment of the CO_3 ion in the mineral phase of enamel during formation and maturation. Calcified Tissue International 49: 259-268

Runia LT. 1987. Strontium and calcium distribution in plants: effect on palaeodietary studies. Journal of Archaeological Science 14: 599-608

Schoeninger MJ. 1985. Trophic level effects on $^{15}N/^{14}N$ and $^{13}C/^{12}C$ ratios in bone collagen and strontium levels in bone mineral. Journal of Human Evolution 14: 515-525

Schoeninger MJ, Iwaniec UT, Glander KE. 1997. Stable isotope ratios indicate diet and habitat use in new world monkeys. American Journal of Physical Anthropology 103: 69-83

Schoeninger MJ, Iwaniec UT, Nash LT. 1998. Ecological attributes recorded in stable isotope ratios of arboreal prosimian hair. Oecologia 113: 222-230

Schoeninger MJ, Moore J, Sept JM. 1999. Subsistence strategies of two "savanna" chimpanzee populations: the stable isotope evidence. American Journal of Physical Anthropology 49: 297-314

Schroeder HA, Tipton IH, Nason AP. 1972. Trace-element metals in: strontium and barium. Journal of Chronic Disease 25: 491-517

Sealy JC, Sillen A. 1988. Sr and Sr/Ca in marine and terrestrial foodwebs in the Southern Cape, South Africa. Journal of Archaeological Science 15: 425-438

Sealy JC, van der Merwe NJ, Sillen A, Kruger FJ, Krueger HW. 1991. $^{87}Sr/^{86}Sr$ as a dietary indicator in modern and archaeological bone. Journal Archaeological Science 18: 399–416

Sillen A. 1986. Biogenic and diagenetic Sr/Ca in Plio-Pleistocene fossils in Omo Shungura Formation. Paliobiology 12: 311-323

Sillen A. 1988. Elemental and isotopic analysis of mammalian fauna from Southern Africa and their implications for paleodietary research. American Journal of Physical Athropology 76: 49-60

Sillen A. 1992. Strontium-calcium ratios (Sr/Ca) of *Australopithecus robustus* and associated fauna from Swartkrans. Journal of Human Evolution 23: 495-516

Sillen A, Kavanagh M. 1982. Strontium and palaeodietary research: a review. Yearbook of Physical Anthropology 25: 67-90

Sillen A, Hall G, Richardson S and Armstrong R. 1995. Strontium calcium ratios (Sr/Ca) and isotopic ratios ($^{87}Sr/^{86}Sr$) of *Australopithecus robustus* and *Homo* sp. from Swartkrans. Journal of Human Evolution 28: 277-285

Singleton M. 2002. Patterns of cranial shape variation in the Papionini (Primates: Cercopithecinae). Joural of Human Evolution 42: 547-578

Smit AJ. 2001 Source identification in marine ecosystems: food web studies using $\delta^{13}C$ and $\delta^{15}N$. In: Unkovich M, Pate J, McNeill A, Gibbs DJ, editors. Stable Isotope Techniques in the Study of Biological Processes and Functioning Ecosystems. Dordrecht: Kluwer Academic Publishers. p219-245

Smith BN, Epstein S. 1971. Two categories of $^{13}C/^{12}C$ ratios for plants. Plant Physiology 47: 380-384

Sponheimer M. 1999. Isotopic ecology of the Makapansgat Limeworks fauna. Ph.D. Dissertation, Rutgers University.

Sponheimer M, Lee-Thorp JA. 1999a. Alteration of enamel carbonate environments during fossilization. Journal of Archaeological Science 26: 143-150

Sponheimer M, Lee-Thorp JA. 1999b. Isotopic evidence for the diet of an early hominid, *Australopithecus africanus*. Science 83: 368-370

Sponheimer M, Lee-Thorp JA. 1999c. Oxygen isotope in enamel carbonate and their ecological significance. Journal of Archaeological Science 26: 723-728

Sponheimer M, Lee-Thorp JA. 2001. The oxygen isotope composition of mammalian enamel carbonate from Morea Estate, South Africa. Oecologia 126: 153-157

Sponheimer M, Lee-Thorp J. 2003a. Using isotope data of fossil bovid communities for palaeoenvironmnetal reconstruction. South African Journal of Science 99: 273-275

Sponheimer M, Lee-Thorp J. 2003b. Three case studies used to reassess the reliability of fossil bone and enamel isotope signals for paleodietary studies. Journal of Anthropological Archaeology 22: 208-216

Sponheimer M, Lee-Thorp. In press. Enamel diagenesis at South African Australopith sites: implications for paleoecolgical reconstruction with trace-elements. Geochimica et Cosmochimica Acta

Sponheimer M, Reed K, Lee-Thorp JA. 1999. Combining isotopic and ecomorphological data o refine bovid paleodietary reconstruction: a case study from Makapansgat Limeworks hominid locality. Journal of Human Evolution 36: 705-718

Sponheimer M, Reed K, Lee-Thorp JA. 2001. Isotopic palaeoecology of Makapansgat Limeworks Perissodactyla. South African Journal of Science 97: 327-329

Sponheimer M, Grant CC, De Ruiter DJ, Lee-Thorp JA, Cordon DM, Cordon J. 2003a. Diets of impala from Kruger National park: evidence from stable carbon isotopes. Koedoe 46: 101-106

Sponheimer M, Lee-Thorp JA, DeRuiter DJ, Smith JM, van der Merwe NJ, Reed K, Grant CC, Ayliffe LK, Robinson TF, Heidelberger C, Marcus W. 2003b. Diets of southern African Bovidae: Stable isotope evidence. Journal of Mammology 84: 471-47

Sponheimer M, Robinson T, Ayliffe L, Roeder B, Hammer J, Passey B, west A, Cerling T, Dearing D, Ehleringer J. 2003c. Nitrogen isotopes in

mammalian herbivores: hair $\delta^{15}N$ values from a controlled feeding study. International Journal of Osteoarchaeology 13: 80-87

Sponheimer M, Robinson TF, Roeder BL, Passey BH, Ayliffe LK, Cerling TE, Dearing MD and Ehleringer JR. 2003d. An experimental study of nitrogen flux in llamas: is ^{14}N preferentially excreted? Journal of Archaeological Science 30: 1-7

Sponheimer M, de Ruiter D, Lee-Thorp J, Spath A. 2005a. Sr/Ca and early hominin diets revisited: new data from modern and fossil tooth enamel. Journal of Human Evolution 48: 147-156

Sponheimer M, Lee-Thorp J, de Ruiter D, Codron D, Codron J, Baugh T, Thackeray F. 2005b. Hominins, sedges and termites: new carbon isotope data from the Sterkfontin valley and Kruger National Park. Journal of Human Evolution 48: 301-312

Teaford MF, Oyen OJ. 1989. In-vivo and in-vitro turnover in dental microwear. American Journal of Physical Anthropology 80: 447-60

Thackeray JF, Myer S. 2004. *Parapapio broomi* and *P. jonesi* from Strekfontein: males and females of one species? Annals of the Transvaal Museum 41: 79-82.

Tieszen LL, Fagre T. 1993. Effect of diet quality and composition on the isotopic composition of respiratory CO2, bone collagen, bioapatite and soft tissue. In: Lambert JB, Grupe G, editors. Prehistoric human bone: archaeology at the molecular level. Springer and Verlag. p 121-155

Tieszen LL, Senyimba MM, Imbamba SK, Troughton JH. 1979. The distribution of C_3 and C_4 grasses and carbon isotope discrimination along an altitudinal and moisture gradient in Kenya. Oecologia 37: 337-350

Toots H, Voorhies MR. 1965. Strontium in fossil bones and the reconstruction of food chains. Science 149: 854-855

Ungar PS, M'Kirera F. 2003. A solution to the worn tooth conundrum in primate functional anatomy. Procedures of the national Academy of Sciences of the United States of America 100: 3874-3877

van der Merwe NJ, Medina E. 1989. Photosynthesis and $^{12}C/^{13}C$ ratios in Amazonian rain forests. Geochimica et Cosmochimica Acta 53:1091-1094.

van der Merwe NJ, Tschauner H. (1999). C_4 plants and the development of human societies. In: Sage RF and Monson RK, editors. C_4 Plant Biology. Academic Press. pp. 509-549

van der Merwe NJ, Thackeray JF, Lee-Thorp JA, Luyt J. 2003. The carbon isotope ecology and diet of Australopithecus africanus at Sterkfontein, South Africa. Journal of Human Evolution 44: 581-597

Vogel JC. 1980. Fractionation of carbon isotopes during photosynthesis. In: Sitzungsberighte der Hiedelberger Akademie der Wisserschaften, Mathematisch – Nuturwissinschaftliche Klasse Jarhgang. 1980. 3. Abhandlung. Berlin: Springer-Verlag. p 111-135

Vogel JC, van der Merwe NJ. 1977. Isotopic evidence for early maize cultivation in New York State. American Antiquity 42: 238-242

Vogel JC, Fulls A, Ellis RP. 1978. The geographical distribution of Kranz grass in South Africa. South African Journal of Science 74:209-15.

Vrba ES. 1983. Biostratigraphy and chronology, based particularly on bovidae, of southern hominid-associated assemblages: Makapansgat, Sterkfontein, Taung, Kromdraai, Swartkrans; also Elandsfontein (Saldana), Broken Hill (now

Kabwe) and Cave of Hearths. Proceeding of the First International Congress Humane Paleontology 2: 707-752

Vrba E. 1995. The fossil record of African antelopes (Mammalia, Bovidae) in relation to human evolution and paleoclimate. In: Vrba E, Denton G, Burckle L, Partridge T. *Paleoclimate and Evolution With Emphasis on Human Origins*. New Haven: Yale University Press. p 385-424

Wang Y, Cerling T. 1994. A model of fossil and bone diagenesis: implications for paleodiet reconstruction from stable isotopes. Palaeogeography, Palaeoclimatology, Palaeoecology 107: 281-289

Williams FL, Ackermann RR, Leigh SR. in press. Facial-masticatory affinities in Parapapio and other Plio-Pleistocene southern African papionins. American Journal of Physical Anthropology

WoldeGabriel G, White TD, Suwa G, Renne P, de Heinzeli J, Hart WK. 1994. Ecological and temporal placement of early Pliocene hominids at Aramis, Ethiopia. Nature 371: 330-333

Zavada MS, Cadman A. 1993. Palynological investigation at the Makapansgat Limeworks: an *Australopithecine* site. Journal of Human Evolution 25: 337 – 350

Zinner D, Peleaz F, Torkler F. 2001. Distrobution and habitat associations of baboons (*Papio hamadryas*) in Central Eritrea. International Journal of Primatology22: 397-413

APPENDICES

APPENDIX A

Appendix A-1. Classification of South African Plio-Pleistocene Fossil Cercopithecoidea

Order: Primates (Linnaeus, 1758)

Suborder: Anthropoidea (Mivart, 1864)

Superfamily 1: Cercopithecoidea (Simpson, 1931)

Family: Cercopithecidae (Gray, 1821)

Subfamily 1: Cercopithecinae (Blanford 1888)

Genera: *Parapapio* (Jones, 1937)

Parapapio antiquuus (Freedman, 1957)

Pp. whitei (Broom, 1940)

Pp. broomi (Broom, 1940)

Pp. jonesi (Broom, 1940)

Dinopithecus (Broom, 1936)

Gorgopithecus (Broom and Robinson, 1949)

Papio (Erxleben, 1777)

Theropithecus (Geoffroy, 1843)

Theropithecus oswaldi (Delson, 1993?)

T. darti (Delson, 1993?)

Subfamily 2: Colobinae (Elliot, 1913)

Genera : *Cercopithecoides* (Mollett, 1947)

Cercopithecoides williamsi (Mollet, 1947)

Adapted from Brain (1981, 1993), Delson (1992, 1993) and Freedman (1957)

Appendix A-2. Specimen information for fossil cercopithecoid specimens from Makapansgat Members 3 and 4 analysed in this investigation.

Table A.1. Accession, sex and age information for individual fossil cercopithecoid specimen analysed in this study.

MP Accession no.	M Accession no.	Taxon	Sex	Age	Digitised	Enamel Sampled
MP36	M236	*Cercopithecoides williamsi* (?)		Adt	N	Y
MP3A	M203	*C. williamsi* (Freedman 1960)	M	Adt	Y	Y
MP239		*Parapapio* sp.	F	Adt	Y	Y
	M3133	*Parapapio* sp.		Adt	Y	Y
	M3147	*Parapapio* sp.		Adt	Y	Y
	M3079	*Parapapio* sp.	F	Adt	Y	Y
	M3084	*Parapapio* sp.		Adt	Y	Y
	M3078	*Parapapio* sp.		Adt	Y	N
MP167	M3053	*Parapapio* sp.		Adt	Y	N
MP47/MP92/MP5	M624	*Parapapio* sp.		Adt	Y	N
MP208		*Parapapio* sp.		Adt	Y	Y
MP151	M3037	*Parapapio broomi* (Freedman 1960)		Adt	N	Y
MP2	M202	*Pp. broomi* (Freedman 1960)	M	Adt	Y	Y
MP75	M2961	*Pp. broomi* (Freedman 1960), *Pp. jonesi* (Maier 1970)	M	Adt	Y	Y
MP170	M3056	*Pp. broomi* (Maier 1970)	F	Adt	Y	Y
	M3070	*Pp. broomi* (Maier 1970) *Pp. whitei* (Freedman 1976)	F	Adt	Y	Y
	M3065	*Pp. broomi* (Maier 1970)	M	Adt	Y	N
MP76	M2062	*Pp. broomi* (Maier 1970), *Pp. whitei* (Freedman 1960/'76)	M	Adt	Y	Y
MP119	M3005	*Pp. broomi* (?), *Pp. whitei* (Freedman 1960)	F	Adt	Y	Y
MP173	M3059	*Pp. jonesi* (Maier 1970)	M	Adt	N	Y
MP164	M3050	*Pp. whitei* (Eisenhart ?)		Adt	Y	Y

MP223		*Pp. whitei* (Freedman 1976)	M	Adt	Y	Y
MP221		*Pp. whitei* (Freedman 1976)	M	Adt	Y	N
MP222		*T. darti* (Freedman 1976)	F	Adt	Y	Y
	M3073	*T. darti* (Maier 1970)		Adt	Y	N

M = Male

F = Female

Adt = Adult

N = No

Y = Yes

Table A.2. Accession, sex and age information for extant chacma baboon specimens analysed in this study.

Accession no.	Sex	Age
ZM33402	F	Adt
ZM33401	F	Adt
ZM33410	M	Adt
ZM33412	M	Adt
ZM33646	M	Adt
ZM12970	M	Adt
ZM17179	M	Adt
ZM33664	M	Adt
ZM33670	M	Adt
ZM33671	M	Adt
ZM33677	F	Adt
ZM33672	F	Adt
ZM33676	M	Adt
ZM33674	M	Adt
ZM33675	M	Adt
ZM35819	F	Adt
ZM35921	F	Adt
ZM35719	M	Adt
ZM35916	M	Adt
ZM35918	M	Adt
ZM35935	F	Adt
ZM35944	F	Adt
ZM35941	F	Adt
ZM35949	F	Adt
ZM35948	F	Adt
ZM36824	F	Adt
ZM36829	F	Adt
ZM37112	F	Adt
ZM40445	M	Adt
UCT73384	M	Adt
Rondeboschkull	M	Adt

ZM = Iziko Museums – Cape Town Natural History Museum Accession Numbers

UCT= University of Cape Town Accession Numbers

"Rondeboschskull" Curated at UCT

APPENDIX B

Appendix B-1. Pre-Treatment Protocol Experiments

Calibration

Table B.1. $\delta^{13}C$ ad $\delta^{18}O$ results and calibrated results for internal standards.

Results for Internal Standards (all δ values in ‰)								
Analysis	Standard	Weight	Exp $\delta^{13}C$	Obs $\delta^{13}C$	Cal $\delta^{13}C$	Exp $\delta^{18}O$	Obs $\delta^{18}O$	Cal $\delta^{18}O$
32175	Cararra Z	0.08	2.25	10.81	2.09	-1.27	-1.35	-1.29
32244	Cararra Z	0.07	2.25	10.68	1.96	-1.27	-1.39	-1.35
Ave		0.08	2.25	10.72	1.99	-1.27	-1.37	-1.32
Stdev		0.008		0.08	0.08		0.03	0.04
32166	*Cav Mbl	0.08	0.34	9.39	0.68	-8.97	-7.51	-8.79
32176	Cav Mbl	0.08	0.34	9.32	0.62	-8.97	-7.33	-8.57
32168	Cav Mbl	0.07	0.34	9.12	0.41	-8.97	-8.26	-9.70
32231	Cav Mbl	0.08	0.34	9.18	0.47	-8.97	-7.57	-8.86
32245	Cav Mbl	0.08	0.34	9.16	0.46	-8.97	-7.49	-8.76
Ave		0.08	0.34	9.23	0.57	-8.97	-7.63	-8.94
Stdev		0.004		0.12	0.11		0.36	0.44
32167	NBS18	0.13	-5.05	3.55	-5.06	-23.03	-23.83	
32177	NBS18	0.12	-5.05	3.65	-4.96	-23.03	-22.76	
32187	NBS18	0.11	-5.05	3.37	-5.24	-23.03	-23.77	
32232	NBS18	0.12	-5.05	3.37	-5.23	-23.03	-23.51	
32246	NBS18	0.13	-5.05	3.69	-4.93	-23.03	-22.16	
Ave		0.12	-5.05	3.53	-5.09	-23.03	-23.21	
Stdev		0.01		0.15	0.15		0.72	

* Cav Mbl = Cavendish Marble

Figure B.1. $\delta^{13}C$ calibration curve calculated from internal standards

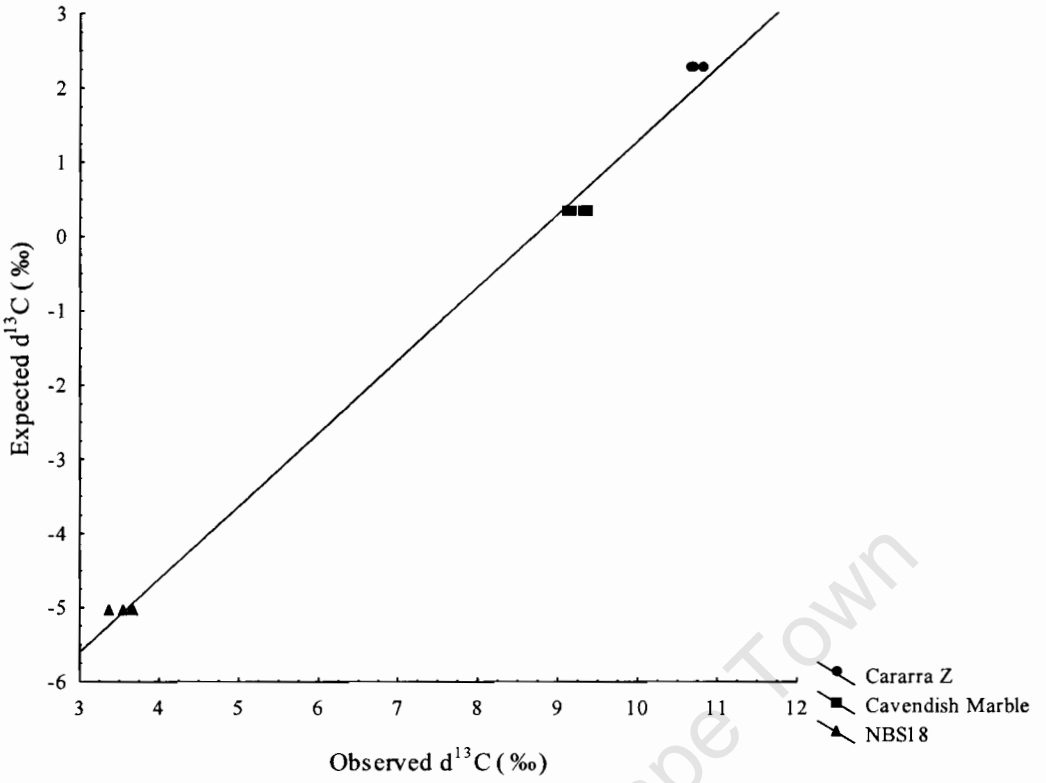

Fit: $r^2 = 0.9956$;
$\delta^{13}C$ calibration equation: $y = -8.5534 + 0.9839*x$

Figure B.2. $\delta^{18}O$ (‰) calibration curve calculated from internal standards

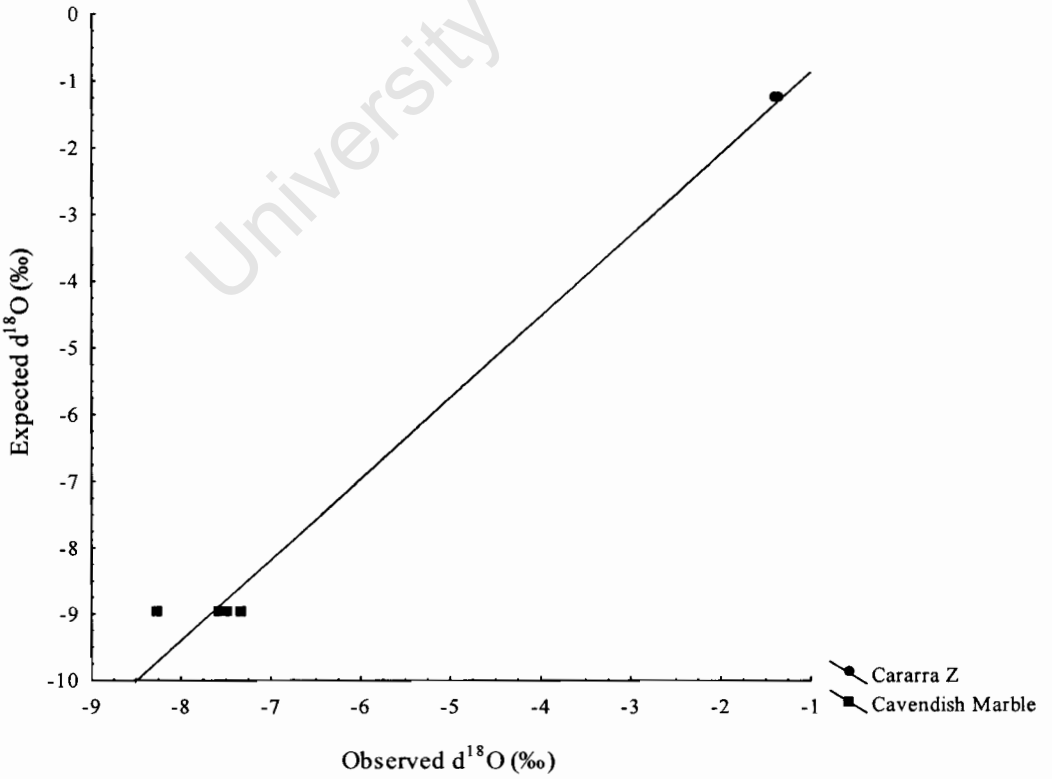

Fit: $r^2 = 0.9907$
$\delta^{18}O$ calibration equation: $y = 0.3476 + 1.2186*x$

Table B.2. Results for different variants of Pre-Treatment Procedure

Results for different variants of Pre-Treatment Procedure (all δ values in ‰)								
Pre-treatment I								
Sample no.	Sample $Weight_{Initial}$	Sample $Weight_{Final}$	Net Weight Loss	% Weight Loss	Analysis	Weight	$\delta^{13}C$	$\delta^{18}O$
AA1	5.95	3.57	2.38	40.00	32172	1.11	-10.51	1.12
AA2	5.87	3.59	2.28	38.84	32173	1.02	-10.55	0.99
AA3	6.39	4.06	2.33	36.46	32242	1.06	-10.89	0.82
Ave			2.33	38.43			-10.65	0.98
Stdev			0.05	1.80			0.21	0.15
Pre-treatment II								
Sample no.	Sample $Weight_{Initial}$	Sample $Weight_{Final}$	Net Weight Loss	% Weight Loss	Analysis	Weight	$\delta^{13}C$	$\delta^{18}O$
BB1	5.41	3.31	2.10	38.82	32235	0.97	-10.6	0.9
BB2	6.16	3.47	2.69	43.67	32236	0.96	-10.7	0.7
BB3	6.67	4.35	2.32	34.78	32243	1.05	-10.9	1.3
Ave			2.37	39.09			-10.7	0.9
Stdev			0.30	4.45			0.1	0.3
Pre-treatment III								
Sample no.	Sample $Weight_{Initial}$	Sample $Weight_{Final}$	Net Weight Loss	% Weight Loss	Analysis	Weight	$\delta^{13}C$	$\delta^{18}O$
CC1	5.47	3.48	1.99	36.38	32174	1.02	-10.5	1.1
CC2	5.32	3.24	2.08	39.10	32178	1.00	-10.5	1.2
CC3	6.47	3.96	2.51	38.79	32241	1.04	-10.8	1.0
Ave			2.19	38.09			-10.6	1.1
Stdev			0.28	1.49			0.2	0.1
Pre-treatment IV								
Sample no.	Sample $Weight_{Initial}$	Sample $Weight_{Final}$	Net Weight Loss	% Weight Loss	Analysis	Weight	$\delta^{13}C$	$\delta^{18}O$
DD1	5.44	3.1	2.34	43.01	32183	0.99	-10.7	1.2
DD2	5.08	2.85	2.23	43.90	32184	1.02	-10.5	0.6
DD3	6.46	3.88	2.58	39.94	32239	1.11	-10.7	0.9
Ave			2.38	42.28			-10.6	0.9
Stdev			0.18	2.08			0.1	0.3
Pre-treatment V								
Sample no.	Sample $Weight_{Initial}$	Sample $Weight_{Final}$	Net Weight Loss	% Weight Loss	Analysis	Weight	$\delta^{13}C$	$\delta^{18}O$
EE1	4.94	2.97	1.97	39.88	32181	1.04	-9.5*	1.2
EE2	5.82	3.4	2.42	41.58	32182	1.02	-10.4	1.3
EE3	4.87	2.66	2.21	45.38	32240	1.04	-10.7	1.3
Ave			2.20	42.28			-10.2	1.3
Stdev			0.23	2.82			0.6	0.1

*EE1 suspected that sample was not thoroughly rinsed after acetone treatment

Results for different variants of Pre-Treatment Procedure (all δ values in ‰) continued…

			Untreated					
Sample no.	Sample $Weight_{Initial}$	Sample $Weight_{Final}$	Net Weight Loss	% Weight Loss	Analysis	Weight	$\delta^{13}C$	$\delta^{18}O$
1	5.08	4.42	0.66	12.99	34671	0.08	-4.7	0.9
2	6.03	5.03	1.00	16.58	34672	0.07	-4.8	0.8
3	6.21	5.47	0.74	11.92	34673	0.08	-4.6	1.1
Ave			0.80	13.83			-4.7	0.9
Stdev			0.18	2.44			0.1	0.2

APPENDIX C

Appendix C-1. $\delta^{13}C$ and $\delta^{18}O$ results for standards and resulting calibrations

Table C.1. $\delta^{13}C$ ad $\delta^{18}O$ results and calibrated results for internal standards.

Results for Internal Standards (all δ values in ‰)								
Analysis	Standard	Weight	Exp $\delta^{13}C$	Obs $\delta^{13}C$	Cal $\delta^{13}C$	Exp $\delta^{18}O$	Obs $\delta^{18}O$	Cal $\delta^{18}O$
32318	Cararra Z	0.08	2.25	10.73	2.02	-1.27	-1.16	-1.91
32332	Cararra Z	0.09	2.25	10.74	2.02	-1.27	-1.34	-2.10
32339	Cararra Z	0.09	2.25	10.71	2.00	-1.27	-1.48	-2.24
32349	Cararra Z	0.08	2.25	10.67	1.96	-1.27	-1.57	-2.34
32358	Cararra Z	0.07	2.25	10.51	1.80	-1.27	-1.94	-2.72
Ave		0.08		10.67	1.96		-1.50	-2.26
Stdev		0.01		0.09	0.09		0.29	0.30
32323	Cav Mbl*	0.08	0.34	9.09	0.37	-8.95	-7.49	-8.38
32324	Cav Mbl	0.09	0.34	9.09	0.37	-8.95	-7.76	-8.66
32325	Cav Mbl	0.09	0.34	9.15	0.43	-8.95	-7.49	-8.38
32326	Cav Mbl	0.09	0.34	9.12	0.40	-8.95	-7.47	-8.36
32340	Cav Mbl	0.08	0.34	9.33	0.61	-8.95	-7.27	-8.16
32350	Cav Mbl	0.08	0.34	9.35	0.63	-8.95	-7.09	-7.98
32355	Cav Mbl	0.08	0.34	9.04	0.32	-8.95	-7.78	-8.68
32359	Cav Mbl	0.08	0.34	9.48	0.76	-8.95	-6.57	-7.44
Ave		0.08		9.21	0.49		-7.36	-8.25
Stdev		0.004		0.16	0.16		0.39	0.40
32319	NBS18	0.12	-5.05	3.82	-4.92	-23.03	-21.07	-22.26
32328	NBS19	0.14	-5.05	3.65	-5.10	-23.03	-22.48	-23.70
32341	NBS20	0.12	-5.05	3.93	-4.82	-23.03	-21.45	-22.65
32351	NBS21	0.11	-5.05	3.70	-5.05	-23.03	-21.33	-22.53
32354	NBS22	0.16	-5.05	3.20	-5.55	-23.03	-24.21	-25.48
Ave		0.13		3.66	-5.09		-22.11	-23.32
Stdev		0.02		0.28	0.28		1.29	1.32
32327	Linc Lime**	0.08	1.10	9.74	1.02	-10.40	-10.22	-11.17
32335	Linc Lime	0.09	1.10	10.19	1.48	-10.40	-8.72	-9.65
32337	Linc Lime	0.08	1.10	10.12	1.41	-10.40	-9.00	-9.93
32360	Linc Lime	0.07	1.10	9.68	0.96	-10.40	-9.82	-10.77
Ave		0.08		9.93	1.22		-9.44	-10.38
Stdev		0.01		0.26	0.26		0.70	0.71

* Cav Mbl = Cavendish Marble

**Linc Lime = Lincoln Limestone

Figure C.1. $\delta^{13}C$ calibration curve calculated from internal standards

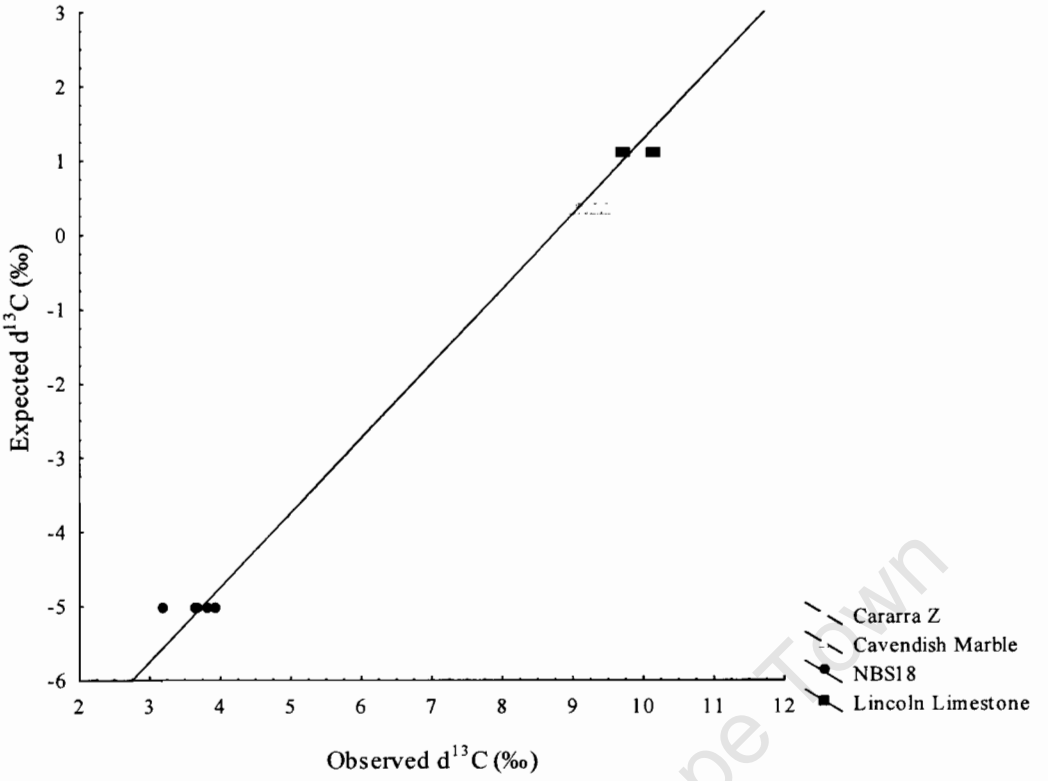

Fit: $r^2 = 0.9911$

$\delta^{13}C$ calibration equation: $y = -8.7646 + 1.0049*x$

Figure C.2. $\delta^{13}C$ calibration curve calculated from internal standards

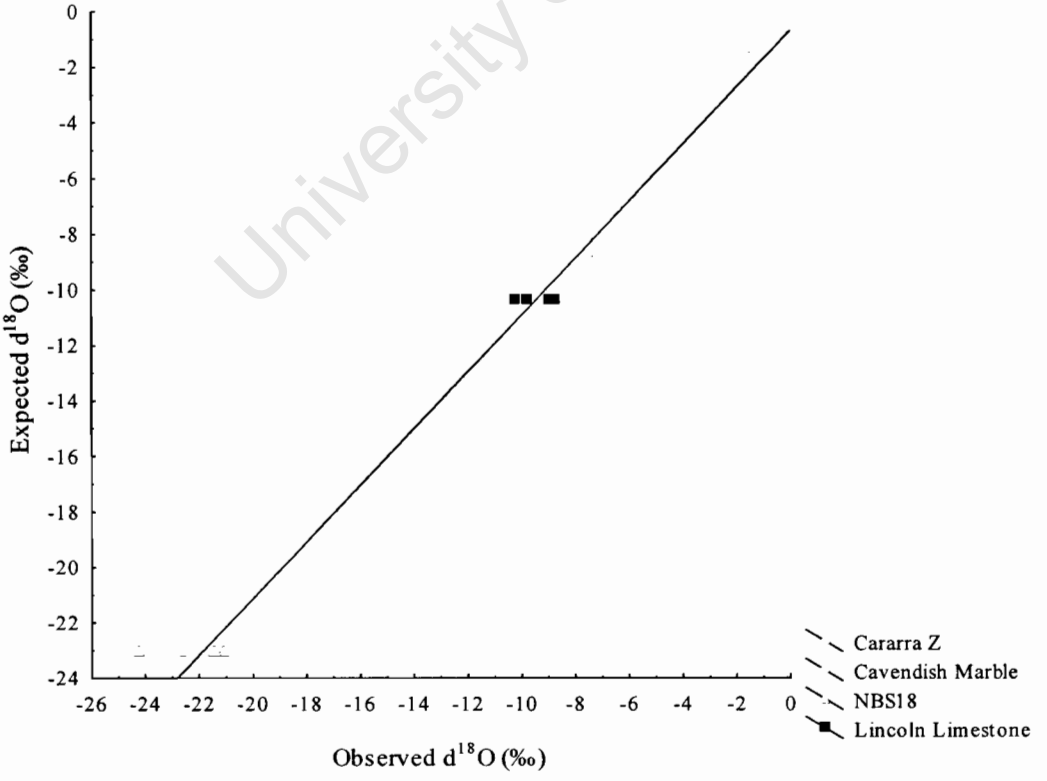

Fit: $r^2 = 0.9844$

$\delta^{18}O$ calibration equation: $y = -0.6989 + 1.0216*x$

Appendix C-2. $\delta^{13}C$ and $\delta^{18}O$ and trace-element results for fossil cercopithecoid sample from Makapansgat Limeworks Members 3 and 4.

Table C.2. $\delta^{13}C$ and $\delta^{18}O$ results for fossil cercopithecoid sample from Makapansgat Limeworks Members 3 and 4.

Stable Isotope Results for Fossil Cercopithecoid Enamel Carbonate (all δ values in ‰)							
Taxon	Analysis	Accession no.	Weight	Obs $\delta^{13}C$	Cal $\delta^{13}C$	Obs $\delta^{18}O$	Cal $\delta^{18}O$
Cercopithecoides williamsi	32356	MP36	0.54	4.58	-4.27	-1.68	-1.80
C. williamsi	32357	MP3A	0.61	0.76	-8.17	-2.51	-2.78
Parapapio sp.	32331	M3133	0.96	1.09	-7.83	-1.30	-1.35
Parapapio sp.	32321	M3084	1.03	2.56	-6.33	-1.51	-1.60
Parapapio sp.	32336	*M3147	0.98	6.62	-2.18	-0.99	-0.99
Parapapio sp.	32343	MP208	1.00	0.99	-7.93	-1.26	-1.31
Parapapio sp.	32353	M3070	1.16	1.33	-7.58	-1.15	-1.17
Parapapio sp.	32346	**M3079	0.98	-0.18	-9.13	-5.09	-5.84
Parapapio sp.	32347	MP239	1.07	-0.50	-9.45	-2.17	-2.38
Pp. broomi	32320	MP151	0.96	-0.51	-9.46	-1.30	-1.35
Pp. broomi	32342	MP2	1.00	-1.02	-9.98	0.80	1.14
Pp. broomi	32338	MP170	1.01	1.32	-7.59	-1.76	-1.89
Pp. jonesi	32352	MP75	1.21	2.42	-6.47	-0.76	-0.71
Pp. jonesi	32344	MP173	1.02	1.46	-7.45	-2.04	-2.23
Pp. whitei	32322	MP164	1.02	2.52	-6.37	-0.73	-0.68
Pp. whitei	32345	MP223	1.04	3.23	-5.65	-2.30	-2.54
Pp. whitei	32329	MP119	1.03	1.63	-7.28	-1.34	-1.39
Pp. whitei	32330	MP76	0.97	-0.57	-9.52	-0.88	-0.85
Theropithecus darti	32348	MP222	1.02	6.41	-2.40	-3.83	-4.35

*M3147 yielded an apparently anomalous $\delta^{13}C$ value inconsistent with $\delta^{13}C$ values reported for *Parapapio* specimens from Makapansgat and elsewhere.

**M3079 yeiled an apparently anomalous $\delta^{18}O$ value inconsistent with $\delta^{18}O$ values obtained for *Parapapio* specimens from Makapansgat

Table C.3. Trace-element results for fossil cercopithecoid sample from Makapansgat Limeworks members 3 and 4.

Trace-element Results for Fossil Cercopithecoid Tooth Enamel (elemental abundances are reported in ppm)							
	Taxon	Ca (ppm)	Sr (ppm)	Ba (ppm)	Sr/Ca*1000	Ba/Ca*1000	Sr/Ba
MP239	*Parapapio* sp.	303530.75	126.40	21.90	0.42	0.07	5.77
M3133	*Parapapio* sp.	332899.77	178.38	63.87	0.54	0.19	2.79
M3079	*Parapapio* sp.	329030.87	88.46	88.44	0.27	0.27	1.00
M3084	*Parapapio* sp.	311450.00	56.87	36.77	0.18	0.12	1.55
MP208	*Parapapio* sp.	312889.99	53.69	20.45	0.17	0.07	2.63
*M3147	*Parapapio* sp.	332120.79	325.43	26.01	0.98	0.08	12.51
MP151	*Pp. broomi*	316209.36	72.40	26.39	0.23	0.08	2.74
MP2	*Pp. broomi*	330626.07	179.92	24.80	0.54	0.08	7.26
MP170	*Pp. broomi*	303576.79	124.78	35.75	0.41	0.12	3.49
MP173	*Pp. jonesi*	251052.78	45.52	16.34	0.18	0.07	2.79
MP75	*Pp. jonesi*	300066.36	116.50	88.17	0.39	0.29	1.32
M3070	*Pp. whitei*	278498.33	56.43	20.89	0.20	0.07	2.70
**MP76	*Pp. whitei*	3862.65	0.92		0.24		
MP119	*Pp. whitei*	326558.42	92.87	53.67	0.28	0.16	1.73
MP164	*Pp. whitei*	305231.79	121.38	42.83	0.40	0.14	2.83
MP223	*Pp. whitei*	291014.47	80.57	43.66	0.28	0.15	1.85
MP222	*Theropithecus darti*	334210.00	142.00	72.10	0.43	0.22	1.97

Appendix C-3. Stable Isotope and trace-element data for fossil fauna from Makapansgat Limeworks, Member 3, that was used for contextual and comparative purposes

Table C.4. Stable Isotope and trace-element data for fossil fauna from Makapansgat Limeworks, Member 3, that was used for contextual and comparative purposes – data was taken from Sponheimer (1999), Sponheimer and Lee-Thorp (1999, unpublished data, in press), Sponheimer et al. (2005)

Stable Isotope and Trace-Element Data for Fossil Fauna from Makapansgat Member 3						
Sample ID	Family	$\delta^{13}C$ (‰)	$\delta^{18}O$ (‰)	Sr/Ca*1000	Ba/Ca*1000	Sr/Ba
M1177	Bovidae	-10.7	-0.4	0.54	0.10	5.70
M1209	Bovidae	-11.8	0.7	0.16	0.15	1.11
M1642	Bovidae	-12.1	3.5			
M183	Bovidae	-9.0	1.7	0.15	0.11	1.38
M183	Bovidae	-9.2	-1.1			
M19	Bovidae	-11.4	1.4	0.19	0.17	1.13
M6281	Bovidae	-11.0	3.1	0.43	0.12	3.51
M6293	Bovidae	-11.1	1.9	0.06	0.04	1.66
M6325	Bovidae	-12.1	2.0			
M6477	Bovidae	-10.3	1.4	0.22	0.23	0.98
M6518	Bovidae	-10.8	1.7	0.09	0.07	1.29
M6769	Bovidae	-11.8	-0.2	0.37	0.39	0.95
M7504	Bovidae	-10.5	2.0			
M760	Bovidae	-10.0	0.8	0.21	0.15	1.35
M766	Bovidae	-11.7	3.8	0.70	0.11	6.61
M767	Bovidae	-10.2	3.0	0.24	0.11	2.28
M7689	Bovidae	-11.2	0.4			
M7805	Bovidae	-11.8	2.2			
M7811	Bovidae	-12.2	1.6			
M8823	Bovidae	-10.4	3.1			
M8876	Bovidae	-12.3	0.8			
M9014	Bovidae	-10.9	1.8			
M9053	Bovidae	-12.0	1.1			
M9172	Bovidae	-11.0	1.6	1.22	0.45	2.71
M9173	Bovidae	-10.7	1.8	0.87	0.13	6.82
M9177	Bovidae	-8.6	-1.4	0.72	0.70	1.04
M9178	Bovidae	-8.6	-2.9	0.41	0.08	5.47
M997	Bovidae	-10.8	3.2	0.51	0.10	5.04
M1113	Giraffidae	-10.8	0.6	0.19	0.11	1.82
M1798	Giraffidae	-9.6	1.1	0.27	0.17	1.56
M1876	Giraffidae	-10.7	2.4			
M2085	Giraffidae	-12.0	4.2	0.49	0.53	0.92
M2086	Giraffidae	-10.3	1.5			
M528	Giraffidae	-10.0	3.1			
M8853	Giraffidae	-9.9	1.5			

Stable Isotope and Trace-Element Data for Fossil Fauna from Makapansgat Member 3 (continued….)

Sample ID	Family	$\delta^{13}C$ (‰)	$\delta^{18}O$ (‰)	Sr/Ca*1000	Ba/Ca*1000	Sr/Ba
M936	Giraffidae	-11.3	5.2			
M938	Giraffidae	-11.1	2.2	0.22	0.12	1.84
M938	Giraffidae	-10.4	2.4			
M1218	Bovidae	-2.0	-1.0			
M1398	Bovidae	-3.3	-0.7			
M3180	Bovidae	-4.0	-0.9	0.29	0.38	0.77
M387	Bovidae	0.4	0.4	0.39	0.22	1.76
M388	Bovidae	-3.7	0.4			
M6269	Bovidae	-4.3	0.1			
M6272	Bovidae	1.2	1.3			
M6274	Bovidae	-1.0	2.3			
M6280	Bovidae	1.3	0.2			
M6305	Bovidae	-0.5	-0.8	0.46	0.26	1.77
M6308	Bovidae	1.2	3.0	0.63	0.61	1.02
M6528	Bovidae	-3.3	1.0			
M6609	Bovidae	-0.5	1.0			
M6669	Bovidae	0.9	-0.8	0.92	0.39	2.36
M6963	Bovidae	-0.2	2.1	0.31	0.19	1.62
M7243	Bovidae	-5.2	-0.6	0.86	0.22	3.92
M7319	Bovidae	-4.1	0.8			
M7685	Bovidae	-0.3	0.0	0.55	0.40	1.38
M774	Bovidae	1.2	-0.6	0.29	0.30	0.94
M8161	Bovidae	-3.2	-1.0			
M8163	Bovidae	-4.1	0.3			
M8351	Bovidae	-2.2	-1.2	0.37	0.28	1.31
M8835	Bovidae	0.6	-0.7			
M8897	Bovidae	-1.3	-2.0			
M977	Bovidae	-1.4	-0.4	0.26	0.24	1.11
M978	Bovidae	-5.0	-1.6			
M193	Equidae	0.2	-2.3			
M2476	Equidae	0.0	-1.4			
M2480	Equidae	-1.2	-1.2			
M2505	Equidae	-1.9	-3.2			
MUE A2651	Equidae	-0.7	-1.6			
M1826/1890	Suidae	-2.1	-4.7			
M1859	Suidae	-2.1	-2.2	0.27	0.10	2.81
M1886	Suidae	-1.6	-5.7	0.13	0.09	1.55
M2025	Suidae	-0.9	-1.8	0.80	0.40	2.02
M8913	Suidae	-0.5	-1.1	0.46	0.23	1.95

APPENDIX D

Appendix D-1. 3D anatomical landmark coordinate data for the extant chacma baboon sample

Table D.1. 3D anatomical landmark coordinate data for the extant *Papio h. ursinus* sample

3D Anatomical Landmark Coordinate Data - Extant *Papio h. ursinus* Sample												
Specimen no. (sex)	Prosthion			Nasospinale			Premaxilla-maxilary suture (R)			Rhinion		
	x	y	z	x	y	z	x	y	z	x	y	z
ZM33402F	-41.97	197.31	-174.60	-41.59	202.58	-169.20	-57.41	196.23	-163.95	-38.59	228.25	-147.61
ZM33401F	-42.19	208.71	-174.82	-40.52	216.07	-167.27	-57.05	208.59	-163.85	-35.10	241.54	-146.01
ZM33410M	-23.12	198.97	-216.31	-21.92	207.07	-209.01	-41.67	200.57	-199.99	-18.15	242.87	-181.74
ZM33412M	-28.41	228.07	-211.66	-26.47	236.38	-203.41	-48.73	230.95	-197.51	-21.63	267.16	-176.90
ZM33646M	-24.82	194.48	-218.80	-23.65	205.93	-213.12	-43.04	197.79	-204.06	-19.54	241.73	-186.23
ZM12970M	-25.49	199.70	-211.02	-24.60	205.48	-205.42	-45.21	200.10	-194.83	-21.65	239.54	-178.63
ZM17179M	-27.68	197.41	-215.84	-26.21	206.38	-210.25	-51.16	200.60	-200.50	-20.81	244.86	-177.96
ZM33664M	-31.11	206.38	-205.16	-29.70	212.15	-198.35	-48.73	208.45	-186.02	-22.41	250.21	-171.55
ZM33670M	-34.86	193.03	-201.46	-33.93	196.13	-197.21	-52.43	193.98	-185.84	-24.91	237.61	-175.46
ZM33671M	-27.18	194.49	-194.23	-25.94	200.43	-189.20	-46.04	201.18	-178.28	-18.98	236.94	-167.80
ZM33677F	-19.46	207.32	-164.08	-18.74	213.09	-159.59	-35.54	211.05	-151.56	-15.57	239.43	-144.30
ZM33672F	-18.46	200.59	-159.80	-16.61	208.55	-156.68	-33.34	203.38	-150.00	-10.39	239.03	-141.63
ZM33676M	-34.89	184.08	-190.19	-33.42	192.83	-186.12	-54.84	193.90	-173.95	-25.96	230.80	-166.85
ZM33674M	-26.30	193.63	-210.49	-25.78	199.49	-205.17	-47.25	193.15	-195.25	-23.74	238.94	-177.63
ZM33675M	-27.31	187.92	-195.66	-26.89	194.90	-191.00	-44.91	192.72	-182.02	-22.34	231.99	-161.98
ZM35819F	-24.40	198.37	-171.50	-24.73	201.17	-168.48	-42.57	199.56	-157.95	-22.24	232.86	-150.48
ZM35921F	-35.62	206.26	-172.44	-34.99	210.71	-168.41	-52.92	210.08	-160.01	-31.36	240.26	-149.58
ZM35719M	-34.48	210.82	-206.56	-34.24	216.94	-201.88	-54.59	215.46	-190.36	-29.11	252.36	-174.44
ZM35916M	-41.81	188.58	-215.15	-40.65	199.72	-206.45	-62.60	190.55	-198.48	-34.91	236.60	-179.72
ZM35918M	-42.87	180.19	-191.99	-41.09	189.35	-188.99	-60.49	187.81	-177.99	-35.77	231.79	-173.30
ZM35935F	-28.30	201.90	-167.21	-28.06	206.57	-163.37	-43.90	200.52	-153.60	-26.58	236.04	-143.83

ZM35944F	-30.43	204.38	-174.14	-29.91	215.94	-162.92	-48.42	205.22	-162.43	-26.62	239.25	-143.40
ZM35941F	-28.14	205.54	-162.97	-27.46	210.26	-158.14	-44.73	204.17	-154.98	-24.59	238.69	-138.38
ZM35949F	-28.17	222.03	-174.15	-27.51	231.13	-168.54	-44.86	226.31	-162.40	-23.72	258.08	-142.48
ZM35948F	-24.57	202.44	-178.51	-24.85	209.45	-170.83	-42.02	201.10	-166.14	-20.19	236.25	-149.49
ZM36824F	-35.26	197.75	-165.52	-34.86	201.87	-162.80	-51.35	201.20	-152.12	-30.24	230.12	-141.60
ZM36829F	-34.88	218.33	-172.59	-33.77	223.73	-166.10	-50.27	217.73	-159.21	-28.60	244.37	-141.71
ZM37112F	134.42	129.06	-173.60	138.68	131.48	-169.86	127.10	143.49	-162.45	164.39	143.98	-146.11
ZM40445M	134.84	125.06	-207.13	141.44	128.00	-199.66	123.37	144.05	-191.32	171.70	141.49	-171.63
UCT73384M	118.73	111.33	-206.74	127.71	117.20	-199.82	107.21	134.26	-195.16	163.96	134.61	-173.77
RondeboschSkull	137.71	123.51	-208.43	142.26	125.34	-204.10	130.66	143.17	-194.91	173.70	141.33	-173.98

3D Anatomical Landmark Coordinate Data - Extant *Papio h. ursinus* Sample (Continued…)

Specimen no. (sex)	Superior premaxilary suture (R)			Zygomaxillary inferior (R)			Nasion			Zygomaxillary superior (R)		
	x	y	z	x	y	z	x	y	z	x	y	z
ZM33402F	-41.97	237.8	-133	-70.03	221.41	-113.8	-34.29	269.01	-114.07	-55.68	247.65	-112.69
ZM33401F	-38.19	250.96	-133.72	-70.08	242.6	-106.11	-28.02	285.83	-113.59	-50.15	267.95	-109.46
ZM33410M	-21.04	255.39	-160.26	-53.82	243.89	-126.79	-9.97	305.39	-131.26	-33.74	282.49	-126.59
ZM33412M	-28.18	273.82	-162.65	-56.99	265.21	-124.28	-13.32	318.42	-113.41	-36.47	301.05	-115.04
ZM33646M	-25.73	252.28	-163.45	-56.26	241.66	-130.55	-10.91	297.86	-123.45	-36.97	280.84	-122.27
ZM12970M	-27.62	249.25	-161.8	-56.12	238.8	-128.6	-12.7	296.73	-127.25	-32.47	274.67	-123.23
ZM17179M	-27.22	251.11	-166.02	-62.54	246.71	-130.22	-13.24	304.75	-126.01	-38.13	281.22	-125.72
ZM33664M	-28.98	254.92	-162.03	-55.94	245.68	-116.93	-14.45	300.86	-116.4	-34.56	281.01	-114.19
ZM33670M	-31.7	244.27	-163.77	-58.86	239.52	-122.15	-12.21	295.05	-126.92	-35.55	278.28	-122.24
ZM33671M	-25.61	245.54	-157.4	-56.45	242.53	-121.83	-9.05	296.76	-125.35	-30.51	274.04	-121.21
ZM33677F	-20.39	246.31	-136.01	-47.16	238.05	-110.18	-9.04	285.61	-116.6	-28.66	263.16	-113.31
ZM33672F	-15.56	247.62	-133.26	-45.59	242.23	-107.5	-3.73	284.84	-118.78	-23.64	269.4	-108.81
ZM33676M	-31.84	241.37	-153.41	-60.64	244.2	-117.85	-15.07	302.32	-119.39	-38.14	279.08	-118.53
ZM33674M	-30.84	244.42	-163.52	-65.47	241.64	-124.84	-16.78	294.54	-128.44	-39.59	272.56	-124.87
ZM33675M	-28.29	238.85	-153.33	-57.83	233.65	-116.68	-17.48	286.64	-117.74	-39.53	267.34	-115.42
ZM35819F	-27.87	240.33	-140.2	-54.63	232.63	-110.89	-17.23	278.1	-118.51	-36.62	256.64	-111.94

ZM35921F	-35.47	248.18	-133.24	-68.2	236.72	-109.61	-25.08	279.21	-114.74	-48.32	261.36	-109.3
ZM35719M	-35.91	258.29	-160.62	-69.22	250.62	-126.6	-24.95	307.14	-118.57	-47.39	283.61	-119.17
ZM35916M	-42.86	243.21	-166.57	-76.02	245.16	-124.4	-24.73	300.73	-125.81	-50.93	282.62	-122.93
ZM35918M	-40.1	247.51	-156.04	-69.27	248.51	-119.26	-25.93	298.21	-126.85	-47.67	280.12	-120.18
ZM35935F	-31.74	243.58	-132.34	-57.14	233.09	-109.33	-21.52	283.73	-114.2	-39.84	259.51	-109.14
ZM35944F	-34.26	243.51	-138.33	-63.31	236	-109.55	-24.46	282.61	-115.09	-45.1	264.73	-109.55
ZM35941F	-31.11	245.78	-130.9	-61.12	236.86	-104.82	-22.29	283.54	-109.36	-43.14	262.58	-104.18
ZM35949F	-28.47	266.13	-127.49	-57.41	254.4	-105.38	-17.71	298.94	-105.94	-37.41	280.55	-103.66
ZM35948F	-25.71	240.98	-141.04	-41.8	200.91	-166.03	-16.6	279.67	-113.62	-33.8	261.48	-110.64
ZM36824F	-33.54	239.4	-128.61	-61.82	231.53	-103.76	-24.65	276.81	-110.55	-42.61	256.2	-107.32
ZM36829F	-32.9	250.76	-132.87	-63.14	241.23	-109.49	-20.87	284.47	-108.06	-43.75	266.51	-107.22
ZM37112F	172.23	151.65	-131.01	142.93	171.13	-114.57	201.24	162.38	-113.77	174.79	168.12	-110.64
ZM40445M	175.48	151.02	-160.38	152.14	176.25	-125.59	222.38	166.77	-121.33	195.79	175.14	-118.27
UCT73384M	163.22	143.47	-167.69	144.39	167.3	-122.91	216.53	160.05	-121.98	189.19	169.06	-118.63
RondeboschSkull	175.34	149.14	-162.24	151.73	175.6	-125.5	216.41	159.82	-124.34	188.29	168.62	-120.09

3D Anatomical Landmark Coordinate Data - Extant *Papio h. ursinus* Sample (Continued…)

Specimen no. (sex)	Frontomalare-orbitale (R)			Orbitalnotch (R)			Frontomalare-temporale (R)			Glabella		
	x	y	z	x	y	z	x	y	z	x	y	z
ZM33402F	-67.39	260.1	-104	-48.89	272.3	-110.03	-70.9	260.84	-94.03	-33.02	277.32	-109.66
ZM33401F	-61.66	280.43	-101.81	-43.75	290.85	-108.57	-64.99	283.69	-90.48	-26.35	294.69	-108.02
ZM33410M	-49.36	293.46	-117.97	-28.98	308.15	-128.16	-57.3	293.13	-107.61	-8.68	315.03	-124.42
ZM33412M	-49.67	312.22	-103.35	-28.06	323.84	-109.16	-53.91	314.63	-91.64	-10.96	328.99	-105.68
ZM33646M	-50.66	292.87	-114.89	-29.46	303.91	-121.68	-55.08	299.42	-105.19	-9.61	310.67	-115.04
ZM12970M	-49.51	289.93	-117.65	-28.03	298.27	-125.58	-56	288.85	-107.09	-10.61	303.45	-123.43
ZM17179M	-54.04	297.38	-113.6	-31.93	308.71	-123.2	-60.06	301.83	-101.65	-12.12	313.24	-118.99
ZM33664M	-48.63	293.45	-104.71	-28.67	304.83	-112.49	-50.73	300.89	-94.67	-12.59	309.88	-109.94
ZM33670M	-47.9	291.14	-114.67	-28.1	300.85	-124.71	-53.19	295.58	-105.67	-10.01	305.65	-122.03
ZM33671M	-45.96	290.87	-114.54	-24.56	300.46	-123.72	-47.04	298.35	-104.65	-7.34	304.28	-119.55
ZM33677F	-41.87	276.17	-105.34	-24.28	289.05	-114.08	-43.53	284.56	-96.37	-7.24	294.57	-112.95
ZM33672F	-36.38	282.46	-106.37	-19.05	290.03	-116.15	-38.99	289.93	-99.46	-2.09	292.45	-117.51

ZM33676M	-53.8	293.53	-110.19	-31.23	304.04	-118.27	-55.34	300.01	-100.81	-13.6	308.04	-114.39
ZM33674M	-56.01	287.86	-116.07	-35.01	299.46	-125.66	-58.59	295.13	-104.56	-15.63	304.59	-124.29
ZM33675M	-53.18	281.65	-108.18	-34.6	293.09	-116.55	-55.58	289.54	-98.92	-17.07	296.66	-113.75
ZM35819F	-48.51	272.47	-107.55	-29.14	281.39	-116.14	-49.75	281.15	-99.05	-15.59	285.95	-115.99
ZM35921F	-59.95	275.86	-104.63	-40.51	284.22	-114.01	-62.49	281.29	-94.76	-23.46	290.49	-111.1
ZM35719M	-62.89	298.56	-108.85	-41.48	311.23	-115.59	-65.16	302.54	-97.03	-23.66	316.51	-112.02
ZM35916M	-65.59	295.51	-113.08	-43.13	308.28	-123.02	-70.47	299.36	-101	-23.66	313.47	-118.75
ZM35918M	-63.3	296.65	-114.41	-44.02	305.09	-126.61	-65.56	304.26	-105.28	-23.48	310.4	-124.13
ZM35935F	-52.97	274.49	-106.74	-36.13	286.02	-112.48	-57.57	277.2	-97.98	-21.6	289.74	-110.28
ZM35944F	-56.6	277.67	-103.99	-40.54	288.63	-113.41	-59.91	280.69	-94.05	-21.99	293.09	-110.09
ZM35941F	-56.11	276.87	-98.05	-34.61	285.05	-106.76	-59.93	279.74	-90.22	-21.77	291.02	-105.1
ZM35949F	-51.8	294.37	-97.2	-32.1	303.94	-104.37	-53.39	300.03	-87.5	-15.38	310.14	-100.57
ZM35948F	-51.57	274.67	-101.78	-30.36	286.13	-111.16	-54.33	277.83	-91.87	-14.99	291.31	-109.62
ZM36824F	-58.6	272	-100.02	-39.57	282.29	-108.18	-59.66	278.22	-92.13	-22.78	284.31	-106.79
ZM36829F	-54.95	281.65	-98.31	-35.34	289.2	-105.52	-60.01	283.72	-90.1	-18.35	292.88	-102.13
ZM37112F	178.45	187.41	-104.03	198.6	178.32	-110.11	182.61	191.81	-95.13	211.75	166.72	-107.61
ZM40445M	198.39	196.21	-113.65	216.77	183.44	-120.42	201.02	205.17	-102.67	233.04	171.24	-115.25
UCT73384M	192.58	189.69	-112.82	212.96	177.44	-121.06	200.4	197.51	-102.01	227.4	164.24	-116.78
RondeboschSkull	192.36	188.39	-113.13	212.6	175.87	-121.81	197.81	193.93	-103.6	226.21	163.44	-118.69

3D Anatomical Landmark Coordinate Data - Extant *Papio h. ursinus* Sample (Continued…)

Specimen no. (sex)	Temporal-frontal-parietal suture (R)			Bregma			Premaxillary-maxillary suture (L)			Premaxillary suture superior (L)		
	x	y	z	x	y	z	x	y	z	x	y	z
ZM33402F	-68.96	261.85	-75.45	-31.71	280.41	-49.2	-28.03	192.26	-164.52	-33.41	237.12	-132.03
ZM33401F	-62.19	277.46	-74.78	-22.42	299.37	-50.93	-25.37	204.5	-165.36	-30.18	251.05	-133.29
ZM33410M	-42.39	292.39	-84.71	-7.29	312.95	-59.57	-1.2	196.96	-201.16	-10.66	257.06	-158.12
ZM33412M	-46.72	302.81	-72.65	-7.25	315.12	-43.65	-8.3	223.81	-199.91	-13.09	272.73	-162.65
ZM33646M	-39.99	298.73	-79.14	-13.69	306.5	-59.78	-3.39	196.23	-206.14	-10.8	249.78	-165.07
ZM12970M	-51.88	284.3	-82.03	-13.55	305.95	-56.52	-5.11	194.19	-193.37	-15.28	248.27	-160.5
ZM17179M	-48.7	292.26	-79.1	-12.2	307.52	-56.61	-4.08	193.57	-198.71	-12.94	248.32	-170.06

ZM33664M	-46.87	289.54	-73.12	-9.21	308.34	-54.49	-11.4	203.9	-190.83	-15.02	251.63	-162.9
ZM33670M	-43.39	294.77	-80.3	-9.94	307.83	-58.74	-13.76	188.97	-188.59	-15.8	245.5	-161.1
ZM33671M	-46.22	287.88	-84.61	-8.93	305.49	-54.77	-7.09	192.65	-178.03	-10.38	243.78	-154.43
ZM33677F	-42.6	279.47	-76.96	-6.43	303.15	-56.3	-2.37	206.72	-151.5	-9.33	246.97	-134.42
ZM33672F	-38.28	284.62	-78.54	0.31	310.02	-53.6	0.42	198.19	-153.17	-3.98	245.85	-133.77
ZM33676M	-49	291.56	-76.21	-15.14	305.54	-49.16	-13.91	182.37	-176.04	-17.33	240.56	-152.2
ZM33674M	-54.46	279.28	-81.06	-17.05	304.96	-59.5	-6.28	189.77	-196.1	-15.91	245	-162.02
ZM33675M	-52	281.48	-74.53	-16.47	301.51	-48.53	-6.69	187.39	-180.61	-16.99	242.17	-148.47
ZM35819F	-49.75	276.91	-75.41	-13.08	298.3	-56.29	-8.21	194.44	-157.07	-16.85	241.25	-136.38
ZM35921F	-61.25	270.72	-74.89	-24.21	299.95	-51.14	-17.29	201.81	-159.58	-25.73	248.29	-131.29
ZM35719M	-61.27	294.49	-75.41	-24.49	311.03	-49.8	-13.05	209.11	-189.65	-22.66	257.73	-158.1
ZM35916M	-60.93	292.89	-78.1	-22.79	312.28	-56.21	-19.2	184.68	-198.69	-26.66	244.26	-164.32
ZM35918M	-60.94	297.02	-78.7	-22.44	322.3	-65.82	-22.62	182.4	-179.4	-25.78	243.48	-158.49
ZM35935F	-57.59	273.37	-78.34	-22.7	300.98	-50.65	-11.25	200.13	-153.27	-22.24	246.38	-129.17
ZM35944F	-55.78	275.73	-77.44	-21.07	300.4	-49.21	-11.2	203.4	-162.06	-21.19	243.61	-136.89
ZM35941F	-56.71	276.04	-68.77	-21.18	298.54	-46.51	-11.26	201.22	-152.54	-19.03	241.83	-133.6
ZM35949F	-50.97	290.68	-69.64	-17.44	306.51	-42.02	-10.34	222.19	-160.88	-18.54	264.18	-130.44
ZM35948F	-51.06	272.03	-74.01	-16.13	296.43	-46.44	-7.4	196.6	-165.75	-15.19	242.62	-136.38
ZM36824F	-57.6	275.18	-69	-23.51	293.99	-47.53	-17.25	196.98	-152.84	-24.36	237.29	-128.55
ZM36829F	-54.59	276.68	-71.02	-19.48	294.7	-47.54	-17.35	211.63	-158.92	-23.09	248.75	-132.47
ZM37112F	175.57	187.88	-75.67	213.39	168.24	-49.26	138.24	113.58	-160.59	173.99	143.41	-134.19
ZM40445M	198.47	190.56	-75.59	228.55	170.2	-54.96	138.78	104.9	-191.08	180.8	139.31	-158.54
UCT73384M	189.53	187.67	-80.08	224.29	167.27	-53.68	124.96	93.02	-195.22	168.45	128.78	-169.15
RondeboschSkull	189.07	186.61	-83.95	226.45	165.81	-55.73	143.43	105.73	-192.96	181.27	138.91	-159.34

3D Anatomical Landmark Coordinate Data - Extant *Papio h. ursinus* Sample (Continued…)

Specimen no. (sex)	Zygomaxillary inferior (L)			Zygomaxillary superior (L)			Frontomalare-orbitale (L)			Orbital notch (L)		
	x	y	z	x	y	z	x	y	z	x	y	z
ZM33402F	-9.30	214.54	-114.85	-17.25	243.18	-112.50	-2.33	254.18	-104.16	-17.85	269.51	-111.33
ZM33401F	-0.96	231.11	-110.45	-10.44	261.82	-109.98	4.80	270.99	-103.78	-9.69	285.13	-109.93
ZM33410M	24.26	237.81	-129.44	8.63	280.26	-127.02	28.51	291.14	-118.61	9.02	306.32	-128.37

ZM33412M	16.20	257.02	-127.45	4.27	295.51	-117.86	21.70	299.91	-108.35	5.13	320.03	-110.69
ZM33646M	25.87	235.34	-128.56	7.30	275.35	-120.76	25.66	282.30	-113.69	8.77	297.59	-121.53
ZM12970M	16.12	229.26	-124.90	0.11	269.68	-121.12	20.24	279.09	-116.24	5.45	293.18	-125.14
ZM17179M	22.65	234.91	-128.69	5.25	274.80	-126.09	26.14	285.53	-114.38	7.51	303.36	-123.65
ZM33664M	11.76	235.44	-121.72	-0.51	276.00	-115.68	17.01	284.55	-107.80	0.69	300.97	-114.72
ZM33670M	14.73	228.17	-124.00	2.26	270.46	-121.87	19.98	277.66	-115.14	6.63	295.16	-124.90
ZM33671M	17.26	229.77	-119.58	2.13	268.85	-122.10	23.15	278.04	-113.63	10.41	294.72	-122.88
ZM33677F	17.52	230.75	-110.79	4.07	260.47	-112.04	21.93	270.43	-105.55	8.70	285.90	-113.82
ZM33672F	21.92	230.41	-107.28	9.09	263.10	-109.95	27.72	271.77	-106.95	12.82	284.20	-117.27
ZM33676M	13.75	232.15	-118.02	0.99	271.54	-118.03	20.24	280.55	-108.94	2.87	298.71	-118.42
ZM33674M	16.03	225.89	-125.33	1.75	267.21	-125.12	21.39	277.50	-116.65	3.65	293.35	-126.66
ZM33675M	10.89	226.50	-118.23	-3.48	264.40	-115.10	15.12	273.74	-108.27	0.26	289.46	-116.46
ZM35819F	8.72	223.40	-111.38	-1.46	251.70	-110.00	12.59	263.52	-107.78	2.23	276.28	-116.40
ZM35921F	5.69	226.91	-110.86	-7.44	255.24	-109.26	8.11	267.05	-103.05	-6.84	280.29	-113.02
ZM35719M	4.80	239.84	-123.06	-8.33	278.93	-119.84	10.76	288.25	-108.90	-7.61	307.25	-115.96
ZM35916M	7.80	231.44	-123.90	-7.27	276.05	-122.02	13.14	284.24	-113.84	-5.41	303.36	-123.78
ZM35918M	5.11	238.02	-119.48	-9.45	274.36	-120.67	9.91	287.26	-114.67	-6.58	299.31	-127.16
ZM35935F	5.52	230.72	-108.39	-9.55	258.59	-108.79	7.88	270.76	-105.16	-4.71	281.82	-111.92
ZM35944F	10.55	230.69	-109.57	-4.06	260.74	-108.15	8.43	271.30	-102.76	-7.10	284.51	-113.08
ZM35941F	7.75	229.80	-103.85	-4.33	258.59	-103.35	8.44	268.36	-97.53	-7.36	282.58	-106.57
ZM35949F	9.08	244.85	-104.38	-1.82	274.87	-104.85	13.10	283.64	-96.32	-1.12	300.58	-103.92
ZM35948F	16.83	227.63	-112.76	-0.29	257.44	-111.13	17.74	268.41	-101.32	1.69	283.90	-111.42
ZM36824F	2.46	221.96	-104.99	-10.79	251.10	-107.51	6.69	261.74	-101.31	-8.22	276.51	-109.28
ZM36829F	6.38	230.86	-110.63	-7.97	259.03	-108.79	10.87	267.75	-99.49	-6.29	284.20	-105.90
ZM37112F	169.02	110.81	-112.80	187.93	138.31	-110.20	205.90	128.13	-103.27	211.02	150.12	-109.76
ZM40445M	185.16	105.53	-125.08	210.03	140.79	-118.64	228.17	126.47	-112.54	233.17	149.17	-120.98
UCT73384M	175.53	101.45	-123.99	205.28	134.07	-117.17	223.27	123.62	-109.56	228.33	142.41	-118.57
RondeboschSkull	178.68	102.32	-123.50	202.63	131.44	-118.39	219.07	122.29	-110.24	225.15	146.15	-120.45

3D Anatomical Landmark Coordinate Data - Extant *Papio h. ursinus* Sample (Continued...)

Specimen no. (sex)	Frontomalare-temporale (L)			Temporal-frontal-parietal suture (L)			Porion (R)			Porion (L)		
	x	y	z	x	y	z	x	y	z	x	y	z
ZM33402F	-0.0426	255.4631	-94.321	-2.0114	254.7187	-79.5555	75.8014	229.1309	-46.5528	-0.0312	218.808	-47.2106
ZM33401F	8.50	272.78	-94.43	4.62	267.75	-76.45	-67.16	248.83	-45.55	3.51	234.01	-49.65
ZM33410M	34.97	294.54	-108.27	22.37	289.47	-85.14	-57.00	263.40	-44.45	33.68	255.18	-45.41
ZM33412M	28.55	304.08	-95.51	20.95	291.68	-77.27	-59.02	264.72	-42.67	26.74	251.96	-48.80
ZM33646M	32.02	284.98	-103.49	19.41	270.73	-81.49	-65.43	251.49	-46.16	28.28	239.57	-44.65
ZM12970M	24.49	287.91	-104.81	20.63	273.07	-79.02	-63.73	249.44	-46.57	21.62	238.17	-44.18
ZM17179M	31.22	292.66	-101.40	19.44	282.55	-82.46	-63.17	254.82	-43.90	25.62	243.12	-44.26
ZM33664M	22.31	293.73	-98.84	17.48	280.44	-77.48	-58.52	255.07	-39.75	24.10	245.36	-45.79
ZM33670M	26.81	286.64	-105.14	19.00	279.56	-80.66	-60.23	255.32	-45.68	21.85	240.69	-47.29
ZM33671M	25.63	283.56	-103.87	21.06	278.66	-80.14	-61.41	255.65	-46.91	23.21	242.63	-45.18
ZM33677F	25.16	274.99	-97.13	23.03	272.13	-79.86	-48.96	252.22	-45.28	25.13	245.85	-46.15
ZM33672F	31.46	276.14	-98.98	29.16	276.36	-81.00	-43.36	261.89	-41.95	27.41	249.71	-46.11
ZM33676M	21.79	289.28	-98.67	13.24	280.86	-77.84	-68.20	254.26	-43.24	18.97	239.94	-44.02
ZM33674M	25.80	283.28	-106.54	15.45	275.13	-83.98	-66.33	250.54	-45.17	21.36	240.63	-42.67
ZM33675M	18.25	282.62	-97.68	14.41	273.56	-75.74	-65.81	249.65	-40.51	19.72	241.51	-43.49
ZM35819F	16.77	269.55	-99.89	15.75	267.61	-78.28	-58.12	246.10	-43.67	16.85	236.67	-44.85
ZM35921F	10.46	272.36	-93.08	6.33	263.74	-73.48	-68.25	246.71	-43.21	6.94	238.92	-41.40
ZM35719M	13.75	292.76	-98.23	6.02	288.49	-77.65	-73.73	261.27	-44.94	10.23	252.23	-45.37
ZM35916M	18.29	286.82	-102.56	8.22	280.64	-80.71	-78.64	260.30	-40.46	14.03	245.55	-39.02
ZM35918M	14.93	290.43	-104.35	7.19	285.48	-79.96	-73.35	272.97	-40.21	13.42	258.14	-39.88
ZM35935F	10.24	276.01	-95.33	9.89	269.79	-74.57	-62.94	243.52	-49.30	11.21	239.97	-44.14
ZM35944F	11.97	273.48	-93.08	6.10	268.35	-80.35	-65.13	249.43	-44.28	8.78	240.49	-43.66
ZM35941F	12.72	272.15	-88.46	8.39	268.91	-70.17	-61.99	251.07	-38.57	8.34	241.48	-40.43
ZM35949F	16.56	285.93	-86.02	9.99	283.69	-70.34	-61.46	260.41	-41.65	11.75	249.44	-40.33
ZM35948F	20.87	270.41	-92.36	16.20	266.20	-72.26	-59.50	243.48	-41.29	18.44	237.60	-41.56
ZM36824F	10.06	266.93	-92.49	7.75	263.77	-73.16	-66.23	244.77	-41.59	8.12	234.84	-43.20
ZM36829F	14.24	273.08	-89.76	7.93	265.21	-73.90	-65.09	245.96	-42.16	8.22	232.80	-43.75
ZM37112F	208.97	126.98	-94.08	201.38	126.99	-76.28	146.46	178.04	-47.34	175.50	112.61	-46.86

ZM40445M	236.75	126.51	-102.07	221.60	131.03	-78.62	152.41	185.53	-49.72	189.67	102.35	-50.31
UCT73384M	232.99	124.75	-98.87	212.00	122.17	-77.01	155.02	183.73	-45.98	188.27	105.91	-42.33
RondeboschSkull	224.98	121.93	-102.26	215.88	124.71	-81.61	158.53	183.53	-46.42	187.99	106.96	-42.17

Appendix D-2. 3D anatomical landmark coordinate data for the fossil cercopithecoid sample

Table D.2. 3D anatomical landmark coordinate data for the fossil cercopithecoid sample from Makapansgat Limework Members 3 and 4.

3D Anatomical Landmark Coordinate Data - Fossil Cercopithecoid Sample												
Specimen no.	Prosthion			Nasospinale			Premaxllary-maxillary suture (R)			Rhinion		
	x	y	z	x	y	z	x	y	z	x	y	z
MP167	216.96	-42.22	-128.15				201.52	-41.44	-121.24	217.77	-5.59	-120.87
	216.95	-42.45	-128.17				201.55	-38.53	-121.07	217.44	-5.65	-121.02
	216.96	-41.70	-128.24				201.55	-39.09	-120.76	216.88	-6.17	-120.83
MP47	210.97	-54.47	-136.99	210.50	-48.21	-126.57	192.58	-54.28	-125.48	211.53	-19.16	-109.38
	211.36	-55.09	-136.61	210.67	-48.31	-127.88	193.24	-55.39	-125.77	211.96	-19.38	-109.53
	211.32	-54.93	-136.52	210.78	-48.51	-127.87	193.16	-54.15	-126.75	211.47	-20.35	-109.82
MP3078	210.70	-40.48	-142.72	207.94	-33.58	-134.28	196.13	-39.83	-135.49	209.47	-10.78	-128.13
	210.43	-40.59	-142.81	208.62	-33.18	-134.57	195.67	-40.01	-134.80	210.43	-9.69	-128.36
	210.41	-40.59	-142.62	208.86	-32.82	-134.57	196.69	-40.24	-135.54	210.28	-10.65	-128.76
MP221	226.30	-85.84	-155.27	225.51	-74.89	-146.51	208.78	-80.26	-147.09	227.05	-45.36	-143.94
	224.77	-86.98	-155.15	223.46	-76.97	-146.66	206.72	-82.06	-147.12	223.65	-47.50	-143.99
	224.80	-87.77	-154.91	223.16	-77.36	-145.29	206.13	-81.97	-146.80	223.48	-46.72	-144.20
MP2				121.72	-211.76	-148.66				144.19	-199.47	-133.19
				121.74	-211.33	-148.98				144.96	-198.71	-131.51
				122.43	-211.87	-149.78				144.24	-198.59	-131.52
MP170							100.15	-210.06	-168.27			
							99.62	-209.50	-168.20			
							99.40	-210.60	-167.90			

MP76							162.26	-168.59	-126.85	192.51	-174.88	-94.74
							161.89	-168.18	-126.14	191.95	-175.58	-94.83
							161.12	-168.36	-126.18	191.20	-174.97	-94.08
MP119	117.16	-195.34	-142.05	123.34	-191.82	-134.71	110.99	-181.77	-133.58			
	117.74	-195.48	-142.49	123.06	-192.09	-135.60	111.39	-181.24	-133.43			
	117.30	-195.90	-142.11	123.28	-192.20	-135.68	111.07	-181.71	-133.60			
MP75										149.73	-195.07	-139.58
										151.12	-194.64	-139.01
										150.65	-194.96	-139.85
MP223	140.86	-196.56	-177.91	146.66	-192.52	-162.66	129.13	-182.38	-167.73	170.73	-174.97	-151.64
	139.86	-197.29	-178.37	146.71	-192.50	-163.20	129.03	-183.30	-168.01	170.47	-174.73	-151.39
	140.67	-197.10	-177.96	147.10	-192.02	-164.27	128.48	-183.29	-167.09	170.06	-175.82	-151.82
MP164												
M3065												
M3084	167.00	-169.91	-139.12	166.80	-170.11	-126.52	153.35	-157.27	-132.44	184.94	-159.05	-106.83
	162.87	-172.33	-140.98	164.91	-169.84	-126.25	151.86	-158.05	-131.46	184.69	-159.25	-107.27
	161.70	-172.48	-140.65	165.00	-170.18	-125.23	151.31	-158.34	-131.41	183.41	-159.75	-106.42
MP239	129.82	-201.58	-146.63	136.93	-195.67	-138.66	125.40	-185.72	-140.06	161.85	-178.02	-126.94
	129.33	-202.04	-146.72	136.99	-195.26	-138.11	123.59	-187.35	-137.79	163.58	-177.67	-126.11
	130.05	-201.37	-146.51	137.01	-195.55	-138.92	123.29	-186.87	-137.54	163.00	-177.38	-126.49
M3070	127.17	-209.66	-119.78	133.67	-203.44	-116.30	118.81	-194.56	-111.85	152.41	-192.68	-111.95
	126.32	-209.21	-120.02	133.70	-204.47	-117.17	119.89	-192.11	-111.74	152.39	-192.71	-112.06
	126.90	-209.09	-119.99	133.19	-204.87	-116.97	118.76	-193.03	-111.42	151.15	-191.85	-113.25
M3079	153.53	-193.76	-131.24	159.72	-189.30	-121.65	145.77	-177.54	-123.74			
	152.14	-192.01	-131.11	160.24	-189.09	-120.75	144.43	-178.82	-122.77			
	154.92	-193.97	-131.02	159.29	-189.37	-121.58	145.63	-179.76	-122.68			
M3147												

M3133												
MP208	127.21	-214.38	-117.48	132.10	-209.98	-111.61	121.68	-200.28	-111.07	152.84	-199.31	-113.47
	127.08	-214.32	-117.06	132.11	-209.79	-111.30	124.80	-199.23	-112.47	152.90	-198.45	-113.31
	125.78	-215.98	-116.76	132.53	-210.39	-111.25	123.07	-197.33	-109.27	152.41	-198.35	-113.05
M3073	215.23	-62.49	-165.63	213.99	-53.01	-157.27	197.67	-57.31	-156.68	217.86	-27.39	-153.07
	214.34	-61.98	-165.57	213.38	-52.23	-156.33	197.56	-57.00	-157.03	217.77	-27.62	-153.04
	213.64	-62.75	-165.47	213.47	-52.05	-155.95	197.67	-56.36	-157.76	217.48	-28.17	-153.23
MP3	108.59	-211.28	-154.54	115.47	-206.38	-145.67	104.96	-198.96	-148.55	147.78	-187.43	-139.43
	108.07	-211.47	-154.50	115.03	-206.77	-146.16	104.33	-199.31	-149.12	147.11	-188.25	-139.59
	108.01	-211.68	-154.61	115.20	-206.60	-145.74	104.12	-199.10	-149.05	147.39	-188.19	-139.46
MP217				126.51	-208.81	-171.13						
				127.89	-209.89	-171.30						
				127.79	-209.76	-171.05						
MP222	110.18	-214.12	-170.92	114.14	-211.29	-163.91	102.21	-205.56	-164.75			
	109.69	-213.87	-170.81	113.80	-210.94	-163.83	102.56	-204.40	-164.79			
	109.80	-214.31	-170.58	113.40	-211.03	-163.63	101.93	-204.87	-164.76			

3D Anatomical Landmark Coordinate Data - Fossil Cercopithecoid sample (Continued…)

Specimen no.	Superior premaxilary suture (R)			Zygomaxillary inferior (R)			Nasion			Zygomaxillary superior (R)		
	x	y	z	x	y	z	x	y	z	x	y	z
MP167							215.20	21.32	-110.67			
							215.67	20.56	-110.80			
							215.53	19.71	-110.86			
MP47							212.26	12.01	-70.59			
							212.16	11.82	-70.65			
							212.24	12.18	-70.01			
MP3078	202.55	-1.71	-118.75				208.92	14.68	-112.74			

	203.33	0.00	-117.61				209.76	12.28	-113.22			
	202.41	-0.01	-117.63				209.59	12.28	-112.97			
MP221	218.72	-24.11	-131.05	189.01	-41.93	-103.54	227.73	3.83	-121.30	203.81	-21.64	-114.87
	215.14	-23.50	-129.44	188.14	-46.61	-105.82	222.78	1.88	-121.70	204.70	-23.46	-115.50
	215.10	-25.24	-130.42	185.85	-44.93	-103.46	222.66	2.76	-121.12	204.58	-23.96	-116.05
MP2	140.35	-190.82	-126.52	112.25	-181.66	-100.14	169.49	-184.74	-104.42	141.82	-178.76	-103.32
	140.44	-191.20	-126.21	112.57	-181.21	-102.91	170.34	-184.93	-104.35	141.95	-179.53	-102.78
	139.98	-191.93	-126.48	112.97	-182.02	-101.81	169.76	-184.54	-103.30	141.69	-179.88	-102.94
MP170				110.98	-177.30	-113.26	167.84	-180.55	-123.90	141.27	-176.60	-123.64
				111.10	-176.46	-113.03	169.81	-180.00	-123.32	140.83	-176.32	-123.65
				110.10	-176.94	-113.19	169.35	-179.73	-123.43	140.49	-176.55	-123.66
MP76	190.60	-169.96	-70.44	141.91	-158.50	-71.33				172.30	-159.06	-64.91
	188.75	-170.66	-72.95	141.53	-158.77	-71.47				171.64	-159.39	-65.09
	189.59	-170.88	-72.80	141.13	-158.81	-71.00				171.11	-159.04	-65.25
MP119				126.45	-153.45	-94.22	172.67	-168.15	-111.32	149.04	-159.36	-105.96
				126.79	-154.00	-96.28	173.11	-167.70	-111.05	148.41	-159.77	-105.89
				126.90	-153.43	-96.51	171.87	-168.23	-111.60	147.93	-159.91	-106.05
MP75	151.58	-186.34	-126.99				179.75	-173.25	-113.29	145.47	-172.52	-112.60
	151.58	-186.27	-126.81				179.73	-172.85	-113.21	145.22	-173.07	-112.41
	152.31	-186.60	-126.85				179.27	-172.94	-113.62	145.80	-172.91	-111.30
MP223	174.05	-164.64	-136.38	137.55	-147.95	-112.50	193.72	-158.40	-124.19	166.02	-148.67	-118.01
	175.07	-164.70	-135.40	137.65	-147.14	-113.23	194.64	-158.46	-124.31	166.89	-149.02	-117.45
	175.19	-164.24	-134.87	137.82	-148.48	-113.30	195.82	-157.82	-123.88	167.64	-149.84	-117.09
MP164							206.22	-151.72	-105.16			
							207.25	-151.31	-104.05			
							206.38	-150.93	-104.48			
M3065				145.72	-151.74	-102.55	201.76	-157.87	-115.49	175.03	-154.64	-112.96
				146.80	-154.13	-104.85	203.05	-157.36	-115.02	174.28	-153.28	-112.82
				147.01	-154.74	-104.63	203.38	-157.57	-114.76	174.74	-153.52	-112.06
M3084	179.78	-156.61	-97.79				195.57	-153.40	-80.96	167.39	-145.25	-82.83
	178.34	-156.64	-98.10				196.64	-154.22	-81.32	167.04	-146.03	-82.66
	178.97	-156.86	-97.41				196.29	-153.08	-80.56	166.07	-144.81	-83.55

MP239	162.24	-171.81	-119.89	131.00	-158.54	-102.31	184.63	-164.37	-114.81	157.86	-158.49	-105.51
	162.19	-171.59	-119.60	130.70	-158.33	-101.62	184.02	-163.44	-114.59	157.79	-158.61	-105.51
	162.02	-171.02	-119.61	131.14	-158.69	-102.46	184.66	-163.98	-114.96	157.29	-158.03	-105.64
M3070	151.94	-183.38	-102.82	128.87	-163.30	-81.88	176.63	-175.81	-98.98	152.48	-168.37	-89.50
	152.22	-183.25	-102.68	128.77	-163.91	-81.79	177.50	-175.03	-98.98	152.93	-167.58	-88.99
	152.10	-183.35	-102.92	128.63	-164.61	-82.80	177.38	-175.20	-98.96	152.73	-168.12	-89.05
M3079	179.18	-172.68	-99.81				197.20	-170.13	-93.35			
	179.00	-172.63	-100.08				196.59	-169.22	-93.08			
	179.22	-172.70	-99.67				194.85	-169.98	-93.56			
M3147												
M3133							188.28	-172.95	-110.06	159.45	-167.98	-101.81
							186.73	-172.93	-110.28	160.68	-168.28	-101.36
							188.36	-172.28	-110.05	161.40	-169.85	-101.48
MP208	154.36	-189.28	-107.48	133.21	-174.70	-85.46	176.09	-183.07	-106.98	154.07	-176.46	-95.18
	155.24	-189.13	-106.96	133.45	-175.27	-85.30	176.03	-183.08	-106.93	154.82	-175.89	-94.37
	156.18	-189.21	-106.61	133.41	-176.63	-85.86	175.99	-183.63	-106.82	154.04	-175.56	-94.23
M3073	211.86	-16.97	-140.69	183.99	-28.54	-119.19	222.61	15.03	-126.42	201.41	-2.78	-121.22
	211.99	-17.40	-140.92	178.82	-28.35	-117.47	221.56	14.18	-126.59	203.29	-2.25	-121.74
	212.21	-16.80	-140.64	186.41	-28.32	-118.89	221.16	9.72	-127.73	200.58	-3.25	-121.47
MP3	144.82	-181.65	-133.36	111.06	-175.92	-115.43	162.56	-177.71	-130.35	131.81	-174.82	-125.38
	144.32	-181.47	-132.89	111.83	-173.38	-116.74	160.57	-179.24	-131.00	133.88	-175.45	-124.88
	143.55	-181.74	-133.33	110.68	-174.25	-116.60	161.34	-179.67	-131.12	131.75	-174.72	-125.71
MP217							174.89	-174.22	-122.60			
							174.32	-174.38	-122.69			
							174.24	-174.58	-122.55			
MP222				113.06	-180.15	-112.12	165.79	-182.75	-126.21	145.15	-169.21	-114.51
				112.28	-176.02	-111.67	165.68	-181.88	-126.36	146.21	-169.51	-116.31
				112.06	-176.06	-111.46	167.55	-180.57	-125.27	145.97	-170.62	-116.78

3D Anatomical Landmark Coordinate Data - Fossil Cercopithecoid sample (Continued…)

Specimen no.	Zygomaxillary superior (R)			Frontomalare-orbitale (R)			Orbital notch (R)			Frontomalare-temporale (R)		
	x	y	z	x	y	z	x	y	z	x	y	z
MP167				189.74	15.77	-97.18	204.60	25.32	-104.94	185.34	14.92	-94.57
				189.81	15.83	-96.95	204.67	25.33	-104.85	185.13	15.30	-94.35
				189.07	15.92	-97.21	215.38	22.25	-110.65	184.90	15.31	-93.90
MP47												
MP3078												
MP221	203.81	-21.64	-114.87	193.69	-3.71	-108.48	212.35	6.00	-118.15	187.41	-2.07	-104.70
	204.70	-23.46	-115.50	188.63	-7.13	-108.41	207.75	3.13	-118.09	183.03	-5.62	-104.38
	204.58	-23.96	-116.05	188.47	-7.56	-108.79	206.92	4.29	-118.38	182.54	-6.53	-105.12
MP2	141.82	-178.76	-103.32	144.75	-159.49	-90.98	164.13	-170.94	-98.77	137.73	-157.16	-86.01
	141.95	-179.53	-102.78	144.29	-159.74	-90.91	163.53	-170.47	-98.39	137.56	-156.67	-86.08
	141.69	-179.88	-102.94	143.83	-160.09	-91.16	163.02	-170.91	-98.40	139.52	-156.08	-86.26
MP170	141.27	-176.60	-123.64	143.49	-157.81	-113.69	164.23	-164.77	-120.26			
	140.83	-176.32	-123.65	144.54	-156.93	-113.52	163.59	-164.59	-120.12			
	140.49	-176.55	-123.66	143.18	-157.53	-113.67	164.10	-164.64	-120.19			
MP76	172.30	-159.06	-64.91	171.25	-146.24	-48.89	194.04	-155.81	-51.22	165.82	-144.83	-36.23
	171.64	-159.39	-65.09	170.60	-147.22	-48.53	193.76	-156.94	-51.46	166.82	-145.43	-37.44
	171.11	-159.04	-65.25	171.33	-148.01	-49.42	192.93	-158.17	-51.47	166.38	-145.64	-37.49
MP119	149.04	-159.36	-105.96									
	148.41	-159.77	-105.89									
	147.93	-159.91	-106.05									
MP75	145.47	-172.52	-112.60									
	145.22	-173.07	-112.41									
	145.80	-172.91	-111.30									
MP223	166.02	-148.67	-118.01	173.84	-133.52	-109.96	192.25	-142.06	-118.74	169.62	-129.41	-100.78
	166.89	-149.02	-117.45	173.65	-133.53	-110.46	192.42	-142.40	-118.90	168.93	-129.41	-100.82

	167.64	-149.84	-117.09	171.90	-133.27	-110.21	192.45	-142.46	-118.83	169.61	-129.64	-100.00
MP164				180.68	-130.13	-92.89	198.23	-138.38	-98.16	176.69	-127.64	-85.76
				180.67	-129.50	-92.87	198.63	-138.71	-98.26	176.60	-127.17	-88.36
				180.62	-130.65	-92.77	198.01	-137.58	-98.03	176.62	-127.08	-87.61
M3065	175.03	-154.64	-112.96	178.23	-135.90	-106.89	194.95	-143.97	-112.57	175.67	-132.69	-100.20
	174.28	-153.28	-112.82	179.59	-136.62	-106.99	196.39	-145.03	-112.71	176.82	-131.74	-99.73
	174.74	-153.52	-112.06	179.66	-136.32	-107.68	195.70	-144.92	-112.72	176.16	-132.02	-99.33
M3084	167.39	-145.25	-82.83	171.02	-132.80	-71.70	189.64	-142.47	-74.36	164.62	-129.21	-63.94
	167.04	-146.03	-82.66	167.52	-132.31	-72.39	189.03	-142.10	-74.18	163.79	-129.70	-63.20
	166.07	-144.81	-83.55	169.94	-131.77	-71.50	189.37	-142.87	-74.36	163.83	-129.33	-63.92
MP239	157.86	-158.49	-105.51	159.24	-143.94	-102.22	180.44	-152.14	-109.51	159.43	-137.62	-95.06
	157.79	-158.61	-105.51	160.02	-141.31	-101.99	180.75	-152.43	-109.57	159.45	-137.66	-94.91
	157.29	-158.03	-105.64	159.77	-143.63	-102.00	180.81	-152.61	-109.56	158.83	-137.37	-94.70
M3070	152.48	-168.37	-89.50	160.00	-151.48	-86.95	173.83	-161.29	-96.20	154.15	-147.22	-81.75
	152.93	-167.58	-88.99	156.22	-152.60	-87.28	174.77	-160.43	-96.75	153.41	-147.81	-82.37
	152.73	-168.12	-89.05	157.76	-151.74	-87.13	173.62	-160.94	-96.37	157.63	-146.57	-82.37
M3079							191.54	-155.31	-86.95			
							190.86	-154.49	-86.90			
							192.45	-155.45	-86.44			
M3147												
M3133	159.45	-167.98	-101.81	164.64	-154.06	-96.61	185.74	-161.09	-105.06	159.90	-150.42	-90.02
	160.68	-168.28	-101.36	163.89	-153.84	-96.50	185.55	-161.87	-104.42	159.07	-150.24	-91.78
	161.40	-169.85	-101.48	165.13	-153.03	-96.67	185.04	-160.43	-104.69	159.98	-149.97	-90.20
MP208	154.07	-176.46	-95.18	158.63	-160.06	-94.69	174.29	-170.27	-105.21	155.10	-156.77	-89.39
	154.82	-175.89	-94.37	158.82	-160.42	-94.81	175.77	-168.96	-106.09	155.80	-156.06	-89.47
	154.04	-175.56	-94.23	159.11	-160.55	-94.88	175.26	-169.99	-105.44	155.66	-156.01	-88.92
M3073	201.41	-2.78	-121.22	191.65	13.18	-114.87	206.75	21.74	-123.56	186.49	11.17	-107.61
	203.29	-2.25	-121.74	192.22	14.46	-115.44	207.00	21.49	-123.60	186.67	11.26	-108.43
	200.58	-3.25	-121.47	191.79	14.35	-115.21	206.86	21.97	-123.61	186.02	11.43	-108.46
MP3	131.81	-174.82	-125.38				156.86	-163.84	-125.53			

	133.88	-175.45	-124.88				155.63	-164.11	-124.97			
	131.75	-174.72	-125.71				157.17	-164.80	-125.76			
MP217												
MP222	145.15	-169.21	-114.51	149.32	-150.54	-107.06	167.32	-161.68	-123.72	147.62	-147.48	-102.55
	146.21	-169.51	-116.31	150.10	-150.83	-107.80	167.53	-161.63	-124.26	148.22	-146.13	-101.96
	145.97	-170.62	-116.78	149.38	-150.78	-106.95	165.32	-160.36	-122.12	147.63	-147.63	-101.61

3D Anatomical Landmark Coordinate Data - Fossil Cercopithecoid sample (Continued…)

Specimen no.	Glabella			Temporal-frontal-parietal suture (R)			Bregma			Premaxillary-maxillary suture (L)		
	x	y	z	x	y	z	x	y	z	x	y	z
MP167				186.47	18.10	-78.93	218.84	48.82	-61.22	228.63	-45.49	-117.15
				186.68	17.65	-79.49	218.20	48.99	-61.04	227.54	-46.57	-117.17
				186.51	17.77	-79.78	218.63	49.09	-61.82	228.77	-45.06	-116.95
MP47	212.61	16.19	-64.46							230.03	-54.47	-126.53
	213.43	16.67	-63.95							230.02	-55.60	-126.24
	213.13	16.32	-64.67							229.60	-55.94	-126.26
MP3078	208.48	20.73	-108.82				205.66	39.04	-59.77	222.83	-37.37	-139.10
	208.63	21.51	-107.73				206.25	39.13	-60.89	221.91	-37.89	-140.34
	209.25	22.02	-107.13				205.93	39.40	-59.62	223.13	-37.41	-138.87
MP221	227.14	7.28	-118.69	197.57	2.09	-85.58	227.86	33.73	-64.77	243.35	-81.04	-146.65
	222.11	6.35	-118.63	191.86	-0.11	-85.26	221.49	31.88	-65.06	241.29	-81.14	-147.69
	222.14	6.74	-118.08	191.25	0.02	-85.58	221.87	31.98	-64.70	242.82	-80.50	-146.83
MP2	174.89	-181.94	-98.18	143.35	-164.06	-61.43	185.25	-175.95	-51.86	129.57	-227.78	-146.63
	176.84	-183.80	-97.42	143.65	-164.01	-61.59	185.50	-176.17	-51.91	127.44	-229.18	-145.15
	174.09	-183.54	-99.20	142.82	-164.77	-61.66	185.17	-176.20	-52.41	126.81	-229.65	-145.21
MP170	176.23	-172.66	-117.29	147.97	-156.25	-80.41	189.04	-163.53	-58.00			
	176.17	-172.85	-117.60	148.20	-156.08	-80.53	189.20	-163.75	-57.67			
	177.03	-173.81	-117.30	147.90	-156.68	-81.45	189.05	-163.41	-57.23			

MP76												
MP119				155.12	-141.45	-70.49				126.30	-209.05	-134.22
				154.26	-142.64	-71.61				125.81	-208.71	-134.46
				154.76	-141.52	-70.51				128.18	-207.62	-134.23
MP75	182.55	-169.44	-109.14	157.99	-153.08	-79.33	196.52	-161.95	-56.04			
	182.30	-169.39	-109.03	158.51	-152.68	-79.23	196.45	-161.52	-56.10			
	182.40	-169.62	-109.26	158.15	-153.00	-79.71	196.27	-161.19	-55.50			
MP223	202.44	-152.91	-119.07							149.79	-213.38	-166.61
	202.79	-154.31	-119.32							150.16	-212.09	-167.41
	202.62	-153.78	-118.67							149.00	-212.30	-167.45
MP164	210.80	-149.82	-99.47	176.93	-134.35	-72.90	213.04	-150.18	-39.63			
	211.55	-149.88	-98.96	177.06	-134.42	-72.81	212.91	-149.74	-40.00			
	210.78	-149.26	-99.28	177.43	-134.36	-72.83	213.12	-149.67	-40.46			
M3065	208.14	-153.91	-110.13	185.25	-131.46	-82.58	222.35	-140.57	-61.27			
	208.19	-153.04	-109.63	185.52	-131.39	-81.99	222.07	-141.11	-60.54			
	207.98	-153.61	-110.28	185.66	-131.56	-81.91	222.09	-141.08	-60.55			
M3084	201.05	-151.65	-75.01							169.89	-189.83	-137.41
	200.97	-151.66	-74.50							168.44	-189.93	-137.06
	200.53	-151.26	-74.50							168.26	-189.95	-137.00
MP239	191.19	-160.06	-108.80	161.98	-143.29	-78.42	208.25	-149.36	-56.45	141.47	-210.87	-137.42
	191.61	-159.75	-107.95	162.60	-142.28	-77.57	208.22	-149.14	-56.12	140.46	-211.00	-137.02
	191.39	-160.34	-108.88	162.71	-141.48	-77.36	208.02	-149.08	-56.51	140.85	-210.87	-137.02
M3070	184.48	-170.19	-95.60							138.43	-219.26	-110.20
	184.91	-170.60	-95.40							137.63	-219.52	-110.29
	184.60	-170.89	-95.58							137.98	-219.39	-111.09
M3079	202.60	-166.44	-85.57				215.84	-156.32	-35.44	158.57	-205.97	-126.96
	203.28	-165.94	-84.26				215.82	-156.43	-35.27	159.41	-205.95	-127.06
	203.72	-167.41	-84.60				215.86	-156.66	-36.37	159.19	-206.28	-127.16
M3147												

M3133	195.45	-168.45	-104.76	172.50	-150.61	-71.44	213.06	-161.38	-53.22			
	195.51	-167.54	-103.61	173.11	-150.51	-71.96	212.83	-161.01	-53.58			
	195.81	-168.78	-104.63	172.24	-150.97	-72.13	212.75	-160.92	-53.90			
MP208				165.24	-153.53	-72.35	212.54	-166.24	-64.23	135.13	-225.73	-108.71
				166.44	-152.54	-72.27	213.06	-166.67	-64.72	136.62	-225.92	-107.64
				166.91	-151.67	-71.76	212.74	-166.10	-64.28	135.94	-225.58	-108.46
M3073	222.58	22.24	-122.36	191.30	15.51	-87.44	226.42	42.41	-63.05	228.80	-59.01	-156.41
	222.03	22.50	-122.05	192.01	16.55	-88.23	226.30	42.56	-63.44	228.05	-59.84	-157.57
	222.66	22.84	-121.74	192.74	17.54	-89.34	225.96	42.41	-63.17	228.22	-59.71	-157.49
MP3	166.92	-175.06	-126.10	145.01	-153.15	-77.05	185.86	-168.79	-70.77	121.39	-222.47	-151.34
	166.61	-175.22	-126.14	143.89	-154.01	-76.35	185.72	-168.62	-70.52	120.22	-221.87	-151.91
	166.45	-175.29	-126.21	142.98	-154.58	-76.79	185.30	-168.19	-70.81	120.51	-221.62	-152.30
MP217	182.79	-168.88	-118.01	154.75	-152.12	-81.18	191.38	-162.98	-57.43	138.50	-220.53	-170.87
	182.71	-168.74	-118.05	154.70	-151.55	-81.63	191.34	-162.53	-58.18	138.19	-223.61	-170.63
	182.31	-169.01	-118.40	155.38	-152.02	-82.14	191.09	-162.97	-57.96	136.87	-225.23	-170.29
MP222	177.88	-173.39	-122.85	159.74	-156.40	-76.88	193.03	-167.45	-68.02	120.06	-224.94	-165.78
	178.10	-172.87	-122.01	150.81	-160.40	-78.45	193.24	-167.31	-66.90	117.72	-225.64	-165.12
	177.79	-173.09	-123.00	150.55	-160.30	-77.89	193.45	-167.56	-67.86	116.92	-225.65	-165.30

3D Anatomical Landmark Coordinate Data - Fossil Cercopithecoid sample (Continued…)

Specimen no.	Premaxillary suture superior (L)			Zygomaxillary inferior (L)			Zygomaxillary superior (L)			Frontomalare-orbitale (L)		
	x	y	z	x	y	z	x	y	z	x	y	z
MP167												
MP47							232.91	-9.61	-70.53	249.85	1.84	-59.39
							233.16	-9.73	-69.84	251.07	2.95	-59.48
							232.72	-9.79	-69.86	250.59	4.33	-59.40
MP3078	212.07	-0.62	-119.43	241.09	-21.01	-97.48	226.38	-2.30	-106.38	237.67	10.48	-100.80
	211.79	0.42	-118.71	241.19	-21.14	-96.88	223.84	-2.32	-107.87	237.47	10.36	-100.81

	211.85	0.61	-118.41	241.14	-21.08	-97.38	226.71	-2.55	-106.98	237.61	10.24	-100.74
MP221	233.47	-29.24	-132.79	265.16	-45.40	-100.54	246.67	-23.12	-113.94	262.65	-5.93	-108.62
	228.99	-27.33	-131.19	258.45	-46.87	-102.66	240.77	-22.19	-113.50	255.99	-5.65	-108.15
	229.20	-28.15	-131.66	260.40	-45.08	-102.40	240.33	-22.67	-113.93	256.52	-6.25	-108.04
MP2	149.38	-203.72	-126.59	152.06	-237.01	-98.98	164.63	-213.10	-103.06	181.44	-220.29	-93.46
	150.00	-202.99	-125.26	152.74	-238.18	-100.35	161.79	-212.22	-103.37	181.28	-220.05	-93.43
	148.10	-205.04	-125.55	152.10	-238.50	-100.18	161.40	-212.84	-103.33	181.03	-220.66	-93.46
MP170												
MP76	197.37	-179.37	-74.12									
	196.48	-180.56	-74.02									
	196.23	-180.66	-74.25									
MP119				155.94	-212.22	-94.68	166.09	-190.91	-105.34			
				153.18	-211.67	-94.49	167.28	-190.31	-103.99			
				154.89	-209.73	-94.30	167.66	-189.29	-105.37			
MP75	158.11	-197.69	-129.48				173.54	-204.94	-112.10			
	157.55	-198.56	-129.84				173.32	-204.75	-111.64			
	157.39	-198.59	-130.11				173.11	-204.96	-112.48			
MP223	181.59	-175.25	-139.02	181.94	-214.53	-112.56	195.59	-187.70	-116.25	215.00	-187.95	-110.43
	183.47	-173.85	-136.20	184.18	-215.33	-113.38	195.66	-188.72	-116.55	214.35	-187.19	-110.54
	183.77	-173.35	-135.86	183.40	-215.27	-112.83	195.10	-187.67	-115.86	214.16	-187.46	-110.52
MP164										215.94	-183.95	-94.96
										215.60	-184.67	-95.02
										216.05	-184.90	-95.05
M3065							194.55	-184.63	-110.37	212.87	-186.44	-105.36
							195.22	-185.24	-109.76	213.44	-185.47	-105.29
							194.14	-182.90	-110.48	214.54	-185.16	-105.66
M3084							190.30	-178.53	-85.07	206.10	-188.30	-74.82
							190.13	-178.69	-85.17	205.28	-188.97	-75.14
							190.24	-179.49	-85.47	206.00	-189.47	-75.15
MP239	168.59	-181.08	-120.70	168.05	-214.61	-101.91	178.96	-190.91	-107.06	197.54	-194.25	-103.18

	169.07	-180.40	-120.71	167.52	-214.41	-101.58	178.78	-191.15	-107.27	197.65	-194.31	-103.20
	169.79	-179.78	-119.73	168.26	-214.48	-102.72	179.25	-190.81	-106.44	196.99	-193.60	-103.44
M3070	160.25	-192.75	-102.84	165.73	-222.38	-80.16	172.86	-200.70	-89.28			
	160.24	-193.04	-102.75	165.85	-222.59	-80.47	172.94	-201.00	-89.01			
	160.58	-193.17	-102.11	166.49	-223.05	-80.04	173.34	-201.84	-88.76			
M3079	186.91	-180.01	-98.57									
	186.64	-180.17	-98.54									
	186.90	-180.71	-98.21									
M3147												
M3133				170.37	-225.54	-92.95	181.15	-200.12	-103.34	199.34	-201.27	-100.29
				171.28	-226.40	-92.70	181.40	-201.06	-103.10	198.92	-201.51	-100.05
				170.82	-225.89	-94.07	181.57	-202.81	-104.67	198.73	-201.93	-100.17
MP208	161.70	-198.10	-107.15	170.70	-227.46	-82.88	172.24	-204.52	-93.97			
	162.49	-197.17	-107.02	171.26	-227.15	-81.48	172.45	-204.77	-94.00			
	163.19	-197.08	-107.17	171.00	-227.31	-83.38	172.38	-205.33	-93.99			
M3073	223.50	-18.18	-139.78	255.06	-38.83	-116.17	238.63	-8.71	-122.47	253.48	7.71	-116.15
	222.63	-18.61	-140.62	252.90	-40.09	-115.62	237.84	-8.23	-122.17	253.53	7.31	-116.08
	222.73	-18.76	-140.53	254.34	-39.54	-115.94	237.10	-8.12	-122.08	252.79	6.63	-115.62
MP3	152.47	-190.48	-132.32	154.87	-230.36	-121.85	157.69	-207.02	-127.04	180.30	-209.81	-120.64
	151.56	-191.76	-133.30	154.24	-230.08	-121.82	155.94	-207.20	-127.70	179.67	-209.63	-120.43
	151.46	-191.63	-132.90	153.41	-230.22	-120.66	156.47	-207.72	-127.88	179.62	-209.89	-120.45
MP217				161.94	-237.42	-117.73	166.85	-202.98	-123.22			
				161.76	-237.45	-117.48	167.40	-206.08	-125.88			
				161.00	-237.81	-117.57	166.60	-205.31	-126.00			
MP222				150.14	-236.28	-115.82	167.11	-206.35	-119.41	189.42	-209.19	-112.67
				150.01	-235.96	-115.93	167.27	-206.07	-119.09	189.54	-207.56	-113.44
				149.77	-235.77	-115.93	167.30	-206.99	-119.03	189.34	-207.49	-113.48

3D Anatomical Landmark Coordinate Data - Fossil Cercopithecoid sample (Continued…)

Specimen no.	Orbital notch (L)			Frontomalare-temporale (L)			Temporal-frontal-parietal suture (L)			Porion (R)			Porion (L)		
	x	y	z	x	y	z	x	y	z	x	y	z	x	y	z
MP167	225.82	23.33	-107.88				247.18	19.82	-81.45	181.39	3.66	-48.53	254.99	5.83	-53.66
	226.17	24.00	-107.92				247.11	20.22	-81.23	181.32	3.73	-48.56	254.83	5.57	-52.71
	227.44	24.66	-107.81				246.77	20.97	-81.25	181.54	4.60	-47.25	254.72	6.74	-52.71
MP47	229.64	13.49	-66.02	256.70	2.76	-50.94									
	230.69	13.58	-65.96	256.99	2.03	-51.34									
	230.29	14.65	-65.84	257.29	0.75	-51.33									
MP3078	220.90	19.23	-108.59	241.87	10.50	-93.73							245.37	1.11	-48.83
	220.75	19.24	-108.59	241.99	11.08	-92.99							245.37	0.97	-48.74
	221.10	18.95	-108.38	240.79	14.06	-91.86							245.61	2.08	-47.82
MP221	240.16	2.92	-118.55	265.99	-6.15	-102.51	257.06	3.72	-83.07	184.42	-7.00	-37.10	271.73	-8.95	-39.07
	235.99	4.15	-118.68	260.70	-5.19	-102.54	251.19	4.50	-83.01	178.81	-8.53	-36.79	265.10	-5.20	-37.08
	235.78	3.24	-118.37	261.04	-5.52	-101.24	251.24	3.94	-83.52	178.81	-9.25	-37.10	264.55	-4.71	-37.08
MP2	179.01	-197.13	-97.93	183.55	-225.38	-84.83									
	180.67	-196.86	-99.16	183.82	-225.96	-85.17									
	180.02	-198.53	-99.23	183.57	-226.46	-85.92									
MP170	184.67	-188.28	-120.24												
	184.66	-188.34	-120.18												
	185.06	-188.15	-119.98												
MP76															
MP119							190.38	-191.35	-68.31				177.42	-206.24	-38.92
							192.31	-189.40	-68.56				177.19	-206.40	-38.65
							194.63	-187.24	-68.19				179.43	-204.57	-38.99
MP75	189.26	-187.00	-111.14				194.35	-201.77	-78.00				184.08	-225.87	-49.01
	188.63	-186.36	-111.16				195.08	-201.00	-78.46				183.86	-225.94	-49.04
	188.78	-186.29	-111.18				195.41	-200.49	-78.75				183.73	-225.94	-48.94
MP223	211.22	-168.77	-116.46	216.94	-191.31	-100.08	207.70	-189.32	-81.34				200.97	-209.53	-47.49
	211.83	-169.03	-116.70	216.91	-191.62	-100.52	207.34	-189.18	-81.94				200.76	-209.67	-47.60
	211.84	-169.22	-116.66	216.82	-191.51	-100.29	206.31	-189.97	-81.90				201.91	-210.51	-49.07
MP164	216.40	-163.63	-100.35	218.23	-187.94	-87.85	212.83	-185.86	-73.46				193.62	-209.31	-43.62
	214.93	-164.13	-100.05	217.42	-188.56	-87.89	212.01	-186.75	-73.37				194.77	-209.47	-43.90

	216.59	-163.93	-100.21	217.52	-188.60	-87.97	212.32	-186.54	-73.40				195.00	-209.73	-44.99
M3065	211.63	-166.78	-113.03	218.18	-187.60	-99.83	218.59	-181.65	-78.90	157.99	-139.24	-52.05	201.66	-201.73	-48.98
	211.78	-166.46	-112.93	218.61	-187.33	-100.23	216.62	-182.48	-79.82	158.13	-139.67	-51.86	201.79	-202.53	-50.30
	210.78	-166.25	-112.89	218.63	-187.02	-99.33	216.91	-182.16	-80.36	157.26	-139.17	-53.74	201.55	-201.92	-49.13
M3084	205.94	-168.10	-76.29	205.62	-196.75	-67.70									
	205.00	-168.07	-76.27	205.26	-196.63	-67.22									
	206.27	-167.70	-76.21	205.57	-196.40	-67.74									
MP239	194.67	-172.59	-111.01	198.97	-198.00	-95.75	204.16	-187.66	-75.60	149.74	-139.44	-41.33	194.52	-205.33	-43.59
	194.62	-172.80	-110.94	198.82	-198.10	-95.72	200.61	-190.24	-75.81	148.88	-140.32	-39.90	194.39	-205.04	-42.63
	194.66	-172.61	-111.00	199.23	-197.88	-95.51	200.32	-190.10	-76.55	148.91	-140.04	-41.04	193.61	-204.98	-42.01
M3070	189.75	-185.85	-96.09												
	189.49	-185.28	-96.23												
	189.19	-185.58	-96.08												
M3079															
M3147															
M3133	199.09	-182.43	-106.53	204.36	-202.50	-92.06	204.45	-200.01	-74.52	158.60	-150.81	-34.24	199.98	-215.68	-37.53
	199.66	-183.36	-105.89	200.59	-204.50	-94.17	204.34	-200.22	-73.34	158.70	-150.65	-34.03	199.38	-217.39	-40.84
	199.44	-183.65	-105.89	202.88	-203.37	-93.20	203.96	-200.50	-73.06	158.89	-151.41	-33.04	199.75	-215.59	-37.11
MP208										155.56	-150.35	-39.19	194.64	-218.67	-41.09
										155.54	-150.48	-39.03	195.62	-218.51	-41.53
										155.10	-150.99	-38.43	195.47	-218.54	-41.38
M3073	237.40	19.69	-125.09	258.68	7.16	-103.89	253.59	12.41	-89.20	179.44	-5.98	-56.48	265.50	-9.18	-51.01
	238.16	19.31	-125.03	259.45	6.95	-104.90	253.18	14.42	-89.33	178.80	-4.97	-57.93	265.86	-8.18	-50.69
	238.05	18.86	-124.77	259.30	7.62	-105.14	253.25	12.96	-89.24	178.45	-2.53	-58.98	265.80	-7.93	-50.70
MP3	178.14	-191.27	-127.48	184.80	-209.68	-111.67	185.89	-208.40	-76.77	127.22	-161.44	-47.86	170.29	-227.34	-59.60
	177.83	-191.69	-127.57	184.65	-210.17	-111.83	185.83	-208.67	-75.41	125.09	-164.78	-56.34	170.14	-227.41	-59.30
	177.15	-191.39	-127.54	184.03	-210.25	-111.56	185.72	-209.07	-74.74	125.67	-164.51	-56.57	170.24	-227.36	-59.51
MP217	191.36	-183.79	-118.76				196.31	-192.45	-80.89				184.54	-222.27	-45.17
	192.25	-183.69	-118.80				196.31	-192.68	-80.56				184.17	-222.29	-44.92
	191.37	-184.39	-118.42				195.78	-192.96	-80.65				183.76	-222.95	-46.27
MP222				194.33	-211.51	-105.44	187.84	-204.79	-78.85	137.82	-159.26	-45.21	181.46	-222.54	-47.80
				194.31	-211.39	-105.30	187.92	-204.15	-79.06	138.98	-158.07	-43.75	182.36	-222.40	-46.69

				194.33	-211.49	-105.29	187.38	-204.63	-78.66	139.12	-158.02	-43.97	183.13	-222.27	-48.32

Appendix D-3. Measurements of the upper third molars of the fossil cercopithecoid specimens and extant chacma baboon specimens used in this investigation.

Table D.3. Measurements of the upper third molars of the fossil cercopithecoid specimens and extant chacma baboon specimens used in this investigation.

Access no.	Buccal/lingual posterior (R)	Buccal/lingual anterior (R)	Mesio-dsital (R)	Buccal/lingual posterior (L)	Buccal/lingual anterior (L)	Mesio-dsital (L)
Fossil Cercopithecoid Sample						
MP2		10.4		9.0	10.3	10.5
M3056				9.3	11.4	11.8
MP151	8.5	11.1	10.9	8.6	10.6	10.5
MP76				10.3	12.3	11.7
MP119				11.0	12.9	12.5
MP223	10.5	12.9		10.5	12.6	12.5
MP173						12.6
MP239	8.3	11.2	11.4	8.4	11.2	
M3070	9.0	12.1	11.5		12.3	
M3079			10.8			11.3
M3147			13.5	10.2	12.5	13.6
M3133	9.7	11.2	10.7		11.3	
MP208		11.5				
Extant Chacma Baboon Sample						
ZM33402F	9.9	10.7	13.8	9.9	11.0	13.5
ZM33401F	9.5	11.5	12.5	10.0	11.5	12.5
ZM33410M	9.5	11.5	13.0	9.5	11.5	13.5
ZM33412M	11.0	12.0	14.5	11.0	12.5	14.5

ZM33646M	10.5	11.5	14.0	11.5	11.5	13.5
ZM12790M	10.5	12.0	14.5	11.0	12.0	14.5
ZM17179M	9.0	12.0	14.0	10.5	12.0	14.0
ZM33664M	10.5	11.5	13.5	10.5	11.5	13.0
ZM33670M	9.5	11.9	13.0	9.9	12.0	14.0
ZM33671M	11.0	12.5	14.5			
ZM33672F	11.0	12.5	13.5	10.5	12.0	13.0
ZM33676M	10.5	11.5	14.5	10.5	12.0	14.5
ZM33764M	10.5	13.0	14.5	11.5	13.0	15.0
ZM33675M	10.5	11.5	13.0	10.5	11.0	13.0
ZM35819F	9.9	11.5	12.5	10.0	12.5	12.5
ZM35912F	9.9	12.0	12.5	10.0	12.5	12.0
ZM35917M	11.5	13.0	15.0	11.5	12.9	15.0
ZM35915M	11.5	12.0	14.0	11.0	12.9	13.5
ZM35918M	10.5	12.5	13.5	11.0	12.5	13.5
ZM35935F	9.0	11.5	12.0	9.5	11.0	12.5
ZM35944F	10.0	11.9	13.0	9.9	11.5	13.0
ZM35941F	10.0	11.9	12.5	9.9	11.5	12.0
ZM35949F	10.0	11.0	12.0	9.9	11.0	12.5
ZM35948F	10.0	12.0	13.0	10.0	12.0	12.9
ZM36824F	9.9	11.5	12.5	9.9	12.0	13.0
ZM362829F	9.0	11.5	12.5	9.5	11.0	12.9
ZM37112F	9.9	11.0	13.0	9.9	11.0	13.0
ZM40445M	10.5	12.5	14.0	11.0	12.5	14.5
Rondebosch Skull	9.9	12.0	14.0	9.9	12.5	14.5